

Notes on mechanical properties of solids

W.E Bailey

January 22, 2020

Contents

1 Microscopic basis of elasticity	7
1.1 Bonding from interatomic potentials	8
1.1.1 General considerations	8
1.1.2 Semiquantitative model: empirical potentials	9
1.1.3 Harmonic components: 'springlike'	11
1.1.4 Anharmonic components	11
1.1.5 Alternate forms	14
1.2 Lattice dynamics: normal modes of the diatomic lattice	14
1.2.1 Equation of motion	15
1.3 Debye model for heat capacity	18
1.3.1 Derivation of Debye model	18
1.3.2 Comparison with experiments	24
2 Stress	33
2.1 Types of forces on a volume element	33
2.2 The stress matrix	34
2.3 Requirements for equilibrium	35
2.3.1 Forces	35
2.3.2 Torques	37
2.4 Stress matrix	38
2.5 Application: beam theory	38
2.5.1 Curvature	38
2.5.2 Translational equilibrium	39
2.5.3 Rotational equilibrium and bending moments	40
3 Principal axes of the stress tensor	47
3.1 Properties of tensors	47
3.1.1 Tensors express a linear relationship between two quantities	48

3.1.2	Rules for coordinate transformations	50
3.1.3	Coordinate transformations for tensors	54
3.1.4	Representation of the stress tensor as a surface	56
3.2	Finding principal axes	57
3.2.1	Three-dimensional stress tensor	57
3.2.2	Single rotation: Mohr's circle	58
4	Strain tensor	63
4.1	Definitions of strain	63
4.1.1	One-dimensional strain	64
4.1.2	Two-dimensional strain	65
4.1.3	Symmetrizing the strain tensor	67
4.1.4	Tensor shear strain and (engineering) shear strain . .	68
4.1.5	Dilation	69
5	Elasticity and thermodynamics	71
5.1	Isotropic elasticity	71
5.1.1	Parameters defining isotropic elasticity	71
5.2	Thermodynamics of elasticity	77
5.2.1	Elastic energy	78
5.2.2	Entropic elasticity in polymers	79
5.2.3	Thermal expansion and compressibility parameters in thermodynamic quantities	81
5.2.4	Grüneisen function	83
6	Anisotropic elasticity	89
6.1	Stiffness and compliance	89
6.1.1	Simple stress configurations: use of compliance . . .	90
6.1.2	Simple strain configurations: use of stiffness	91
6.2	General restrictions on elastic tensors	91
6.2.1	Experimental inaccessibility	92
6.2.2	Symmetry of stiffness and compliance matrices . . .	92
6.3	Matrix notation	94
6.3.1	Utility of the matrices: crystal and physical axes aligned	96
6.3.2	Transformation of matrix to tensor elasticities	96
6.3.3	Elastic energy in matrix notation	98
6.4	Crystal symmetry	98
6.4.1	Neumann's principle	99
6.4.2	Expression in tensor transformations	99
6.4.3	Cubic systems	101

CONTENTS	5
6.5 Young's modulus in a given cubic direction	104
6.6 Transforming compliances to stiffnesses	108
6.7 Polycrystalline averages: return to isotropy	109
6.7.1 Stiffness and compliance matrices for isotropic materials	112
7 Elastic waves	119
7.1 Elastic modes	119
7.1.1 Vibrating string	120
7.1.2 Longitudinal vibrations of an isotropic beam	122
7.1.3 Transverse vibrations of an isotropic beam	124
7.2 Solutions for phase velocity	128
7.2.1 General: Cauchy equation of motion	129
7.2.2 Cubic materials	130
7.2.3 Isotropic materials	132
8 Composite elasticity and anelasticity	137
8.1 Neglecting Poisson contraction	137
8.1.1 Isostrain: fibers	137
8.1.2 Isostress: plates	137
8.2 Including Poisson contraction	137
8.3 Anelasticity and viscoelasticity	139
8.3.1 Shear viscosity	140
8.3.2 Discrete-element models	141
8.4 Internal friction	145
8.4.1 Cyclic stress; complex modulus	145
8.4.2 Response of the standard linear solid	151
8.4.3 Snoek damping	152
9 Introduction to plasticity: tensile	159
9.1 Engineering stress and engineering strain	159
9.1.1 Engineering stress s	159
9.1.2 Engineering strain e	160
9.2 Volume conservation in plasticity	161
9.3 The flow curve	163
9.3.1 Instability in tension: Considère's criterion	164
10 Forces on a dislocation	169
10.1 Strain and dislocation density	170
10.1.1 Strain as a function of dislocation density	170
10.1.2 Strain rate as a function of dislocation velocity	170

10.1.3	Dislocation accumulation	170
10.2	Peach-Koehler forces	171
10.2.1	Edge dislocation under simple shear	171
10.2.2	Mixed dislocation under arbitrary σ	173
10.2.3	Glide force on a dislocation loop	175
10.3	Strain fields and self-energy of dislocations	177
10.3.1	Screw dislocation	177
10.3.2	Edge dislocation	180
10.3.3	Force between two dislocations	183
10.4	Line tension of a dislocation	184
10.5	Dislocation - point-defect interactions	188
10.5.1	Chemical force in dislocation climb	189
10.5.2	Glide pinned by point defects	193
10.6	Dislocation dynamics	196
10.6.1	Power-law creep	197
10.6.2	Strain rate	197
10.6.3	Tensile test: yield drop	199
11	Strength of metals	205
11.1	Yield stress of perfect single crystals	205
11.1.1	Microscopic crystals	205
11.1.2	Macroscopic crystals	207
11.2	Strengthening mechanisms	207
11.2.1	Work hardening	207
11.2.2	Solid-solution strengthening	210
11.2.3	Precipitation hardening	215
11.2.4	Finite-size strengthening (Hall-Petch)	215
12	Fracture	223
12.1	Griffith critical crack length	223
12.1.1	Square beam	223
12.1.2	Elliptical crack	225
12.2	Weibull distribution	226
A	Moments of inertia	233
A.1	Area moments of inertia	233
A.2	Mass moments of inertia	234

Chapter 1

Microscopic basis of elasticity

The goal of this course is to understand the mechanical response of materials used in structural applications. Some materials are stronger than others. Why? Can a given type of material be made stronger? What does strength mean; how is it defined? These are the sorts of questions we will try to answer over the semester. The only way to answer these questions is to consider materials at the *microscopic* level, viewing the constituent atoms and how their positions change when forces are applied to the outer surfaces of the body.

We will see that there are two types of mechanical responses to forces. The first type is *reversible*: a *force* is applied, the outer surfaces of the body are *displaced* by some distance, but when the force is removed, the body returns to its original dimensions. This is an *elastic response*. The second type of response, more relevant for the strength of materials, is an *irreversible*, or *plastic response*. Here the displacement of atoms, or deformation, is permanent, remaining after the force is removed.

In Section 1.1, we will see how elasticity originates in the atomic bonding of a crystal. This view will also make it possible to understand how slight deviations from linear elasticity, with force and displacement proportional to each other, come about; these *anharmonic* effects are the origin of thermal expansion. In section 1.2, we will see how elasticity can be measured not only in static deformation, but also in vibration, through *elastic waves*. Much of the experimental evidence for elasticity and elastic bonding comes from a counterintuitive source: calorimetric measurements, especially heat capacity C_V , which answers: how much heat is absorbed in changing the

temperature of a sample by 1 K? We will explore the success of Debye model for understanding heat capacity in Section 1.3 and show how all its parameters can be determined by measurements of elasticity.

1.1 Bonding from interatomic potentials

First, we will consider a simple and general model for bonding in a solid, based on competing attractive and repulsive potentials. The model provides a microscopic basis for ‘spring forces’ between atoms, underlying both our treatment of lattice vibrations in Section 1.2 and our eventual continuum description of elasticity.

1.1.1 General considerations

Bonding lowers the energy of a crystal The internal energy U of a crystal is lowered through its bonding. As a sort of proof, consider:

- For temperatures below the melting point T_m , the Gibbs free energy of the solid (crystal) phase is lower than that of the liquid phase, proven by the fact that crystallization is spontaneous at constant pressure P and $T < T_m$.
- The Gibbs free energy has contributions from internal energy, pressure P , and entropy S , through $G = U + PV - TS$.
- In the liquid, configurational entropy S will be larger than that for a crystal, in which $S \rightarrow 0$ as $T \rightarrow 0$, according to the fourth law of thermodynamics.
- At atmospheric pressure, PV is relatively negligible.
- By process of elimination, the internal energy U is the quantity lowered in bonding.

Existence of the lattice parameter For a crystal at a given temperature, the interatomic spacing is well-defined, through the unit cell parameters. This imples that the potential energy *reduction* $-|U|$ through the bonding reaches a *minimum* for the interatomic spacing reached at the lattice parameter. Qualitatively, the energy minimum (potential well) is relatively easy to understand. Whatever binds the atoms – metallic bonds, covalent bonds, or ionic bonds – becomes weaker when the atoms are spaced

further apart. On the other hand, whatever repels the atoms from each other, keeping them from collapsing in on themselves to form a black hole – Pauli exclusion, basically – becomes stronger when the atoms are pushed closer together.

1.1.2 Semiquantitative model: empirical potentials

For a semiquantitative model, we can consider the bonding between two atoms separated by a distance d . We would like to find the bond energy $U(d)$, which reaches a minimum for $d = 2R$, where R is the radius of a hard-sphere model for the atoms. For ionic bonding, for example, we know that the electrostatic energy can be written in terms of the electrostatic potential through

$$U(d) = |Z_+ q_e| V(d) \quad (1.1)$$

The electrostatic potential can be written with

$$V(d) = \frac{-Z_- q_e}{4\pi\epsilon_0 d} \quad (1.2)$$

where Z is the number of ionic charges per atom. We can express this term as $U_-(d) = -Ad^{-1}$. The repulsive term from Pauli exclusion is less simple and not as well defined as the electrostatic interaction. We assume that it depends on interatomic spacing as $U_+(d) = Bd^{-n}$, with $6 \leq n \leq 11$. The sum of the two terms, with both A and B positive, is

$$U(d) = U_-(d) + U_+(d) \quad (1.3)$$

$$U(d) = -Ad^{-1} + Bd^{-n} \quad (1.4)$$

The interatomic spacing of the crystal structure (or here, the interatomic spacing of the diatomic molecule) will be found, for $T = 0$, where the energy $U(d)$ is minimized. To find the equilibrium, we take the zero of the interatomic force, $F = -\partial U / \partial d$,

$$F(d_0) = Ad_0^{-2} - n Bd_0^{-(n+1)} = 0 \quad (1.5)$$

$$d_0 = \left(\frac{nB}{A} \right)^{1/(n-1)} \quad (1.6)$$

where d_0 is the equilibrium interatomic spacing. d_0 decreases with increasing attractive potential strength A and increases with increasing repulsive potential strength B .

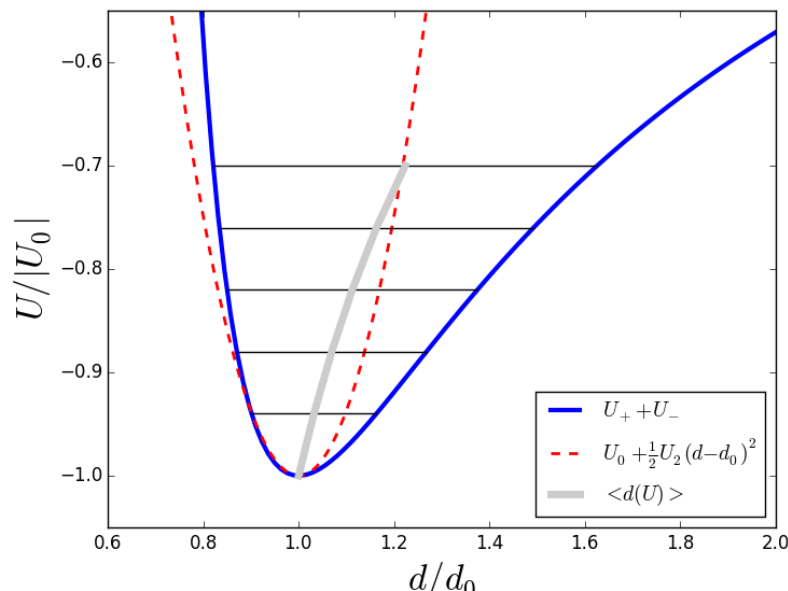


Figure 1.1: Solid line: interatomic potential defined in Eq 1.4. Dashed line: harmonic approximation, defined in Eq. 1.7. Shaded line: average interatomic spacing as a function of energy $\langle d(U) \rangle$ above the minimum, showing thermal expansion.

1.1.3 Harmonic components: 'springlike'

For very small displacements about the equilibrium spacing, the combined action of the bonding and repulsive terms is like a spring force between the atoms, restoring the spacing from d to d_0 . This can be seen more quantitatively by Taylor-expanding the potential for small displacements $d - d_0$,

$$U(d) \simeq U(d_0) + \frac{1}{2} \left(\frac{\partial^2 U}{\partial d^2} \right)_{d=d_0} (d - d_0)^2 \dots \quad (1.7)$$

Clearly, the first-order term is left out of this expression because it is zero at $d = d_0$ – the potential is minimized and the first derivative is zero. Including more terms, and defining $u \equiv d - d_0$ as the displacement of an atom,

$$U(d) \simeq U_0 + \frac{f}{2!} u^2 + \frac{g}{3!} u^3 + \frac{h}{4!} u^4 \dots \quad (1.8)$$

where f, g, h are the second, third, and fourth-order derivatives of U in terms of u about $u = 0$. Note that the coefficient for the third-order term is negative, $g < 0$: there is positive curvature in U for $d < d_0$ and negative curvature for $d > d_0$. The force can be written $F = -\partial U / \partial d$, so keeping only the first term,

$$F(d) = - \left(\frac{\partial^2 U}{\partial d^2} \right)_{d=d_0} (d - d_0) \quad (1.9)$$

Through comparison with the spring constant expression, $F = -k\Delta x$, we can identify a spring constant with the curvature of the interatomic potential,

$$k \leftrightarrow \partial^2 U(d) / \partial^2 d \quad (1.10)$$

It is straightforward but tedious to show that for the power law model,

$$f = (n+3) (n^{-3} A^{n+2} B^{-3})^{1/(n-1)} \quad (1.11)$$

1.1.4 Anharmonic components

As shown in Figure 1.1, the potential $U(d)$ begins to deviate from the harmonic approximation for moderate displacements $u/d_0 < 1$. The first correction for anharmonicity is the third-order, $gu^3/3!$ term. While the harmonic approximation is even about $u = 0$, the actual potential rises more

steeply for negative displacements $u < 0$ than for positive displacements, $u > 0$. This feature has effects on the temperature dependence of mechanical properties.

Thermal expansion As shown in Figure 1.1, when the system of bound atoms is excited to higher energies $U > U_0$, the average interatomic spacing $\langle d(U) \rangle$ will increase. The horizontal lines in Figure 1.1 indicate the effect of increasing average energies. This phenomenon is known as *thermal expansion*. The coefficient of thermal expansion α ($=\text{K}^{-1}$) is defined by the dimensionless strain per degree of rise of temperature,

$$\alpha = 1/L (\partial L / \partial T)_P \quad (1.12)$$

or

$$\alpha = (\epsilon / \partial T)_P \quad (1.13)$$

For a quantitative estimate, we can consider the effect of the anharmonic term on the vibrational characteristics of a molecule with displacement u . For the equation of motion of one atom with mass m under the force F exerted by another, fixed atom, we have (neglecting rotation), to third order in u , $\ddot{u} = F/m$

$$\ddot{u} = -\frac{1}{m} \left(fu + \frac{g}{2} u^2 \right) \quad (1.14)$$

$$\ddot{u} = -\omega_0^2 (u + su^2) \quad s \equiv \frac{g}{2f} \quad (1.15)$$

where $s [=] \text{m}^{-1}$. We can seek solutions including a second harmonic term,

$$u(t) = v_0 + A \cos \omega t + \eta \cos 2\omega t \quad (1.16)$$

with small amplitude η , $\eta \ll A$, and $v_0 \ll A$ is a time-averaged displacement. We neglect terms second order in η and v_0 (and ηv_0) as well as higher-harmonic terms, and approximate the new term quadratic in u as

$$u^2(t) \simeq \frac{A^2}{2} (1 + \cos 2\omega t) + 2Av_0 \cos \omega t \quad (1.17)$$

giving for Equation 1.14

$$\begin{aligned} \frac{\omega^2}{\omega_0^2} (A \cos \omega t + 4\eta \cos 2\omega t) = \\ v_0 + A \cos \omega t + \eta \cos 2\omega t + s \frac{A^2}{2} (1 + \cos 2\omega t) + 2sAv_0 \cos \omega t \end{aligned} \quad (1.18)$$

Equating the constant terms gives, for the time-averaged displacement v_0 ,

$$v_0 = -\frac{sA^2}{2} \quad (1.19)$$

and equating the $\cos \omega t$ terms, using Eq 1.19, gives for the frequency,

$$\frac{\omega^2}{\omega_0^2} = (1 + 2sv_0) \quad (1.20)$$

$$\frac{\omega^2}{\omega_0^2} = 1 - s^2 A^2 \quad (1.21)$$

Each of these terms shows that there is a nonlinear effect of vibration amplitude A on the resonance properties. Equation 1.19 shows that a time-averaged displacement v_0 , absent for infinitesimally small displacement, develops proportional to the square of the vibrational amplitude and the magnitude of the third-order term g . Equation 1.21 shows that there is a reduction (softening) in the resonance frequency proportional the square of the vibrational amplitude.

Equation 1.19 is the origin of thermal expansion. Classically, the mean energy of the molecule, vibrating with amplitude A as $u(t) = Ae^{-i\omega t}$, can be expressed in terms of the spring constant $f = k$ as $fA^2/2$. This limit holds at *high temperatures* compared with the Debye temperature, as will be shown in Section 1.3.

Equating the energy with the thermal energy yields $k_B T = fA^2/2$, or

$$A^2 \sim \frac{2k_B T}{f} \quad (1.22)$$

$$v_0 = -\frac{g}{4f} \frac{2k_B T}{f} \quad (1.23)$$

Taking $\epsilon = v_0/d_0$ for the strain, the thermal expansion coefficient is then

$$\alpha = -s \frac{k_B}{d_0 f}$$

(1.24)

Temperature-dependence of the elastic modulus Equation 1.21 shows that the elastic modulus is also dependent on temperature, but weakly so. Remembering that the resonant frequency ω_0 can be expressed in terms of the spring constant (here f) as $\omega_0^2 = f/m$, we see

$$\frac{E(T)}{E(0)} = 1 - \frac{2s^2 k_B}{f} T \quad (1.25)$$

which shows that anharmonicity also predicts a linear decrease in the elastic constant $E(T)$ with increasing temperature, at high temperature. Experiments prove this prediction to be true, although the temperature dependence is rather weak, negligible for most purposes far from the melting point. The change in the stiffness for Ag over $4.2 \text{ K} \leq T \leq 300 \text{ K}$ is only about 6% of the total[1]. This can be explained by the small magnitude of s^2/f .

1.1.5 Alternate forms

The power-law model for interatomic potentials is shown here for illustrative purposes, not because it is the most widely used or most accurate. The Morse potential,

$$U(d) = D \left(e^{-2\alpha(d-d_0)} - 2e^{-\alpha(d-d_0)} \right) \quad (1.26)$$

appears to be the best validated through experimental values of elastic modulus E , cohesive energy U_0 , thermal expansion α , and temperature dependence of elastic modulus $E(T)/E(0)$, at least for cubic metals, as described in Ref [2]. This potential also has competing long-ranged attractive and short-ranged repulsive terms, and will be explored in the Exercises.

1.2 Lattice dynamics: normal modes of the diatomic lattice

The interatomic potential model suggests that interatomic bonds are mostly like springs, keeping atoms at a fixed separation at equilibrium. The massive part of the atom is the ion core; the outer-shell valence electrons, with negligible mass, are the springs. To model *lattice dynamics*, the equations of motion for atoms in a solid, we can treat an array of masses connected to each other by springs.

If two atoms are bound together and initially displaced from their equilibrium spacing d_0 , they will oscillate about their equilibrium separation

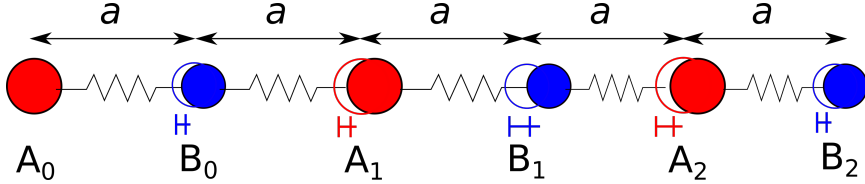


Figure 1.2: Illustration of diatomic model for lattice vibrations. Displacements are measured as A_i, B_i for atom A, B at site i . The illustration shows the longitudinal acoustic mode with wavelength $\lambda \simeq 6a$

with a frequency $\omega_0 = \sqrt{k/m}$, where the spring constant k is given by the interatomic potential in Equation 1.10 and m is the atomic mass. In a crystal, arbitrary motions can be described as linear combinations of the normal collective modes; we will calculate normal modes for the simplest example below.

1.2.1 Equation of motion

We will consider a 1-D crystal (on x) with two atoms, A and B , in the unit cell, as illustrated in Figure 1.2. A and B atoms are separated by a , and the structure is $A_0B_0A_1B_1A_2B_2\dots$, such that the lattice parameter is $2a$. Displacements from these positions will be zero at equilibrium.

We can consider displacements along any direction. The spring constants will be the same as what we have considered so far if the displacements are along \hat{x} , or if the displacements are longitudinal. There are also two possibilities for transverse modes, with displacements along \hat{y} and along \hat{z} . The spring constants here are different, in principle, and longitudinal and transverse modes can then have different frequencies.

We can write the equation of motion for atom A_i in terms of nearest-neighbor interactions only, with B_{i-1} and B_i . We consider wavelike solutions for the displacements of A and B atoms at position i ,

$$A_i = A \exp j(kx_{A,i} - \omega t) \quad (1.27)$$

$$B_i = B \exp j(kx_{B,i} - \omega t) \quad (1.28)$$

where A and B are in principle complex vectors (with the direction giving the wave polarization.) Here the positions of the atoms are $x_{A,i} = 2i a$ and $x_{B,i} = (2i + 1) a$. For A atoms, Newton's law is

$$m_A \ddot{A}_i(t) = -k_{AB} (A_i - B_{i-1}) - k_{AB} (A_i - B_i) \quad (1.29)$$

Substituting in for the spatial dependence,

$$-\omega^2 m_A A e^{jk(2ia)} = -k_{AB} \left(A e^{jk(2ia)} - B e^{jk(2i-1)a} + A e^{jk(2ia)} - B e^{jk(2i+1)a} \right) \quad (1.30)$$

yielding for the dispersion relation $\omega(k)$

$$-\omega^2 A = -\frac{k_{AB}}{m_A} (2A - 2B \cos ka) \quad (1.31)$$

and for B atoms, similarly,

$$-\omega^2 B = -\frac{k_{AB}}{m_B} (2B - 2A \cos ka) \quad (1.32)$$

Defining an averaged resonant frequency ω_0 and a mass ratio η

$$\omega_0^2 \equiv \frac{k_{AB}}{\sqrt{m_A m_B}} \quad \eta \equiv \sqrt{\frac{m_A}{m_B}} \quad (1.33)$$

So the 2×2 eigenvalue equation is

$$0 = \begin{bmatrix} 1 - \eta (\omega^2 / \omega_0^2) / 2 & -\cos ka \\ -\cos ka & 1 - \eta^{-1} (\omega^2 / \omega_0^2) / 2 \end{bmatrix} \begin{bmatrix} A \\ B \end{bmatrix} \quad (1.34)$$

where solutions exist only for the determinant equal to zero:

$$(1 - \eta \omega^2 / (2\omega_0^2)) (1 - \eta^{-1} \omega^2 / (2\omega_0^2)) - \cos^2 ka = 0 \quad (1.35)$$

$$(\omega^2 / 2\omega_0^2)^2 - (\eta + \eta^{-1}) (\omega^2 / 2\omega_0^2) + (1 - \cos^2 ka) = 0 \quad (1.36)$$

$$\frac{\omega^2}{2\omega_0^2} = \left(\frac{\eta + \eta^{-1}}{2} \right) \pm \sqrt{\left(\frac{\eta + \eta^{-1}}{2} \right)^2 - \sin^2 ka} \quad (1.37)$$

This defines the dispersion relation for lattice vibrations $\omega(k)$. Here the *positive* root, at higher frequency, is the *optical* mode, and the *negative* root, at lower frequency, is the *acoustic* mode. The frequencies are so named because in the long-wavelength (low-k) limit, lattice vibrations can be excited by sound ($< 10^3 \text{s}^{-1}$) or light ($\sim 10^{15} \text{s}^{-1}$). Numerical solutions are shown in Figure 1.3. In the limit of equal masses $m_A = m_B$, $\eta = 1$, and the two modes are

$$\frac{\omega^2}{2\omega_0^2} = 1 \pm \cos ka \quad (1.38)$$

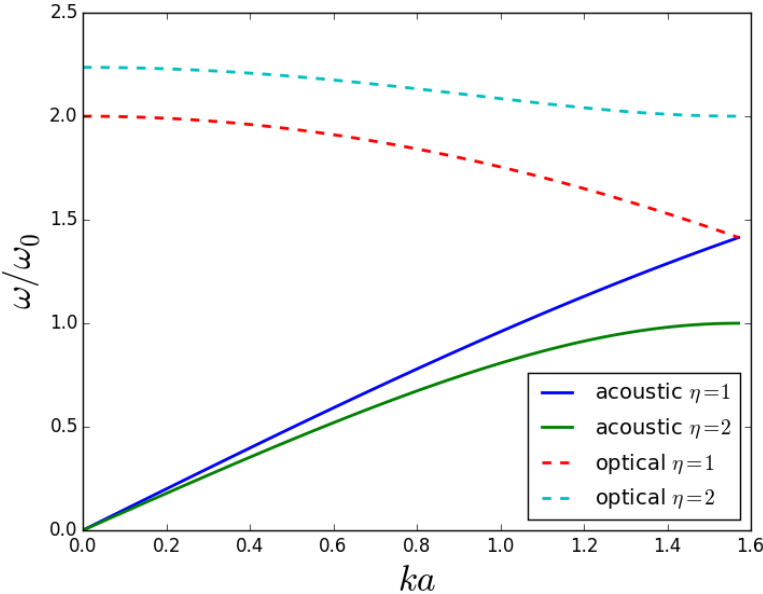


Figure 1.3: Phonon dispersion relation $\omega(k)$, diatomic model as pictured in Figure 1.2, for $\eta = 1$ ($m_A = m_B$) and $\eta = 2$ ($m_B = 2m_A$). Solid lines: acoustic modes. Dashed lines: optical modes.

For $ka \ll 1$, the modes are

$$\omega_- \simeq \omega_0 ka \quad \omega_+ \simeq \sqrt{2}\omega_0 \sqrt{2 - \frac{(ka)^2}{2}} \simeq 2\omega_0 \quad (1.39)$$

The former is known as the Debye approximation and the latter is known as the Einstein approximation. For the Debye approximation, the speed of sound is

$$\partial\omega/\partial k = v_m = \omega_0 a \quad (1.40)$$

, and then varies as the square root of the interatomic 'spring constant.' In Cu, for example, $v_m \simeq 5$ km/s for longitudinal mode, and roughly half that for the transverse mode. Taking $a \simeq 0.25$ nm, the resonant frequency for the bond is $\omega_0 \sim 20$ THz.

1.3 Debye model for heat capacity

Early experimental evidence for the role of lattice vibrations in heat absorption came from measurements of the temperature-dependent heat capacity $C_V(T)$. The Debye model (with dispersion $\omega = v_m k$) was successful in explaining the low-temperature limit, $C_V \simeq T^3$.

1.3.1 Derivation of Debye model

The allowed phonon modes are much the same as the allowed modes for free electrons, or for a vibrating string. In each Cartesian direction, there is one allowed mode per $\Delta k = \pi/L$, and as before,

$$k_n = \Delta k n \quad \Delta k = \frac{\pi}{L} \quad (1.41)$$

Also, we treat only the acoustic phonons, with $\omega = v_m k$, where v_m is the speed of sound, and

$$\omega_n = \frac{\pi}{L} v_m n \quad (1.42)$$

We can solve this problem like the total number of electrons below E_F . The k -space density of phonon modes is

$$D_{k^3} = \frac{3}{(\pi/L)^3} \quad (1.43)$$

where instead of two allowed spin states, we have three polarizations: one longitudinal (compression) and two transverse.

Particle representation; occupancy At this point, it is necessary to introduce the particle representation for lattice vibrations. Like electrons, lattice vibrations have fundamental, quantized values for energy, $E_n = \hbar\omega_n$. They are created when thermal energy is added to the system and annihilated when thermal energy is removed. Phonons are bosons; unlike electrons, they can all populate a single mode. Their thermal occupancy is described by the Bose-Einstein distribution,

$$f_{BE}(E) = \frac{1}{\exp(E - \mu)/k_B T - 1} \quad (1.44)$$

For particles which are not conserved, like phonons, the chemical potential can be taken as constant, zero for convenience:

$$f_p(E) = \frac{1}{\exp E/k_B T - 1} \quad (1.45)$$

which is the Planck distribution.

The assumption of $\mu = 0$ for non-conserved "particles," such as phonons (lattice vibrations) or photons (light), can be justified in the following way. Gradients in the chemical potential μ keep track of particle flow. Diffusive equilibrium of particle type i is reached when the chemical potential for that species, μ_i , is everywhere the same, and there is no gradient $\nabla\mu_i$ to drive diffusion. Phonons are more or less equivalent to heat absorbed by the lattice, as will be seen. The transport of heat is governed by thermal gradients ∇T , so there is no reason to introduce a separate quantity for their chemical potential.

The Debye temperature To quantify the excitation of lattice motion by heat, it will be convenient to define a temperature which sets the temperature or energy scale. It will take more energy to set the atoms into motion in some lattices than in others. If the bonding "springs" are very stiff, or if there are more atoms in a given volume, an vibration with a given amplitude stores more energy (which has to be absorbed from heat) than it does in a low-density solid with floppy bonds. The *Debye temperature* θ defines the energy scale (through $k_B\theta$) for the excitation.

To develop an expression for θ , we will make some counterfactual assumptions, and justify these later through our success in obtaining a convenient closed-form expression for the heat capacity C_V . Remember that θ is only a temperature scaling parameter so there is no real hazard in making these assumptions.

We will assume, counterfactually, that the phonons obey the Pauli exclusion principle. In this, we assume that each set of vibrational polarization and mode number (i.e. quantum numbers k_x , k_y , k_z for the phonon) can be occupied only singly by the phonon, and that the states fill from low energy (where they are completely occupied) to high energy (where they are completely empty). There will be a limit to the highest energy which can be occupied under these circumstances, given by the fact that there are only so many ways in which the solid can vibrate (a limit to the number of phonon modes.) The heat energy of the highest-energy lattice vibration under these assumptions is defined by the *Debye temperature* $k_B\theta$.

In reality, nothing prevents a single mode to be occupied by *all* the phonons, each "particle" increasing the vibrational amplitude by a tiny

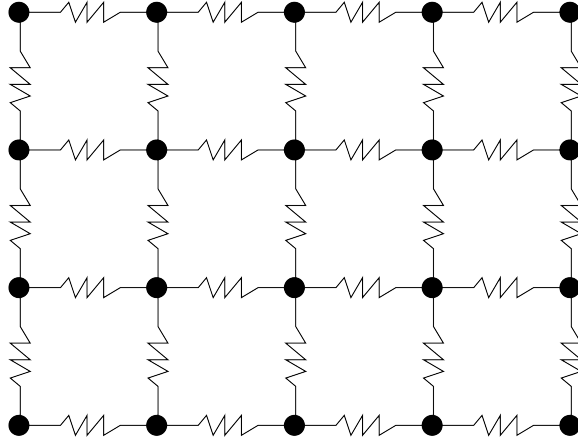


Figure 1.4: Debye model for crystal lattice: masses (nuclei) on springs (electrons).

amount. Creating an overpopulation of coherent phonons in the lowest-energy mode is nothing exotic; it is what happens when one plucks a guitar string!¹

We assume that all phonon states are occupied singly up to a 'cutoff' value of scalar wavenumber k , called the *Debye* wavenumber k_D ; beyond this, they are unoccupied. Because energy increases with scalar k , for $k > k_D$, if phonons were Fermions (obeying Pauli exclusion) at zero temperature, the states would be completely unoccupied. The total number of phonons excited, defined here as Q , *would be* (counterfactually)

$$Q = D_{k^3} \frac{1}{8} \frac{4\pi}{3} k_D^3 \quad (1.46)$$

where the factor $1/8$ comes in because we consider only the positive octant of wavenumbers; $\pm k_x$ define the same mode and cannot be double-counted. Substituting Eq 1.43, and taking $L^3 = V$ as the volume of the system, the total number of phonons will be

$$Q = \frac{V}{2\pi^2} k_D^3 \quad (1.47)$$

The higher is k_D , the larger will be the number Q of phonons excited. Alternatively, expressing k_D as an energy E , through $E = \hbar v_m k$,

¹It would be more remarkable if one cooled the guitar down, not driving it mechanically, and at a certain temperature, the string started to oscillate—this might be called a Bose-Einstein condensation of phonons.

$$Q(E) = \frac{V}{2\pi^2} \frac{1}{(\hbar v_m)^3} E^3 \quad (1.48)$$

There is a limit to Q given by the total number of possible mechanical normal modes in the system. N atoms with three polarizations support $3N$ normal modes. For example, for two atoms, one polarization, there are two normal modes: the "acoustic mode" (motion in the same direction) and the "optical mode" (moving in opposite directions.) This poses an upper limit on k_D . Taking $Q = 3N$:

$$3N = \frac{V}{2\pi^2} k_D^3 \quad (1.49)$$

The Debye k can be expressed in terms of the atomic number density $n_{at} = N/V$ as

$$k_D = (6\pi^2 n)^{1/3} \quad (1.50)$$

or in terms of the Debye frequency $\omega_D = v_m k_D$ and temperature $\hbar\omega_D = k_B\theta$,

$$\theta = \frac{\hbar v_m}{k_B} (6\pi^2 n_{at})^{1/3} \quad (1.51)$$

where n_{at} can be expressed as $n_{at}^{-1} = (6\pi^2)(\hbar v_m/k_B)^3 \theta^{-3}$.

Energy density of states: In terms of ω_D , the density of states can be expressed as

$$g_E(E) = \frac{\partial Q}{\partial E} \quad (1.52)$$

We can express Q in terms of energy as

$$Q = D_{k^3} \frac{\pi}{6} k_D^3 \quad (1.53)$$

$$Q = D_{k^3} \frac{\pi}{6} \left(\frac{E}{\hbar v_m} \right)^3 \quad (1.54)$$

$$g_E(E) = \frac{3V}{2\pi^2 \hbar^3 v_m^3} E^2 \quad (1.55)$$

Now the total energy for the system can be expressed as

$$U = \int_0^{k_B \theta} dE E f_p(E) g_E(E) \quad (1.56)$$

and per atom as

$$u \equiv \frac{U}{N} = \frac{3n^{-1}}{2\pi^2 \hbar^3 v_m^3} \int_0^{k_B \theta} dE \frac{E^3}{\exp E/\tau - 1} \quad (1.57)$$

Changing variables to $x \equiv E/\tau$, $E^3 = \tau^3 x^3$, $dE = \tau dx$,

$$u = \frac{3n_{at}^{-1}}{2\pi^2 \hbar^3 v_m^3} \tau^4 \int_0^{\theta/T} dx \frac{x^3}{e^x - 1} \quad (1.58)$$

$$u = \frac{3(6\pi^2)(\hbar v_m/k_B)^3 \theta^{-3}}{2\pi^2 \hbar^3 v_m^3} \tau^4 \int_0^{\theta/T} dx \frac{x^3}{e^x - 1} \quad (1.59)$$

$$u = 9 \frac{k_B T^4}{\theta^3} \int_0^{\theta/T} dx \frac{x^3}{e^x - 1} \quad (1.60)$$

Differentiating the upper limit of integration, we have for the heat capacity per atom $c_V \equiv C_V/N = (\partial u / \partial T)_V$,

$$c_V = 36k_B \left(\frac{T}{\theta} \right)^3 \int_0^{\theta/T} dx \frac{x^3}{e^x - 1} - 9 \frac{k_B T^4}{\theta^3} \left(\frac{\theta}{T^2} \right) \left(\frac{x^3}{e^x - 1} \right)_{x=\theta/T} \quad (1.61)$$

$$c_V = 36k_B \left(\frac{T}{\theta} \right)^3 \int_0^{\theta/T} dx \frac{x^3}{e^x - 1} - 9 \frac{k_B \theta}{T} \left(\frac{1}{e^{\theta/T} - 1} \right)_{x=\theta/T} \quad (1.62)$$

Equation 1.62 is plotted in Figure 1.5.

Low-temperature limit of heat capacity In the limit $T \ll \theta$, the upper limit of the integration can be expressed as infinity. From tables of integrals, $\int_0^\infty dx x^3 (e^{-x} - 1)^{-1} = \pi^4/15$

$$u = 9 \frac{k_B T^4}{\theta^3} \frac{\pi^4}{15} \quad (1.63)$$

$$c_V = \frac{12\pi^4}{5} k_B \left(\frac{T}{\theta} \right)^3 \quad T \ll \theta \quad (1.64)$$

This is the Debye T^3 law for low-temperature heat capacity, very important in the historical development of solid state.

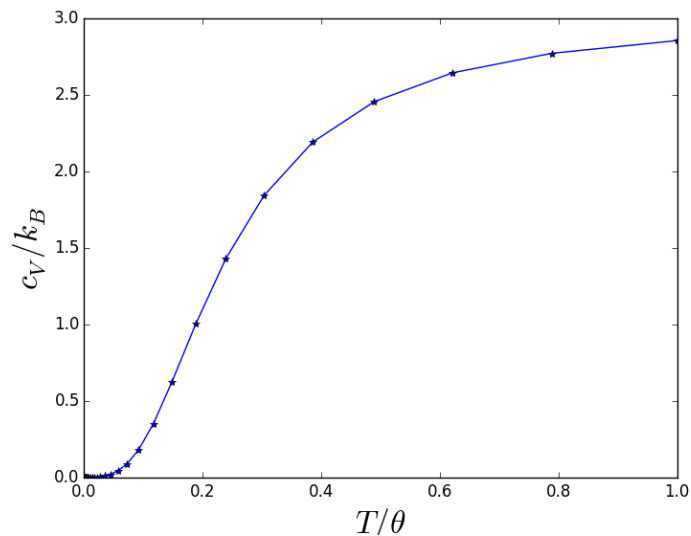


Figure 1.5: Temperature-dependent heat capacity per atom, c_V , in units of the Boltzmann constant, from the Debye model (Eq 1.62.) Temperature scale is normalized to the Debye temperature θ . Note the low-temperature variation as $(T/\theta)^3$ and the classical high-temperature limit of $3k_B$.

High-temperature limit For $T \gg \theta$, the integrand in Eq 1.60 can be approximated as $x^3/(1+x-1.) = x^2$, and the definite integral evaluates to $(\theta/T)^3/3$. Thus the high-temperature limit for the heat capacity per atom is

$$c_V = 3k_B \quad T \gg \theta \quad (1.65)$$

which is the result for an ideal gas. This result is known as the Dulong-Petit law.

1.3.2 Comparison with experiments

The agreement between the Debye theory and experimental heat capacities is remarkably good. The temperature-dependent heat capacity $C_V(T)$, measured from calorimetry and plotted as a function of reduced temperature T/θ is shown in Figure 1.6. The single fit parameter in these experiments is the Debye temperature θ . A universal temperature dependence is seen for diverse classes of materials: cubic metals, diamond cubic insulators, a hexagonal insulator and a cubic ionic compound (KCl). This is all as predicted by Eq 1.62, which holds irrespective of any details of the bonding.

Debye temperature and elasticity Next comes the question: is the Debye temperature simply a fitting parameter for heat capacity measurements, or can it be predicted? Recasting the Debye temperature, we see that it depends on two materials parameters which can be determined from independent experiments: the density ρ and the speed of sound v_m :

$$\theta = \frac{\hbar}{k_B} \left(6\pi^2 \frac{N_A \rho}{M} \right)^{1/3} v_m \quad (1.66)$$

where N_A is Avogadro's number and M is the molecular weight. The isotropic speed of sound can be extracted from tables of longitudinal and shear speeds, v_l and v_s , by

$$v_m = \left(\frac{1}{3} \left[\frac{2}{v_s^3} + \frac{1}{v_l^3} \right] \right)^{-1/3} \quad (1.67)$$

which are themselves functions of elastic moduli, as would be expected from $v_p = \omega/k$: a stiffer medium will allow a wave to propagate more quickly.

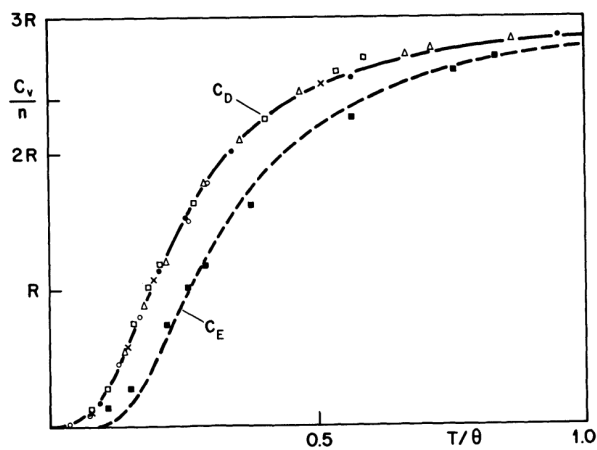


Fig.3.10. Einstein and Debye specific heat as a function of reduced temperature. θ is either the Einstein or the Debye temperature, depending on which curve is being examined. The Debye specific heat is compared with the observed specific heats of Ag(\bullet), $\theta_D = 215$ K; Al(Δ), $\theta_D = 394$ K; C(diamond)(\square), $\theta_D = 1860$ K; $\text{Al}_2\text{O}_3(\circ)$, $\theta_D = 937$ K; KC1(x), $\theta_D = 227$ K; and the Einstein specific heat with C(diamond) (\blacksquare) $\theta_E = 1320$ K, [3.11,12]

Figure 1.6: Experimental heat capacities for a range of different materials.
From Ref [3] p.79

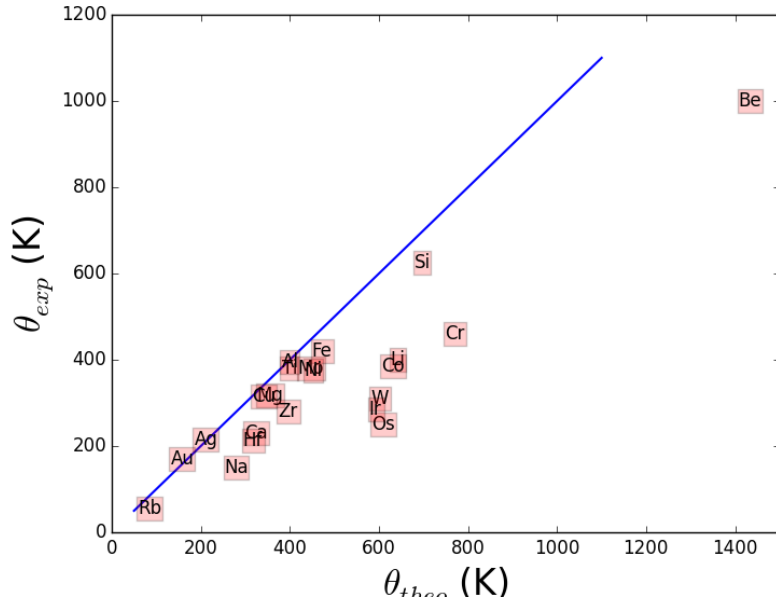


Figure 1.7: Experimental Debye temperatures for 22 elemental solids, measured by calorimetry, as a function of values predicted from ultrasonic measurements of the speed of sound v_m using Eq 1.66. Debye temperatures tabulated in Ref [3], speeds of sound. Line indicates perfect agreement. Theoretical values generally predict or overestimate θ .

For illustrative purposes, I compare the experimental Debye temperatures, measured by calorimetry, with those predicted from elasticity, estimated (crudely) through Eq 1.67. The longitudinal and shear speeds of sound have been measured through ultrasonic transmission; I have (inadvisably) taken values of v_l and v_s for different solids from Wikipedia. Combining these values of v_l and v_s , with tabulated densities and atomic weights (*ibid*), with measured Debye temperatures θ from heat capacity as tabulated in [3], we can determine how predictive the theory is. The comparison for several elemental solids is presented in Figure 1.7. We see that the Debye temperatures are predicted reasonably well for these materials from the speeds of sound; the error in many cases results from incomplete measurements of v_l and v_s .

In cases where the speeds of sound have been calculated accurately from suitably averaged single-crystal anisotropy elastic moduli, the agreement is

Crystal	θ_{exp} (K)	v_l (km/s)	v_s (km/s)	ρ (g cm $^{-3}$)	M	θ/θ_{theo}
Ag	215	3.51	1.61	10.49	107.88	0.97

Table 1.1: Comparison of experimental Debye temperature from calorimetry with that calculated from longitudinal and shear speeds of sound v_l and v_s , including density ρ , for Ag.

much better than that shown here. Better than 10% agreement between 'mechanical' (from elastic moduli) and 'thermal' (from calorimetry) Debye temperatures has been found across a set of 60 polycrystalline solids of various types in Ref [4].

Exercises

1. One widely used empirical potential for the energy between two atoms with spacing d is the Morse potential, written as

$$U(d) = D \left(e^{-2\alpha(d-d_0)} - 2e^{-\alpha(d-d_0)} \right) \quad (1.68)$$

Sample values for Cu are $D = 343$ meV, $\alpha = 1.36 \text{ \AA}^{-1}$. For a diatomic bond of Cu_2 ,

- (a) Calculate the "spring constant" f , assuming an interatomic spacing of 0.209 nm.
- (b) Calculate the anharmonic coefficient g and parameter s
- (c) Calculate the coefficient of thermal expansion α for the bond
- (d) Estimate the ratio of elastic modulus at room temperature to that at zero temperature, $E(300K)/E(0K)$ considering one bond only.

For (FCC) Cu, with lattice parameter 0.36nm,

- (e) calculate the cohesive energy. For simplicity, consider only nearest-neighbor interactions (12 in the crystal).
2. Determine the polarization character of the optical and acoustic modes of the diatomic lattice by backsubstituting the eigenfrequencies ω in Eq 1.39 into the eigenvalue Equation 1.34, and solving for A and B . How do the atoms move?
3. Derive the dispersion relation for a monatomic lattice: A atoms only, separated by a lattice spacing of a , with spring constant k . Using the Bloch theorem, show (graphically) that the result is identical to that for the diatomic lattice with $m_A = m_B$ shown in Figure 1.3. *Hint:* the first Brillouin zone boundary for a lattice with lattice parameter $2a$ is at half the value of that for a lattice with lattice parameter a , and the reduced representation for one is in the extended representation for the other.
4. Will there be a relationship between cohesive energy and the Debye temperature, according to the power law model for potentials? Assume two scenarios: one where the A and B coefficients change by a common factor, and one where they do not. What do you expect? Make a table of cohesive energies (in eV/atom) and Debye temperatures θ (in

K) for Si, Ge, Sn; Cu, Ag, Au and rationalize your results. (Debye temperatures are available as an e-book on clio for ref. [3]; find cohesive energies on www.springermaterials.com or wikipedia.)

5. Calculate the Debye temperature for a fictitious FCC crystal with 100 g/mol, lattice parameter of 0.4 nm, and isotropic speed of sound 5 km/s.
6. Derive the low-temperature limit of heat capacity, $C_V(T)$, for a two-dimensional lattice, in terms of the Debye temperature θ and the Boltzmann constant k_B only.

Bibliography

- [1] J.R. Neighbors and G.A. Alers. “Elastic constants of silver and gold”. In: *Phys. Rev.* 111 (3 1958), pp. 707–712.
- [2] L.A. Girifalco and V.G. Weizer. “Application of the Morse potential to cubic metals”. In: *Physical Review* 114 (1959), pp. 687–690.
- [3] P. Brüesch. *Phonons: Theory and Experiment I. Lattice dynamics and models of interatomic forces*. Springer Verlag, 1982.
- [4] Orson L. Anderson. “A simplified method for calculating the Debye temperature from elastic constants”. In: *Journal of Physics and Chemistry of Solids* 24 (1963), pp. 909–917.

Chapter 2

Stress

In this chapter, we will introduce the concept of *stress* in a solid, derive constitutive equations for time-dependent and equilibrium stress distributions in solids, and apply the equations to some common material shapes.

2.1 Types of forces on a volume element

There are two types of forces which can be exerted on a differential volume element of a solid, dV :

- **Body forces** exerted per unit **volume** of dV . These exert a force per unit volume of the material, essentially on each atom contained within the element. Examples include the gravitational force, centrifugal forces, or diamagnetic forces. Body forces will be denoted as \mathbf{g} ; body torques will be denoted as \mathbf{G} .
- **Surface tractions** exerted per unit **area** of dV . These come from the elastic continuum, and are nearest-neighbor interactions with other atoms. Atoms just outside the volume element *pull out* the atoms just inside the volume element when the element is under *tensile* stress. Atoms just outside the volume element *push in* the atoms at the boundary of a differential volume element when the element is under *compressive* stress. These forces per unit area are denoted as σ .

For most of our discussion, we will focus on the latter **surface tractions**, called **stresses** σ .

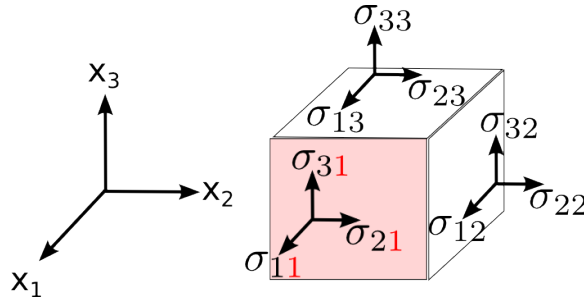


Figure 2.1: *Left:* Cartesian axes x_i ; *right:* stresses. Highlighted: forces acting on face with normal x_1 (boundary in yz plane).

2.2 The stress matrix

We will take our Cartesian coordinate system as (x_1, x_2, x_3) , where x_i stand in for the typical x, y, z , as shown in Figure 2.1, left. The position O is the origin. Defining axes in this way allows us to generalize results more easily: no direction x_i is privileged.

The stress which acts on the element $dV = \delta x_1 \delta x_2 \delta x_3$ is accounted for using two indices. The force per unit area

$$F = \sigma(\delta x)^2 \quad (2.1)$$

is exerted **on** the element face with normal Ox_j , **by** surrounding material, **in** the direction Ox_i . This defines the stress element σ_{ij} . So

$\sigma_{ij} :$	force direction: \mathbf{i} ,	face normal: \mathbf{j}	(2.2)
-----------------	---------------------------------	---------------------------	-------

In Figure 2.1, the forces acting on the face with normal x_1 are highlighted.

Normal and shear stresses There are two types of stresses.

- **Normal stresses** have forces per unit area exerted along the face normal, with $i = j$. So for σ_{11} , the force from the surrounding atoms acts in the direction x_1 , normal to the boundary of the element in that direction. Similarly, σ_{22}, σ_{33} go along the x_2 and x_3 axes respectively.
- **Shear stresses** have $i \neq j$. The forces from the surrounding atoms exert forces in the plane of the element boundary. σ_{12} then describes a force from surrounding atoms, acting in the x direction, on the face in the xz plane, with normal in the positive y direction.

The sign of the force is implicit in the definition. For an element in tension, $\sigma_{ii} > 0$, the force from the surrounding atoms pulls out the atoms within the element. The force is exerted in the $+x$ direction for the face with normal $+x$, but for the opposite face, with normal $-x$, the force points in the opposite direction, $-x$. The sign convention means that the sense of the force reverses at opposite boundaries. For shear stresses, it is less obvious, but also true that the force direction for a given value of σ_{ij} will reverse on opposite sides of the element.

2.3 Requirements for equilibrium

Typically, we are interested in the forces acting on bodies in mechanical equilibrium. Mechanical equilibrium implies that all elements within the solid are not accelerating, so there is no net force or torque upon each differential element dV .

2.3.1 Forces

We can write Newton's law for a differential cubic element, δx on a side, located at $\mathbf{x} = x_1 \hat{\mathbf{x}}_1 + x_2 \hat{\mathbf{x}}_2 + x_3 \hat{\mathbf{x}}_3$. For total forces in the x_3 direction, for example, there are six tractions (two from opposite faces) for the three stresses. First we will write the two from the normal stresses and the body force in the x_3 direction, g_3 ,

$$m\ddot{u}_3 = \sigma_{33}(\mathbf{x} + \frac{\delta x}{2} \hat{\mathbf{x}}_3)(\delta x)^2 - \sigma_{33}(\mathbf{x} - \frac{\delta x}{2} \hat{\mathbf{x}}_3)(\delta x)^2 + g_3 (\delta x)^3 \dots \quad (2.3)$$

where m is the mass of the element, u_3 is the displacement of the element in the x_3 direction, and g_3 is a **force per unit volume**. If we are interested in the force due to gravity, acting here on $\hat{\mathbf{z}}$, we would have

$$g_3 = -\rho g \quad (2.4)$$

where $g = 9.8 \text{ m/s}^2$ is the acceleration due to gravity and ρ is the density. There are four more forces from the shear stresses,

$$\dots + \sigma_{32}(\mathbf{x} + \frac{\delta x}{2} \hat{\mathbf{x}}_2)(\delta x)^2 - \sigma_{32}(\mathbf{x} - \frac{\delta x}{2} \hat{\mathbf{x}}_2)(\delta x)^2 + \\ \sigma_{31}(\mathbf{x} + \frac{\delta x}{2} \hat{\mathbf{x}}_1)(\delta x)^2 - \sigma_{31}(\mathbf{x} - \frac{\delta x}{2} \hat{\mathbf{x}}_1)(\delta x)^2$$

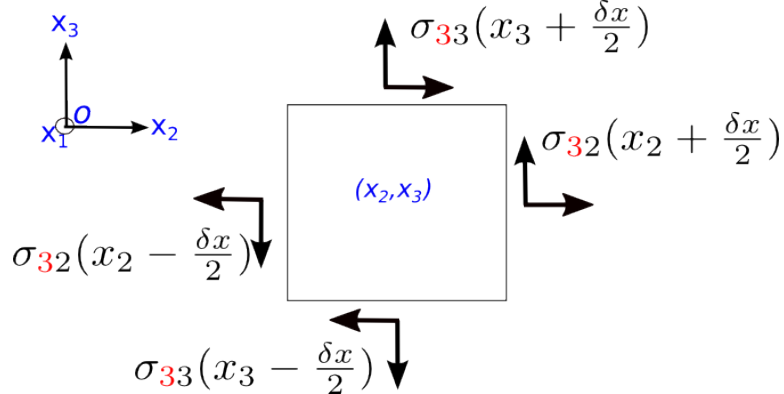


Figure 2.2: Differential element, forces in x_3 . (Two other tractions σ_{31} are not shown.)

If we Taylor expand the stress for small δx , we can write $\sigma(x + \delta x/2) \simeq \sigma(x) + (\delta\sigma/\delta x)\delta x/2$. Recognizing the density as $\rho = m/(\delta x)^3$, we then have

$$\rho \ddot{u}_3 = \frac{\partial \sigma_{31}}{\partial x_1} + \frac{\partial \sigma_{32}}{\partial x_2} + \frac{\partial \sigma_{33}}{\partial x_3} + g_3 \quad (2.5)$$

Using **dummy suffix notation**, a repeated index j implies a sum over $j = 1 \dots 3$; e.g. a dot product for two vectors \mathbf{u} and \mathbf{v} could be written $u_j v_j$. The equilibrium for forces in x_1 can then be written

$$\frac{\partial \sigma_{3j}}{\partial x_j} + g_3 = \rho \ddot{u}_3 \quad (2.6)$$

and now, generalizing to a force in the direction x_i ,

$$\boxed{\rho \ddot{u}_i = \frac{\partial \sigma_{ij}}{\partial x_j} + g_i} \quad (2.7)$$

This is *Cauchy's equation of motion* for deformation. For mechanical equilibrium, $\ddot{u} = 0$, so

$$\boxed{0 = \frac{\partial \sigma_{ij}}{\partial x_j} + g_i \quad (\text{equilibrium})} \quad (2.8)$$

2.3.2 Torques

We can now consider the torques on the element. For a net torque about axis x_i , there will be an angular acceleration about that axis $\ddot{\theta}_i$, given through the moment of inertia about that axis I_i ,

$$\tau_i = I_i \ddot{\theta}_i \quad (2.9)$$

Only the shear tractions will give a torque; the normal tractions will not, since those forces act through the center of the element. For torques about axis x_1 ,

$$\tau_1 = I_1 \ddot{\theta}_1 \quad (2.10)$$

where some review of the *moment of inertia* is in order. The moment of inertia is defined as

we can write the moment of inertia of a cube with side length a , $I = ma^2/6$ (see Eq A.10), and evaluate the torques. Here, in the Taylor expansion, the differentials drop out:

$$(\sigma_{32} - \sigma_{23} + G_1)(\delta x)^3 = \ddot{\theta}_1 \frac{\rho}{6} (\delta x)^5 \quad (2.11)$$

According to this equation, in the limit where $\delta x \rightarrow 0$ (and δx is an arbitrary choice, as long as it is small enough), if the left hand side is nonzero, the angular acceleration will have to increase as $(\delta x)^{-2}$. That cannot be allowed, so in the general case of nonzero body torques,

$$\begin{aligned} \sigma_{32} - \sigma_{23} + G_1 &= 0 \\ \sigma_{13} - \sigma_{31} + G_2 &= 0 \\ \sigma_{21} - \sigma_{12} + G_3 &= 0 \end{aligned}$$

Body torques are present only in some very special cases. A hard ferromagnet experiences a body torque in a strong applied magnetic field H as $\mathbf{G} = -\mu_0 \mathbf{M} \times \mathbf{H}$. However, this is quite rare, and we can write in the absence of body torques,

$$\boxed{\sigma_{ij} = \sigma_{ji}} \quad (2.12)$$

valid for $G_i = 0$, but general for any angular acceleration.

2.4 Stress matrix

We can then arrange the nine values of stress in a 3×3 matrix form,

$$(\sigma) = \begin{bmatrix} \sigma_{11} & \sigma_{12} & \sigma_{13} \\ \sigma_{21} & \sigma_{22} & \sigma_{23} \\ \sigma_{31} & \sigma_{32} & \sigma_{33} \end{bmatrix} = \begin{bmatrix} \sigma_{11} & \sigma_{12} & \sigma_{13} \\ \boldsymbol{\sigma}_{12} & \sigma_{22} & \sigma_{23} \\ \boldsymbol{\sigma}_{13} & \boldsymbol{\sigma}_{23} & \sigma_{33} \end{bmatrix} \quad (2.13)$$

of which only six values are independent. The stress matrix is symmetric.

2.5 Application: beam theory

Beams, which are long in one dimension, short in another, and bend slightly about the orthogonal axis, are a common structural element. *Bernoulli-Euler beam theory* expresses the radius of curvature R of the beam in terms of its bending moment M and area moment of inertia about the z -axis I_z . All aspects of this theory can be derived straightforwardly from Eq 2.41, as will be shown. The expressions found are widely used in civil and mechanical engineering.

2.5.1 Curvature

We will consider a rectangular (prismatic) beam with height profile $y = y(x)$. The beam is long in the x direction and thin in the y direction. For simplicity, we will consider a beam with constant cross-sectional area $A = Wh$, where h is the beam height in y and W is the width in z . The beam may be supported on the surfaces with normal on $\pm\hat{x}$, but is assumed traction-free on the $\pm\hat{y}, \pm\hat{z}$ surfaces.

We assume that the beam develops some curvature in the xy plane, as shown in Figure 2.3. If for example the beam is clamped on one end, at $x = 0$, and pushed downwards in $-y$ on the other end, at $x = L$, the beam profile $y = y(x)$ will be curved. For small displacements, the radius of curvature R is given by the reciprocal of the curvature,

$$R^{-1} \simeq \frac{\partial^2 y}{\partial x^2} \quad (2.14)$$

Purely due to geometry, the curvature dictates that parts of the beam will be in compression and parts in tension, with normal strain along the x -direction, ε_{11} , nonzero. For positive curvature, the top of the beam ($+y$) will compressed, and the bottom of the beam ($-y$) will be expanded. There will be a normal strain along the beam length,

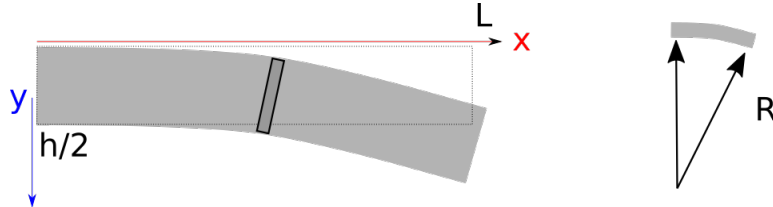


Figure 2.3: Beam supported at left end ($x = 0$), length L in x , height h in y , width W in z (not shown). *Right:* far view, radius of curvature R .

$$\varepsilon_{11} = -\frac{y}{R} \quad (2.15)$$

where y is the distance away from the *neutral axis*, a height in the beam at which $\varepsilon_{11} = 0$. We can guess that such a point must exist because the normal strain changes in sign as a function of y . The response is assumed proportional because the deformations are small. The neutral axis position will be a height Δ above the bottom of the beam.

We assume further that the normal strains in bending are created by normal stresses. This is intuitive enough but can be proven.¹ Applying the Young's modulus to the strain, we have for the stress

$$\sigma_1 = -E \frac{y}{R} \quad (2.16)$$

as illustrated in Figure 2.4, a).

2.5.2 Translational equilibrium

The tractions at the $x = 0$ and $x = L$ surfaces can have force components in both x and y ; z forces are neglected. Thus both σ_{xy} and σ_{xx} are nonzero. There can be no *net* forces in the \hat{x} direction because there are no body forces g_1 and the beam is at equilibrium in \hat{x} . Thus

$$F_x = 0 \quad (2.17)$$

$$F_x = W \int_{-\Delta}^{h-\Delta} dy \sigma_1(y) = 0 \quad (2.18)$$

¹In the sum $\epsilon_1 = s_{1j}\sigma_j$, recall that s_{14}, s_{15} , are zero cubic or isotropic materials: shear cannot create an elongation. Because the surfaces facing \hat{y} and \hat{z} are traction-free and small in dimension, the normal stresses $\sigma_2 \simeq \sigma_3 \simeq 0$. Thus we have only a single component to the ϵ_1 , with $s_{11} = 1/E$.

For a beam with one axis of curvature, about \hat{z} , we can consider that there is no stress gradient along the axis of curvature, or in z , but that there exists a nonzero stress gradient in y , so $\sigma(y, z) = \sigma(y)$ only. Substituting in Eq 2.16 for $\sigma_1(y')$,

$$-\frac{E}{R}W \int_{-\Delta}^{h-\Delta} dy y = 0 \quad (2.19)$$

which tells us that the neutral axis must be at the midpoint of the beam, $\Delta = h/2$. Net forces in \hat{y} for each differential length element Δx will be nonzero when we consider beam vibrations in \hat{y} , with accelerations in \hat{y} . We neglect normal stresses in \hat{y} , $\sigma_2 \simeq 0$: no tractions are applied on the $\pm\hat{y}$ -facing surfaces, so $\sigma_2 = 0$ at the surfaces, and the beam is considered to be thin enough in y that no substantial values of σ_2 can build up in the interior.

2.5.3 Rotational equilibrium and bending moments

The forces in \hat{y} therefore have to come from shear stresses, $\sigma_{12}(y) \neq 0$. To determine the shear, we must consider rotational equilibrium of the differential length element δx . A differential volume element of the beam $A\delta x$, where the cross-sectional area $A \simeq Wh$, does rotate about \hat{z} . A nonzero torque τ_z will be required to change its angular velocity according to its mass moment of inertia ζ_z (See Section A),

$$\tau_z = \zeta_z \ddot{\theta}_3 \quad (2.20)$$

but we assume that the mass moment of inertia in z , ζ_z , is negligibly small, such that there is no rotational moment of inertia. As we will see, $\zeta_z \sim h^3$, and so is very small for thin plates. This thin-plate assumption is one of the key assumptions of B-E theory. Therefore, rather than a dynamic equation, we have the equilibrium expression that net torques about \hat{z} are zero.

Torques act through stresses exerted at the interior faces at x and $x + \Delta x$. We can distinguish between two contributions, due to normal stresses σ_{11} and to shear stresses σ_{12} . The torques from normal stresses can be expressed through *bending moments* M , and given as τ_1 and τ_2 for the contributions from the two interior surfaces. The torques from shear stresses are designated τ_3 . All three sum to give zero torque.

For the normal stress contributions, we define the *bending moment* M at any point to be the integrated torque τ , where the differential torque for an interior area element is $\delta\tau = \mathbf{r} \times \delta\mathbf{F}(y)$:

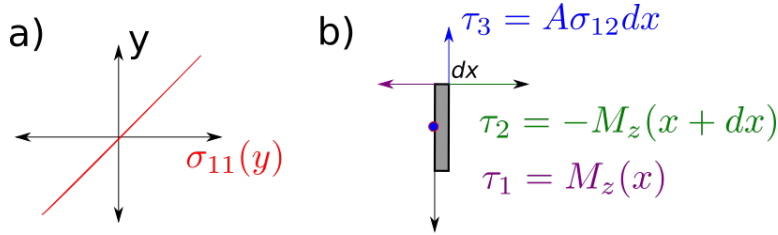


Figure 2.4: a): Stress profile $\sigma_{11}(y)$ under bending as shown in Figure 2.3.
b): Torques acting on the differential length element x to $x+dx$ of the beam shown in Figure 2.3.

$$M_z(x) = - \int_{-\Delta}^{h-\Delta} y \delta F_x(x) \quad (2.21)$$

For this interior differential element at x , defined to $x + \Delta x$, a tensile stress ($\sigma_{xx} > 0$) is a force directed in $-\hat{x}$

$$M_z(x) = W \int_{-\Delta}^{h-\Delta} dy y \sigma_{11}(x, y) \quad (2.22)$$

Substituting in Eq 2.22 for the normal stress from the bending,

$$M_z(x) = -\frac{E}{\rho(x)} W \int_{-\Delta}^{h-\Delta} dy y^2 \quad (2.23)$$

The integral is the area moment of inertia about the z-axis, I_z for the differential element Δx .

$$I_z \equiv \int_{-\Delta}^{h-\Delta} dA y^2 \quad (2.24)$$

where dA is the differential cross-sectional area element $dy dz$; replacing the integration in z by W ,

$$I_z = W \int_{-\Delta}^{h-\Delta} dy y^2 \quad (2.25)$$

For a rectangular beam with dimensions W on z and h on y , the quantity A/I_z is (see Eq A.4 of Section A),

$$\frac{A}{I_z} = \frac{\int dA}{\int_{-h/2}^{h/2} y^2 dA} = \frac{Wh}{W \left(\int_{-h/2}^{h/2} y^2 dy \right)} = \frac{12}{h^2} \quad (2.26)$$

so the equation can be rewritten as

$$M_z = -\frac{E}{R} I_z \quad (2.27)$$

$$M_z = -EI_z \left(\frac{\partial^2 y}{\partial x^2} \right) \quad (2.28)$$

or

$$\boxed{\frac{\partial^2 y}{\partial x^2} = -\frac{M_z}{EI_z}} \quad (2.29)$$

i.e., the curvature increases proportionally with the bending moment, as one might guess. The beam resists curvature with larger moments of inertia and larger elastic moduli.

We can also see that if curvature varies along the beam, i.e. is a function of x , as would be the case for e.g. a sinusoidal profile, it implies a variable bending moment M and a torque which depends on x . Torques M will then not be equal in magnitude at x and $x + \delta x$. We first consider the torque on the face at x . The forces for positive σ_{11} (tension) are in $-\hat{x}$, so the moment is positive. Designating this torque as τ_1 ,

$$\tau_1 = M_z(x) \quad (2.30)$$

The torque from the face at $x + \delta x$ is oppositely directed, because the normal stress has a force which changes sign with the direction of the normal; designating this as τ_2 ,

$$\tau_2 = -M_z(x + \delta x) = -M_z(x) - \frac{\partial M_z(x)}{\partial x} \delta x \quad (2.31)$$

thus the net torque from the bending moment is

$$\tau_1 + \tau_2 = -\frac{\partial M_z(x)}{\partial x} \delta x \quad (2.32)$$

which is nonzero only in the case that the curvature $\partial^2 y / \partial x^2$ is not constant in x , i.e., that the third derivative is nonvanishing. These two torques are illustrated in Figure 2.4, b).

Calculating the torque τ_3 , due to shear stresses σ_{12} , requires an additional identity. The shear force in \hat{y} at $x + \delta x$, over area A , is $F_y = \sigma_{xy}(x + \delta x)A$, creating a torque $\sigma_{xy}A\delta x$. Because we took the fulcrum at x , there is no torque from the opposite face at x . Assuming that the shear stress σ_{12} is independent of y

$$\tau_3 = A\sigma_{12}\delta x \quad (2.33)$$

This is justified through our assumption that the beam is thinner than it is long: $h \ll L$. Summing up torques $\tau_1 + \tau_2 + \tau_3 = 0$ at equilibrium,

$$A\sigma_{xy}\delta x - \frac{\partial M_z}{\partial x}\delta x = 0 \quad (2.34)$$

so at equilibrium, the first x -derivative of the bending moment is

$$\boxed{\frac{\partial M_z}{\partial x} = A\sigma_{xy}} \quad (2.35)$$

and the second, for cross-sectional area independent of length, is

$$\boxed{\frac{\partial^2 M_z}{\partial x^2} = A \frac{\partial \sigma_{xy}}{\partial x}} \quad A \neq A(x) \quad (2.36)$$

To relate stresses to the beam profile, take the x -derivative of Eq 2.29, again assuming that the cross-section properties, here the moments of inertia, do not change:

$$\left(\frac{\partial^2 y}{\partial x^2} \right) = -\frac{M_z}{EI_z} \quad \rightarrow \quad \left(\frac{\partial^3 y}{\partial x^3} \right) = -\frac{1}{EI_z} \frac{\partial M_z}{\partial x} \quad (I_z \neq I_z(x)) \quad (2.37)$$

rearranging,

$$\left(\frac{\partial M_z}{\partial x} \right) = -EI_z \left(\frac{\partial^3 y}{\partial x^3} \right) \quad (2.38)$$

and substituting the shear stress for the moment derivative, from Eq 2.35,

$$\boxed{A\sigma_{xy} = -EI_z \left(\frac{\partial^3 y}{\partial x^3} \right)} \quad (2.39)$$

rearranged, again assuming uniform cross-sectional area, and taking the x -derivative of the shear:

$$\boxed{\frac{\partial \sigma_{xy}}{\partial x} = -\frac{EI_z}{A} \left(\frac{\partial^4 y}{\partial x^4} \right)} \quad (2.40)$$

These identities hold for the assumptions made: small deformation, thin beam / negligible rotational moment of inertia.

Equilibrium under gravity The equilibrium expression, for forces in the y -direction, will be

$$0 = \frac{\partial \sigma_{yx}}{\partial x} + \frac{\partial \sigma_{yy}}{\partial y} + g_2 \quad (2.41)$$

Since the normal stresses in y are zero,

$$0 = \frac{\partial \sigma_{yx}}{\partial x} + g_y \quad (2.42)$$

Substituting in from Eq 2.40,

$$0 = -\frac{EI_z}{A} \left(\frac{\partial^4 y}{\partial x^4} \right) + g_y \quad (2.43)$$

$$\left(\frac{\partial^4 y}{\partial x^4} \right) = -\frac{A}{EI_z} \rho g \quad (2.44)$$

where g is the acceleration due to gravity on $-\hat{y}$. Assume that the beam is supported at the left end, at $x = 0$, with some very strong glue along the $-x$ face. Because it will be held straight at this point, its slope will be zero,

$$\left(\frac{\partial y(0)}{\partial x} \right) = 0 \quad (2.45)$$

At the wall, the (positive) moment about \hat{z} , M_z , will be equal and opposite to the negative moment from gravity, $M_z(0) = +m|g|L/2$, so

$$\left(\frac{\partial^2 y(0)}{\partial x^2} \right) = -\frac{1}{EI_z} M_z = -\frac{1}{EI_z} g \frac{L}{2} \rho V \quad (2.46)$$

where V is the beam volume $V = LWh$. The shear force at the left edge is what holds the beam up. Note that for the outward face on $-\hat{x}$, a positive shear has a force exerted in $-\hat{y}$, so the sign of σ_{xy} is negative.

$$A\sigma_{xy}(0) = -\rho LWh \quad (2.47)$$

but from Eq 2.39, the shear stress at this point is related to the third derivative of the profile

$$-EI_z \left(\frac{\partial^3 y(0)}{\partial x^3} \right) = -\rho Lwh \quad (2.48)$$

With all these constraints, the beam will take the profile

$$y(x) = y_2(0)x^2 + y_3(0)x^3 + y_4(0)x^4 \quad (2.49)$$

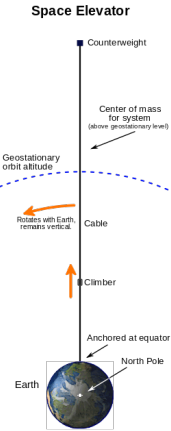


Figure 2.5: Space elevator diagram, copied from Wikipedia.

Exercises

1. Consider a solid cylinder, radius R , length l , density ρ standing up on its end, so that its total height (in x_3) above the pavement is l . Assume normal stresses only. Derive an expression for the stress in the material as a function of x_3 , and plot $\sigma_{33}(x_3)$. How tall can a solid column of concrete ($\rho = 2 \text{ g/cm}^3$) be made before the maximum shear stress exceeds the critical shear stress for fracture, $\tau_c = 10 \text{ MPa}$? Take $\sigma_{33} \sim \tau_{max}$ at fracture. (Recall that the total forces exerted on the body have to sum to zero.)
2. Consider a small sphere of NdFeB permanent magnet material in a large, uniform, superconducting magnetic field of 10 T. If its magnetization \mathbf{M} is initially orthogonal to the applied field $\mu_0\mathbf{H}$ when the field is (instantaneously) turned on, does the sphere shatter? Take $\tau_c = 50 \text{ MPa}$ and $\mu_0 M_s = 0.5 \text{ T}$
3. There is a longstanding proposal for a *space elevator*, as pictured in Figure 2.5. If a mass M can be attached to a long cable, length l , and $l \gg R$, where R is the radius of the earth, gravity is less strong than the centrifugal force, the cable might be supported. 1) Assume that there is no counterweight ($M = 0$). For a cable density ρ , how long does the cable need to be for it to stand up (i.e. all sections in tension)? Estimate l/R for a density of $\rho = 2 \text{ g/cm}^3$, appropriate for carbon fiber. 2) Plot the stress in the cable, and calculate the

maximum stress.

Chapter 3

Principal axes of the stress tensor

We saw last time that the stress, σ_{ij} , can be represented in matrix form as

$$[\sigma] = \begin{bmatrix} \sigma_{11} & \color{red}{\sigma_{12}} & \color{red}{\sigma_{13}} \\ \color{blue}{\sigma_{12}} & \sigma_{22} & \color{red}{\sigma_{23}} \\ \color{blue}{\sigma_{13}} & \color{blue}{\sigma_{23}} & \sigma_{33} \end{bmatrix} \quad (3.1)$$

where the symmetric property of the matrix shown,

$$\sigma_{ij} = \sigma_{ji} \quad (3.2)$$

holds as long as no body torques are present ($G_i = 0$).

In this document, we will see how to choose coordinate axes for the (symmetric) stress such that it consists of normal stresses only. *Mohr's circle* gives a convenient, graphical method for this transformation in the special case where one of the normal stress axes is already known.

3.1 Properties of tensors

We will review some basic properties of tensors, making reference to the stress. The arguments are given in general form since we will encounter other tensors in the mechanical properties of materials. For elasticity, the strain tensor ε_{ij} and the stiffness tensor c_{ijkl} are important. 'Smart' mechanical properties such as piezoelectric effects also require tensor representation.

The stress matrix is symmetric for the (nearly) general case of $G_i = 0$, but apart from this restriction, the quantities σ_{ij} can take any value. There

are two properties which make the matrix (σ), itself just a collection of stresses σ_{ij} , a tensor [σ]:

- The tensor [σ] expresses a **linear relationship between two quantities**. For the stress, the two quantities are force exerted across a plane inside the medium, and the area of the plane in the medium.
- The tensor [σ] refers to a **physical property which exists in space**. Thus if the spatial coordinate system changes,

$$\mathbf{x}(\text{old}) \rightarrow \mathbf{x}'(\text{new}) \quad (3.3)$$

the stress tensor in the new coordinate system [σ'] represents the same stress, so its components σ'_{ij} have a definite relationship with the values in the old representation σ_{ij} .

3.1.1 Tensors express a linear relationship between two quantities

Consider that we have two physical quantities p and q . The quantities can each be (0-D) scalars p or q , (1-D) vectors \mathbf{p} or \mathbf{q} , (2-D) square matrices (p) or (q), or on to N -dimensional square arrays. A tensor [T] expresses a linear relationship between the two,

$$p = [T]q \quad (3.4)$$

so that p can be a proportional response to a stimulus q .

Generally, the dimension of p has to be equal to the dimension of [T] reduced by the dimension of q . If [T] is a matrix (2D), and q is a column vector (1D), p is a column vector (1D).

The classic example for a 2D (or *second rank*) tensor property is electrical conductivity, which relates two vectors, current density \mathbf{J} and applied electric field \mathbf{E}

$$\begin{bmatrix} J_1 \\ J_2 \\ J_3 \end{bmatrix} = \begin{bmatrix} \sigma_{11} & \sigma_{21} & \sigma_{31} \\ \sigma_{21} & \sigma_{22} & \sigma_{32} \\ \sigma_{31} & \sigma_{32} & \sigma_{33} \end{bmatrix} \begin{bmatrix} E_1 \\ E_2 \\ E_3 \end{bmatrix} \quad (3.5)$$

also asserted here to be symmetric ($\sigma_{ij} = \sigma_{ji}$, but σ in this context is electrical conductivity in $\Omega^{-1}m^{-1}$). Taking an individual component of the matrix multiplication, for the current along x_1 , $J_1 = \sigma_{11}E_1 + \sigma_{12}E_2 + \sigma_{13}E_3$. For something like graphite, which has a very high conductivity in the basal

plane but a very low conductivity normal to the basal planes, the current depends very strongly on the direction of the applied field \mathbf{E} ; taking x_3 as the plane-normal direction, σ_{33} is very small, for example. The electric field \mathbf{E} is the stimulus and the current density is the response \mathbf{J} .

This same matrix multiplication can be expressed in dummy suffix notation as

$$J_i = \sigma_{ij} E_j \quad (3.6)$$

where the repeated index j refers to a sum over $j = 1..3$. This notation has several advantages: it is compact, it does not make recourse to special fonts, and it shows explicitly the dimension of each of the quantities through the number of suffixes. The **rank** of a tensor is its dimension, so a scalar has rank 0, a vector p_i has rank 1, a matrix A_{ij} has rank 2, etc.

Both third-rank and fourth-rank tensors exist and describe physical behavior. The piezoelectric effect, relating electrical polarization \mathbf{P} to an applied stress $[\sigma]$, is described through a third-rank tensor d , through

$$P_i = d_{ijk} \sigma_{jk} \quad (3.7)$$

where d_{ijk} has $3^3 = 27$ components. Elastic compliance, relating stress ε and strain σ , is described through the fourth-rank tensor s ,

$$\epsilon_{ij} = s_{ijkl} \sigma_{kl} \quad (3.8)$$

where s_{ijkl} has $3^4 = 81$ components. For both d and s , the total number of independent components is reduced by crystal symmetry.

In all cases, for each component, there is a simple proportionality between each element of the response p and the stimulus q .

Linear relationship expressed by $[\sigma]$ Consider a differential element at a given location inside a medium under stress. We would like to know how much force \mathbf{F} is exerted across the surface area of this element, if it has surface area $\delta\mathbf{A} = dS\hat{\mathbf{n}}$, where $\hat{\mathbf{n}}$ is the surface normal and dS is the differential area. For the sign convention, the force is positive if the force is exerted *by* the material on the positive $\hat{\mathbf{n}}$ side *on* the material on the negative $\hat{\mathbf{n}}$ side. Under these conditions, in vector form, we have $\mathbf{F} = (\sigma)\mathbf{A}$, or

$$F_i = \sigma_{ij} n_j dS \quad (3.9)$$

3.1.2 Rules for coordinate transformations

Forward transformation: matrix (a) ('old' to 'new.')

We can define a matrix (a) for a transformation between two coordinate systems. Let \mathbf{x} denote the unit vectors $\hat{\mathbf{x}}_1, \hat{\mathbf{x}}_2, \hat{\mathbf{x}}_3$, which form the (orthonormal, unit vector) basis of the 'old' coordinate system, with $\hat{\mathbf{x}}_i \cdot \hat{\mathbf{x}}_j = \delta_{ij}$.¹ Let \mathbf{x}' denote the unit vectors for the 'new' coordinate system, $\hat{\mathbf{x}}'_1, \hat{\mathbf{x}}'_2, \hat{\mathbf{x}}'_3$. If we take a vector \mathbf{p} in the 'old' basis, it is

$$\mathbf{p} = p_1 \hat{\mathbf{x}}_1 + p_2 \hat{\mathbf{x}}_2 + p_3 \hat{\mathbf{x}}_3 \quad (3.10)$$

which we refer to as p_i . In the 'new' basis, it is

$$\mathbf{p}' = p'_1 \hat{\mathbf{x}}'_1 + p'_2 \hat{\mathbf{x}}'_2 + p'_3 \hat{\mathbf{x}}'_3 \quad (3.11)$$

which we refer to as p'_i . However, if the vector is a physical quantity, it exists in space independent of our definition of a coordinate system, so it must be the case that $\mathbf{p} = \mathbf{p}'$.

We can set up a matrix of cosine angles, (a), where the element a_{ij} is the cosine of the angle between new axis $\hat{\mathbf{x}}'_i$ and old axis $\hat{\mathbf{x}}_j$. In other words

$$a_{ij} = \hat{\mathbf{x}}'_i \cdot \hat{\mathbf{x}}_j \quad (3.12)$$

The vector in the old representation projects onto the vector in the new representation as

$$\begin{bmatrix} p'_1 \\ p'_2 \\ p'_3 \end{bmatrix} = \begin{bmatrix} a_{11} & a_{12} & a_{13} \\ a_{21} & a_{22} & a_{23} \\ a_{31} & a_{32} & a_{33} \end{bmatrix} \begin{bmatrix} p_1 \\ p_2 \\ p_3 \end{bmatrix} \quad (3.13)$$

or in dummy suffix notation,

$$p'_i = a_{ij} p_j \quad (3.14)$$

Where for the forward transformation, the indices are *close together*.

¹ δ_{ij} is the Kroenicker delta, $\delta_{ij} = 0$ for $i \neq j$, $\delta_{ij} = 1$ for $i = j$.

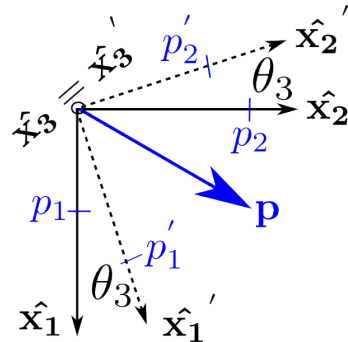


Figure 3.1: Illustration of a coordinate transformation by a single rotation of θ_3 about \hat{x}_3

Single rotation

For a single rotation, e.g. about \hat{x}_3 by θ_3 , the new coordinates are given by

$$\begin{bmatrix} p'_1 \\ p'_2 \\ p'_3 \end{bmatrix} = \begin{bmatrix} \cos \theta_3 & \sin \theta_3 & 0 \\ -\sin \theta_3 & \cos \theta_3 & 0 \\ 0 & 0 & 1 \end{bmatrix} \begin{bmatrix} p_1 \\ p_2 \\ p_3 \end{bmatrix} \quad \text{single rotation} \quad (3.15)$$

This form can be recognized by inspection of Figure 3.1; $a_{12}' = \sin \theta$ is just the projection of new axis \hat{x}_1' onto old axis \hat{x}_2 . Here, in this special case, the transformation matrix a_{ij} is antisymmetric, $a_{ij} = -a_{ji}$.

Example Consider a rotation $\theta_3 = \pi/4$, and vector $\mathbf{p} = 10\hat{x}_1 + 5\hat{x}_2$. What is p' ? The transformation matrix is

$$\begin{bmatrix} p'_1 \\ p'_2 \\ p'_3 \end{bmatrix} = \frac{1}{\sqrt{2}} \begin{bmatrix} 1 & 1 & 0 \\ -1 & 1 & 0 \\ 0 & 0 & 1 \end{bmatrix} \begin{bmatrix} 10 \\ 5 \\ 0 \end{bmatrix} \quad p' = \frac{1}{\sqrt{2}}[15, -5] \quad (3.16)$$

Arbitrary transform

In the most general case, \mathbf{x}' , and a_{ij} , are completely defined through three rotations of the 'old' coordinate system. Take $\hat{\mathbf{x}}'$ to be coincident with $\hat{\mathbf{x}}$ at first, then rotate \mathbf{x}' by θ_1 (right hand sense) about the old axis \hat{x}_1 , preserving $\hat{x}_1 = \hat{x}_1'$, then by θ_2 about \hat{x}_2 , then θ_3 about \hat{x}_3 .

However, if we examine an arbitrary sequence of rotations, $\theta_1, \theta_2, \theta_3$, three matrix multiplications,

$$\begin{bmatrix} p'_1 \\ p'_2 \\ p'_3 \end{bmatrix} = \begin{bmatrix} \cos \theta_3 & \sin \theta_3 & 0 \\ -\sin \theta_3 & \cos \theta_3 & 0 \\ 0 & 0 & 1 \end{bmatrix} \begin{bmatrix} \cos \theta_2 & 0 & \sin \theta_2 \\ 0 & 1 & 0 \\ -\sin \theta_2 & 0 & \cos \theta_2 \end{bmatrix} \begin{bmatrix} 1 & 0 & 0 \\ 0 & \cos \theta_1 & \sin \theta_1 \\ 0 & -\sin \theta_1 & \cos \theta_1 \end{bmatrix} \begin{bmatrix} p_1 \\ p_2 \\ p_3 \end{bmatrix}$$

define the matrix a . The result for (a) is, after some evaluation,

$(a) =$

$$\begin{bmatrix} \cos \theta_2 \cos \theta_3 & -\sin \theta_1 \sin \theta_2 \cos \theta_3 + \sin \theta_1 \sin \theta_3 & \cos \theta_1 \sin \theta_2 \cos \theta_3 + \sin \theta_1 \sin \theta_3 \\ -\cos \theta_2 \sin \theta_3 & \sin \theta_1 \sin \theta_2 \sin \theta_3 + \cos \theta_1 \cos \theta_3 & -\cos \theta_1 \sin \theta_2 \sin \theta_3 + \sin \theta_1 \cos \theta_3 \\ -\sin \theta_2 & -\sin \theta_1 \cos \theta_2 & \cos \theta_1 \cos \theta_2 \end{bmatrix}$$

a form which is not to be memorized or used much. Notice however that there is *no (anti)symmetric property of the matrix (a)* ; $a_{ij} \neq \pm a_{ji}$. The projection of the new axis \hat{x}_i' onto the old axis \hat{x}_j has no general relationship with the projection of the new axis \hat{x}_j' onto the old axis \hat{x}_i .

Orthonormality properties of (a)

The transformation matrix (a) has some properties which constrain the values of a_{ij} . Clearly, since (a) is completely defined through three angles θ_i , the nine values a_{ij} must be related through six equations, reducing the free parameters to three. This can be seen by noticing that any two unit vectors in the old representation, \hat{x}_i and \hat{x}_j , form an orthonormal pair. We can then take unit vectors in the old representation, $p = [1, 0, 0]$, $p = [0, 1, 0]$, $p = [0, 0, 1]$, and transform them:

$$p'_i = a_{ik} p_k \quad p'_j = a_{jl} p_l \quad (3.17)$$

For unit vectors in \hat{x}_k and \hat{x}_l , respectively, each cartesian component p'_i, p'_j has one term

$$p'_i = a_{ik} \quad p'_j = a_{jl} \quad (3.18)$$

where there is no implied sum on the right hand side; k and l are single-valued. To express the dot product of the two vectors in dummy suffix

notation, there must be a repeated index on the left hand side, so we convert $j \rightarrow i$ for p'_j . (j is a free index so this is allowed.)

$$p'_i p'_i = a_{ik} a_{il} \quad (3.19)$$

Two cases need to be considered for k, l . If $k = l$, the dot product of p'_i with itself must be 1.². Thus for $k = l$, $a_{ik} a_{il} = 1$, $a_{i1} a_{i1} = 1$, $a_{i2} a_{i2} = 1$, $a_{i3} a_{i3} = 1$, or

$$a_{11}^2 + a_{21}^2 + a_{31}^2 = 1 \quad (3.20)$$

$$a_{12}^2 + a_{22}^2 + a_{32}^2 = 1 \quad (3.21)$$

$$a_{13}^2 + a_{23}^2 + a_{33}^2 = 1 \quad (3.22)$$

Alternatively, if $k \neq l$, the dot product $a_{ik} a_{il} = 0$, so these cases include $a_{i1} a_{i2} = 0$, $a_{i2} a_{i3} = 0$, $a_{i3} a_{i1} = 0$, or

$$a_{11} a_{12} + a_{21} a_{22} + a_{31} a_{32} = 0 \quad (3.23)$$

$$a_{12} a_{13} + a_{22} a_{23} + a_{32} a_{33} = 0 \quad (3.24)$$

$$a_{13} a_{11} + a_{23} a_{21} + a_{33} a_{31} = 0 \quad (3.25)$$

Cartesian to spherical coordinates

In spherical coordinates, the three orthonormal directions are $(\hat{r}, \hat{\theta}, \hat{\phi})$. We would like to take a vector in the Cartesian coordinate system, $[p_x, p_y, p_z]$, and convert it to a vector in the spherical coordinate system, $[p_r, p_\theta, p_\phi]$. The Cartesian system is then 'old' and the spherical system is 'new.' The transformation will then be defined by

$$\begin{bmatrix} p_r \\ p_\theta \\ p_\phi \end{bmatrix} = \begin{bmatrix} \cos \theta_3 & \sin \theta_3 & 0 \\ -\sin \theta_3 & \cos \theta_3 & 0 \\ 0 & 0 & 1 \end{bmatrix} \begin{bmatrix} p_x \\ p_y \\ p_z \end{bmatrix} \quad (3.26)$$

Reverse transformation ('new' to 'old')

The orthonormality relations make finding the reverse transformation relatively simple. If we express the coordinate transformation as a matrix

²Caution: substituting $k = l$ in this term would be misleading, since there can be no implied sum over k or l , each being single-valued

multiplication (*a*), with $\mathbf{p}' = (a)\mathbf{p}$, we would like to know the reverse transformation matrix (*b*), $\mathbf{p} = (b)\mathbf{p}'$.

It must be true that $(b)(a) = (I)$, where (I) is the identity matrix ($I_{ij} = \delta_{ij}$). This implies that $(b) = (a)^{-1}$, (*b*) is the inverse matrix of (*a*). Because of the orthonormality conditions described in Section 3.1.2, the inverse matrix can be found through the transpose of (*a*): $b_{ij} = a_{ji}$. Verifying this is left as an exercise. Thus

$$\mathbf{p} = (a)^T \mathbf{p}' \quad (3.27)$$

or in dummy suffix notation,

$$p_i = a_{ji} p'_j \quad (3.28)$$

Notice that the indices are *far apart* in the new \rightarrow old transformation.

Eq. 3.28 is very easy to understand from the definition of the coordinate transformation matrix. The element a_{ij} is defined such that it is the cosine of the angle between new axis \hat{x}_i' and old axis \hat{x}_j . In Eq 3.28, we swapped indices: the left hand side indexes the old axis by *j* and the right hand side indexes the new axis by *i*.

3.1.3 Coordinate transformations for tensors

We can transform vector coordinates from 'old' to 'new' representations through

$$p'_i = a_{ik} p_k \quad (3.29)$$

However, rewriting the definition of a tensor from Eq 3.4, for a second-rank tensor, in dummy-suffix notation,

$$p_k = T_{kl} q_l \quad (3.30)$$

The repeated (dummy) suffix can take any name, and the free suffixes on left and right hand sides need to match. Also, the old representation for q_j can be transformed into the new through $q_l = a_{jl} q'_j$, so

$$p'_i = a_{ik} T_{kl} a_{jl} q'_j \quad (3.31)$$

In the dummy suffix notation, each term is a product, summed over repeated indices, so the positions can be interchanged on the right hand side

Rank	Description	'old' → 'new' (forward)	'new' → 'old' (reverse)
1	vector	$p'_i = a_{ij}p_j$	$p_i = a_{ji}p'_j$
2	second-rank tensor	$T'_{ij} = a_{ik}a_{jl}T_{kl}$	$T_{ij} = a_{ki}a_{lj}T'_{kl}$
3	third-rank tensor	$T'_{ijk} = a_{il}a_{jm}a_{kn}T_{lmn}$	$T_{ijk} = a_{li}a_{mj}a_{nk}T'_{lmn}$
4	fourth-rank tensor	$T'_{ijkl} = a_{im}a_{jn}a_{ko}a_{lp}T_{mnop}$	$T_{ijkl} = a_{mi}a_{nj}a_{ok}a_{pl}T'_{mnop}$

Table 3.1: Coordinate transformation rules, tensors of rank 1-4.

$$p'_i = a_{ik}a_{jl}T_{kl}q'_j \quad (3.32)$$

Thus the tensor T'_{ij} , defined in the new coordinate system through $p'_i = T'_{ij}q'_j$, is (going from 'old' to 'new')

$$T'_{ij} = a_{ik}a_{jl}T_{kl} \quad (3.33)$$

and to go from 'new' to 'old',

$$T_{ij} = a_{ki}a_{lj}T'_{kl} \quad (3.34)$$

where the indices in a are simply reversed.

The same process, already shown for first-rank tensors (vectors) and shown here for second-rank tensors, can be extended to third and fourth-rank tensors straightforwardly. The transformation rules for tensors of rank one to four are tabulated in Table 3.1. Note that in all cases, the reverse transformation has reversed indices $a_{ij} \rightarrow a_{ji}$ compared with the forward transformation.

Example: simple transformation of $[\sigma]$ Let's take a classic example for the transformation of a stress tensor with only biaxial shear, $\tau = \sigma_{12} = \sigma_{21}$:

$$[\sigma] = \begin{bmatrix} 0 & \tau & 0 \\ \tau & 0 & 0 \\ 0 & 0 & 0 \end{bmatrix} \quad (3.35)$$

If we choose new axes which are rotated about \hat{x}_3 by $\theta_3 = \pi/4$, what stress results on those axes? We previously found for (a)

$$(a) = \begin{bmatrix} a_{11} & a_{12} & a_{13} \\ a_{21} & a_{22} & a_{23} \\ a_{31} & a_{32} & a_{33} \end{bmatrix} = \frac{1}{\sqrt{2}} \begin{bmatrix} 1 & 1 & 0 \\ -1 & 1 & 0 \\ 0 & 0 & 1 \end{bmatrix} \quad (3.36)$$

So $\sigma'_{ij} = a_{ik}a_{jl}\sigma_{kl}$ has only two terms, for σ_{12} and σ_{21} :

$$\sigma'_{ij} = a_{i1}a_{j2}\sigma_{12} + a_{i2}a_{j1}\sigma_{21} \quad (3.37)$$

$$[\sigma]' = \begin{bmatrix} \tau & 0 & 0 \\ 0 & -\tau & 0 \\ 0 & 0 & 0 \end{bmatrix} \quad (3.38)$$

3.1.4 Representation of the stress tensor as a surface

A graphical representation is helpful for finding the principal axes of the stress tensor $[\sigma]$. Any symmetric, second-rank tensor $[T]$ can be represented as a three-dimensional surface, defined through

$$T_{ij}x_i x_j = 1 \quad (3.39)$$

This compact expression includes a double sum over i and j , with nine terms. We will switch our discussion from a general $[T]$ to $[\sigma]$, but all that follows is true for any symmetric tensor

$$\sigma_{11}x_1^2 + \sigma_{22}x_2^2 + \sigma_{33}x_3^2 + 2\sigma_{12}x_1x_2 + 2\sigma_{23}x_2x_3 + 2\sigma_{31}x_3x_1 = 1 \quad (3.40)$$

where we made use of the symmetry of σ , $\sigma_{ij} = \sigma_{ji}$. Proof can be seen by transforming the axes of x_i and x_j :

$$\sigma_{ij}a_{ki}x'_k a_{lj}x'_l = 1 \quad (3.41)$$

and changing the indices

$$a_{ki}a_{lj}\sigma_{kl} x'_i x'_j = 1 \quad (3.42)$$

we can see that the transformed quantity $\sigma'_{ij} = a_{ki}a_{lj}\sigma_{kl}$ is consistent with the definition of a tensor in Eq 3.33.

Two-dimensional example Taking a two-dimensional σ_{ij} , with $\sigma_{i3} = \sigma_{3i} = 0$, the surface in Eq 3.40 takes a simpler form,

$$\sigma_{11}x_1^2 + 2\sigma_{12}x_1x_2 + \sigma_{22}x_2^2 = 1 \quad (3.43)$$

The normal to the surface can be found from the gradient of the surface function (a scalar):

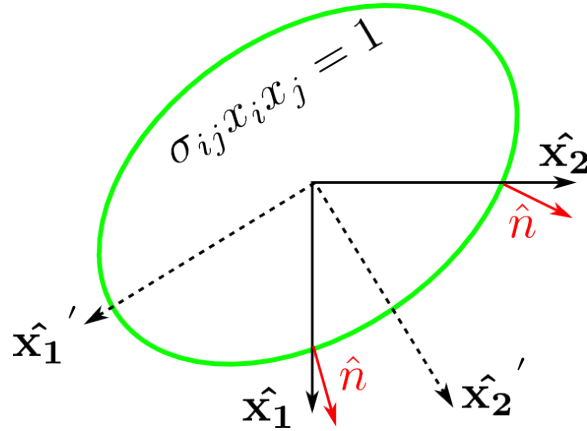


Figure 3.2: Surface representation of a two-dimensional stress. Note that in the 'old' representation $\hat{\mathbf{x}}$, the surface normal $\hat{\mathbf{n}}$, indicating the direction of force \mathbf{F} , is not parallel to the coordinate axes. Along 'new' principal axes $\hat{\mathbf{x}}'$, the surface normal $\hat{\mathbf{n}}$ and force are parallel to the coordinate axes.

$$\hat{\mathbf{n}} = \nabla (\sigma_{11} x_1^2 + 2\sigma_{12} x_1 x_2 + \sigma_{22} x_2^2) \quad (3.44)$$

This evaluates to

$$\hat{\mathbf{n}} = (2\sigma_{11} x_1 + 2\sigma_{12} x_2) \hat{\mathbf{x}}_1 + (2\sigma_{21} x_1 + 2\sigma_{22} x_2) \hat{\mathbf{x}}_2 \quad (3.45)$$

More compactly

$$n_i = \sigma_{ij} x_j \quad (3.46)$$

where n_i can be recognized from Eq 3.9 as the direction of the force exerted across the surface of a differential area element.

3.2 Finding principal axes

3.2.1 Three-dimensional stress tensor

If the force exerted is parallel to the axis x'_i , the axis experiences only normal forces, and is a **principal axis** for the stress tensor. Graphically, then, the principal axes $\hat{\mathbf{x}}'$ are normal to the stress surface, or parallel to $\hat{\mathbf{n}}$ as is illustrated in Figure 3.2. The condition illustrated for two dimensions in

Figure 3.2 holds just as well for three dimensions. The graphical condition can be expressed in matrix form as

$$\begin{bmatrix} \sigma_{11} & \sigma_{12} & \sigma_{13} \\ \sigma_{12} & \sigma_{22} & \sigma_{23} \\ \sigma_{13} & \sigma_{23} & \sigma_{33} \end{bmatrix} \begin{bmatrix} x_1 \\ x_2 \\ x_3 \end{bmatrix} = \lambda \begin{bmatrix} x_1 \\ x_2 \\ x_3 \end{bmatrix} \quad (3.47)$$

or

$$\begin{bmatrix} \sigma_{11} - \lambda & \sigma_{12} & \sigma_{13} \\ \sigma_{12} & \sigma_{22} - \lambda & \sigma_{23} \\ \sigma_{13} & \sigma_{23} & \sigma_{33} - \lambda \end{bmatrix} \begin{bmatrix} x_1 \\ x_2 \\ x_3 \end{bmatrix} = 0 \quad (3.48)$$

This is an eigenvalue equation for the tensor (σ) in the 'old' representation. It has solutions for λ where the determinant of the matrix $(\sigma) - \lambda(\mathbf{I})$, where \mathbf{I} is the identity matrix, is zero, or

$$\begin{vmatrix} \sigma_{11} - \lambda & \sigma_{12} & \sigma_{13} \\ \sigma_{12} & \sigma_{22} - \lambda & \sigma_{23} \\ \sigma_{13} & \sigma_{23} & \sigma_{33} - \lambda \end{vmatrix} = 0 \quad (3.49)$$

Backsubstitution of the three eigenvalues of $\lambda_1, \lambda_2, \lambda_3$ determined this way into Eq 3.48 yield three eigenvectors $\mathbf{X}_1, \mathbf{X}_2, \mathbf{X}_3$. These vectors are the principal axes.

3.2.2 Single rotation: Mohr's circle

In cases where one of the principal axes is already known, \mathbf{X}_3 can be taken along $\hat{\mathbf{x}}_3$, and the whole problem of finding the other two principal axes is a question of finding θ_3 , the rotation of \mathbf{x}' about $\hat{\mathbf{x}}_3$. If we know the stresses $\sigma_{11}, \sigma_{22}, \sigma_{12} = \sigma_{21}$, how can we find θ_3 ?

We seek θ_3 such that σ'_{ij} has only diagonal components.

$$[\sigma]' = \begin{bmatrix} \sigma_1 & 0 & 0 \\ 0 & \sigma_2 & 0 \\ 0 & 0 & \sigma_3 \end{bmatrix} \quad (3.50)$$

The transformation matrix (a) for a single rotation θ_3 has already been written in Section 3.1.2 and illustrated in Figure 3.1. We are interested in the *reverse* transformation. Using Eq 3.34,

$$\sigma_{ij} = a_{ki} a_{lj} \sigma'_{kl} \quad (3.51)$$

notice again that the indices are far away from each other in the reverse transformation ('new' to 'old'.) We have $a_{11} = a_{22} = \cos \theta_3$, $a_{12} = \sin \theta_3$, $a_{21} = -\sin \theta_3$, and $a_{33} = 1$, all other $a_{ij} = 0$. We can designate principal stresses as $\sigma_1, \sigma_2, \sigma_3$, so we can evaluate

$$\sigma_{11} = a_{k1}a_{l1}\sigma'_{kl} \quad (3.52)$$

$$\sigma_{22} = a_{k2}a_{l2}\sigma'_{kl} \quad (3.53)$$

$$\sigma_{12} = a_{k1}a_{l2}\sigma'_{kl} \quad (3.54)$$

simplified because σ'_{ij} has only diagonal components. Expanding the dummy suffix sums,

$$\sigma_{11} = a_{11}a_{11}\sigma_1 + a_{21}a_{21}\sigma_2 \quad (3.55)$$

$$\sigma_{22} = a_{12}a_{12}\sigma_1 + a_{22}a_{22}\sigma_2 \quad (3.56)$$

$$\sigma_{12} = a_{11}a_{12}\sigma_1 + a_{21}a_{22}\sigma_2 \quad (3.57)$$

Note that there is no point in evaluating σ_{21} since a symmetric tensor is also symmetric on transformation. Substituting in for a_{ij} ,

$$\sigma_{11} = \cos^2 \theta_3 \sigma_1 + \sin^2 \theta_3 \sigma_2 \quad (3.58)$$

$$\sigma_{22} = \sin^2 \theta_3 \sigma_1 + \cos^2 \theta_3 \sigma_2 \quad (3.59)$$

$$\sigma_{12} = \sin \theta_3 \cos \theta_3 \sigma_1 - \sin \theta_3 \cos \theta_3 \sigma_2 \quad (3.60)$$

Through the use of the half-angle formulae, $\sin^2 \theta = (1 - \cos 2\theta)/2$, $\cos^2 \theta = (1 + \cos 2\theta)/2$

$$\sigma_{11} = \left(\frac{\sigma_1 + \sigma_2}{2} \right) + \left(\frac{\sigma_1 - \sigma_2}{2} \right) \cos 2\theta_3 \quad (3.61)$$

$$\sigma_{22} = \left(\frac{\sigma_1 + \sigma_2}{2} \right) - \left(\frac{\sigma_1 - \sigma_2}{2} \right) \cos 2\theta_3 \quad (3.62)$$

$$\sigma_{12} = \left(\frac{\sigma_1 - \sigma_2}{2} \right) \sin 2\theta_3 \quad (3.63)$$

Eqs. 3.63 define a circle in the $\sigma_{ii}\sigma_{12}$ plane. The origin of the circle is on the σ_{ii} axis at the average of σ_1 and σ_2 . The radius of the circle is given by the difference, $(\sigma_1 - \sigma_2)/2$. The shear stress is given by the y coordinate on the circle at a rotation of $2\theta_3$, σ_{11} is given by the x coordinate at a rotation of $2\theta_3$, and σ_{22} is given by the x coordinate at a rotation of $2\theta_3 + \pi$.

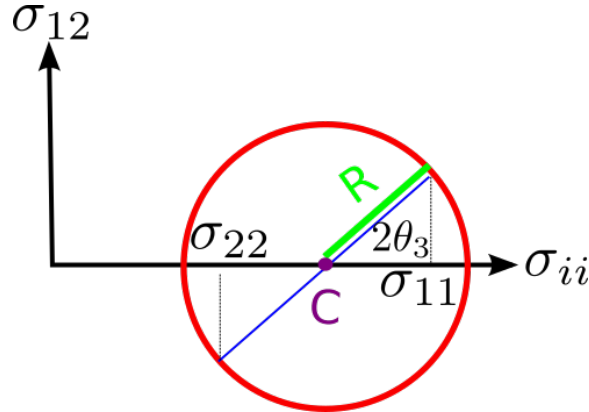


Figure 3.3: Mohr's circle representation of a biaxial stress. Point C gives $(\sigma_1 + \sigma_2)/2$; length R gives $(\sigma_1 - \sigma_2)/2$.

The angle θ_3 can be found by summing the first two relations and dividing into the third:

$$\boxed{\tan 2\theta_3 = \frac{2\sigma_{12}}{\sigma_{11} - \sigma_{22}}} \quad (3.64)$$

This is the (right-hand) angle through which the coordinate system must be rotated about \hat{x}_3 to find the principal axes in the $\hat{x}_1\hat{x}_2$ plane. The magnitudes of the principal stresses are found by taking the square of the difference of the first two relations, and summing with the square of the third

$$R = \left(\frac{\sigma_1 - \sigma_2}{2} \right) = \sqrt{\sigma_{12}^2 + \left(\frac{\sigma_{11} - \sigma_{22}}{2} \right)^2} \quad (3.65)$$

which forms the radius of the circle R . Combined with the sum of the first two $\cos 2\theta_3$ relations,

$$C = \left(\frac{\sigma_1 + \sigma_2}{2} \right) = \left(\frac{\sigma_{11} + \sigma_{22}}{2} \right) \quad (3.66)$$

This gives a complete solution for the principal stresses:

$$\boxed{\sigma_1 = C + R \quad \sigma_2 = C - R} \quad (3.67)$$

Utility: The construction allows one to determine graphically the angle through which the coordinate system needs to be rotated to find principal

axes, as shown in Figure 3.3. On a piece of graph paper, with a ruler, draw a horizontal line, parallel to the x -axis, with y -intercept of σ_{12} . Next, draw two vertical lines, parallel to the y -axis, with x -intercept of σ_{11} and σ_{22} . The midpoint defined between these two intercepts on the x -axis is C ; from C , draw a line to the intersection of the σ_{12} and σ_{11} lines. This defines R . Then use a compass to draw a circle (with radius R from point C) and a protractor to measure the angle.

Going *from* axes which include nonzero shear σ_{12} *to* principal axes, which include only normal stresses, requires a right-hand rotation about \hat{x}_3 by θ_3 . We defined principal axes as the "new" axes in Eq 3.51 and the a -matrix defined in Eq 3.15.

The Mohr's circle construction is not as useful a computational tool now as it may have been in the days of the slide rule. One can use the 'arctan' function on a calculator or programming language to evaluate Eq 3.64 directly for the angle θ_3 , and/or Eq 3.67 for the principal stresses σ_1, σ_2 . Nevertheless, Mohr's circle helps us visualize how normal and shear stresses vary as the coordinate system is rotated away from the principal axes.

Simple examples

- **Uniaxial stress:** $\sigma_{11} = \sigma, \sigma_{22} = 0, \sigma_{12} = 0$. $C = \sigma/2; R = \sigma/2$. The points lie on the σ_{ii} axis, so no rotation is needed to find the principal axes; $\theta_3 = 0$.
- **Hydrostatic stress:** $\sigma_{11} = \sigma_{22} = -P$. What is the radius R of the circle? How can you rotate the axes to get shear components? (A: you cannot; the stress state is hydrostatic for all rotations.)
- **Pure shear:** $\sigma_{12} = \tau, \sigma_{11} = \sigma_{22} = 0$. What is C ? When you rotate by $\theta_3 = \pi/4$, what happens?

Exercises

1. For a solid cylinder under uniaxial normal stress along x_2 , $\sigma_{22} = \sigma$
 - Find the shear stress $\sigma_{\alpha\beta}$ for orthonormal (α, β, x_3) and α, β rotated by θ_3 about x_3 with respect to x_1, x_2 .
 - Find the shear stress $\sigma_{\alpha\beta}$ for a general rotation θ , and show that it is maximum for $\theta = \pi/4$.

2. Consider the following biaxial stress state: $\sigma_{11} = 300 \text{ MPa}$, $\sigma_{22} = 100 \text{ MPa}$, $\sigma_{12} = 100 \text{ MPa}$, with α, β axes defined as before
 - (a) Determine the rotation θ_3 such that α, β are principal axes
 - (b) Determine the principal stresses $\sigma_{\alpha\alpha}, \sigma_{\beta\beta}$
 - (c) Determine the θ_3 for maximum in-plane shear and the magnitude of the maximum $\sigma_{\alpha\beta}$
3. Take the following stress tensor:

$$[\sigma] = \begin{bmatrix} 0 & \sigma_{12} & 0 \\ \sigma_{12} & \sigma_{22} & \sigma_{23} \\ 0 & \sigma_{23} & 0 \end{bmatrix} \quad (3.68)$$

Note that no principal stress axis is known *a priori*.

- (a) Write an expression for the principal stresses. How many nonzero principal stresses are there?
- (b) Verify that the dilation Δ is invariant on transforming to the principal axes.
- (c) Solve the principal stresses for $\sigma_{22} = 200 \text{ MPa}$, $\sigma_{12} = \sigma_{23} = \sqrt{2} \cdot 100 \text{ MPa} \sim 141 \text{ MPa}$
- (d) Determine the principal axes. If there is plane stress in the transformed coordinates, determine the normal to the plane.

Chapter 4

Strain tensor

We represented the stress σ_{ij} as a tensor $[\sigma]$ last time. We know that stress σ and strain ϵ are closely related. It is plausible that a tensor representation of strain, perhaps $[\epsilon]$, is coming next. We will denote this **tensor strain** with the symbol $[\epsilon]$, or ϵ_{ij} .

$$[\epsilon] = \begin{bmatrix} \epsilon_{11} & \epsilon_{12} & \epsilon_{13} \\ \epsilon_{21} & \epsilon_{22} & \epsilon_{23} \\ \epsilon_{31} & \epsilon_{32} & \epsilon_{33} \end{bmatrix} \quad (4.1)$$

This nomenclature is not universal¹, but one can recognize tensor strain from the fact that it has two indices. For the moment, I will not say anything about the symmetry of this tensor; we will try to figure out what sort of form it should have.

4.1 Definitions of strain

We can first consider strain in one dimension in a continuous medium, then move on to the discussion of two and three dimensions. For macroscopic, uniform strain, we often say

$$\epsilon = \frac{\Delta l}{l_0} \quad (4.2)$$

where Δl is the elongation of the body under uniaxial stress and l_0 is its initial length, before the application of the stress. This is valid for a uniform, normal stress (here ϵ is uniform ϵ_{11} , ϵ_{33} , or ϵ_{33} , as will be shown.) However,

¹The text by Nye denotes ϵ_{ij} as the tensor strain

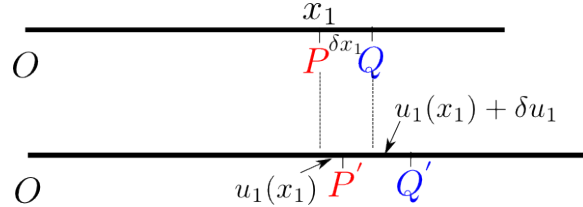


Figure 4.1: Illustration of a uniaxial strain on a wire. See text for details.

we need a more detailed description to consider nonuniform strains in one dimension, and multiaxial and shear strains in two and three dimensions. The quantity which we would like to consider is the displacement vector \mathbf{u} .

Displacement vector The displacement vector \mathbf{u} (or u_i) connects, for any point P in the material with coordinates p_i , the position of the atoms surrounding point P before the deformation with the position of those same atoms after the deformation.

4.1.1 One-dimensional strain

Imagine that we have two points, marked P and Q , on an elastic string under just enough tension to hold it straight, as illustrated in Fig 4.1. The points are some distance away from the end of the string, which is held fixed. Point P is distance x_1 away from the clamped end; point Q is a distance $x_1 + \delta x_1$, where $\delta x_1 \ll x_1$.

Next, we exert enough force on the free end to start to stretch the string out. Points P and Q will move to points P' and Q' , respectively. The free end of the string will move by Δl , as in Eq 4.2, but the rest of the string will move less. The displacement $u_1(x_1)$ will vary from zero, at the clamped end, to Δl , at the free end. We can then define a continuum analog of Eq 4.2 for the differential element between P and Q as

$$\epsilon_1(x_1) = \frac{\overline{P'Q'} - \overline{PQ}}{\overline{PQ}} \quad (4.3)$$

If the displacement $u_1(x_1)$ is known, we can evaluate Eq 4.3 as

$$\epsilon_1(x_1) = \frac{u(x_1 + \delta x_1) - u(x_1)}{\delta x_1} \quad (4.4)$$

$$\epsilon_1(x_1) = \frac{\partial u_1(x_1)}{\partial x_1} \quad (4.5)$$

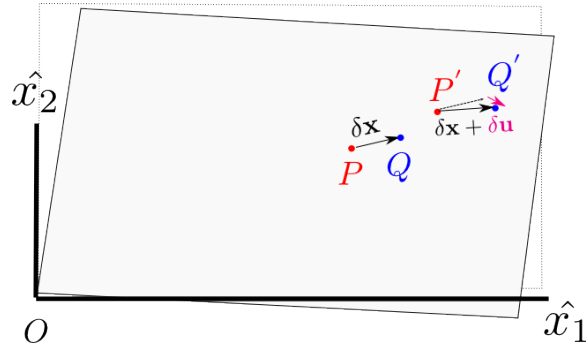


Figure 4.2: Illustration of a two-dimensional strain on a sheet. See text for details.

One thing to see in this expression is that rigid translations of the string do not cause any strain to develop: if displacement is uniform and $u(x)$ has no gradient at a point, no strain exists at that point. Additionally, nothing in this expression says that strain needs to be uniform in the string – if for example the cross-sectional area of the string varies (such that stress σ varies) or the elastic modulus of the string varies over x , the strain can vary. We can then define the point strain according to Eq 4.5,

$$\boxed{e_{11} = \frac{\partial u_1}{\partial x_1}} \quad (4.6)$$

4.1.2 Two-dimensional strain

We can extend the above discussion to an elastic sheet in two dimensions, as illustrated in Figure 4.2. Here we allow points P and Q to sit at points \mathbf{x}_0 and $\mathbf{x}_0 + \delta\mathbf{x}$, respectively, before the deformation. After the deformation, points P' and Q' have each undergone a vector displacement, \mathbf{u} for point $P \rightarrow P'$, and $\mathbf{u} + \delta\mathbf{u}$ for point $Q \rightarrow Q'$.

The infinitesimal strain in two dimensions can be defined exactly the same as in Eq 4.3. Here, we have

$$\overline{PQ} = |\delta\mathbf{x}| = \sqrt{(\delta x_1)^2 + (\delta x_2)^2} \quad (4.7)$$

$$\overline{P'Q'} = |\delta\mathbf{u} + \delta\mathbf{x}| = \sqrt{(\delta x_1 + \delta u_1)^2 + (\delta x_2 + \delta u_2)^2} \quad (4.8)$$

We always consider small displacements, so the quantity under the radical in $\overline{P'Q'}$ can be expanded, neglecting terms of order δu_i^2 .

$$\overline{P'Q'} = |\delta\mathbf{u} + \delta\mathbf{x}| = \sqrt{|\delta\mathbf{x}|^2 + 2(\delta u_1 \delta x_1 + \delta u_2 \delta x_2)} \quad (4.9)$$

Making use of $\sqrt{a^2 + x} \simeq a + x/2a$ for small x ,

$$\overline{P'Q'} - \overline{PQ} = |\delta\mathbf{x}|^{-1}(\delta u_1 \delta x_1 + \delta u_2 \delta x_2) \quad (4.10)$$

Here it is important to consider both cross-derivatives of u_1 and u_2 :

$$\delta u_1 = \frac{\partial u_1}{\partial x_1} \delta x_1 + \frac{\partial u_1}{\partial x_2} \delta x_2 \quad (4.11)$$

$$\delta u_2 = \frac{\partial u_2}{\partial x_1} \delta x_1 + \frac{\partial u_2}{\partial x_2} \delta x_2 \quad (4.12)$$

Defining, as before

$$e_{ij} = \frac{\partial u_i}{\partial x_j} \quad (4.13)$$

these expressions can be rewritten as

$$\delta u_1 = e_{11} \delta x_1 + e_{12} \delta x_2 \quad (4.14)$$

$$\delta u_2 = e_{21} \delta x_1 + e_{22} \delta x_2 \quad (4.15)$$

which substituted in Eq 4.10 and Eq 4.3 become

$$\epsilon = |\delta\mathbf{x}|^{-2} [e_{11}(\delta x_1)^2 + e_{22}(\delta x_2)^2 + (e_{12} + e_{21}) \delta x_1 \delta x_2] \quad (4.16)$$

There is something important to notice in the last term of this expression. For arbitrary e_{12} and e_{21} , it would be possible to express a tensor $[e]$ or e_{ij} through the sum of two tensors, one which is symmetric, $e_{ij} = e_{ji}$, and one which is antisymmetric $e_{ij} = -e_{ji}$. **Only symmetric shear strains contribute to the elongation** and the point strain. It is clear that anti-symmetric terms would give no contribution to ϵ .

Antisymmetric terms are a rotation To see why, think about the transformation of point $P \rightarrow P'$ and $Q \rightarrow Q'$ through an infinitesimal rotation about the origin (or \hat{x}_3 axis) by an angle ϕ . The displacement for the first case would be given through the matrix

$$\begin{bmatrix} u_1 \\ u_2 \end{bmatrix} = \begin{bmatrix} 0 & -\phi \\ \phi & 0 \end{bmatrix} \begin{bmatrix} x_1 \\ x_2 \end{bmatrix} \quad P \rightarrow P' \quad (4.17)$$

and for the second case,

$$\begin{bmatrix} u_1 + \delta u_1 \\ u_2 + \delta u_2 \end{bmatrix} = \begin{bmatrix} 0 & -\phi \\ \phi & 0 \end{bmatrix} \begin{bmatrix} x_1 + \delta x_1 \\ x_2 + \delta x_2 \end{bmatrix} \quad Q \rightarrow Q' \quad (4.18)$$

such that taking the difference of the two matrices gives us

$$\begin{bmatrix} \delta u_1 \\ \delta u_2 \end{bmatrix} = \begin{bmatrix} 0 & -\phi \\ \phi & 0 \end{bmatrix} \begin{bmatrix} \delta x_1 \\ \delta x_2 \end{bmatrix} \quad (4.19)$$

Here we can recognize the cross-derivatives for the displacement vectors in the matrix

$$e_{12} = \frac{\partial u_1}{\partial x_2} = -\phi \quad e_{21} = \frac{\partial u_2}{\partial x_1} = \phi \quad (4.20)$$

Here we can see that the introduction of an infinitesimal rotation ϕ gave us an *antisymmetric* shear, $e_{12} = -e_{21}$. This rotation did nothing to change the positions of the points P and Q relative to each other, so no strain was built up in the transformation. Asymmetric $[e]$ tensors do not contribute to strain. The extension to three dimensions is straightforward.

4.1.3 Symmetrizing the strain tensor

To define a strain tensor, we need to remove the antisymmetric portion. It is relatively easy to do so by defining the strain tensor ε_{ij} from the e_{ij} as

$$\boxed{\varepsilon_{ij} = \frac{1}{2} (e_{ij} + e_{ji})} \quad (4.21)$$

ε_{ij} is the *tensor strain*. More explicitly, in two dimensions, this is

$$[\varepsilon] = \begin{bmatrix} \varepsilon_{11} & \varepsilon_{12} \\ \varepsilon_{21} & \varepsilon_{22} \end{bmatrix} = \begin{bmatrix} e_{11} & \frac{1}{2} (e_{12} + e_{21}) \\ \frac{1}{2} (e_{12} + e_{21}) & e_{22} \end{bmatrix} \quad (4.22)$$

and three dimensions

$$[\varepsilon] = \begin{bmatrix} \varepsilon_{11} & \varepsilon_{12} & \varepsilon_{13} \\ \varepsilon_{21} & \varepsilon_{22} & \varepsilon_{23} \\ \varepsilon_{31} & \varepsilon_{32} & \varepsilon_{33} \end{bmatrix} = \begin{bmatrix} e_{11} & \frac{1}{2} (e_{12} + e_{21}) & \frac{1}{2} (e_{13} + e_{31}) \\ \frac{1}{2} (e_{12} + e_{21}) & e_{22} & \frac{1}{2} (e_{23} + e_{32}) \\ \frac{1}{2} (e_{13} + e_{31}) & \frac{1}{2} (e_{23} + e_{32}) & e_{33} \end{bmatrix} \quad (4.23)$$

Note that in this new definition, if the body is under two-dimensional shear strain, the angle formed between each axis and the side of the body is now *one half* ε_{12} .

4.1.4 Tensor shear strain and (engineering) shear strain

Very often, the strain tensor is written

$$[\varepsilon] = \begin{bmatrix} \epsilon_x & \gamma_{xy}/2 & \gamma_{xz}/2 \\ \gamma_{xy}/2 & \epsilon_y & \gamma_{yz}/2 \\ \gamma_{xz}/2 & \gamma_{yz}/2 & \epsilon_z \end{bmatrix} \quad (4.24)$$

In terms of *engineering strains*, equivalent to the *matrix strains*, about which we will say more in Section 6.3. The normal components of engineering strains $\epsilon_x, \epsilon_y, \epsilon_z$ are the same as the tensor strains $\varepsilon_{11}, \varepsilon_{22}, \varepsilon_{33}$. The shear components of engineering strains, $\gamma_{yz}, \epsilon_{xz}, \epsilon_{xy}$ differ from their tensor counterparts by a factor of two, e.g.

$$\gamma_{yz} = 2\varepsilon_{yz} \quad (4.25)$$

such that γ_{yz} is, if a cube is oriented with the $\hat{\mathbf{z}}$ axis along the vertical and the direction of sight along $\hat{\mathbf{x}}$, the angle formed between the cube sides (with initial normal on $\hat{\mathbf{y}}$) and the vertical axis on shearing.

Antisymmetric tensor $[w_{ij}]$ The antisymmetric part of the $[e]$ tensor also has meaning. Analogously with the symmetric portion, the antisymmetric portion can be found through

$$w_{ij} \equiv \frac{1}{2} (e_{ij} - e_{ji}) \quad (4.26)$$

where $w_{ij} = -w_{ji}$ by definition. In three dimensions,

$$[w] = \begin{bmatrix} w_{11} & w_{12} & w_{13} \\ w_{21} & w_{22} & w_{23} \\ w_{31} & w_{32} & w_{33} \end{bmatrix} = \begin{bmatrix} 0 & \frac{1}{2}(e_{12} - e_{21}) & \frac{1}{2}(e_{13} - e_{31}) \\ \frac{1}{2}(e_{12} - e_{21}) & 0 & \frac{1}{2}(e_{23} + e_{32}) \\ \frac{1}{2}(e_{13} - e_{31}) & \frac{1}{2}(e_{23} - e_{32}) & 0 \end{bmatrix} \quad (4.27)$$

As we saw for a simple rotation about $\hat{\mathbf{x}}_3$, $[w]$ corresponds to a rotation. Generalizing the small-angle rotation matrix shown about $\hat{\mathbf{x}}_3$, we can take a small-angle rotation about an arbitrary vector $\hat{\mathbf{u}}$ or u_i , by a right-handed rotation ϕ . w can be expressed

$$[w] = \begin{bmatrix} 0 & -u_3\phi & u_2\phi \\ u_3\phi & 0 & -u_1\phi \\ -u_2\phi & u_1\phi & 0 \end{bmatrix} \quad (4.28)$$

which reduces to the form shown earlier if $u_1 = u_2 = 0, u_3 = 1$.

4.1.5 Dilation

Because the strain $[\varepsilon]$ is a symmetric second-rank tensor, just like the stress $[\sigma]$, it can be transformed to principal axes. Along the principal axes, there are only normal strains ε_{ii} , indexed as ϵ_i .

$$[\varepsilon] = \begin{bmatrix} \varepsilon_{11} & \varepsilon_{12} & \varepsilon_{13} \\ \varepsilon_{21} & \varepsilon_{22} & \varepsilon_{23} \\ \varepsilon_{31} & \varepsilon_{32} & \varepsilon_{33} \end{bmatrix} \rightarrow \begin{bmatrix} \epsilon_1 & 0 & 0 \\ 0 & \epsilon_2 & 0 \\ 0 & 0 & \epsilon_3 \end{bmatrix} \quad (4.29)$$

where the second matrix is in "matrix" formalism (one index for strain). Even though all strains are normal along the principal strain axes, there can still be a rotation of the system, specified independently through $[w]$. It is simple to calculate the change in volume for a system, given the principal strains ϵ_i . If the strain is homogeneous, lengths L_1, L_2, L_3 (L_i) will change by an amount $\Delta L_1 = L_1\epsilon_1$, $\Delta L_2 = L_2\epsilon_2$, $\Delta L_3 = L_3\epsilon_3$ ($\Delta L_i = L_i\epsilon_i$). The relative change in volume, normalized to the volume, is

$$\Delta \equiv \frac{\delta V}{V} = \frac{V' - V_0}{V_0} = \frac{(1 + \epsilon_1)(1 + \epsilon_2)(1 + \epsilon_3)L_1L_2L_3 - L_1L_2L_3}{L_1L_2L_3} \quad (4.30)$$

Since the strains ϵ_i are small, powers of ϵ^2 and ϵ^3 can be neglected, so

$$\Delta = \epsilon_1 + \epsilon_2 + \epsilon_3 \quad (4.31)$$

Dilation is invariant There is a useful property of tensors which can help us calculate Δ . In a coordinate transformation, some properties of tensors (*invariants*) do not change. The sum of the diagonal components is an invariant. It is then always possible to find the dilation through

$$\Delta = \epsilon_1 + \epsilon_2 + \epsilon_3 \text{ (principal axes)} = \varepsilon_{11} + \varepsilon_{22} + \varepsilon_{33} \text{ (arbitrary axes)} \quad (4.32)$$

Exercises

1. To monitor strain, it is possible to use optical marks (fiducials) and keep track of them in a microscope during an experiment. Imagine that there are two fiducials A, B , separated in x and y by 1 cm. On heating a plate from 300 K to 400 K, fiducial A moves in (x,y) by (10, 20) in μm ; fiducial B moves by (15,40) in μm . Assuming that the strain is uniform in the plate, calculate

- Drift (total displacement) of the plate
- Rotation of the plate
- The tensor strain
- The thermal expansion coefficient α , neglecting any strain normal to the surface.

Chapter 5

Elasticity and thermodynamics

In this chapter, we will introduce elasticity and elastic moduli, and see what elasticity has to do with thermodynamic quantities. We will focus on isotropic elasticity and consider anisotropy later on.

5.1 Isotropic elasticity

If the properties of a sample have no dependence on direction with respect to the sample axes, the properties are *isotropic*. Properties with a directional dependence are *anisotropic*. Physical anisotropy always relates to a microscopic anisotropy, an arrangement of atoms which is different in different directions, so glassy materials must be isotropic. Randomly-oriented polycrystalline samples of crystalline materials will also be isotropic, if the properties are averaged over scales larger than the grain size; we will return to this question in Section 6.7.

5.1.1 Parameters defining isotropic elasticity

There are six quantities used to describe isotropic elasticity. Out of the six quantities, only two are independent; any two can be used to determine the other four. This usually involves the choice of a relevant stress or strain state in which many terms drop out. The equivalences are tabulated in textbooks, e.g. *Elasticity: theory, applications, and numerics* by M. Saad, p. 85 (available as an e-book here.)

1. **Young's modulus E** In linear elasticity, uniaxial stress σ and strain ϵ are related through the Young's modulus E ,

$$\sigma_{11} = E\epsilon_{11} \quad (5.1)$$

if the stress σ is uniaxial: $\sigma_{ij} = \sigma_{11}$. This stress state can be brought about by applying a stress along one axis (aligned with $\hat{x_1}$) and keeping the other surfaces traction-free. The strain ϵ_{ij} will not be uniaxial, in general, under uniaxial stress.

The Young's modulus is always positive, and the maximum known value is for diamond, $E = 1035$ GPa. E has units of Pa.

2. **Poisson ratio ν** If a uniaxial stress σ_{11} is imposed on a solid, two orthogonal principal strains with opposite sign will also develop, given by the Poisson ratio ν ,

$$\epsilon_{22} = \epsilon_{33} = -\nu\epsilon_{11} \quad (5.2)$$

or

$$\nu = -\frac{\epsilon_{22}}{\epsilon_{11}} \quad (5.3)$$

If the imposed strain is tensile ($\epsilon_{11} > 0$), there is a *Poisson contraction* ($\epsilon_{22}, \epsilon_{33} < 0$); if the imposed strain is compressive ($\epsilon_{11} < 0$), there is a *Poisson expansion* ($\epsilon_{22}, \epsilon_{33} > 0$). Clearly ν is dimensionless.

There are restrictions on the Poisson ratio. From thermodynamic principles,

$$-1 \leq \nu \leq 0.5 \quad (5.4)$$

These limits are imposed by the bulk compressibility K and shear modulus μ , which must always be positive. It is always true that $\nu < 0.5$. A material with $\nu = 0.5$ is incompressible and a material with $\nu > 0.5$ would expand spontaneously. Most materials have $0.2 \leq \nu \leq 0.4$. A special case of $\nu = 0$ is cork, which makes it ideal for sealing wine bottles. (Incompressible rubber, $\nu = 0.5$, does not work at all since it expands outwards and jams when you try to push it in.) This is the only value of ν for which volume is conserved – there is

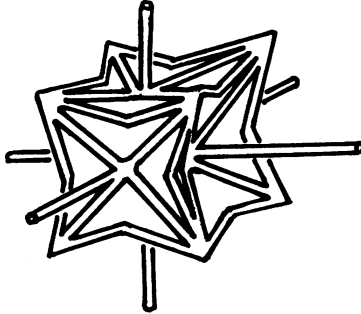


Fig. 3. Idealized reentrant unit cell produced by symmetrical collapse of a 24-sided polyhedron with cubic symmetry.

Figure 5.1: Idealization of an isotropic auxetic material, $\nu < 0$, taken from [1].

no general requirement of conservation of volume for a material under stress.

There is no restriction that ν needs to be positive. Negative effective values of ν can be seen in anisotropic materials, as will be seen. *Auxetic* materials have a negative Poisson ratio: they expand in the direction transverse to uniaxial tensile stress. This effect was first discovered in certain types of isotropic polymer foams in the late 1980s[1] and was understood as the unfolding of some structural links, as pictured in Figure 5.1.

Equivalences : If we choose (E, ν) as the basis, we can express all other elastic constants (shear modulus μ or G , bulk modulus K , Lamé coefficient λ , p-wave modulus M) in their terms. The choice of basis is arbitrary; we could equivalently choose (λ, G) or any other two of the six.

3. Compressibility β or bulk modulus K

If we exert a hydrostatic stress $-P = \sigma_{11} = \sigma_{22} = \sigma_{33}$ on the sample, the *bulk compressibility* β (also denoted as K^{-1}) is defined as

$$\beta \equiv -\frac{1}{V} \left(\frac{\partial V}{\partial P} \right)_T \quad (5.5)$$

Recalling the dilation,

$$\Delta = \varepsilon_{11} + \varepsilon_{22} + \varepsilon_{33} \quad (5.6)$$

which is invariant on coordinate transformations of the strain tensor, we can also express β as

$$\beta \equiv - \left(\frac{\partial \Delta}{\partial P} \right)_T \quad (5.7)$$

In the case of a uniaxial stress, $\sigma = \sigma_{11}$ only,

$$\Delta = \varepsilon_{11} + \varepsilon_{22} + \varepsilon_{33} = \frac{\sigma_{11}}{E} (1 - 2\nu) \quad (\sigma_{22} = \sigma_{33} = 0) \quad (5.8)$$

so that for an incompressible solid, with no change in volume for uniaxial stress, $\nu = 0.5$.

... in terms of E, ν Next imagine a sample under *hydrostatic stress*, $\sigma_1 = \sigma_2 = \sigma_3 = -P$. (The sign convention on P is such that positive work is done on the sample, increasing its energy, for positive pressure P : $\delta W = -PdV$, and $dV < 0$ in compression.) All the components are equal, and we have

$$\Delta = \varepsilon_{11} + \varepsilon_{22} + \varepsilon_{33} = - \frac{3P}{E} (1 - 2\nu) \quad (5.9)$$

so the sample shrinks on compression with $P > 0$. The ratio $\delta\Delta/\delta P$ is known as the bulk compressibility in thermodynamics,

$$\beta \equiv - \frac{1}{V} \left(\frac{\partial V}{\partial P} \right)_T = \frac{3}{E} (1 - 2\nu) \quad (5.10)$$

and $\beta > 0$. The thermal expansion α and compressibility β are important quantities in thermodynamic calculations; with the heat capacity C_p and density V^{-1} , they can be used to calculate most thermodynamic quantities of a given material.

The bulk modulus K is just the inverse of the compressibility β :

$$K \equiv \frac{1}{\beta} = \frac{E}{3(1 - 2\nu)} \quad (5.11)$$

where the units are the same as those of the Young's modulus (Pa). As ν approaches 0.5, the material becomes more and more difficult to compress under hydrostatic stress. The compressibility must be positive to obey the second law of thermodynamics (otherwise a system can spontaneously do work on the surroundings without generation of heat), so it is always true that $\nu \leq 0.5$.

4. **Shear modulus μ (G)** The shear modulus μ , also written as G , is given through e.g.

$$\tau_{xy} = \mu \gamma_{xy} \quad (5.12)$$

where γ_{xy} is the engineering shear strain, measured through the total angle through which two initially orthogonal \hat{x} and \hat{y} axes are rotated towards each other, on shear. Here $\tau_{xy} = \sigma_{xy}$ is the shear stress (exerted on the y -normal face in the x -direction). In terms of the tensor stresses and strains, the modulus would be

$$\sigma_{ij} = 2\mu \varepsilon_{ij} \quad (5.13)$$

as shown in Eq 4.25, for $i \neq j$. The shear modulus μ is also known as the second Lamé coefficient.

... in terms of E, ν Here we will find a formula for the shear modulus μ (or G) in terms of (E and ν). We can take a bar under uniaxial stress σ_{11} . It is possible, taking separate axes α and β to transform the uniaxial stress to pure shear stress through a $\pi/4$ (45°) rotation. Taking $a_{\alpha 1}$ as the cosine of the angle between α and x_1 , etc, the transformation is

$$\sigma_{\alpha\beta} = a_{\alpha i} a_{\beta j} \sigma_{ij} \quad (5.14)$$

$$\sigma_{\alpha\beta} = a_{\alpha 1} a_{\beta 1} \sigma_{11} \quad (5.15)$$

$$\sigma_{\alpha\beta} = \frac{1}{\sqrt{2}} \left(-\frac{1}{\sqrt{2}} \right) \sigma_{11} = -\frac{\sigma_{11}}{2} \quad (5.16)$$

Similarly, the strain tensor transforms

$$\varepsilon_{\alpha\beta} = a_{\alpha 1}a_{\beta 1}\varepsilon_{11} + a_{\alpha 2}a_{\beta 2}\varepsilon_{22} + a_{\alpha 3}a_{\beta 3}\varepsilon_{33} \quad (5.17)$$

$$\varepsilon_{\alpha\beta} = -\frac{1}{2}\varepsilon_{11} + \frac{1}{2}\varepsilon_{22} \quad (5.18)$$

$$\varepsilon_{\alpha\beta} = -\frac{\sigma_{11}}{2E}(1+\nu) \quad (5.19)$$

From $\mu = \sigma_{\alpha\beta}/2\varepsilon_{\alpha\beta}$,

$$G = \mu = \frac{E}{2(1+\nu)}$$

(5.20)

where G and μ are used interchangably for the shear modulus. Only positive values of the shear modulus are possible: for $\mu < 0$, the material will shear spontaneously without application of a shear stress or heat. Since $E > 0$, it has to be the case that $\nu > -1$.

5. First Lamé coefficient λ

The first and second Lamé coefficients λ and μ express the total elastic energy stored by an isotropic medium. The first Lamé coefficient, λ , contributes to the elastic energy only through normal strains; the second coefficient, the shear modulus μ (or G), contributes through both normal and shear strains. In dummy suffix notation, we can for now (until the discussion of elasticity parameters in Section ??) only assert, without proof, that the elastic energy expression takes the compact form

$$U = \frac{\lambda}{2}\varepsilon_{kk}\varepsilon_{ll} + \mu\varepsilon_{ij}\varepsilon_{ij} \quad (5.21)$$

which requires a bit of unpacking. There are implied sums in each of the repeated indices k , l , and ij : ε_{jj} and ε_{kk} (three terms each) as well as $\varepsilon_{ij}\varepsilon_{ij}$ (nine terms). More explicitly,

$$U = \frac{\lambda}{2} \left(\sum_{i=1}^3 \varepsilon_{ii} \right)^2 + \mu \sum_{i=1}^3 \sum_{j=1}^3 \varepsilon_{ij}^2 \quad (5.22)$$

Material	E (GPa)	ν	other info
Al	69	0.33	$T_M = 933$ K
Ti	107	0.34	$T_M = 1941$ K
Cu	110	0.34	$T_M = 1358$ K
Ni	207	0.31	$T_M = 1728$ K
W	407	0.28	$T_M = 3695$ K
C (diamond)	1035	0.1-0.3	-
pyrex	64	-	-
wood	5-15	-	-
silicone rubber	0.05	-	-
PTFE	0.4-0.6	0.46	-

Table 5.1: Some elastic properties, mostly from Callister.

$$U = \frac{\lambda}{2} (\varepsilon_{11} + \varepsilon_{22} + \varepsilon_{33})^2 + \mu (\varepsilon_{11}^2 + \varepsilon_{22}^2 + \varepsilon_{33}^2) + 2\mu (\varepsilon_{12}^2 + \varepsilon_{23}^2 + \varepsilon_{31}^2) \quad (5.23)$$

where we made use of the symmetry of the strain tensor, $\varepsilon_{ij} = \varepsilon_{ji}$. The first Lamé parameter does not need to be positive (although it typically is.) A sample under hydrostatic stress needs to have positive strain energy, but some of this energy is stored in the μ term.

6. p-wave modulus M

The *p* – wave modulus M is useful in problems on elastic waves. It is defined as the ratio of longitudinal stress to longitudinal strain in a uniaxial strain state:

$$\sigma_{11} = M\varepsilon_{11} \quad \varepsilon_{22} = \varepsilon_{33} = \varepsilon_{12} = \varepsilon_{23} = \varepsilon_{31} = 0 \quad (5.24)$$

5.2 Thermodynamics of elasticity

Mechanical work done on an elastic solid will store energy in the solid. A general form for the elastic energy will be derived in Section 5.2.1. In Section 5.2.2, we will see that there exists an alternate microscopic origin for the elastic response, separate from the energetic origin discussed in Chapter 1: strain-induced changes in *entropy* can also create elastic forces. These are

relevant for some polymers, as well as for certain types of oxides. Because heat and work are relevant for thermal expansion α and compressibility β , one might guess that there are thermodynamic limits to these quantities; the limits are discussed in Section 5.2.3, and the relationship between the parameters, the *Grüneisen function*, is discussed in Section 5.2.4.

5.2.1 Elastic energy

If deformation is entirely elastic, *all* mechanical work done on a solid is conserved, and stored in elastic energy. Only when some departure from elasticity exists – either anelasticity, discussed in Section 8.3, or plasticity, discussed thereafter, can mechanical work be lost to heat. Therefore we assume elastic displacements: zero force, $F = 0$, for zero displacement, $\delta x = 0$, and $F = -k\delta x$, where k is some spring constant. The forces applied are in the direction of the displacement.

Elongation First, we can consider the material under a normal stress. The differential mechanical work done on the crystal, if carried out reversibly, will increase the (extensive) internal elastic energy δu :

$$\delta w = \delta u = F_x \delta x \quad (5.25)$$

and taking $F = \sigma_{11}A_0$, $\Delta x = l_0\varepsilon_{11}$,

$$\delta w = \delta u = A_0 l_0 \sigma_{11} \delta \varepsilon_{11} \quad (5.26)$$

$$\delta u = A_0 l_0 \sigma_{11} \delta \varepsilon_{11} \quad (5.27)$$

now for the stored energy density in this reversible deformation, with normal stress and strain in the x direction, $U = u/V$, where the volume $V = A_0 l_0$, we find for the *differential* increase in elastic energy

$$\boxed{\delta U = \sigma_{11} \delta \varepsilon_{11}} \quad (5.28)$$

without any factor of two. To find the total elastic energy stored, we cannot just take constant σ_{11} and let the change in strain be $\delta \varepsilon_{11}$, because the stress (force) changes with strain (elongation), as in a spring. Assuming an elastic response, $\sigma_{11} = E\varepsilon_{11}$,

$$\delta U = E \varepsilon_{11} \delta \varepsilon_{11} \quad (5.29)$$

Integrating from $0 \leq \varepsilon_{11} \leq \varepsilon_{11,f}$, the final elastic energy U_1 , taking $U_0 = 0$, will be

$$U_1 = \frac{E}{2} \varepsilon_{11,f}^2 \quad (5.30)$$

Alternatively, in terms of the **final** stress σ_{11} and strain ε_{11} , the *final* elastic energy volume density will be

$$U = \frac{\sigma_{11}\varepsilon_{11}}{2} \quad (5.31)$$

where we dropped f from the notation. The other faces of the crystal may also be displaced in the deformation, due to e.g. Poisson contractions, but no traction is exerted upon them and so no work is done upon them. may change in area, but their centers are not displaced in the x_1 direction, so no work is done upon them. This argument can be extended to all normal stresses.

Shear For a shear strain, the situation will be similar. Taking the shear stress σ_{21} as an example, the only face which undergoes a displacement in the direction of the σ_{21} shear force (i.e. \hat{x}_2) will be the face with normal \hat{x}_1 . Thus, similarly to the case for normal stresses σ_{ii} which do work only through strains ε_{ii} , shear stresses σ_{ij} do work only through strains ε_{ij} . The net result is that all terms for work done on the material take the form $\sigma_{ij} \varepsilon_{ij}$. These will sum in the total elastic energy:

$$\Delta W = \frac{1}{2} (\sigma_{11}\varepsilon_{11} + \sigma_{22}\varepsilon_{22} + \sigma_{33}\varepsilon_{33} + 2\sigma_{12}\varepsilon_{12} + 2\sigma_{23}\varepsilon_{23} + 2\sigma_{31}\varepsilon_{31}) \quad (5.32)$$

or in dummy suffix notation,

$$U \equiv \Delta W = \frac{\sigma_{ij}\varepsilon_{ij}}{2} \quad (5.33)$$

Since the deformation is elastic, all the work which has gone into deformation is recoverable, so the internal energy per unit volume U is equated with the work ΔW .

5.2.2 Entropic elasticity in polymers

In perfectly crystalline solids (metals, ceramics), elastic deformation would seem to be an energy-conserving process. The positions of atoms do not change with respect to each other during the deformation, regardless of the strain rate, so little or none of the strain energy can be dissipated as heat. Here as we saw before in our discussion of empirical potential models, the

change in free energy $F = U - TS$ of the solid (where U is the internal energy and S is the entropy) is dominated by the internal energy U . Elastic deformation in a perfect crystal is then adiabatic, without heat flow to the surroundings. (If we allow atoms to move with respect to each other, they will lose energy; this will be covered in anelasticity or *internal friction*.)

In polymers, the situation is different. If you hold a rubber band up to your lip and stretch it (the rubber band, not your lip) out, you can feel the rubber band get hot. If you let the rubber band relax, it cools down. The dominant term to the free energy which changes with strain is the entropy S of the polymer. When it stretches out, its entropy goes down, and heat ($\delta Q \geq TdS$) flows to the surroundings.

To see how entropy has an effect on elasticity, consider the internal energy U ,

$$dU = T dS - P dV \quad (5.34)$$

or rearranged,

$$dS = \frac{1}{T} dU + \frac{P}{T} dV \quad (5.35)$$

where we can identify

$$dS = \left(\frac{\partial S}{\partial U} \right)_V dU + \left(\frac{\partial S}{\partial V} \right)_U dV \quad (5.36)$$

This implies

$$P = T \left(\frac{\partial S}{\partial V} \right)_U \quad (5.37)$$

or if we just consider that the length l of the solid changes and its area A stays the same, $V = Al$, $dV = Adl$, $P = f/A$, where f is the force:

$$f = T \left(\frac{\partial S}{\partial l} \right)_U \quad (5.38)$$

The entropy of the polymer changes with its length l , so this derivative is negative. We can remember the result of the random walk problem. If one takes N steps randomly, either to the left or the right with equal probabilities, the most likely outcome is equal numbers of right and left steps and no net displacement. The total number of N step configurations to create a given value of s , known as the multiplicity $g(s, N)$, is

$$\ln g(s, N) = \ln g(0) - \frac{2s^2}{N} \quad (5.39)$$

A polymer is a number of carbon backbone links which can point to the left or right, and for no net displacement, the end-to-end length of the polymer chain is $l = 0$. However a difference in the number of up and down steps $2s$, $N^\uparrow - N^\downarrow = 2s$, is possible, with finite length; for an excess s , link length $|\rho|$, $l \sim 2s|\rho|$. This means the entropy can be expressed in terms of the length as

$$\ln g(s, N) = \ln g(0) - \frac{l^2}{2|\rho|^2 N} \quad (5.40)$$

Here the entropy S is just $S = k_B \ln g$. This gives

$$\left(\frac{\partial S}{\partial l} \right)_U = - \frac{k_B}{|\rho|^2 N} l \quad (5.41)$$

The entropy of the polymer decreases when it is stretched out. In the extreme limit where it is fully stretched out with $l = \rho N$, there is only one possible configuration ($g = 1$), so it is in a highly ordered state, and its entropy is at a minimum. One has to pull on the system in order to decrease its entropy, and its resistance is the 'spring constant' of a rubber. We can recognize here a spring constant for the rubber

$$k = \frac{k_B T}{|\rho|^2 N} \quad (5.42)$$

in units of J/m² or N/m. The model predicts that the Young's modulus of the polymer (neglecting Poisson contraction) is proportional to temperature, becoming stiffer as the temperature is increased.

5.2.3 Thermal expansion and compressibility parameters in thermodynamic quantities

We defined the thermal expansion and compressibility before,

$$\alpha \equiv \frac{1}{V} \frac{\partial V}{\partial T}_P \quad K^{-1} = \beta \equiv - \frac{1}{V} \left(\frac{\partial V}{\partial P} \right)_T \quad (5.43)$$

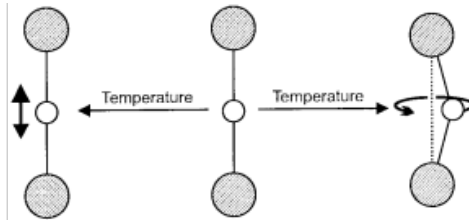


Figure 5.2: Illustration of NTE material, right. Figure taken from [2].

Sign of α : negative thermal expansion (NTE)

Note that α does not need to be positive. There do exist crystals for which the thermal expansion coefficients are isotropic and negative: the material shrinks on heating. A recently discovered example is cubic tungsten zirconate, $Zr W_2O_8$. This shows a negative dilation of $\sim -0.25\%$ on increasing the temperature from 4.2 to 300 K, or $\alpha_1 \sim 3 \times 10^{-6} K^{-1}$ ¹

Here the negative response can be understood from one of the Maxwell relations in thermodynamics,

$$\bar{\alpha} = \frac{1}{V} \left(\frac{\partial V}{\partial T} \right)_P = - \left(\frac{\partial S}{\partial P} \right)_T \quad (5.44)$$

where S is the entropy and P is the pressure. Typically entropy decreases with pressure, since the number of internal degrees of freedom of a system decreases when a system (e.g. a gas) is compressed, but in a compound of this type, the opposite might be true. As illustrated in Figure 5.2, on the right, the compression of an $A - B - A$ bond might allow B to vibrate more freely in the transverse direction. Thus increasing P also increases entropy S , leading to NTE.

Additionally, in covalent compounds Si, Ge, and similar, α becomes negative at low temperature.

Use in equivalences

Taken together, α and β can be used as differential volume expansion coefficients,

$$dV = \left(\frac{\partial V}{\partial T} \right)_P dT + \left(\frac{\partial V}{\partial P} \right)_T dP \quad (5.45)$$

¹"Negative Thermal Expansion from 0.3 to 1050 Kelvin in ZrW_2O_8 ," T.A. Mary, J.S.O. Evans, T. Vogt, A.W. Sleight, **Science** 272 90 (1996).

$$dV = \alpha V dT - \beta V dP \quad (5.46)$$

Any thermodynamic differential ($dU, dS, dV, dH, dF, dG \dots$) can be expressed in terms of α, β, C_p , and differentials in pressure and temperature (dP, dT). This makes it possible to express any of these quantities in terms of these three experimentally determined variables. As an example, take the heat capacities at constant pressure $C_P(T)$ and constant volume $C_V(T)$:

$$\left(\frac{\partial H}{\partial T} \right)_P \equiv C_P(T) \quad C_V(T) = C_P(T) - \frac{TV\alpha^2}{\beta} \quad (5.47)$$

So α and β are even more useful than they would first appear to be.

5.2.4 Grüneisen function

At the same time, the thermal expansion and compressibility (or inverse bulk elastic modulus K^{-1}) are not entirely independent. We got a feeling for their interdependence already from the bonding model in Chapter 1. The thermal expansion arises from the anharmonicity of the potential, but this also gave a softening of the elastic modulus E (or here $K = E/(3[1 - \nu])$) with increasing temperature.

Grüneisen defined a parameter γ which describes the interdependence, relating a change in the lattice vibration frequency ω to a change in the atomic volume V :

$$\gamma_i = -\frac{\partial \ln \omega_i}{\partial \ln V} \quad (5.48)$$

for mode ω_i . We are somewhat familiar with the idea of the interdependence described by γ from the temperature-dependence of bonding parameters. The resonance frequency softens ($\Delta\omega < 0$) and the interatomic spacing expands ($\Delta V > 0$) with higher-amplitude vibrations of the bound atoms, so $\gamma > 0$. Both phenomena are described by the anharmonicity s of the bond. In the Debye model, Gruneisen showed that α, β , and C_V will be related through

$$\alpha = \gamma \frac{\beta C_V}{V} \quad (5.49)$$

if all modes have the same Grüneisen parameter γ_i . Particularly in the high-temperature limit above the Debye temperature $T \gg \theta$, the heat capacity is constant, $C_V \sim 3k_B$. Thus

$$\alpha \sim (3k_B n_A \gamma) \beta \quad (5.50)$$

where the atomic density is written $n_A = V^{-1}$. This form is useful for earth scientists since a full set of α, β data as a function of high temperature or pressure may not be available for a given type of core material, so one can be used to estimate the other.

The Grüneisen parameter is not always a constant as a function of temperature. Particularly for Si, Ge, and similar compounds, γ is not very meaningful; α (but obviously not β) changes sign at low temperature. However it is roughly constant and around 1 – 2 for most materials. It explains that soft materials with low bulk modulus K and high compressibility will, usually, have high coefficients of thermal expansion α .

Exercises

1. Derive a relationship for the p-wave modulus M in terms of the Young's modulus E and Poisson ratio ν .
2. Under what circumstances can the (volumetric) thermal expansion coefficient α be calculated from a single measurement of linear thermal expansion $\delta l/l$?
3. Gold has a Debye temperature of $\theta \sim 162$ K, a Young's modulus of $E = 79$ GPa, and a Poisson ratio of $\nu = 0.43$. Estimate its thermal expansion coefficient, making a reasonable assumption about γ .
4. Derive an approximate expression for the Gruneisen parameter in terms of anharmonicity s and equilibrium interatomic spacing d_0 of the bonds, using the diatomic model. (*Hint:* how do the vibrational frequency and interatomic spacing change with temperature?) You can assume the solid is isotropic and that the changes are small (i.e. Taylor expand quantities where relevant.) Use your results for Cu₂ from HW 1 to estimate γ in Cu. (The experimental value is 1.9)

Bibliography

- [1] Roderic Lakes. “Foam Structures with a Negative Poissons Ratio”. In: *Science* 235.4792 (1987), pp. 1038–1040. DOI: [10.1126/science.235.4792.1038](https://doi.org/10.1126/science.235.4792.1038).
- [2] John S. O. Evans. “Negative thermal expansion materials”. In: *J. Chem. Soc., Dalton Trans.* (19 1999), pp. 3317–3326. DOI: [10.1039/A904297K](https://doi.org/10.1039/A904297K).

Chapter 6

Anisotropic elasticity

In the previous chapter, we examined the isotropic elastic properties of materials. Here we will examine anisotropic elasticity. Quantities like the Young's modulus E and Poisson ratio ν generally depend on the directions of stress and strain in crystalline materials. Artificial, composite materials can also be elastically anisotropic, usually by design.

6.1 Stiffness and compliance

The elastic properties of materials can be defined either in terms of tensor *stiffnesses* [c] or in terms of tensor *compliances* [s]. To find the stresses from the strains, use the stiffnesses c

$$\sigma_{ij} = c_{ijkl} \varepsilon_{kl} \quad (6.1)$$

Note the implied sum over k and l , with nine terms to each σ_{ij} . Alternatively, to find the strains from the stresses, use the compliances s

$$\varepsilon_{ij} = s_{ijkl} \sigma_{kl} \quad (6.2)$$

The stiffnesses c_{ijkl} are useful when we have a well-known *strain state* ε_{kl} ; the compliances s_{ijkl} are useful when we have a well-known *stress state* σ_{kl} .

Mnemonic : The symbol does **not** match the first letter of the name: s for compliance, c for stiffness. The word describes the tendency of a larger value: a stiffer material (c) means a greater stress for imposed strain, a more compliant material (s) means a greater strain for an imposed stress.

6.1.1 Simple stress configurations: use of compliance

If we know the forces that are exerted on the sample boundaries, but not necessarily the dimensions of the sample after the response, the stress state is well-defined, and we use the compliances s .

1. **Uniaxial normal stress:** If tractions are exerted only on one set of faces of a body, normal to those faces, the stress state will be uniaxial and normal at the surface, $\sigma_{11} = \sigma$. If the body has a constant cross-sectional area along \hat{x}_1 , the stress $\sigma_{11} = \sigma$ will be constant. This would be the case for a cylinder, without body forces, under tension at the ends. Here we would use the value s_{1111} :

$$\varepsilon_{11} = s_{1111} \sigma_{11} \quad (6.3)$$

to calculate the elongation. The compliance s_{ijkl} relates the imposed stress σ_{kl} to the resultant strain ε_{ij} , and we are interested in σ_{11} causing ε_{11} . In this case, we know the tension T in the line, and we know the cross-sectional area S of the line, so $\sigma = T/S$.

2. **Young's modulus equivalent:** The Young's modulus is defined for uniaxial stress as

$$\varepsilon_{11} = \frac{\sigma_{11}}{E} \quad (6.4)$$

Therefore to find the Young's modulus, we need the compliance:

$$E \equiv \frac{1}{s_{1111}} \quad (6.5)$$

3. **Shear modulus equivalent**

Similarly, the shear modulus is found for an imposed shear stress σ_{12} :

$$\varepsilon_{12} = s_{1212} \sigma_{12} \quad (6.6)$$

We will see later on, in Eq 6.48, that a number of factors of two need to be taken into account to translate s_{1212} to the isotropic shear modulus μ or G , so that for an isotropic solid,

$$\mu \equiv \frac{1}{4s_{1212}} \quad (6.7)$$

and $\mu = 1/s_{44}$ in matrix notation. However it is this compliance which is relevant for an imposed simple shear stress $\sigma_{12} = \sigma_{21}$, without other components; $\sigma_{ij} = 0$ for $i, j \neq 1, 2$ and $2, 1$.

6.1.2 Simple strain configurations: use of stiffness

If the dimensions of the sample are specified, but the forces exerted on the sample boundaries are not, we use the stiffnesses c to find the stresses:

1. **Uniaxial strain** states are relevant if one dimension of the sample geometry is constrained. For example, we can take a plate of a sample, thickness t which fits exactly in a gap between two rigid walls, also of thickness t . If we imagine that the sample heats up, but the walls do not, thermal expansion will dictate that $\delta\varepsilon_{11} = \alpha\Delta T/3$ (for a cubic or isotropic material.) What happens? The material cannot expand, so the sum of the thermal and traction strains must be zero

$$\varepsilon_{11}^{th} + \varepsilon_{11}^{traction} = 0 \quad (6.8)$$

So here we would take $\varepsilon_{11} = -\varepsilon_{11}^{th}$ and find the thermal stress through

$$\sigma_{11} = -c_{1111}\varepsilon_{11}^{th} \quad (6.9)$$

where $\sigma_{11} < 0$, a compressive stress.

2. **Biaxial strain** Biaxial strains are important in epitaxial thin-film growth. Here we know that the crystal structure of the substrate must match the crystal structure of the film. For homoepitaxy, e.g. Si grown on top of Si, there is no misfit and no strain. For heteroepitaxy, e.g. $\text{Si}_{1-x}\text{Ge}_x$ on Si(100), the alloy has a lattice constant which can be about 1% different from that of the substrate. This places the film in a biaxial strain state, $\varepsilon_{11} = \varepsilon_{22}$.

6.2 General restrictions on elastic tensors

Because the stiffnesses c_{ijkl} and the compliances s_{ijkl} are fourth-rank tensors, there are $3^4 = 81$ components to each, and, in principle, 81 possible elastic constants for each. However, many of these constants have to be equal to each other, and many need to be zero. Formal considerations alone reduce the number of independent values to **21**, before considering anything about the material symmetry.

6.2.1 Experimental inaccessibility

Imagine that in an experiment we would like to measure c_{1223} . This means that we would impose a known strain ε_{23} and try to measure the shear stress σ_{12} . This stiffness can be nonzero.

However, because the tensor strain is symmetric, at the same time as we impose ε_{23} , we impose an equal ε_{32} . Therefore we will have

$$\sigma_{12} = c_{1223}\varepsilon_{23} + c_{1232}\varepsilon_{32} \quad (6.10)$$

$$\sigma_{12} = (c_{1232} + c_{1223})\varepsilon_{23} \quad (6.11)$$

and because there is no way to vary these two strains independently of each other in an experiment, one could never detect a difference in c_{1232}, c_{1223} , if it existed. It then makes sense to set

$$c_{ijkl} = c_{ijlk} \quad (6.12)$$

Similarly, if we look at the transposed strain σ_{ji} , here

$$\sigma_{21} = c_{2123}\varepsilon_{23} + c_{2132}\varepsilon_{32} \quad (6.13)$$

it too must be equal to σ_{ij} (here σ_{12}), since the stress tensor is symmetric. This is possible only if

$$c_{ijkl} = c_{jikl} \quad (6.14)$$

This reduces the number of independent elements dramatically. For each ij in c_{ijkl} , there were nine components specifying kl pairs before considering the symmetry $c_{ijkl} = c_{ijlk}$, but afterwards, there are six. Similarly, for each kl pair in $c_{ijkl} = c_{jikl}$, the symmetry reduces the number of independent ij components to six. The same argument could be made for s_{ijkl} . The total number of independent c_{ijkl} or s_{ijkl} values is therefore reduced from **81** to **36**.

6.2.2 Symmetry of stiffness and compliance matrices

Next we can make a thermodynamic argument to reduce the number of independent values of c_{ijkl} , s_{ijkl} further. The form for the elastic energy will place further constraints on the values of c_{ijkl} , s_{ijkl} . We will consider the energy in a biaxial strain state, ε_{11} , ε_{22} , although the relation will hold for any combination of strains for which the relevant stiffnesses are nonzero. The elastic energy $U = \Delta W$ can be written for a differential strain $\delta\varepsilon_{ij}$ as

$$\delta U = \sigma_{ij} \delta \varepsilon_{ij} \quad (6.15)$$

expressed in terms of the stiffness, using Eq 6.1, as

$$\delta U = c_{ijkl} \varepsilon_{kl} \delta \varepsilon_{ij} \quad (6.16)$$

Next, assuming that there are only two strain components, ε_{11} and ε_{22}

$$\delta U = (c_{1111} \varepsilon_{11} + c_{1122} \varepsilon_{22}) \delta \varepsilon_{11} + (c_{2211} \varepsilon_{11} + c_{2222} \varepsilon_{22}) \delta \varepsilon_{22} \quad (6.17)$$

Now we can see what happens to the total energy if we strain the crystal in different sequences. We will change the strain state from $(\varepsilon_{11}, \varepsilon_{22})$ to $(\varepsilon_{11} + \delta \varepsilon_{11}, \varepsilon_{22} + \delta \varepsilon_{22})$, through two different paths. The values of the strains are taken to be equal: $\delta \varepsilon_{11} = \delta \varepsilon_{22}$. In path A, we will strain first in ε_{11} , then in ε_{22} . The total energy here is:

$$\delta U^A = (c_{1111} \varepsilon_{11} + c_{1122} \varepsilon_{22}) \delta \varepsilon_{11} + (c_{2211} [\varepsilon_{11} + \delta \varepsilon_{11}] + c_{2222} \varepsilon_{22}) \delta \varepsilon_{22} \quad (6.18)$$

In path B, we can strain first in ε_{22} and then in ε_{11} . The total energy change then is

$$\delta U^B = (c_{2211} \varepsilon_{11} + c_{2222} \varepsilon_{22}) \delta \varepsilon_{22} + (c_{1111} \varepsilon_{11} + c_{1122} [\varepsilon_{22} + \delta \varepsilon_{22}]) \delta \varepsilon_{11} \quad (6.19)$$

If we take the difference of the elastic energies for straining the crystal along these two different paths, since $\delta \varepsilon_{11} = \delta \varepsilon_{22} = \delta \varepsilon$, all terms in a single differential are equal. We will have finally

$$\delta U^A - \delta U^B = (\delta \varepsilon)^2 (c_{2211} - c_{1122}) \quad (6.20)$$

The elastic energy depends only on the final strain state, according to Eq 5.33, so there can be no dependence of the total energy on the path taken to that state, and the difference in Eq 6.20 has to vanish. We carried out the problem for $ij = 11$, $kl = 22$, but it would hold for any pair of values. This implies that the stiffness matrix must be symmetric:

$$\boxed{c_{ijkl} = c_{klji}} \quad (6.21)$$

The same holds true for the compliances,

$$\boxed{s_{ijkl} = s_{klji}} \quad (6.22)$$

This relationship says that the elasticity has to be the same if the stress and strain directions are interchanged.

Example We can consider a Poisson contraction. We impose a uniaxial stress and are interested in the transverse strain. Taking stress σ_{11} (on x), for the transverse strain ε_{22} (on y),

$$\varepsilon_{22} = s_{2211}\sigma_{11} \quad (6.23)$$

Now, if we exchange the stress and strain directions, so that the stress is on y and the strain is on x

$$\varepsilon_{11} = s_{1122}\sigma_{22} \quad (6.24)$$

In this case, the Poisson (transverse) strain does no work: $\sigma_{ij}\varepsilon_{ij} = 0$. Nevertheless, the requirement that elastic energy is path-independent says

$$s_{2211} = s_{1122} \quad (6.25)$$

even in the absence of any crystal symmetry. Thus the ratio of longitudinal stress σ to transverse strain ϵ_{\perp} , for unit uniaxial stress σ is the same in both configurations:

$$\frac{\varepsilon_{11}}{\sigma} \quad ([\sigma] = \sigma_{22}) \quad = \quad \frac{\varepsilon_{22}}{\sigma} \quad ([\sigma] = \sigma_{11}) \quad (6.26)$$

$$(6.27)$$

The symmetry reduces the total number of independent values for c_{ij} and s_{ij} from **36** to **21**.

Summary: the first two or last two indices may be interchanged: $ijkl \rightarrow jikl$, or $ijkl \rightarrow ijlk$. Also, the first pair of indices may be interchanged with the last pair: $ijkl \rightarrow klji$.

Example: I know c_{1112} ; what other terms do I know? Reversing the first two indices gives nothing new, so just $c_{1112} = c_{1121} = c_{1211}$; however, I may then combine operations, giving $= c_{2111}$.

6.3 Matrix notation

The elastic constants for anisotropic crystals are usually represented as a matrix, rather than as a fourth-rank tensor. The matrix is easier to write on a (two-dimensional) page. The matrix (tensor) stress gets flattened to a one-dimensional vector first by collapsing indices:

$$11 \rightarrow 1 \quad 22 \rightarrow 2 \quad 33 \rightarrow 3 \quad 23 \rightarrow 4 \quad 13 \rightarrow 5 \quad 12 \rightarrow 6 \quad (6.28)$$

represented in the matrix, there are only these six values to consider, since the matrix is symmetric:

$$\begin{bmatrix} \sigma_{11} & \sigma_{12} & \sigma_{13} \\ \sigma_{21} & \sigma_{22} & \sigma_{23} \\ \sigma_{31} & \sigma_{32} & \sigma_{33} \end{bmatrix} \rightarrow \begin{bmatrix} \sigma_1 & \sigma_6 & \sigma_5 \\ \cdot & \sigma_2 & \sigma_4 \\ \cdot & \cdot & \sigma_3 \end{bmatrix} \rightarrow \begin{bmatrix} \sigma_1 \\ \sigma_2 \\ \sigma_3 \\ \sigma_4 \\ \sigma_5 \\ \sigma_6 \end{bmatrix} \quad (6.29)$$

and the six-element vector holds all the matrix stresses σ_i , $i = 1 \dots 6$. Similarly, the tensor strain ε_{ij} is converted to the matrix engineering strain using the same scheme.

$$\begin{bmatrix} \varepsilon_{11} & \varepsilon_{12} & \varepsilon_{13} \\ \varepsilon_{21} & \varepsilon_{22} & \varepsilon_{23} \\ \varepsilon_{31} & \varepsilon_{32} & \varepsilon_{33} \end{bmatrix} \rightarrow \begin{bmatrix} \epsilon_1 & \epsilon_6/2 & \epsilon_5/2 \\ & \epsilon_2 & \epsilon_4/2 \\ & & \epsilon_3 \end{bmatrix} \rightarrow \begin{bmatrix} \epsilon_1 \\ \epsilon_2 \\ \epsilon_3 \\ \epsilon_4 \\ \epsilon_5 \\ \epsilon_6 \end{bmatrix} \quad (6.30)$$

Here the matrix shear strains are engineering strains, defined in Eq 4.21 to be a factor of two larger than the tensor shear strains:

$$\epsilon_4 = \gamma_{23} = 2\varepsilon_{23} \quad \epsilon_5 = \gamma_{13} = 2\varepsilon_{13} \quad \epsilon_6 = \gamma_{12} = 2\varepsilon_{12} \quad (6.31)$$

The matrix formulation becomes useful through the matrix stiffnesses c_{ij} and compliances s_{ij} :

$$\sigma_i = c_{ij} \epsilon_j \quad (6.32)$$

$$\epsilon_i = s_{ij} \sigma_j \quad (6.33)$$

The equality of elasticities c_{ij} when we interchange strain directions ϵ_i and stress directions σ_j , discussed in Section 5.2.1 implies

$$\boxed{c_{ij} = c_{ji}} \quad (6.34)$$

and similarly for the compliances,

$$\boxed{s_{ij} = s_{ji}} \quad (6.35)$$

and since there are six indices, this reflects the reduction of independent elements from 36 to 21.

6.3.1 Utility of the matrices: crystal and physical axes aligned

Tabulated elasticities are always given in terms of the matrix c_{ij} and s_{ij} . If the crystal axes are a convenient frame for a stress-strain calculation, particularly for a cubic, tetragonal, or orthorhombic system with orthonormal axes, and the stresses / strains aligned along them, the problem can be attacked just with the matrix stiffness / compliances. This saves work. However if we are interested in stresses or strains not along orthonormal crystal axes, we will have to convert the matrix c_{ij} to tensor c_{ijkl} , or the matrix s_{ij} to tensor s_{ijkl} , and transform the tensor to new axes according to the relations in Eq 3.34. An example is shown in Section 6.5.

Example An orthorhombic crystal is deformed in compression, with $\sigma = -P$ along the [100] axis such that it cannot expand along [010] and [001]. What is its elastic modulus for the deformation? *Answer:* Here we know the strain state of the crystal: we have $\epsilon_{11} \rightarrow \epsilon_1$ only. The stiffnesses are needed

$$\sigma_i = c_{i1}\epsilon_1 \quad (6.36)$$

where the other strains $\epsilon_i = 0$. Stresses will develop along other axes as well, but to relate σ_1 to ϵ_1 , we can write

$$\frac{\sigma_1}{\epsilon_1} = c_{11} \quad (6.37)$$

6.3.2 Transformation of matrix to tensor elasticities

The matrix elasticities include many tensor components implicitly, so translation from matrix to tensor stiffness and compliance is not transparent. Conversion is straightforward for stiffnesses: matrix indices i, j are each converted to their two-index counterpart according to the relations 6.28. In matrix notation, for simple shear ϵ_6

$$\sigma_6 = c_{66}\epsilon_6 \quad (6.38)$$

where the same relation in tensor notation would be, due to the inevitable symmetric tensor strain component,

$$\sigma_{12} = c_{1212}\varepsilon_{12} + c_{1221}\varepsilon_{21} \quad (6.39)$$

and because $c_{ijkl} = c_{ijlk}$,

$$\sigma_{12} = c_{1212} 2\varepsilon_{12} \quad (6.40)$$

where $\epsilon_6 = 2\varepsilon_{12}$, so the components c are equal in the two representations. Generally, we can write for the stiffnesses

$$c_{1111} = c_{11} \quad c_{1122} = c_{12} \quad c_{1211} = c_{61} \quad c_{1212} = c_{66} \quad (6.41)$$

etc. However, for the compliances, there are factors of two involved. Here, for simple shear σ_6 , in a triclinic system, there could be a normal strain ϵ_1 , represented in the two systems

$$\epsilon_1 = s_{16}\sigma_6 \quad (6.42)$$

$$\varepsilon_{11} = s_{1112}\sigma_{12} + s_{1121}\sigma_{21} \quad (6.43)$$

$$\varepsilon_{11} = 2s_{1112}\sigma_{12} \quad (6.44)$$

implying

$$s_{1112} = s_{16}/2 \quad (6.45)$$

Where a factor 1/2 comes in for s_{ij} . Or for the shear modulus,

$$\epsilon_6 = 2\varepsilon_{12} = s_{66}\sigma_6 \quad (6.46)$$

$$\varepsilon_{12} = 2s_{1212}\sigma_{12} \quad (6.47)$$

$$s_{1212} = s_{66}/4 \quad (6.48)$$

Thus $\boxed{\mathbf{s}_{mn}}$ add factors of two and four as follows:

- $\boxed{s_{mn} = s_{ijkl} \text{ for } m, n = 1, 2, 3 :}$

cubics: $s_{1111} = s_{2222} = s_{3333} = s_{11}$

cubics: $s_{1122} = s_{2233} = s_{3311} = s_{2211} = s_{3322} = s_{1133} = s_{12}$

- $s_{mn}/2 = s_{ijkl}$ for m or $n = 4, 5, 6$
cubics: no such terms
- $s_{mn}/4 = s_{ijkl}$ for m and $n = 4, 5, 6$
cubics: $s_{1212} = s_{2323} = s_{3131} = s_{44}/4$

6.3.3 Elastic energy in matrix notation

Recall Eq 5.33 for the elastic energy in terms of the tensor stresses and strains,

$$U = \frac{\sigma_{ij}\varepsilon_{ij}}{2} = \frac{1}{2}(\sigma_{11}\varepsilon_{11} + \sigma_{22}\varepsilon_{22} + \sigma_{33}\varepsilon_{33}) + \sigma_{12}\varepsilon_{12} + \sigma_{23}\varepsilon_{23} + \sigma_{31}\varepsilon_{31} \quad (6.49)$$

where we made use of the symmetry of the tensors (adding two terms each for the strain terms.) In terms of the matrix stresses and strains, the above equation can be written

$$U = \frac{\sigma_i\varepsilon_i}{2} = \frac{1}{2}(\sigma_1\epsilon_1 + \sigma_2\epsilon_2 + \sigma_3\epsilon_3) + \frac{1}{2}(\sigma_6\epsilon_6 + \sigma_5\epsilon_5 + \sigma_4\epsilon_4) \quad (6.50)$$

where we used the relation between matrix shear and tensor shear strains, $\varepsilon_{12} = \epsilon_6/2$ etc. Thus we can sum elastic energies up also over the single matrix index $1 \leq i \leq 6$,

$$U = \frac{\sigma_i\epsilon_i}{2} \quad (6.51)$$

Recall that this relationship is the integration, over variable stress σ_i , of the differential relationship $\delta U = \sigma_i \delta \epsilon_i$ (no factor of one half, and over which σ_i is constant). We can then write equivalently, in matrix or tensor notation

$$\sigma_i = \left(\frac{\partial U}{\partial \epsilon_i} \right) \quad \sigma_{ij} = \left(\frac{\partial U}{\partial \epsilon_{ij}} \right) \quad (6.52)$$

6.4 Crystal symmetry

The symmetry of the crystal further reduces the number of independent c_{ijkl} and s_{ijkl} components. Neumann's principle describes the symmetry of the

physical properties of a crystal. We will examine Neumann's principle and its expression in tensor transformations.

6.4.1 Neumann's principle

Neumann's principle states

The symmetry elements of a physical property of a crystal must contain the symmetry elements of the point group of the crystal

Point groups refer to rotational symmetries of a crystal. We can think about rotations about a given axis; some axes in crystals have rotational symmetries, and 2-, 3-, 4-, and/or 6-fold rotations about these axes (by 180° , 120° , 90° , and 60° , respectively), depending on the type of crystal, bring about identical arrangements of atoms. For HCP metals, for example, the c-axis has sixfold rotational symmetry: rotations of 60° about lattice points bring about identical atomic arrangements. In FCC metals, all $\langle 111 \rangle$ axes have threefold rotational symmetry: 120° rotations bring about identical atomic arrangements.

Neumann's principle means that if we consider a physical property, like elasticity, in different crystal directions, the physical property needs to have *at least* the same rotational symmetry, but could also have even higher symmetry. For example, we can take a cubic crystal, and consider the Young's modulus $\varepsilon'_{ii} = s'_{iiii}\sigma'_{ii}$ in the (001) plane. Most classes of cubic crystal have fourfold rotational symmetry on (001). This means that if we look at the Young's modulus, $1/s'_{1111}$ as a function of angle, it has to *include*, i.e. respect, the symmetry of the crystal. It must be possible to rotate the stress/strain axis within the (001) plane and come up with the same compliance at 90° increments.

Newman's principle does *not* mean that there will be an evident fourfold symmetry of the Young's modulus in the (001) plane. The Young's modulus might be isotropic for the case considered. Isotropy implies that we can rotate by an infinitesimal or arbitrary angle and observe the same stiffness. One could call this a ∞ -fold axis; this symmetry is *higher* than fourfold, and obviously includes fourfold symmetry. We can still rotate by 90° and see the same properties.

6.4.2 Expression in tensor transformations

If we have a fourth-rank tensor, obeying

$$T'_{ijkl} = a_{im}a_{jn}a_{ko}a_{lp} T_{mnop} \quad (6.53)$$

and the rotation matrix (a) expresses a rotation defined by the point group of the crystal, then it will be true that

$$T_{ijkl} = T'_{ijkl} \quad (6.54)$$

This is a restatement of Neumann's principle: the physical properties will be the same after the rotation, and will therefore include the symmetry expressed in (a). Expanding the coordinate transformation for T'_{ijkl} ,

$$T_{ijkl} = a_{im}a_{jn}a_{ko}a_{lp} T_{mnop} \quad (6.55)$$

Notice that the left hand side, like the right, is in the *old* representation: it expresses equivalence between tensor components of a given crystal in a given representation tied to crystal axes.

Example: Consider the application of a uniaxial stress to a cubic crystal and the measurement of a normal strain along \hat{x}_1 only, described therefore by c_{1111} . If we consider the same operation along \hat{x}_2 only, this would be described by c_{2222} . Because the two crystal directions are related through a 90 deg. rotation (tetrad) about \hat{x}_3 , consistent with the point group of the crystal, the values c_{1111} and c_{2222} must be equal, according to Neumann's principle.

We can define a new coordinate system so that the new axes have been rotated with respect to the old through a rotation defined by the point group. For the 90 deg. right-hand rotation about \hat{x}_3 , we can take the transformation to be one which maps $\hat{x}_1 \rightarrow \hat{x}_2'$, $\hat{x}_2 \rightarrow -\hat{x}_1'$. The direction \hat{x}_2 will, in the crystal, have equivalent to the direction \hat{x}_1 .

If the transformation respects the symmetry of the crystal, it will be the case that

$$c'_{1111} = c_{1111} \quad (6.56)$$

but since all \hat{x}_1 directions are transformed as $\hat{x}_1 \rightarrow \hat{x}_2'$, this can be restated equivalently as

$$c_{2222} = c_{1111} \quad (6.57)$$

They are related by a symmetry operation (a) such that \hat{x}_1'

6.4.3 Cubic systems

Generalizing this result for other elements of the stiffness tensor for a cubic crystal, Neumann's principle can be restated as

$$c_{ijkl} = c'_{ijkl} \quad (6.58)$$

where

$$c'_{ijkl} = a_{im}a_{jn}a_{ko}a_{lp} c_{mnop} \quad (6.59)$$

and the a_{ij} values between new axis \hat{x}_i' and old axis \hat{x}_j describe a $\theta_3 = \pi/2$ rotation, a tetrad included in the point group:

$$(a) = \begin{bmatrix} 0 & 1 & 0 \\ -1 & 0 & 0 \\ 0 & 0 & 1 \end{bmatrix} \quad (6.60)$$

We can see according to this transformation which elements will be equal to each other and which need to be zero. In this discussion, we will consider only those components for which the product $a_{im}a_{jn}a_{ko}a_{lp} \neq 0$, because where they are zero, we cannot be sure that the terms c_{mnop} are zero.

Equal elements

In our prior example, taking the tensor normal stiffness along the new axis 1, c'_{1111}

$$c'_{1111} = a_{12}^4 c_{2222} \quad (6.61)$$

Because the individual elements of the new representation, also must be equal to those of the old, $c'_{ijkl} = c_{ijkl}$, this implies

$$c_{1111} = c_{2222} \quad (6.62)$$

or $c_{11} = c_{22}$ in matrix notation. The equalities $c_{22} = c_{33}$ and $c_{11} = c_{33}$ could be shown by taking tetrad axes along x_1 and x_2 respectively.

Using the same matrix (a) for the fourfold rotation about \hat{x}_3 , c_{1133} is

$$c'_{1133} = a_{1m}a_{1n} c_{mn33} \quad (6.63)$$

Note that when we write terms on the right hand side, because the matrix (a) preserves the x_3 component of a vector, any indices 3 must remain the same in the transformation, and we consider elements $mn33$ only. An

element with e.g. c_{mn32} would be zero in the transformation since $a_{32} = 0$. Similarly, from the terms in (a), there will be nonzero components only for $m = n = 2$, so again applying Neumann's principle (to drop the prime),

$$c_{1133} = c_{2233} \quad (6.64)$$

In matrix form, these are $c_{13} = c_{23}$, and since all three axes are equivalent, $c_{13} = c_{23} = c_{12}$. Next, for the shear component c_{2323} ,

$$c'_{2323} = a_{2m}a_{2o} c_{m3o3} \quad (6.65)$$

with nonzero components only for $m = o = 1$, so through Neumann's principle,

$$c_{2323} = c_{1313} \quad (6.66)$$

For the matrix shear stiffnesses, we can write $c_{44} = c_{55}$, and since all three axes are equivalent, $c_{44} = c_{55} = c_{66}$ also.

Elements equal to zero

Next, we would like to see if normal strains can result in a shear stress:

$$c'_{1233} = a_{1m}a_{2o} c_{mn33} \quad (6.67)$$

nonzero only for

$$c_{1233} = -c_{2133} \quad (6.68)$$

or from general symmetry, we can interchange the first two indices

$$c_{1233} = -c_{1233} \quad (6.69)$$

only possible if this element is equal to zero. Thus in matrix notation, $c_{63} = c_{62} = c_{61} = c_{53} = c_{52} = c_{51} = c_{43} = c_{42} = c_{41} = 0$ for cubic systems.

Similarly, what about a shear strain about one axis causing a shear stress about another? We take a shear strain on 23 giving us a shear stress on 12:

$$c_{2331} = a_{2m}a_{1p} c_{m33p} \quad (6.70)$$

$$c_{2331} = -c_{1332} \quad (6.71)$$

After carrying out the three transpositions, this is equal to

$$c_{2331} = -c_{2331} \quad (6.72)$$

Therefore this element also must be equal to zero. The matrix components which must vanish in cubic systems are then $c_{45} = c_{46} = c_{56} = 0$.

Result for cubics

For cubic crystals, independent stiffnesses c_{ij} are reduced by crystal symmetry from (21 to 3). The matrix is relatively simple:

$$(c) = \begin{bmatrix} c_{11} & c_{12} & c_{12} & \cdot & \cdot & \cdot \\ c_{11} & c_{12} & \cdot & \cdot & \cdot & \cdot \\ c_{11} & \cdot & \cdot & \cdot & \cdot & \cdot \\ c_{44} & \cdot & \cdot & \cdot & \cdot & \cdot \\ c_{44} & \cdot & & & & \\ c_{44} & & & & & c_{44} \end{bmatrix} \quad (6.73)$$

- $\boxed{c_{11}}$ refers to the stiffness for a normal stress along one crystal direction and a normal strain along *the same* crystal direction. Describes (tensor notation) the relationship between σ_{ii} and ε_{ii} . $\sigma_{ii} = \dots + c_{1111}\varepsilon_{ii}$ (tensor notation) or $\sigma_i = \dots + c_{11}\epsilon_i$ ($i \leq 3$) (matrix notation.) Three identical entries: $\boxed{c_{11} = c_{22} = c_{33}}$, or three tensor values: $c_{1111}, c_{2222}, c_{3333}$.
- $\boxed{c_{12}}$ refers to the stiffness for a normal stress along one crystal direction and a normal strain along *another* crystal direction. Describes (tensor notation) the relationship between σ_{ii} and ε_{jj} . $\sigma_{ii} = \dots + c_{1122}\varepsilon_{jj}$ (tensor notation) or $\sigma_i = \dots + c_{12}\epsilon_j$ (matrix notation.) Three identical entries: $\boxed{c_{12} = c_{23} = c_{31}}$, or six tensor values: $c_{1122}, c_{2211}, c_{1133}, c_{3311}, c_{2233}, c_{3322}$.
- $\boxed{c_{44}}$ refers to the stiffness for a *shear stress* about one crystal direction and a shear strain about *the same* crystal direction. Describes (tensor notation) the relationship between σ_{ij} and ε_{ij} . $\sigma_{ij} = \dots + c_{ijij}\varepsilon_{ij}$ (tensor notation) or $\sigma_i = \dots + c_{44}\epsilon_i$ ($i \geq 4$) (matrix notation.) Three identical entries: $\boxed{c_{44} = c_{55} = c_{66}}$, and six tensor values: $c_{1212}, c_{2121}, c_{1313}, c_{3131}, c_{2323}, c_{3232}$.

6.5 Young's modulus in a given cubic direction

To calculate the Young's modulus in an arbitrary direction l_i (unit length), define a new compliance matrix s'_{ijkl} in new axes such that the direction l_i is set along the x'_1 axis. The vector l_i is defined in the 'old' coordinate system. The rotations of the other new axes x'_2, x'_3 do not matter. We can then see that

$$a_{1i} = l_i \quad (6.74)$$

Our job will be to calculate s'_{1111} : stress and strain both applied along l_i . To carry out the tensor transformation, we have, in general for a fourth-rank tensor,

$$T'_{ijkl} = a_{im}a_{jn}a_{ko}a_{lp}T_{mnop} \quad (6.75)$$

so in this case, it is

$$s'_{1111} = a_{1m}a_{1n}a_{1o}a_{1p}s_{mnop} \quad (6.76)$$

or

$$s'_{1111} = l_i l_j l_k l_l s_{ijkl} \quad (6.77)$$

after changing axes. Remember that there are only three types of nonzero components: three s_{11} (E -type) terms,

$$s_{1111} = s_{2222} = s_{3333} = s_{11} \quad (6.78)$$

six s_{12} (ν -type) terms

$$s_{1122} = s_{2233} = s_{3311} = s_{2211} = s_{3322} = s_{1133} = s_{12} \quad (6.79)$$

and **twelve** s_{44} (μ -type),

$$s_{1212} = s_{2323} = s_{3131} = \dots \quad (6.80)$$

$$s_{2121} = s_{3232} = s_{1313} = \dots \quad (6.81)$$

$$s_{1221} = s_{2332} = s_{3113} = \dots \quad (6.82)$$

$$s_{2112} = s_{3223} = s_{1331} = \frac{s_{44}}{4} \quad (6.83)$$

$$(6.84)$$

We have seen why the factor $1/4$ multiplies s_{44} in Eq ???. This gives a total of **21** terms to consider. (This will be necessary for all cubic elasticity transformation problems.) Then we have in the implicit sum,

$$\begin{aligned}s'_{1111} = & (l_1^4 + l_2^4 + l_3^4) s_{11} + 2(l_1^2 l_2^2 + l_2^2 l_3^2 + l_3^2 l_1^2) s_{12} + \\ & 4(l_1^2 l_2^2 + l_2^2 l_3^2 + l_3^2 l_1^2) \frac{s_{44}}{4}\end{aligned}$$

Next, recognize that because l_i is a unit vector,

$$(l_1^2 + l_2^2 + l_3^2)^2 = 1 \quad (6.85)$$

$$(l_1^4 + l_2^4 + l_3^4) + 2(l_1^2 l_2^2 + l_2^2 l_3^2 + l_3^2 l_1^2) = 1 \quad (6.86)$$

$$(6.87)$$

so that

$$(l_1^4 + l_2^4 + l_3^4) = 1 - 2(l_1^2 l_2^2 + l_2^2 l_3^2 + l_3^2 l_1^2) \quad (6.88)$$

Rewriting the equation for s'_{1111} ,

$$s'_{1111} = s_{11} + (2s_{12} - 2s_{11} + s_{44})(l_1^2 l_2^2 + l_2^2 l_3^2 + l_3^2 l_1^2) \quad (6.89)$$

or

$$\boxed{\bar{s} = s_{11} - 2(s_{11} - s_{12} - \frac{s_{44}}{2})(l_1^2 l_2^2 + l_2^2 l_3^2 + l_3^2 l_1^2)} \quad (6.90)$$

where the term in the parentheses is an anisotropy factor: if it is zero, the response is isotropic.

For stiffnesses, the transformation to \bar{c} is just the same, except that in the conversion from tensor to matrix shear, there is no factor of four; $c_{44} = c_{1212}$, etc, where $s_{44} = 4s_{1212}$. This means we can replace s_{11} with c_{11} , s_{12} with c_{12} , but s_{44} with $4c_{44}$:

Example: (110) plane We can see how this works out for a thin plane sample of a FCC crystal, cut along 110 planes. Normal stress and strain are applied along a given plane direction. We define the angle θ as the right-handed rotation of the stress σ'_{11} and strain ϵ'_{11} directions away from [110]. The direction of stress and strain in the crystal, along the crystal axes, is then

material	$s_{11}(\text{TPa})^{-1}$	$s_{12}(\text{TPa})^{-1}$	$s_{44}(\text{TPa})^{-1}$
Cu	15.0	-6.3	13.3

Table 6.1: Compliances for (FCC) Cu, Landolt-Bornstein tables. Note that s_{12} is negative since it reflects the Poisson contraction.

$$\mathbf{l} = [001] \sin \theta + \frac{1}{\sqrt{2}} [\bar{1}10] \cos \theta \quad (6.91)$$

$$\mathbf{l} = -\cos \theta / \sqrt{2} \hat{\mathbf{x}}_1 + \cos \theta / \sqrt{2} \hat{\mathbf{x}}_2 + \sin \theta \hat{\mathbf{x}}_3 \quad (6.92)$$

The directional factor $Q = l_1^2 l_2^2 + l_2^2 l_3^2 + l_3^2 l_1^2$ then becomes

$$Q = \cos^4 \theta / 4 + \cos^2 \theta \sin^2 \theta / 2 + \cos^2 \theta \sin^2 \theta / 2 \quad (6.93)$$

$$Q = \frac{1}{4} \cos^4 \theta + \cos^2 \theta \sin^2 \theta \quad (6.94)$$

Notice that Q has limiting values of $Q_{<001>} = 0$, $Q_{<110>} = 1/4$, and $Q_{<111>} = 1/3$, all of which are contained within the (110) plane, at angles of $\theta = 90^\circ$, $\theta = 0$, and $\theta = \pm 35.3^\circ$, respectively. The compliances for Cu, taken from the Landolt-Bornstein tables, are given above. This gives an anisotropy factor

$$a_2 = -2 \left(s_{11} - s_{12} - \frac{s_{44}}{2} \right) \quad (6.95)$$

$$a_2 = -29.3 \text{ TPa}^{-1} \quad (6.96)$$

and we can express

$$s'_{11} = a_1 + a_2 Q \quad (6.97)$$

where $a_1 = s_{11}$. The minimum value will be $a_1 - |a_2|/3$, for [111]; the maximum value will be s_{11} , for [001]. The direction-resolved compliance is plotted in Figure 6.1. The degree of anisotropy is quite large, where s' changes by a factor of three in the rotation of the pulling direction from [001] to [111]

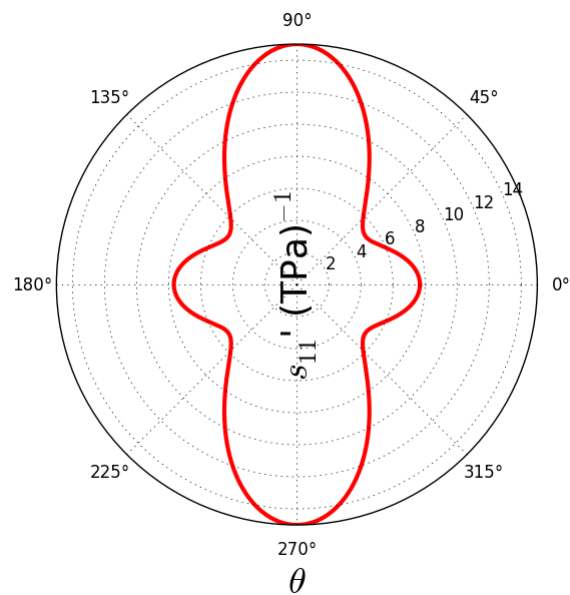


Figure 6.1: Compliance s'_{11} (where $\epsilon'_{11} = s'_{11}\sigma'_{11}$) as a function of applied stress direction. Angle θ is in the (110) plane, right hand rotation from [110]. Parameters are for (FCC) Copper.

6.6 Transforming compliances to stiffnesses

We can recast the definitions $\sigma_i = c_{ij}\epsilon_j$ and $\epsilon_i = s_{ij}\sigma_j$ in matrix form, as

$$\boldsymbol{\sigma} = (c)\boldsymbol{\epsilon} \quad \boldsymbol{\epsilon} = (s)\boldsymbol{\sigma} \quad (6.98)$$

where (c) and (s) are matrices with the same elements as c_{ij} , s_{ij} , and $\boldsymbol{\sigma}$ and $\boldsymbol{\epsilon}$ are column vectors with the stress components and strain components respectively.

If we multiply the first equation by the inverse of the (c) matrix,

$$(c)^{-1}\boldsymbol{\sigma} = (c)^{-1}(c)\boldsymbol{\epsilon} \quad (6.99)$$

so

$$\boldsymbol{\epsilon} = (c)^{-1}\boldsymbol{\sigma} \quad (6.100)$$

and clearly

$$(s) = (c)^{-1} \quad (s)(c) = (\mathbf{I}) \quad (6.101)$$

where (\mathbf{I}) is the identity matrix, $I_{ij} = \delta_{ij}$.

This means that we just have to multiply the matrices together:

$$\begin{bmatrix} c_{11} & c_{12} & c_{12} & 0 & 0 & 0 \\ c_{12} & c_{11} & c_{12} & 0 & 0 & 0 \\ c_{12} & c_{12} & c_{11} & 0 & 0 & 0 \\ 0 & 0 & 0 & c_{44} & 0 & 0 \\ 0 & 0 & 0 & 0 & c_{44} & 0 \\ 0 & 0 & 0 & 0 & 0 & c_{44} \end{bmatrix} \begin{bmatrix} s_{11} & s_{12} & s_{12} & 0 & 0 & 0 \\ s_{12} & s_{11} & s_{12} & 0 & 0 & 0 \\ s_{12} & s_{12} & s_{11} & 0 & 0 & 0 \\ 0 & 0 & 0 & s_{44} & 0 & 0 \\ 0 & 0 & 0 & 0 & s_{44} & 0 \\ 0 & 0 & 0 & 0 & 0 & s_{44} \end{bmatrix} = \begin{bmatrix} 1 & 0 & 0 & 0 & 0 & 0 \\ 0 & 1 & 0 & 0 & 0 & 0 \\ 0 & 0 & 1 & 0 & 0 & 0 \\ 0 & 0 & 0 & 1 & 0 & 0 \\ 0 & 0 & 0 & 0 & 1 & 0 \\ 0 & 0 & 0 & 0 & 0 & 1 \end{bmatrix} \quad (6.102)$$

Multiplying the fourth through sixth rows by fourth through sixth columns gives either zero or

$c_{44} = \frac{1}{s_{44}}$

(6.103)

and out of the nine products for the upper left blocks, only two are independent:

$$s_{11}c_{11} + 2s_{12}c_{12} = 1 \quad (6.104)$$

$$s_{12}c_{11} + s_{11}c_{12} + s_{12}c_{12} = 0 \quad (6.105)$$

Notice that in these relationships, we can interchange s with c , so the solution we will find for c in terms of s can be expressed in the same way for s in terms of c . This is not generally true for all crystal systems, just for cubics. Solving for c_{11}, c_{12} ,

$$c_{11} = \frac{1}{s_{11}}(1 - 2s_{12}c_{12}) \quad (6.106)$$

$$\frac{s_{12}}{s_{11}}(1 - 2s_{12}c_{12}) + \frac{1}{s_{11}}(s_{11}^2 + s_{11}s_{12})c_{12} = 0 \quad (6.107)$$

Multiplying through by s_{11} ,

$$c_{12}(s_{11}^2 + s_{11}s_{12} - 2s_{12}^2) = -s_{12} \quad (6.108)$$

$$c_{12} = -\frac{s_{12}}{(s_{11} - s_{12})(s_{11} + 2s_{12})} \quad (6.109)$$

and backsubstituting,

$$c_{11} = \frac{s_{11} + s_{12}}{(s_{11} - s_{12})(s_{11} + 2s_{12})} \quad (6.110)$$

Now interchanging s and c ,

$$s_{12} = -\frac{c_{12}}{(c_{11} - c_{12})(c_{11} + 2c_{12})} \quad (6.111)$$

$$s_{11} = \frac{c_{11} + c_{12}}{(c_{11} - c_{12})(c_{11} + 2c_{12})} \quad (6.112)$$

6.7 Polycrystalline averages: return to isotropy

There are two types of polycrystalline averages for the elastic constants used to determine an average Young's modulus E and Poisson ratio ν from the c_{ij} and s_{ij} coefficients. The *Voigt average* assumes uniform strain (*isostrain*) in the polycrystalline sample. The *Reuss average* assumes uniform stress (*isostress*) in the polycrystalline sample.

Voigt average The Voigt average assumes uniform strain, seeking values of c'_{ij} as transformed to new axes from the crystal axes. All values of a_{ij} are then averaged over all equally weighted orientations for the crystal to find average values of the stiffnesses $\bar{c}_{11}, \bar{c}_{12}, \bar{c}_{44}$. We have already determined an expression for s'_{11} in Eq 6.90; for c'_{11} , there is just a difference of a factor of four in the c_{44} term:

$$c'_{11} = c_{11} - 2(c_{11} - c_{12} - 2c_{44})(a_1^2 a_2^2 + a_2^2 a_3^2 + a_3^2 a_1^2) \quad (6.113)$$

Now the task is to take a spatial average of the orientation-dependent term Q ; consider an average of e.g. $a_1^2 a_3^2$, for the middle term, over all possible orientations of the grain. If we take spherical coordinates with $a_3 = \cos \theta, a_2 = \sin \phi \sin \theta$

$$\langle a_1^2 a_3^2 \rangle = \frac{\int_0^{2\pi} \int_0^\pi \sin \theta \cos^2 \phi \sin^2 \theta \cos^2 \theta d\phi d\theta}{\int_0^{2\pi} \int_0^\pi \sin \theta d\phi d\theta} \quad (6.114)$$

$$\langle a_1^2 a_3^2 \rangle = \frac{\int_0^{2\pi} \cos^2 \phi d\phi \int_0^\pi \sin \theta (\cos^2 \theta - \cos^4 \theta) d\theta}{4\pi} \quad (6.115)$$

$$\langle a_1^2 a_3^2 \rangle = \frac{2\pi (1/3 - 1/5)}{4\pi} = \frac{1}{15} \quad (6.116)$$

Since all directions x_i are equivalent, all terms in the sum $\langle a_1^2 a_2^2 \rangle + \langle a_2^2 a_3^2 \rangle + \langle a_3^2 a_1^2 \rangle$ are the same, and the sum evaluates to 1/5. Thus

$$\bar{c}_{11} = \frac{3}{5}c_{11} + \frac{2}{5}c_{12} + \frac{4}{5}c_{44} \quad (6.117)$$

for cubic materials. A similar analysis gives

$$\bar{c}_{12} = \frac{1}{5}c_{11} + \frac{4}{5}c_{12} - \frac{2}{5}c_{44} \quad (6.118)$$

$$\bar{c}_{44} = \frac{1}{5}c_{11} - \frac{1}{5}c_{12} + \frac{3}{5}c_{44} \quad (6.119)$$

These satisfy the isotropy condition

$$\bar{c}_{44} = \frac{1}{2}(\bar{c}_{11} - \bar{c}_{12}) \quad (6.120)$$

The Voigt-average Young's modulus E_V is expressed for uniaxial stress as $E_V = 1/s_{11}$; transforming from c_{11} using Eq 6.112

$$E_V = \frac{(\bar{c}_{11} - \bar{c}_{12})(\bar{c}_{11} + 2\bar{c}_{12})}{\bar{c}_{11} + \bar{c}_{12}} \quad (6.121)$$

$$E_v = \frac{1}{5} \frac{(2c_{11} - 2c_{12} + 6c_{44})(5c_{11} + 10c_{12})}{4c_{11} + 6c_{12} + 2c_{44}} \quad (6.122)$$

$$E_v = \frac{(c_{11} - c_{12} + 3c_{44})(c_{11} + 2c_{12})}{2c_{11} + 3c_{12} + c_{44}} \quad (6.123)$$

$$G_v = \frac{c_{11} - c_{12} + 3c_{44}}{5} \quad (6.124)$$

verified in Ref [1].

Reuss average The Reuss average is simpler. Here we assume isostress in the grains, so we can evaluate directly from a spatial average of s_{11} . The result we had for \bar{c}_{11} in Eq 6.117 can be reproduced, substituting s for c and dividing by a factor 4 in the c_{44} term:

$$\bar{s}_{11} = \frac{3}{5}s_{11} + \frac{2}{5}s_{12} + \frac{1}{5}s_{44} \quad (6.125)$$

Thus the Reuss-averaged Young's modulus E_R is

$$E_R = \frac{5}{3s_{11} + 2s_{12} + s_{44}} \quad (6.126)$$

This expression¹ can be found in Ref [1]. "Translating" the result for \bar{c}_{44} , by taking $c_{11} \rightarrow s_{11}, c_{12} \rightarrow s_{12}, c_{44} \rightarrow s_{44}/4$,

$$\bar{s}_{44}/4 = \frac{1}{5}s_{11} - \frac{1}{5}s_{12} + \frac{3}{5}s_{44}/4 \quad (6.127)$$

so for the shear modulus,

$$G_R = \frac{5}{4s_{11} - 4s_{12} + 3s_{44}} \quad (6.128)$$

For both the Voigt and Reuss averages, the elasticity is isotropic, so we can use Eq 5.20 to find the Poisson ratio ν :

$$\nu_v = \frac{E_v}{2G_v} - 1 \quad \nu_R = \frac{E_R}{2G_R} - 1 \quad (6.129)$$

¹in distinction to that in Newnham, Properties of Materials, chapter 13.8, which has an erroneous $5s_{11}$ term

Crystal	c_{11}	c_{12}	c_{44}	s_{11}	s_{12}	s_{44}	E_V	E_R	\bar{E}
Fe	230	135	117	7.67	-2.83	8.57	227	193	210
Cu	169	122	75.3	15	-6.3	13.3	144	109	127

Table 6.2: Cubic elastic constants, from Landolt-Bornstein tables, converted to polycrystalline, isotropic Young's moduli. Stiffnesses c_{ij} and Young's moduli (Voigt, Reuss, and VRH) E_V , E_R , and \bar{E} in GPa; compliances s_{ij} in TPa^{-1} .

Polycrystalline averages The Voigt and Reuss averages are upper and lower bounds on isotropic elastic moduli of polycrystals. Both isostress and isostrain are extreme approximations. In isostrain (Voigt), stress varies discontinuously across grain boundaries, so the grains cannot be in equilibrium; the estimate of E_V is an upper bound for the elastic modulus. In isostress (Reuss), strain at grain boundaries must be discontinuous, implying that lattices no longer match on deformation, and E_R is a lower bound for the elastic moduli.

6.7.1 Stiffness and compliance matrices for isotropic materials

Compliances s_{ij} The compliance matrix for an isotropic material takes the same form as that for a cubic. The elements are

$$s_{11} = \frac{1}{E} \quad s_{44} = \frac{1}{G} \quad s_{12} = -\frac{\nu}{E} \quad (6.130)$$

This can be seen very simply. We already defined the Young's modulus in terms of s_{1111} and the shear modulus in terms of $4/s_{1212}$, in tensor notation, in Section 6.1.1. The value for s_{12} is clear from the definition of the Poisson ratio: since $\epsilon_2 = -\nu\epsilon_1$ for a uniaxial stress σ_1 , $\epsilon_2 = s_{12}\sigma_1$, and $s_{12} = -\nu/E$.

Writing these out explicitly for the normal strains,

$$\epsilon_1 = \frac{\sigma_1}{E} - \frac{\nu}{E}(\sigma_2 + \sigma_3) \quad (6.131)$$

$$\epsilon_2 = \frac{\sigma_2}{E} - \frac{\nu}{E}(\sigma_1 + \sigma_3) \quad (6.132)$$

$$\epsilon_3 = \frac{\sigma_3}{E} - \frac{\nu}{E}(\sigma_1 + \sigma_2) \quad (6.133)$$

and the shear strains are diagonal in the shear stresses, dependent only on the same type:

$$\frac{\epsilon_4}{\sigma_4} = \frac{\epsilon_5}{\sigma_5} = \frac{\epsilon_6}{\sigma_6} = \frac{1}{G} \quad (6.134)$$

Similarly, the elements of the stiffness matrix can be expressed in terms of the shear modulus μ and Lame coefficient λ , defined in Section 5.

Stiffnesses c_{ij} Substituting the expressions for s_{ij} into the conversion formulae, Eqs 6.110 and 6.109

$$c_{11} = \frac{s_{11} + s_{12}}{(s_{11} - s_{12})(s_{11} + 2s_{12})} \quad c_{11} = \frac{E(1 - \nu)}{(1 + \nu)(1 - 2\nu)} \quad (6.135)$$

$$c_{12} = -\frac{s_{12}}{(s_{11} - s_{12})(s_{11} + 2s_{12})} \quad c_{12} = \frac{E\nu}{(1 + \nu)(1 - 2\nu)} \quad (6.136)$$

We will next show that the three unique stiffness elements, including c_{11} and c_{12} defined above, can be expressed more simply in terms of the Lamé parameters. Recall that the Lamé parameters λ, μ are defined in terms of the elastic energy, Eq 5.21,

$$U \equiv \frac{\lambda}{2} \varepsilon_{kk} \varepsilon_{ll} + \mu \varepsilon_{ij} \varepsilon_{ij} \quad (6.137)$$

or in terms of the matrix stresses and strains,

$$U = \frac{\lambda}{2} (\epsilon_1 + \epsilon_2 + \epsilon_3)^2 + \mu (\epsilon_1^2 + \epsilon_2^2 + \epsilon_3^2) + \frac{\mu}{2} (\epsilon_4^2 + \epsilon_5^2 + \epsilon_6^2) \quad (6.138)$$

Taking the derivatives of the elastic energy to find the matrix strains, according to Eq 6.52

$$\sigma_1 = \frac{\partial U}{\partial \epsilon_1} = (2\mu + \lambda) \epsilon_1 + \lambda (\epsilon_2 + \epsilon_3) \quad (6.139)$$

$$\sigma_2 = (2\mu + \lambda) \epsilon_2 + \lambda (\epsilon_1 + \epsilon_3) \quad (6.140)$$

$$\sigma_3 = (2\mu + \lambda) \epsilon_3 + \lambda (\epsilon_1 + \epsilon_2) \quad (6.141)$$

On the other hand, using the stiffnesses c_{ij} with imposed strains ϵ_j , the stresses from $\sigma_i = c_{ij} \epsilon_j$ are

$$\sigma_1 = c_{11} \epsilon_1 + c_{12} (\epsilon_2 + \epsilon_3) \quad (6.142)$$

etc. Thus we find for the matrix stiffnesses of an isotropic solid, in terms of the Lamé parameters,

$$\boxed{c_{11} = 2\mu + \lambda \quad c_{12} = \lambda \quad c_{44} = \mu} \quad (6.143)$$

Exercises

1. Determine an expression for the bulk modulus K of a cubic crystal in terms of the matrix stiffnesses c_{ij} . You can assume that the normal strain axes ϵ_i are along the unit cell axes.
2. Using the Python function `sprime` distributed in class, plot the Young's modulus s'_{1111} for Cu for a full rotation of stress and strain axes through 2π in the (100) and (111) planes. How do your plots obey Neumann's principle?.
3. Using the Python function `sprime`, show that an average of 100 random orientations for the stress/strain axis l_i converges to the Reuss average. *Hint:* use the function `2*np.pi*np.random.random((100,2))` to create random values for spherical angles θ, ϕ and generate l_i from these angles.
4. Derive an expression for the p-wave modulus M for different directions of uniaxial strain defined by l_i .
5. Modify the Python function to calculate the p -wave modulus, according to your result in the last problem. Plot the modulus for a full rotation of 2π in the (100) and (111) planes, and be sure to show that your computed result agrees with analytic results for some low-index orientations.
6. Using the Landolt-Bornstein tables values, calculate the Voigt, Reuss, and Voigt-Reuss-Hill average isotropic Young's modulus E for Al.
7. Derive the Young's modulus for the Reuss average of a [111]-fiber-textured polycrystalline cubic solid.

Bibliography

- [1] J M J den Toonder, J A W van Dommelen, and F P T Baaijens. “The relation between single crystal elasticity and the effective elastic behaviour of polycrystalline materials: theory, measurement and computation”. In: *Modelling and Simulation in Materials Science and Engineering* 7.6 (Nov. 1999), pp. 909–928. doi: 10.1088/0965-0393/7/6/301.

Chapter 7

Elastic waves

We have already seen in Chapter 1 that atoms can oscillate about their equilibrium positions in a solid, participating in wavelike motion under the influence of forces from neighboring atoms. Lattice vibrations, or phonons, are the primary mechanism through which solids absorb and store thermal energy from their surroundings. In our prior consideration of the Debye temperature, there was a single 'speed of sound' v_p , said to be in some way proportional to the Young's modulus E of the solid.

In this section, we will take a closer look at what the speed of sound has to do with the elastic moduli of a solid, and what the elastic moduli have to do with acoustic vibrations.

7.1 Elastic modes

First, we will look at the influence of the elasticity parameters on resonant frequencies and displacement shapes – elastic modes – for vibrations of two different types of bodies. A *string* under tension is considered thin enough that the stress is uniform throughout the body. The vibrations of a *beam*, with finite thickness orthogonal to the flexural axis, are complicated by the fact that the stress needs to be nonuniform throughout the thickness h . We will see that the resonant frequencies are influenced by the elasticity and density of the material, but also that the geometry, dimensions, and pinning conditions at the boundaries all play a strong role.

7.1.1 Vibrating string

We will first consider the vibrations of a string under a uniform tension (force per unit area) T . Assume, first, that the angle that the string makes with the x -axis at any point, $\theta = \theta(x)$ is not constant: the string *curves*, and second, that θ is small, allowing us to make a small-angle approximation. At any point $x, y(x)$,

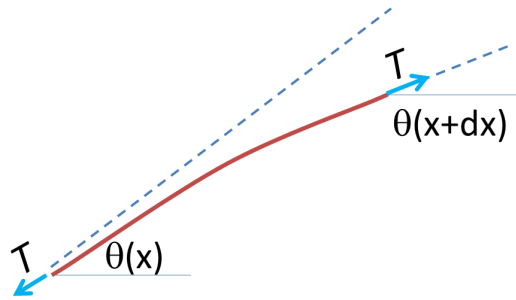


Figure 7.1: Differential length dx of spring under tension T with curvature

Taking a differential length element dx , x to $x + dx$, mass m , we can write Newton's law for the acceleration in y as

$$F_y = m \frac{\partial^2 y}{\partial t^2} \quad (7.1)$$

Net forces in \hat{y} , for uniform tension T , require string curvature. The total forces are

$$T (\sin \theta(x + dx) - \sin \theta(x)) = m \frac{\partial^2 y}{\partial t^2} \quad (7.2)$$

Taking a small-argument approximation $\theta \ll 1$, we approximate $\sin \theta \simeq \theta$, so

$$T (\theta(x + dx) - \theta(x)) = m \frac{\partial^2 y}{\partial t^2} \quad (7.3)$$

$$T \left(\frac{\partial y(x + dx)}{\partial x} - \frac{\partial y(x)}{\partial x} \right) = m \frac{\partial^2 y}{\partial t^2} \quad (7.4)$$

For the differential length element dx , x to $x + dx$, mass m :

$$F_y = m \frac{\partial^2 y}{\partial t^2} \quad (7.5)$$

$$T \delta x \frac{\partial^2 y}{\partial x^2} = m \frac{\partial^2 y}{\partial t^2} \quad (7.6)$$

The string vibrations are then described by the partial differential equation (PDE)

$$\left(\frac{\partial^2 y}{\partial t^2} \right) = \frac{T}{\rho_l} \left(\frac{\partial^2 y}{\partial x^2} \right) \quad (7.7)$$

a.k.a. the wave equation, describing waves with velocity v ,

$$\left(\frac{\partial^2 y}{\partial t^2} \right) = v^2 \left(\frac{\partial^2 y}{\partial x^2} \right) \quad (7.8)$$

satisfying $y(x, t) = y(x - vt)$, i.e. a fixed profile in y travels down x at a speed v_p (phase velocity.) Consider a sinusoidal wave:

$$y(x, t) = A \cos(kx - \omega t) \quad (7.9)$$

substituted in the wave equation, this solution is

$$\frac{\partial^2}{\partial t^2} \cos(kx - \omega t) = v^2 \frac{\partial^2}{\partial x^2} \cos(kx - \omega t) \quad (7.10)$$

where ω is temporal frequency (s^{-1}); k is spatial frequency (m^{-1}), aka *wavenumber*, $k = 2\pi/\lambda$, inverse in wavelength. The phase velocity is

$$v_p = \frac{\omega}{k} \quad (7.11)$$

For the string, the wave equation is

$$v_p = \sqrt{\frac{T}{\rho_l}} \quad (7.12)$$

The elastic wave travels on the string at a speed given by the root of the ratio of tension T (N) to mass per unit length ρ_l (kg/m). High tension or low mass creates a fast wave! On a system of length L , such as a string, in which the displacement is pinned at the boundaries $x = 0$, $x = L$, the lowest frequency is

$$k_1 = \frac{\pi}{L} \quad (7.13)$$

So for the lowest frequency (sinusoid):

$$\omega_1 = 2\pi\nu_1 = v_p k_1 \quad \nu_1 = \frac{1}{2\pi} v_p \frac{\pi}{L} \quad \rightarrow \quad \boxed{\nu_1 = \frac{1}{2L} v_p} \quad (7.14)$$



Figure 7.2: Unfretted string lengths: guitar $L = 65$ cm, bass $L = 84$ cm

For a stringed instrument, the tone can be changed by placing a finger on the string, effectively shortening L , or by changing the tension T . Substituting in for the strain ϵ in terms of the Young's modulus E , $T = E\epsilon A$, linear mass density $\rho_l = M/L$, volume mass density $\rho = M/(AL)$, the phase velocity will be given by

$$v_p = \sqrt{\frac{E}{\rho}} \quad (7.15)$$

we will see that the ratio of elastic modulus to mass density $\sqrt{E/\rho}$ appears generically in the velocity of elastic waves, even in the more detailed treatments for crystals later on.

7.1.2 Longitudinal vibrations of an isotropic beam

We will now consider elastic waves in beams. Beams resist displacements not because they are under tension, as in the case for the string, but because they are rigid bodies. There is an energy penalty (Eq 5.33) for strain in a rigid elastic body. In the Cauchy equation, Eq 7.60,

$$\rho \ddot{u}_i = g_i + \left(\frac{\partial \sigma_{ij}}{\partial x_j} \right) \quad (7.16)$$

we will be interested in time-dependent, harmonic $e^{-i\omega t}$ solutions for u_i . The body forces g_i , such as gravity, tend to be time-independent, so we

can leave these out of the discussion. In Section 2.5, we considered a beam with profile $y(x)$, so there are variations in the x_1 direction, which we will designate as x :

$$\ddot{u}_i - \frac{1}{\rho} \left(\frac{\partial \sigma_{ix}}{\partial x} \right) = 0 \quad (7.17)$$

For a longitudinal vibration, the displacements in the material are in the same direction as the length of the beam, here x , so $i = x$

$$\left(\frac{\partial^2 u_x}{\partial t^2} \right) = \frac{1}{\rho} \left(\frac{\partial \sigma_{xx}}{\partial x} \right) \quad (7.18)$$

Differentiate this expression with respect to x ,

$$\frac{\partial^2}{\partial t^2} \left(\frac{\partial u_x}{\partial x} \right) = \frac{1}{\rho} \left(\frac{\partial^2 \sigma_{xx}}{\partial x^2} \right) \quad (7.19)$$

where we recognize the normal strain ϵ_{xx} in the first term, from Eq ??:

$$\left(\frac{\partial^2 \epsilon_{xx}}{\partial t^2} \right) = \frac{1}{\rho} \left(\frac{\partial^2 \sigma_{xx}}{\partial x^2} \right) \quad (7.20)$$

The stress and strain are related through the Young's modulus, so

$$\left(\frac{\partial^2 \sigma_{xx}}{\partial t^2} \right) = \frac{E}{\rho} \left(\frac{\partial^2 \epsilon_{xx}}{\partial x^2} \right) \quad (7.21)$$

Recognize the wave equation here, $\partial_x^2 z(x, t) = v_p^2 \partial_t^2 z(x, t)$. The phase velocity $v_p = \omega/k$ is given by

$$v_p - \frac{\omega}{k} = \sqrt{\frac{E}{\rho}} \quad (7.22)$$

and we can write solutions for the displacement as

$$u_x(x, t) = u_x^0 e^{i(kx - \omega t)} \quad (7.23)$$

and taking the x -derivative,

$$\epsilon_{xx}(x, t) = -i k u_x^0 e^{i(kx - \omega t)} \quad (7.24)$$

Application of boundary conditions If the bar has free ends, the normal stresses are zero at the ends, $\sigma_{xx}(0) = \sigma_{xx}(L) = 0$ at the ends, and by Hooke's law, so are the normal strains $\epsilon_{xx}(0) = \epsilon_{xx}(L) = 0$. The stress can then be written, for a standing wave with equal, counterpropagating $\pm v_p$ components,

$$\sigma_{xx}(x, t) = \frac{\sigma_0}{2} (\sin(k_n x - \omega t) + \sin(k_n x + \omega t)) \quad (7.25)$$

where σ_0 is the maximum stress during a cycle, the boundary conditions are $k_n L = n\pi$ and n is an integer. The strain will be related to this through the Young's modulus,

$$\epsilon_{xx}(x, t) = \frac{\sigma_0}{2E} (\sin(k_n x - \omega t) + \sin(k_n x + \omega t)) \quad (7.26)$$

and the displacement is the integral over x ,

$$u_x(x, t) = \frac{\epsilon_0 L}{2n\pi E} \left(-\cos\left(n\pi \frac{x}{L} - \omega t\right) + \cos\left(n\pi \frac{x}{L} + \omega t\right) \right) \quad (7.27)$$

7.1.3 Transverse vibrations of an isotropic beam

We will next consider the *flexural* (or transverse) vibrations of a beam or rod, with small harmonic displacements in \hat{y} . The basic theory of beams has been developed in Section 2.5. Here too the restoring stiffnesses with respect to vibrations are due to Hooke's law and normal stresses, but to the extent that they are generated by bending moments. We will see that the boundary conditions at the ends have a very noticeable effect on the elastic modes and discrete resonant frequencies ω_n ; here the situation is more complicated than for longitudinal vibrations with free ends.

Bernoulli beam theory showed, in Section 2.5, Equation 2.29, that the beam curvature is given by

$$\frac{\partial^2 y}{\partial x^2} = -\frac{M_z}{EI_z} \quad (7.28)$$

We can develop a PDE for the deformation by differentiating twice with respect to x :

$$\left(\frac{\partial^4 y}{\partial x^4} \right) + \frac{1}{EI_z} \left(\frac{\partial^2 M_z}{\partial x^2} \right) = 0 \quad (7.29)$$

where at (approximate) rotational equilibrium, having neglected the mass moment of inertia, we can substitute in for the second derivative of the moment from Eq 2.36

$$\left(\frac{\partial^4 y}{\partial x^4} \right) + \frac{A}{EI_z} \left(\frac{\partial \sigma_{xy}}{\partial x} \right) = 0 \quad (7.30)$$

Because the force in y has only the shear component, and it varies only in the x direction according to the assumptions of $B - E$ theory, Cauchy's equation of motion in the y direction is now given by

$$\left(\frac{\partial \sigma_{xy}}{\partial x} \right) = -\rho g + \rho \ddot{y} \quad (7.31)$$

Substituting back in the kinematic equation,

$$\left(\frac{\partial^4 y}{\partial x^4} \right) + D^{-1} \left(\frac{\partial^2 y}{\partial t^2} \right) = \frac{1}{\rho D} g_y(x, t) \quad D \equiv \frac{EI_3}{A\rho} \quad (7.32)$$

applying the I_z/A ratio from Eq 2.26, the constant D for a prism is

$$D = \frac{Eh^2}{12\rho} \quad (7.33)$$

Again, to develop oscillatory solutions, the body forces are probably not interesting, as they are typically not oscillatory, so we set them equal to zero:

$$\left(\frac{\partial^4 y}{\partial x^4} \right) + D^{-1} \left(\frac{\partial^2 y}{\partial t^2} \right) = 0 \quad (7.34)$$

If we seek sinusoidal solutions, $y(x, t) = y_0 \cos(kz - \omega t)$, the dispersion relation for elastic waves along the beam will be

$$\omega^2 = Dk^4 \quad (7.35)$$

Interestingly, the elastic waves in a beam will be *dispersive*, with phase velocity ω/k not constant as a function of frequency.

Application of boundary conditions

The supports at the $x = 0$ and $x = L$ ends of the beam have a very noticeable effect on the elastic modes of the beam. Both the vibration profiles $y(x)$ and the discrete resonance frequencies ω_n depend strongly upon how the beam is constrained at the ends. We will consider two of three typical symmetric

pinning conditions: simple supports (*SS*), which impose zeros (nodes) in the deflection at the ends, and free boundary conditions (*F*), which assume no tractions on the end surfaces. The third boundary condition is *clamped* (*C*), which requires that both the beam height and beam slope are zero at the boundaries. These boundary conditions were named by Leissa[1]. Other boundary conditions, such as a dashpot attached to the ends, can also be imagined; these are tabulated in [2].

Simply supported ends (SS) For a beam supported at $x = 0$ and $x = L$, there is no displacement at the ends, so

$$y(0) = 0 \quad y(L) = 0 \quad (7.36)$$

The solutions are easy to write; just like those of a vibrating string, they are sinusoidal,

$$y(x) = y_n \sin k_n x \quad k_n = n\pi/L \quad (7.37)$$

Because the wavenumber k_n is well-defined, the frequency ω_n can be found simply through the dispersion relationship in Eq 7.35,

$$\omega_n = \sqrt{D} \left(\frac{\pi}{L} \right)^2 n^2 \quad (7.38)$$

Free ends (F) For free ends, stresses are zero at every point, so normal stresses are zero all along the height y of the beam

$$\sigma_{xx}(0, y) = 0 \quad \sigma_{xx}(L, y) = 0 \quad (7.39)$$

and shear stresses are also zero at all heights,

$$\sigma_{xy}(0, y) = 0 \quad \sigma_{xy}(L, y) = 0 \quad (7.40)$$

The absence of normal stresses implies that there can be no bending moments exerted at the free ends, and with $M_z(0) = 0$, $M_z(L) = 0$, this implies zero curvature from Eq 7.28,

$$\frac{\partial^2 y(0)}{\partial x^2} = 0 \quad \frac{\partial^2 y(L)}{\partial x^2} = 0 \quad (7.41)$$

Because the shear stress $\sigma_{xy}(0) = \sigma_{xy}(L)$ is also zero, from Eq 2.35, the x -derivative of the moment $\delta M_z / \delta x = 0$, and then the third derivative is zero as well,

$$\left(\frac{\partial^3 y(0)}{\partial x^3} \right) = 0 \quad \left(\frac{\partial^3 y(L)}{\partial x^3} \right) = 0 \quad (7.42)$$

Note that from the biharmonic operator (fourth x-derivative), sinusoids with real and imaginary wavenumbers are equally valid solutions, so we can express a trial solution as

$$y(x) = A_0 \cos k_n x + A_1 \cosh k_n x + B_0 \sin k_n x + B_1 \sinh k_n x \quad (7.43)$$

$$k_n^{-2} \left(\frac{\partial^2 y}{\partial x^2} \right) = -A_0 \cos k_n x + A_1 \cosh k_n x - B_0 \sin k_n x + B_1 \sinh k_n x \quad (7.44)$$

$$k_n^{-3} \left(\frac{\partial^3 y}{\partial x^3} \right) = -B_0 \cos k_n x + B_1 \cosh k_n x + A_0 \sin k_n x + A_1 \sinh k_n x \quad (7.45)$$

Applying the $x = 0$ boundary condition leads simply to

$$A_0 = A_1 \equiv A \quad B_0 = B_1 \equiv B \quad (7.46)$$

and applying the $x = L$ boundary condition leads to

$$\begin{bmatrix} -\cos k_n L + \cosh k_n L & -\sin k_n L + \sinh k_n L \\ \sin k_n L + \sinh k_n L & -\cos k_n L + \cosh k_n L \end{bmatrix} \begin{bmatrix} A \\ B \end{bmatrix} = 0 \quad (7.47)$$

for the determinant to be zero,

$$1 - 2 \cos k_n L \cosh k_n L + \cosh^2 k_n L - \sinh^2 k_n L = 0 \quad (7.48)$$

$$\cos k_n L \cosh k_n L = 1 \quad (7.49)$$

This equation can be solved numerically for $k_n L$. Solutions are found for approximately

$$k_n L = 1.50\pi, 2.50\pi, 3.50\pi \dots \quad (7.50)$$

Because the wavenumber k_1 for the first solution is a factor $\sim 3/2$ higher than the fundamental for the *SS* case, $k_1 L = \pi$, the "effective length" for the fundamental mode could be considered to be a factor $2/3$ shorter.

The first several solutions for the free beam are shown in Figure 7.3.

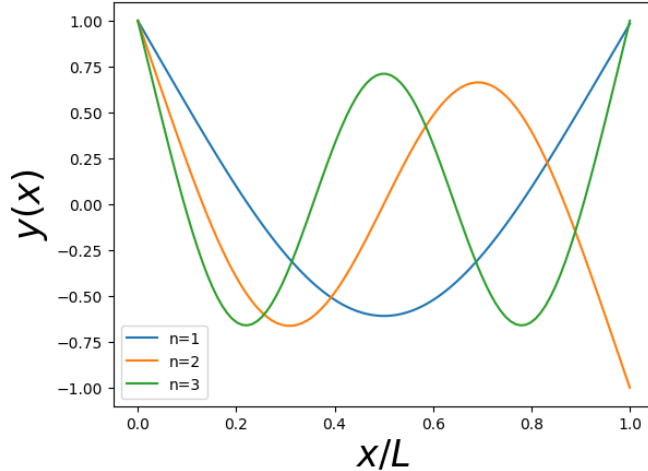


Figure 7.3: Profile of vibrating beam with free (F) boundary conditions, with no tractions at either end, $x = 0$ and $x = L$. Eigenmodes $n = 1, 2, 3$ are shown. Note that the outer $\sim L/6$ on either end has an evanescent form, whereas the interior part $L/6 \leq x \leq 5L/6$ is more sinusoidal. Total number of central nodes is $n + 1$.

Example: resonant frequency for fundamental frequency of free beam, two central nodes, $n = 1$ The lowest-frequency eigenmode, interestingly, has two central nodes, two points x_n for which $y(x_n) = 0$, away from the edges of the beam. We have found that $k_1 L = 1.50\pi$. Taking $L = 0.26$ m, $h = 0.91$ mm, and parameters appropriate for Al, $E = 69$ GPa, $\nu = 0.33$, and $\rho = 2700$ kg/m³, we can estimate the expected frequency $\omega/2\pi$,

$$\frac{\omega_1}{2\pi} = \frac{1}{2\pi} \sqrt{\frac{E}{12\rho}} h k^2 = \frac{0.91 \text{ mm}}{2\pi\sqrt{12}} \sqrt{\frac{69 \text{ GPa}}{2700 \text{ kg/m}^3}} \left(\frac{1.505\pi}{0.26 \text{ m}} \right)^2 \simeq 70 \text{ Hz} \quad (7.51)$$

7.2 Solutions for phase velocity

For the most general consideration of sound wave propagation, we will develop solutions for elastic waves in a single crystal, with stiffnesses c_{ijkl} , as a function of direction of propagation. We will then consider two interesting special cases: cubic crystals and isotropic materials.

7.2.1 General: Cauchy equation of motion

We can remember our equation of motion, Eq 2.7, valid for any point in a medium, under the influence of stresses and body forces g_i

$$\rho \ddot{u}_i = \frac{\partial \sigma_{ij}}{\partial x_j} + g_i \quad (7.52)$$

We will seek oscillatory, plane-wave solutions of this equation. The direction of propagation \mathbf{k} is arbitrary. In vector form,

$$\mathbf{u}(\mathbf{r}, t) = \mathbf{u}_0 \exp i(\mathbf{k} \cdot \mathbf{r} - \omega t) \quad (7.53)$$

where \mathbf{u}_0 is the polarization of the wave. Alternatively, we can write in index form

$$\mathbf{u}(\mathbf{r}, t) = u_i \exp i(|k|l_j x_j - \omega t) \quad (7.54)$$

where $\mathbf{k} = |k|l_i$, and l_i are the cosines of the propagation direction with respect to the Cartesian axes. The constants u_i determine the amplitudes of motion along cartesian axis x_i .

We would like to find solutions for this equation of motion. Specifically, we would like to relate the phase velocity $v_p = \omega/k$ to the direction of elastic wave propagation l_i , and determine the polarization character of the motion: in what direction do the atoms move? We can remember that transverse waves $\mathbf{u} \perp \mathbf{k}$, which are shear-like, should have different frequencies from longitudinal waves $\mathbf{u} \parallel \mathbf{k}$, which are tensile/compressive-like.

Solutions of this form will oscillate as a function of time and position. Thus unless body forces g_i are also oscillatory, which is rare, we can neglect them in the solution, and set $g_i = 0$. The stresses σ_{ij} relate to the strains through the stiffness through Eq 6.1,

$$\sigma_{ij} = c_{ijkl} \varepsilon_{kl} \quad (7.55)$$

Substituting in,

$$\rho \ddot{u}_i = \frac{\partial}{\partial x_j} c_{ijkl} \varepsilon_{kl} \quad (7.56)$$

with implied sums over j, k, l . Next, from the definition of the tensor stress in Eq 4.21

$$\varepsilon_{kl} = \frac{1}{2} \left(\frac{\partial u_k}{\partial x_l} + \frac{\partial u_l}{\partial x_k} \right) \quad (7.57)$$

Eq 7.56 becomes

$$\rho \ddot{u}_i = \frac{\partial}{\partial x_j} \left(\frac{\partial u_k}{\partial x_l} + \frac{\partial u_l}{\partial x_k} \right) \frac{c_{ijkl}}{2} \quad (7.58)$$

Since the second time derivative yields $-\omega^2 u_i$ and the two spatial derivatives yield a factor of $|k|^2$, we have

$$\rho \frac{\omega^2}{|k|^2} u_i = l_j (l_l u_k + l_k u_l) \frac{c_{ijkl}}{2} \quad (7.59)$$

The two sums are equal because we can reverse the last two indices in c_{ijkl} without changing its value, as shown in Section 6.2.1. Finally,

$$\boxed{\rho v_p^2 u_i = l_j l_l c_{ijkl} u_k} \quad (7.60)$$

This is Cauchy's law of motion, the most general form for sound-wave propagation in a crystal. Note that the displacements u_i, u_k have three cartesian components, so there are three equations contained here, each of which has 27 possible terms (for the sum over three indices in c_{ijkl}) in a triclinic crystal.

7.2.2 Cubic materials

In cubic materials, as we have seen, many of the c_{ijkl} terms are zero, and many are equivalent. We can consider the equation for u_1 , and expand Eq 7.60:

$$\rho v_p^2 u_1 = l_j l_l c_{1jkl} u_k \quad (7.61)$$

We can look first at $k = 1$. Here,

$$\rho v_p^2 u_1 = l_j l_l c_{1jl1} u_1 \quad (7.62)$$

There will be only three terms to this sum, because of the zero values of the cubic stiffness tensor: $jl = 11$, for $c_{1111} = c_{11}$, and $jl = 22, 33$, for $c_{1212} = c_{1313} = c_{44}$:

$$\rho v_p^2 u_1 = [l_1^2 c_{11} + (l_2^2 + l_3^2) c_{44}] u_1 \quad (7.63)$$

$$\rho v_p^2 u_1 = [l_1^2 c_{11} + (1 - l_1^2) c_{44}] u_1 \quad (7.64)$$

This relationship could be considered generic for the three elements $i = k$, here $= 1$. Next, we can consider a relationship between u_1 and u_2 . Taking $k = 2$,

$$\rho v_p^2 u_1 = l_j l_l c_{1j2l} u_2 \quad (7.65)$$

Here there are nonzero components only for c_{1122} ($jl = 12$) and c_{1221} ($jl = 21$).

$$\rho v_p^2 u_1 = l_1 l_2 (c_{12} + c_{44}) u_2 \quad (7.66)$$

This could be considered generic for the six cases where $i \neq k$. Carrying this out for all nine i, k combinations, we have

$$\begin{bmatrix} [l_1^2 c_{11} + (1 - l_1^2) c_{44}] & l_1 l_2 (c_{12} + c_{44}) & l_3 l_1 (c_{12} + c_{44}) \\ l_1 l_2 (c_{12} + c_{44}) & [l_2^2 c_{11} + (1 - l_2^2) c_{44}] & l_2 l_3 (c_{12} + c_{44}) \\ l_3 l_1 (c_{12} + c_{44}) & l_2 l_3 (c_{12} + c_{44}) & [l_3^2 c_{11} + (1 - l_3^2) c_{44}] \end{bmatrix} \begin{bmatrix} u_1 \\ u_2 \\ u_3 \end{bmatrix} = \rho v_p^2 \begin{bmatrix} u_1 \\ u_2 \\ u_3 \end{bmatrix}$$

The motion for a given set of l_i can then be solved in terms of eigenvalues of the left-hand matrix. There will in general be three solutions.

Simplest case: $l_1 = 1$ We can consider sound wave propagation on the \hat{x}_1 axis first. The other directional components l_2, l_3 are zero. The matrix simplifies quite a bit:

$$\begin{bmatrix} c_{11} & 0 & 0 \\ 0 & c_{44} & 0 \\ 0 & 0 & c_{44} \end{bmatrix} \begin{bmatrix} u_1 \\ u_2 \\ u_3 \end{bmatrix} = \rho v_p^2 \begin{bmatrix} u_1 \\ u_2 \\ u_3 \end{bmatrix}$$

giving us the world's easiest eigenvalue problem. Here we have, for the first row,

$$v_{p,1} = \sqrt{\frac{c_{11}}{\rho}} \quad (7.67)$$

Backsubstituting, this solution satisfies motion with $u_1 \neq 0$ only, so the wave is longitudinally polarized (parallel to \hat{k}) on \hat{x}_1 . The sound wave is a

pure compression wave, just like a sound wave travelling through air. The other two solutions are identical in velocity,

$$v_{p,2} = v_{p,3} = \sqrt{\frac{c_{44}}{\rho}} \quad (7.68)$$

corresponding to polarizations on $\hat{x_2}$ and $\hat{x_3}$ respectively. These are pure shear wave solutions. Shear waves do not exist in liquids or gases.

7.2.3 Isotropic materials

For the speeds of sound of isotropic materials, we just have to substitute the stiffness found in Section 6.7.1,

$$c_{11} = \frac{E(1-\nu)}{(1+\nu)(1-2\nu)} \quad c_{44} = \frac{E}{2(1+\nu)} = \mu \quad (7.69)$$

Substituting in Eqs 7.67 and 7.68,

$$v_{p,1} = \sqrt{\frac{(1-\nu)}{(1+\nu)(1-2\nu)}} \sqrt{\frac{E}{\rho}} \quad (7.70)$$

Remembering the p -wave modulus M , the isotropic elastic constant for uniaxial strain, $v_{p,1}$ and $v_{p,2}$ can be expressed as

$$v_l = v_{p,1} = \sqrt{\frac{M}{\rho}} \quad (7.71)$$

$$v_t = v_{p,2} = \sqrt{\frac{\mu}{\rho}} \quad (7.72)$$

where we explicitly call out the longitudinal and transverse (or compressional and shear) wave velocities v_l and v_t .

Exercises

1. Calculate the strain required for a nylon guitar string to reach the high-E tone on a guitar (330 hz.) (Use your internet skills for constants if they are not in the notes.)
2. Consider longitudinal vibrations in a $L = 1$ m brass rod. If the ends are clamped so that they cannot move, determine 1) the fundamental frequency, taking $E = 100$ GPa and $\nu = 0.3$, 2) the displacement profile as a function of x .
3. What is the resonant frequency for the lowest-frequency transverse mode of 10 cm x 0.1 mm Al bar a) simply supported at the ends, b) with free ends?
4. Determine the mode profile and resonant frequencies for a bar which is *clamped* at both ends, i.e. cannot be displaced in any direction, and fixed in both x and y .
5. An earthquake strikes the San Francisco Bay Area; how long does it take for the tremors to be felt in Los Angeles, 600 km away? Assume that the elastic waves propagate as through bulk (not surface) rock with density of 2.65 g/cm³ and Young's modulus of 10 GPa. Calculate for the P - (primary) wave due to compression and the S -secondary wave due to shear, assuming a poisson ratio of $\nu = 0.25$.
6. Compare longitudinal wave velocities in a single crystal of Ag for elastic wave propagation along the [100] and [110] directions. Is there a directional dependence of the velocity? Why or why not?

Bibliography

- [1] A.W. Leissa. “The free vibration of rectangular plates”. In: *Journal of Sound and Vibration* 31.3 (Dec. 1973), pp. 257–293. DOI: 10.1016/s0022-460x(73)80371-2.
- [2] Karl F. Graff. In: *Wave motion in elastic solids*. Dover Publications, 1991. Chap. 3: Flexural waves in thin rods.

Chapter 8

Composite elasticity and anelasticity

8.1 Neglecting Poisson contraction

8.1.1 Isostrain: fibers

Result here is

$$E_f = V_A E_A + V_B E_B \quad (8.1)$$

8.1.2 Isostress: plates

Result here is

$$E_c^{-1} = V_A E_A^{-1} + V_B E_B^{-1} \quad (8.2)$$

8.2 Including Poisson contraction

Still a stress σ pulling normal to the plates. Because the sides are free surfaces, there will be no net force on them,

$$V_A \sigma_{\perp}^A + V_B \sigma_{\perp}^B = 0 \quad (8.3)$$

There will be shear strains keeping the layers together but they are short-ranged to the edges, so we neglect these. The transverse strains need to be the same for the material to cohere,

$$\epsilon_{\perp}^A = \epsilon_{\perp}^B \quad (8.4)$$

The transverse strains are

$$\epsilon_{\perp}^A = \frac{\sigma_{\perp}^A}{E_A} - \frac{\nu_A}{E_A} (\sigma_{\perp}^A + \sigma) \quad (8.5)$$

$$\epsilon_{\perp}^B = \frac{\sigma_{\perp}^B}{E_B} - \frac{\nu_B}{E_B} (\sigma_{\perp}^B + \sigma) \quad (8.6)$$

Equating the transverse strains,

$$\frac{\sigma_{\perp}^A}{E_A} - \frac{\nu_A}{E_A} (\sigma_{\perp}^A + \sigma) = \frac{\sigma_{\perp}^B}{E_B} - \frac{\nu_B}{E_B} (\sigma_{\perp}^B + \sigma) \quad (8.7)$$

$$\left(\frac{1}{E_A} - \frac{\nu_A}{E_A} \right) \sigma_{\perp}^A - \left(\frac{1}{E_B} - \frac{\nu_B}{E_B} \right) \sigma_{\perp}^B = \left(\frac{\nu_A}{E_A} - \frac{\nu_B}{E_B} \right) \sigma \quad (8.8)$$

substituting in to isolate for σ_{\perp}^B

$$\left[\left(\frac{1}{E_A} - \frac{\nu_A}{E_A} \right) + \frac{V_A}{V_B} \left(\frac{1}{E_B} - \frac{\nu_B}{E_B} \right) \right] \sigma_{\perp}^A = \left(\frac{\nu_A}{E_A} - \frac{\nu_B}{E_B} \right) \sigma \quad (8.9)$$

$$\left[(E_B - \nu_A E_B) + \frac{V_A}{V_B} (E_A - \nu_B E_A) \right] \sigma_{\perp}^A = (\nu_A E_B - \nu_B E_A) \sigma \quad (8.10)$$

$$\sigma_{\perp}^A = \frac{(\nu_A E_B - \nu_B E_A) V_B}{V_A E_A (1 - \nu_B) + V_B E_B (1 - \nu_A)} \sigma \quad (8.11)$$

and the result for σ_{\perp}^B can be found by exchanging indices A, B

$$\sigma_{\perp}^B = \frac{(\nu_B E_A - \nu_A E_B) V_A}{V_A E_A (1 - \nu_B) + V_B E_B (1 - \nu_A)} \sigma \quad (8.12)$$

which leaves the denominator unchanged. Next, we can substitute the transverse stresses into the expression for the normal strain in each layer, remembering that the normal stresses are equal: $\sigma^A = \sigma^B = \sigma$.

$$\epsilon^A = \frac{\sigma}{E_A} - \frac{2\nu_A}{E_A} \sigma_{\perp}^A \quad (8.13)$$

$$\epsilon^B = \frac{\sigma}{E_B} - \frac{2\nu_B}{E_B} \sigma_{\perp}^B \quad (8.14)$$

and for the total strain proportional to stress,

$$\epsilon = V_A \epsilon_A + V_B \epsilon_B \quad (8.15)$$

$$\frac{\epsilon}{\sigma} = E_C^{-1} = \frac{V_A}{E_A} + \frac{V_B}{E_B} - \frac{2V_A V_B [\nu_A E_B (\nu_A E_B - \nu_B E_A) + \nu_B E_A (\nu_B E_A - \nu_A E_B)]}{V_A E_A (1 - \nu_B) + V_B E_B (1 - \nu_A)} \quad (8.16)$$

simplifying,

$$\frac{\epsilon}{\sigma} = E_C^{-1} = \frac{V_A}{E_A} + \frac{V_B}{E_B} - \frac{2V_A V_B}{E_A E_B} \frac{(\nu_A E_B - \nu_B E_A)^2}{V_A E_A (1 - \nu_B) + V_B E_B (1 - \nu_A)} \quad (8.17)$$

The third term on the right hand side represents the additional stiffness due to differential Poisson contraction. The term is always negative, so it always decreases E_C^{-1} and increases the stiffness. As can be seen, for realistic parameters ($\nu = 0.33$), the Poisson correction is relatively small. This expression reduces to the one we found neglecting the Poisson contraction if

$$\nu_A E_B = \nu_B E_A \quad (8.18)$$

8.3 Anelasticity and viscoelasticity

So far, we have considered only elastic displacements, which are entirely reversible, conserving energy. There has to be some additional term to the equation of motion for atomic displacements (the Cauchy Equation, Eq 7.60) which causes elastic waves to die out. Friction is familiar in mechanics, but we usually think about it as a force which acts at surfaces, between a rigid body and another medium, expressed through a coefficient of friction (rolling or sliding friction between solid surfaces, or air resistance.)

There also exists *internal friction*. When atoms move with respect to each other in an otherwise well-crystallized solid, energy is lost. If a solid is well-isolated from its surroundings, when it is strained cyclically, it will eventually heat up. For small-amplitude motion of atoms *within* their potential wells, formed by nearest-neighbors in a crystal, energy losses due to internal friction are relatively small. Internal friction becomes large when atoms move out of their potential wells.

Energy dissipation / friction implies that there is a time-delayed response of the strain to the stress or vice-versa, as we will show. The delayed

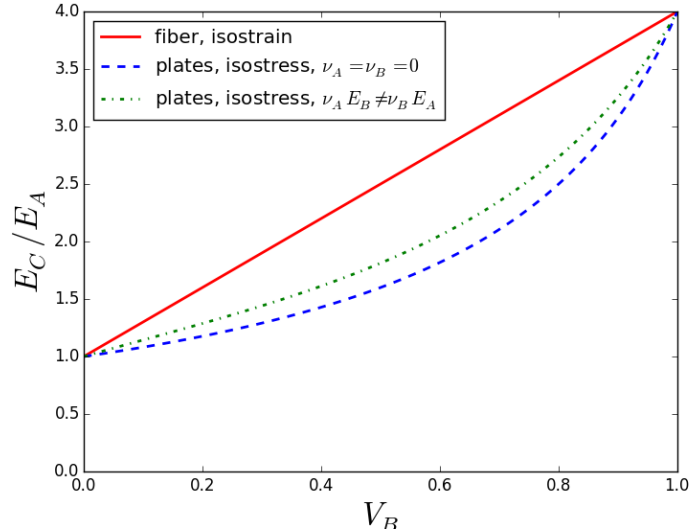


Figure 8.1: Elastic moduli for composites: stress parallel to fibers (isostrain), stress perpendicular to plates (isostress), neglecting or including the Poisson contraction (here $\nu_A = \nu_B = 0.33$.) Assumes $E_B = 4E_A$.

response is called 'anelastic' or 'viscoelastic.' In this section we will look at anelastic phenomena from a macroscopic level, and discuss the microscopic origins later. The models used to describe anelasticity are close to those used to describe composites.

8.3.1 Shear viscosity

Previously, we considered the bulk shear modulus μ ,

$$\sigma_{12} = \mu \gamma_{12} = 2\mu \varepsilon_{12} \quad (8.19)$$

We can now introduce a shear *viscosity*, where the shear stress is proportional not to the shear, but the rate of shear

$$\sigma_{12} = \eta \left(\frac{\partial \gamma}{\partial t} \right) \quad \rightarrow \quad \boxed{\eta \equiv \frac{\sigma_{12}}{\dot{\gamma}}} \quad (8.20)$$

Similarly, we can remember that for an isotropic, incompressible ($\nu = 1/2$) elastic medium, we can write

$$\mu = \frac{E}{2(1+\nu)} \rightarrow E = 3\mu \quad (8.21)$$

$$\sigma = 3\mu \epsilon \quad (8.22)$$

Thus we can express the stress - strain *rate* relationship through the shear viscosity,

$$\boxed{\sigma_i = 3\eta \dot{\epsilon}_i} \quad (8.23)$$

This is an anelastic term in the sense that it depends on time derivatives of ϵ ; it is also *viscous* in the sense that it dissipates energy, with a force opposing the direction of motion. Anelasticity and viscoelasticity are very closely related.

8.3.2 Discrete-element models

To model solids with anelasticity / viscoelasticity, we consider that there are elastic elements (since some strain is recoverable) and viscous elements (since the response is not instantaneous), arranged in different ways. Elastic elements are represented as *springs*, with associated elastic strain ϵ_s and elastic stress σ_s ,

$$\epsilon_s = \frac{\sigma_s}{E} \quad \rightarrow \quad \dot{\epsilon}_s = \frac{\dot{\sigma}_s}{E} \quad (8.24)$$

and anelastic / viscous elements are represented as *dashpots*, with associated anelastic strain ϵ_d and anelastic stress σ_d ,

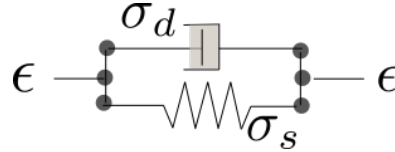
$$\dot{\epsilon}_d = \frac{1}{3\eta} \sigma \quad (8.25)$$

Maxwell solids assume the elements bear a load in *series* (isostress), Voigt assume the elements to bear a load in *parallel* (isostrain). The standard linear solid puts a Voigt element in series with an elastic element.

Voigt solid

For a Voigt solid, the spring and dashpot elements are in parallel, or isostrain. Now the stresses sum and the strains are equal,

$$\sigma = \sigma_s + \sigma_d \quad (8.26)$$

Figure 8.2: Voigt solid (isostrain ϵ , $\sigma = \sigma_s + \sigma_d$.)

$$\epsilon = \epsilon_s = \epsilon_d \quad (8.27)$$

Substituting in for the stresses,

$$\sigma(t) = E\epsilon + 3\eta\dot{\epsilon} \quad (8.28)$$

we define a time constant τ as

$$\tau \equiv \frac{3\eta}{E}$$

(8.29)

such that the prior equation is

$$\epsilon + \tau\dot{\epsilon} = E^{-1}\sigma \quad (8.30)$$

For a constant stress $\sigma(t) = \sigma_1$,

$$\epsilon(t) = \frac{\sigma_1}{E} \left(1 - e^{-t/\tau} \right) \quad (8.31)$$

we will have a long-term strain response reached only after a few time constants. There is then a *delayed* response, where the strain lags behind the strain that would be present in the absence of anelasticity ($\eta = 0$). The time delay of strain is key for irreversibility, as we will see particularly clearly for the case of cyclic stresses. Energy dissipation is a feature of anelasticity / viscoelasticity regardless of the specific model.

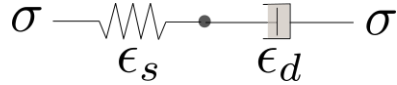
Maxwell solid

For the Maxwell solid, stress is everywhere the same and the strains sum,

$$\sigma = \sigma_s = \sigma_d \quad (8.32)$$

$$\epsilon = \epsilon_s + \epsilon_d \quad \rightarrow \quad \dot{\epsilon} = \dot{\epsilon}_s + \dot{\epsilon}_d \quad (8.33)$$

Substituting in,

Figure 8.3: Maxwell solid (isostress σ , $\epsilon = \epsilon_s + \epsilon_d$.)

$$\dot{\epsilon} = \frac{1}{E} \dot{\sigma} + \frac{1}{3\eta} \sigma \quad (8.34)$$

Two cases are interesting for the Maxwell solid. For a constant stress, $\sigma(t) = \sigma_1$, we can solve for the strain,

$$\epsilon(t) = \epsilon_0 + \frac{\sigma_1}{3\eta} t \quad (\sigma(t) = \sigma_1) \quad (8.35)$$

which increases linearly with time, with a strain rate inversely proportional to the shear viscosity. Alternatively, for a constant strain rate, $\dot{\epsilon}(t) = \dot{\epsilon}_1$,

$$E\tau\dot{\epsilon}_1 = \tau\dot{\sigma} + \sigma \quad (8.36)$$

$\sigma(t)$ is solved with

$$\sigma(t) = E\tau\dot{\epsilon}_1 \left(1 - e^{-t/\tau} \right) \quad (8.37)$$

Here τ gives the characteristic time for the stress to increase from zero to its asymptotic value $\sigma_\infty = E\tau\dot{\epsilon}_1$.

Standard linear solid

A standard linear solid considers a spring, E_u (unrelaxed modulus), in series with a Voigt element, characterized by E_1 and η . We will designate the Voigt element as 1 and the spring as u . The two elements are in isostress:

$$\sigma = E_u \epsilon_u \quad (8.38)$$

$$\sigma = E_1 (\epsilon_1 + \tau \dot{\epsilon}_1) \quad (8.39)$$

and the total strains sum

$$\epsilon = \epsilon_1 + \epsilon_u \quad (8.40)$$

The differential equation for stress and strain can be found by eliminating ϵ_1 and ϵ_u from the above equations and expressing a relationship between $\sigma, \epsilon, \dot{\sigma}$ and $\dot{\epsilon}$. We can eliminate ϵ_u simply,

$$\epsilon_u = \frac{\sigma}{E_U} \quad (8.41)$$

so

$$\epsilon_1 = \epsilon - \frac{\sigma}{E_U} \quad (8.42)$$

and for the strain rates,

$$\dot{\epsilon}_1 = \dot{\epsilon} - \frac{\dot{\sigma}}{E_U} \quad (8.43)$$

Rewriting the stress in the Voigt element,

$$E_1^{-1}\sigma = \epsilon_1 + \tau\dot{\epsilon}_1 \quad (8.44)$$

$$E_1^{-1}\sigma = \epsilon - E_U^{-1}\sigma + \tau(\dot{\epsilon} - E_U^{-1}\dot{\sigma}) \quad (8.45)$$

Next, we can define a *relaxed* Young's modulus,

$$E_R^{-1} \equiv E_U^{-1} + E_1^{-1} \quad (8.46)$$

which leaves

$$E_R^{-1}\sigma + \tau E_U^{-1}\dot{\sigma} = \epsilon + \tau\dot{\epsilon} \quad (8.47)$$

This is the general differential equation relating stress, strain, stress rate, and strain rate.

Step stress: We can now consider the strain response to a step stress,

$$\sigma(t) = 0 \quad t < 0 \quad (8.48)$$

$$\sigma(t) = \sigma_0 \quad t \geq 0 \quad (8.49)$$

and consider the initial, transient motion, and the equilibrium stress and strain. When the material is first loaded, the strain is zero, and stress rate $\dot{\sigma}$ is infinite. The Young's modulus is defined by the unrelaxed term,

$$\epsilon_0 = \frac{\sigma_0}{E_U} \quad t \ll \tau \quad (8.50)$$

where the strain ϵ_0 appears instantaneously. In the steady state, the time derivatives go to zero:

$$\epsilon_\infty = \frac{\sigma_0}{E_R} \quad t \gg \tau \quad (8.51)$$

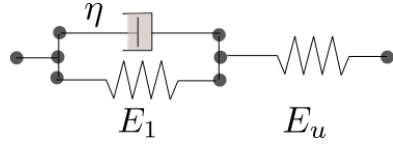


Figure 8.4: Standard linear solid: spring E_u and Voigt element (E_1, η) in isostress.

Between these limits, the strain responds with a characteristic time τ ,

$$\epsilon(t) = \epsilon_\infty + (\epsilon_0 - \epsilon_\infty) e^{-t/\tau} \quad (8.52)$$

$$\epsilon(t) = \sigma_0 \left[E_R^{-1} + (E_U^{-1} - E_R^{-1}) e^{-t/\tau} \right] \quad (8.53)$$

8.4 Internal friction

8.4.1 Cyclic stress; complex modulus

We can now consider how the standard linear solid behaves under a cyclic stress. We apply an alternating, sinusoidal stress at frequency ω .

$$\sigma(t) = \sigma_0 \cos \omega t \quad (8.54)$$

which can be represented as

$$\sigma(t) = \operatorname{Re} [\sigma_0 e^{-i\omega t}] \quad (8.55)$$

Here σ_0 is real-valued: we control the cyclic stress, know its phase, and set $t = 0$ to when it is maximized. The strain response will, for stresses not too large, also respond sinusoidally,

$$\epsilon(t) = \operatorname{Re} [\tilde{\epsilon}_0 e^{-i\omega t}] \quad (8.56)$$

where a complex $\tilde{\epsilon}_0 = |\epsilon_0| e^{i\delta}$ represents a phase delay of the strain response by an angle δ . For positive $0 \leq \delta \leq \pi$, the strain *lags behind* the stress, reaching its maximum value after the stress reaches its maximum value, delayed by $\Delta t = \delta/\omega$. We now define the complex Young's modulus

$$\tilde{\epsilon}_0 = \tilde{E}^{-1}(\omega) \sigma_0 \quad (8.57)$$

$$\tilde{E}(\omega) = E'(\omega) + iE''(\omega) \quad (8.58)$$

$$\tilde{E}(\omega) = |E|e^{-i\delta} = |E|(\cos \delta - i \sin \delta) \quad (8.59)$$

The ratio between the imaginary and real components of the modulus gives the tangent of the phase delay:

$$\tan \delta = -\frac{E''}{E'} \quad (8.60)$$

where a negative imaginary modulus corresponds to a delayed response.

Relationship of phase delay to energy loss

To consider the work done in cyclic stress, we can imagine first the response of strain ϵ to a positive stress σ . We know that the work done on the system, for increasing strain $\delta\epsilon > 0$ is

$$dW = +\sigma(\epsilon)\delta\epsilon \quad (8.61)$$

and the work done on the system will tend to increase the internal energy dU , through the elastic energy. If the stress is released, the system will do work on the surroundings: $\delta\epsilon < 0$, and $dW < 0$, tending to decrease the internal energy dU . If then we look at loading from $\sigma = 0$ to $\sigma = \sigma_{max}$ and back to $\sigma = 0$, there will be two contributions to work

$$W_{0,\sigma_{max},0} = \int_0^{\epsilon_{max}} \sigma_+(\epsilon)\delta\epsilon - \int_0^{\epsilon_{max}} \sigma_-(\epsilon)\delta\epsilon \quad (8.62)$$

where $\sigma_+(\epsilon)$ is the stress for strain on loading and $\sigma_-(\epsilon)$ is the stress for strain on unloading. The total work done on the system will be

$$W_{0,\sigma_{max},0} = \int_0^{\epsilon_{max}} (\sigma_+(\epsilon) - \sigma_-(\epsilon)) \delta\epsilon \quad (8.63)$$

Clearly, if the response is perfectly elastic, $\sigma = E'\epsilon$, the integral vanishes, and no net work is done on the system: as much is stored as is released, since the elastic response is reversible. For total work to be done on the sample, there must be some difference in the stress $\sigma_\pm(\epsilon)$ in loading and unloading. The difference requires *hysteresis*: the stress-strain relationship depends on the stress-strain history.

Moreover, for the total work to be positive, we must have $\sigma_+(\epsilon) > \sigma_-(\epsilon)$. (We cannot have the total work negative, produced by the system on the surroundings, according to the second law, unless we add heat.) In other

words, the stress-strain cycle in the $\epsilon - \sigma$ plane must go clockwise, as pictured. This implies that the strain is always behind where it would be in the elastic case: on loading, the strain is lower; on unloading, the strain is higher.

To extend this reasoning over the full cycle, we can consider the cyclic integration of terms in the first law,

$$\oint dU = \oint dW + \oint dq \quad (8.64)$$

where q is the heat flow. Of course the internal energy U is a single-valued function of state variables ϵ, σ only, and its integration will be zero, leaving

$$\oint dq = - \oint dW \quad (8.65)$$

so the work done on the system flows out to the surroundings as heat.
Therefore

- a finite phase lag δ implies energy dissipation.
- From the relation in Eq 8.60, an imaginary modulus E'' is a frictional term.
- Because friction can only be positive, $E'' < 0$.

Note that the sign of E'' depends on our sign convention for time; for $e^{+i\omega t}$ variation, E'' would be positive.

Q-factor

We can form a spring out of our viscoelastic material and see how it responds to a cyclic stress. Our material of interest, with complex modulus $\tilde{E}(\omega)$, is in the shape of a cylinder: top and bottom surface area A_0 , length l_0 . We impose a cyclic force $F_0 e^{-i\omega t}$ to the bottom surface and place a point-mass m at the top. The strain ϵ is uniform: the displacement within the cylinder (elastic wave) goes as $u = u_0 e^{ikx}$, but in the long-wavelength limit $kl_0 \ll 1$, so $u = u_0 kx$. The "spring constant" for the elastic force F_{el} from displacement $u(L, t)$ is

$$F_{el}(t) = -\frac{A_0}{l_0} E' u(L, t) \quad (8.66)$$

or with $F = -ku(L)$, $k = A_0 E' / l_0$, proportional to the real modulus with dimensional constants. The dissipative force from the shear viscosity, acting opposite to the direction of motion and not recoverable, is

$$F_{diss}(t) = -\frac{A_0}{l_0} 3\eta \frac{\partial u}{\partial t}(L, t) \quad (8.67)$$

If we substitute in sinusoidal variations for $u(t) = u_0 e^{-i\omega t}$, the total force is

$$F_{0,tot} = -\frac{A_0}{l_0} (E' - 3i\omega\eta) u_0 \quad (8.68)$$

suggesting that we can represent the complex modulus by

$$E'' = 3\eta\omega \quad (8.69)$$

We next compare the energy dissipated per cycle to maximum energy stored. Energy dissipated is

$$-\Delta q = \oint F_{diss}(t) du = -\frac{A_0}{l_0} 3\eta \int_0^{2\pi/\omega} \Re[-i\omega \widetilde{u}_0 e^{-i\omega t}] \Re[-i\omega \widetilde{u}_0 e^{-i\omega t} dt] \quad (8.70)$$

To evaluate the integral, we can use the trick

$$\Re[ab]\Re[cd] = \frac{1}{4} (abcd + a^*b^*c^*d^* + abc^*d^* + a^*b^*cd) \quad (8.71)$$

where b and d contain the time-dependent part $e^{-i\omega t}$. The only terms which survive the integration are the last two, bd^* and b^*d , since the others have sinusoidal components at 2ω and integrate to zero over the cycle. So

$$-\Delta q = -\frac{A_0}{l_0} 3\eta \frac{2\pi}{\omega} \frac{1}{2} (-i\omega \widetilde{u}_0) (-i\omega \widetilde{u}_0)^* \quad (8.72)$$

$$-\Delta q = -\frac{A_0}{l_0} \pi 3\eta\omega |\widetilde{u}_0|^2 \quad (8.73)$$

$$-\Delta q = -\frac{A_0}{l_0} \pi E'' |\widetilde{u}_0|^2 \quad (8.74)$$

We compare this energy dissipated with the maximum energy stored,

$$U_{max} = \frac{k}{2} |u_0|^2 = \frac{A_0}{2l_0} E' |u_0|^2 \quad (8.75)$$

The ratio of maximum energy stored to energy dissipated per cycle is called the *Q-factor*, or quality factor, of the oscillator:

$$Q \equiv 2\pi \frac{U_{max}}{-\Delta q} = -\frac{E'}{E''} \quad (8.76)$$

We will refer to the *Q*-factor more typically as its inverse,

$$\boxed{Q^{-1} = -\frac{E''}{E'}} \quad (8.77)$$

This is the *damping* of the oscillator.

Q-factor in free oscillation If the spring is given some initial displacement u_0 , it will oscillate freely at its resonance frequency. It will have an initial energy $U = ku_0^2/2$. For low damping, the elastic energy will decrease per cycle N as

$$\frac{dU}{dN} = -Q^{-1}U \quad (8.78)$$

$$\frac{\partial \ln U}{\partial N} = -(2\pi)Q^{-1} \quad (8.79)$$

So there will be an exponential decay of the elastic energy as a function of the number of cycles as

$$U(N) = U_0 e^{-2\pi Q^{-1} N} \quad (8.80)$$

and since the elastic energy is quadratic in the displacement, we can take the square root of this equation for the displacement,

$$u(N) = u_0 e^{-\pi Q^{-1} N} \quad (8.81)$$

We can now define a characteristic number of cycles, N_C , for the spring to reach $1/e$ of its initial amplitude:

$$u(N) = u_0 e^{-N/N_C} \quad N_C \equiv Q/\pi \quad (8.82)$$

This could also be expressed as a function of time, since each cycle requires a period $\tau = 2\pi/\omega_0$:

$$u(N) = u_0 e^{-t/\tau_C} \quad \tau_C \equiv Q\tau/\pi \quad (8.83)$$

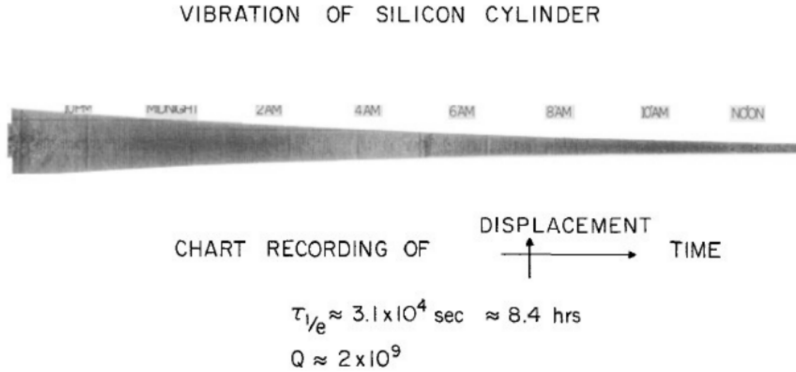


Fig. 5. Amplitude of vibration in first longitudinal mode of vibration vs. time. The value of $Q \approx 2 \times 10^9$ corresponding to a relaxation time $1/e$ of 3.1×10^4 sec = 8.6 h was measured. The oscillation in amplitude is caused by a slight frequency difference (which is deliberate) between the local oscillator and the cylinder.

Figure 8.5: Free vibrations of a Si spring at 4.2 K, from McGuigan et al[1].

The higher the quality factor of the spring, the longer it vibrates freely. The highest Q -factors in mechanical oscillation recorded are $Q \sim 4 \times 10^9$ for large (~ 20 cm) bulk quartz crystals. Very pure single-crystal Si can have similarly high values of Q [1], as shown in Figure [1]. For a frequency $\nu = 19553 \text{ s}^{-1}$, $Q = 2 \times 10^9$ translates to $\tau_C = 2 \times 10^9 \cdot 1/19553 \text{ s}^{-1}/\pi \simeq 9 \text{ hrs}$! Low temperatures are important for the high Q so that all free electrons can be frozen out of the system; conduction electrons provide another energy loss mechanism.

Q-factor in forced vibrations The amplitude under a sinusoidal force $F_0 e^{-i\omega t}$ is

$$\widetilde{u}_0 = \frac{F_0/m}{\omega_0^2 - \omega^2} \quad (8.84)$$

$$\widetilde{u}_0 = \frac{F_0/m}{\omega_0^2 (1 - iQ^{-1}) - (\omega_0 + \Delta\omega)^2} \quad (8.85)$$

$$\widetilde{u}_0 = \frac{F_0/(m\omega_0)}{2\Delta\omega - iQ^{-1}\omega_0} \quad (8.86)$$

$$\widetilde{u}_0 = \frac{F_0/(4m\omega_0)}{(\Delta\omega)^2 + Q^{-2}\omega_0^2/4} (2\Delta\omega + iQ^{-1}\omega_0) \quad (8.87)$$

We take $\Delta\omega_{1/2}$ as the circular frequency detuning away from the resonance. The imaginary amplitude (proportional to power dissipation) has a FWHM in frequency of

$$2\Delta\omega_{1/2} = \omega_0 Q^{-1} \quad (8.88)$$

$$2\Delta\nu_{1/2} = \nu_0 Q^{-1} \quad (8.89)$$

For the example of the Si single crystal, we would have a frequency FWHM of 10^{-7} Hz!

8.4.2 Response of the standard linear solid

We can calculate the sinusoidal response of the response in the limit of small differences between the relaxed and unrelaxed moduli,

$$E_R \equiv (1 - \Delta) E_U \quad |\Delta| \ll 1 \quad (8.90)$$

and $\Delta > 0$, since the unrelaxed modulus (single spring) is always larger than the relaxed modulus (which adds a spring in series.) For small Δ , the reciprocal is

$$E_R^{-1} \equiv (1 + \Delta) E_U^{-1} \quad (8.91)$$

from the Taylor series $(1+x)^{-1} \simeq 1-x$. Substituting the cyclic response into the standard linear solid equation of motion,

$$E_R^{-1} \sigma + \tau E_U^{-1} \dot{\sigma} = \epsilon + \tau \dot{\epsilon} \quad (8.92)$$

$$(E_R^{-1} - i\omega\tau E_U^{-1}) \sigma_0 = (1 - i\omega\tau) \tilde{\epsilon}_0 \quad (8.93)$$

Next substituting in for Δ ,

$$(1 + \Delta - i\omega\tau) E_U^{-1} \sigma_0 = (1 - i\omega\tau) \tilde{\epsilon}_0 \quad (8.94)$$

$$\left[1 + \Delta (1 - i\omega\tau)^{-1} \right] E_U^{-1} \sigma_0 = \tilde{\epsilon}_0 \quad (8.95)$$

making use of the Taylor series expansion for small Δ again,

$$\tilde{E}(\omega) = \left[1 - \Delta (1 - i\omega\tau)^{-1} \right] E_U \quad (8.96)$$

$$\tilde{E}(\omega) = \left[1 - \Delta \frac{1 + i\omega\tau}{1 + \omega^2\tau^2} \right] E_U \quad (8.97)$$

Taking the ratio of the imaginary to the real modulus, we see (again for small Δ)

$$\tan \delta = \Delta \frac{\omega \tau}{1 + \omega^2 \tau^2} \quad (8.98)$$

The phase lag is maximized for $\omega \tau = 1$, with maximum value $\tan \delta_m = \Delta/2$. Remembering that $\tan \delta = Q^{-1}$, we have

$$Q^{-1} = [Q^{-1}]_{max} \frac{2\omega \tau}{1 + \omega^2 \tau^2} \quad (8.99)$$

This equation implies that there is a strongly peaked frequency dependence of internal friction. If the frequency of cyclic stress is close to the frequency with which the stress relaxes, the damping is maximized, for $\omega \tau = 1$. If the cyclic stress is at such a high frequency that the relaxation does not have time to occur, $\omega \tau \gg 1$, the Voigt element bears no strain and does not dissipate energy. If on the other hand the cyclic stress is applied very slowly compared with the relaxation time, $\omega \tau \ll 1$, the dashpot element does not contribute any force to the Voigt element, and all the stress is elastic.

8.4.3 Snoek damping

We have not yet addressed what microscopic, atomic mechanisms can be involved in viscoelasticity. A classic example, one which is technologically relevant for steels, was identified by Snoek in 1941[2]. Snoek found that the damping in steels was proportional to interstitial carbon (C) concentration. The mechanism is shown in Figure 8.6 a). For stresses σ along the x, y , or z directions, the energy of C impurities in octahedral sites, initially equal, changes: if a tensile (compressive) stress is applied along the long axis of the interstitial site (along the cube edge upon which it sits), its energy increases (decreases) compared with the interstitial sites of different types. This creates a chemical potential difference which drives short-ranged C diffusion: the C atoms hop from one site to an adjacent site.

The diffusion constant (defined as the ratio of atomic flux to concentration gradient, $\mathbf{J} = -D\nabla c$) is thermally activated, with

$$D(T) = D_0 \exp - \frac{\Delta H}{RT} \quad (8.100)$$

where R is the ideal gas constant $R = N_A k_B = 8.314 \text{ J/mol/K}$ in a molar basis. The thermal activation of diffusion comes about because the hopping frequency of the atoms from one site to another is also thermally

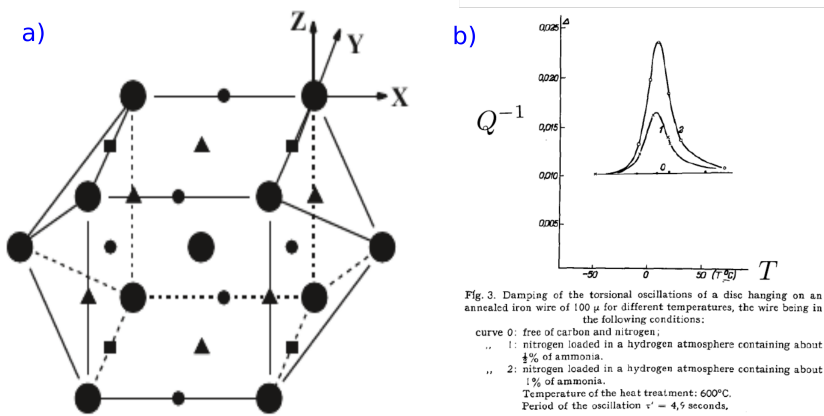


Fig. 3. Damping of the torsional oscillations of a disc hanging on an annealed iron wire of 100μ for different temperatures, the wire being in the following conditions:
curve 0: free of carbon and nitrogen;
.. 1: nitrogen loaded in a hydrogen atmosphere containing about $\frac{1}{2}\%$ of air;
.. 2: iron loaded in a hydrogen atmosphere containing about 1% of ammonia.
Temperature of the heat treatment: 600°C .
Period of the oscillation $\tau' = 4.5$ seconds.

Figure 8.6: Snoek damping, relevant for steels. a) (Left): location of octahedral interstitial sites for small impurities (e.g. C,N,O) in BCC metals (e.g. Fe, Cr, V.) The different sites (circles, squares, triangles) become lowered (raised) in energy when a compressive stress is applied along (transverse to) their edge direction. (Taken from [3].) b) (Right) Snoek's data, showing a damping maximum for small percentages of C in Fe (steel) as a function of temperature, from Ref [2]. The damping is proportional to C concentration in the steel.

activated, since the atoms must squeeze through a high-energy state during the jump,

$$\nu(T) = \nu_0 \exp - \frac{\Delta H}{RT} \quad (8.101)$$

This hopping frequency can be related to the characteristic time for the hop, $\nu = \tau^{-1}$,

$$\tau(T) = \tau_0 \exp + \frac{\Delta H}{RT} \quad (8.102)$$

where we can now equate the hopping time with the relaxation time $\sigma = E\tau\dot{\epsilon}$. The hopping is irreversible because the jump excites short-wavelength lattice vibrations of the Fe lattice, which (when propagating to the edges of the sample) allow heat to flow out of the sample. The relaxation time is then strongly temperature dependent. Using the mathematical identity

$$\operatorname{sech} [\ln x] = \frac{2}{e^{\ln x} + e^{-\ln x}} \quad (8.103)$$

$$\operatorname{sech} [\ln x] = \frac{2}{x + 1/x} \quad (8.104)$$

$$\operatorname{sech} [\ln x] = \frac{2x}{1 + x^2} \quad (8.105)$$

we can rewrite our damping expression as

$$Q^{-1} = [Q^{-1}]_{max} \operatorname{sech} [\ln \omega \tau] \quad (8.106)$$

Now substituting in for $\tau(T)$,

$$Q^{-1} = [Q^{-1}]_{max} \operatorname{sech} \left[\ln \omega \tau_0 + \frac{\Delta H}{RT} \right] \quad (8.107)$$

The $\operatorname{sech} x$ function is peaked with maximum value of 1 and FWHM of ~ 2.5 at $x = 0$. For a given frequency, with $\omega_{ref}/2\pi = 1$ Hz taken as standard, there will then be a *temperature T_m for which the damping is maximum*. The temperature for maximum damping is then given by

$$\ln \omega_{ref} \tau_0 + \frac{\Delta H}{RT_m} = 0 \quad (8.108)$$

and we can rewrite the damping expression as

$$Q^{-1} = [Q^{-1}]_{max} \operatorname{sech} \left[\frac{\Delta H}{R} \left(\frac{1}{T} - \frac{1}{T_m} \right) \right] \quad (8.109)$$

From the tables in Blantner, p. 16, we have for C in $\alpha - Fe$, $[Q^{-1}]_{max} = 0.215$, $T_m = 314$ K, $\tau_0 = 1.89$ fs, and $\Delta H = 83.7$ kJ/mol. We can calculate the damping under two conditions of interest:

- $\nu = 1$ Hz, $T = 295$ K. At room temperature, the damping will be different from its maximum at 314 K. We have:

$$\frac{Q^{-1}}{[Q^{-1}]_{max}} = \operatorname{sech} \left[\frac{83700}{8.314} \left(\frac{1}{295} - \frac{1}{314} \right) \right] = 0.25 \quad (8.110)$$

so that the damping is one quarter as strong at room temperature as it is at its maximum.

- $\nu = 440$ Hz, $T = 295$ K The reference tone near the middle of a piano, A4, is tuned to this frequency. This tone is the resonant frequency of a steel string (piano wire) placed under tension, produced by striking the string with a hammer. Now at room temperature,

$$\frac{Q^{-1}}{[Q^{-1}]_{max}} = \operatorname{sech} \left[\ln 2\pi 1.89 \text{ fs } 440 \text{ s}^{-1} + \frac{83700}{8.314 295} \right] = 5.8 \times 10^{-4} \quad (8.111)$$

For 0.5% atomic of interstitial C in Fe, representative for piano wire, there would be $Q^{-1} = 6.2 \times 10^{-5}$ contributed by the Snoek mechanism. We can convert this to a decay time for the amplitude vibration of $\tau_C = Q/(\pi\nu) = 1./(\pi 440 \text{ s}^{-1} 6.2 \times 10^{-5})$ of 11.6 s; the decay time for the sound (varying as the square of the amplitude) is roughly 5.8 s according to our estimate.

Exercises

1. Compare the effective Young's modulus for a 10% volume fraction of hard material A in a matrix of soft material B , $E_A = 10E_B$, in two geometries:
 - Fiber geometry (long axes of fibers along stress)
 - Plate geometry (composition modulation in direction of primary stress), neglecting Poisson contraction
 - Plate geometry (composition modulation in direction of primary stress), including Poisson contraction. Take $\nu_A = 0.3, \nu_B = 0.45$.
2. Derive a relationship for the Young's modulus of plates in the $x_1 - x_2$ plane, σ_1/ϵ_1 where the primary stress σ_1 is applied along one of the in-plane directions of the plate. Express your answer in terms of the volume fractions V_A, V_B and isotropic elastic constants E_A, E_B, ν_A, ν_B .
3. Consider a model of a viscoelastic solid in which a Maxwell element (E_a, η) is in parallel (isostrain) with an elastic element E_b . Derive the equation of motion relating $\epsilon, \sigma, \dot{\epsilon}, \dot{\sigma}$. Solve for the Young's modulus in the $t = 0+$ and $t = \infty$ limits, and plot the stress σ as a function of time under a step stress.
4. The elongation of a cylinder of slightly viscoelastic material is found to be 1 % greater for a step stress σ_0 measured after 1 day compared with after 100 fs. If the viscoelasticity of the cylinder is dominated by a single defect with a single relaxation time, what will be the *shortest* time for a spring made from this material set into free vibration to decay to 10% of its initial amplitude, if measurements are taken for a full range of masses applied to the end of the spring?
5. The notes on a piano span a range from 27.5 Hz to 4186 Hz. The A keys are tuned to 440 Hz for A4, with each octave doubling in frequency in the following sequence: 27.5, 55, 110, 220, 440, 880, 1760, 3520 Hz for A1-A8 on the keyboard. Plot (using python) as a function of frequency over $A0 - A7$ the *sustain time* for a given note struck on the piano, defined as the time needed for the volume (square of amplitude) to decay to $1/e$ its initial value. Use a logarithmic scale for the frequency. Make your estimate a) assuming that the Q value for the oscillation is that for A4 as calculated in the lectures, b) taking into account the frequency dependence of Q expected for piano wire. Does the result seem reasonable?

Bibliography

- [1] D.F. McGuigan et al. “Measurements of the Mechanical Q of Single-Crystal Silicon at Low Temperatures”. In: *Journal of Low-Temperature Physics* 30 (5 1978), pp. 621–629.
- [2] J.L. Snoek. “Effect of small quantities of carbon and nitrogen on the elastic and plastic properties of iron”. In: *Physica* 8 (1941), pp. 711–733.
- [3] M.S. Blantner et al. *Internal Friction in Metallic Materials: a Handbook*. Springer, 2007.

Chapter 9

Introduction to plasticity: tensile

For small enough stresses σ , applied slowly enough ($\omega \rightarrow 0$ limit), on any crystalline material, the strain response ϵ will be fully elastic. Strains are reversible: when σ is reduced to zero, the strain also goes to zero, and the material regains its initial shape. No energy is lost to heat in this kind of response. Fortunately, elasticity is not the whole story. For stresses larger than a critical value, applied to a metal, the strain becomes permanent, or *plastic*. Plasticity (or *ductility*) is one of the most useful engineering properties of metals: it allows us to form metals into shapes by applying enough pressure, through hot-rolling, drawing, etc. Ceramics are usually *brittle* at room temperature: they simply fracture when the stress is too large. (At elevated temperatures, ionic compounds too can have a plastic strain response.) In this section we will look at some basic phenomenology of plasticity in metals, expressed in a tensile test.

9.1 Engineering stress and engineering strain

Up until now, we have concerned ourselves with true stress and true strain, but the engineering quantities s and e are the ones which are measured directly in tensile tests and more relevant for service.

9.1.1 Engineering stress s

The true stress for a material bearing a load P is

$$\sigma = \frac{P}{A} \quad (9.1)$$

where A is the cross sectional area of the material *at that stress*, $A = A(\sigma)$. For a cylinder under simple tension along the axial direction ϵ_3 , there will certainly be a Poisson contraction of the area,

$$\frac{\Delta A}{A_0} = \epsilon_1 + \epsilon_2 \quad (9.2)$$

$$\frac{\Delta A}{A_0} = -2\nu\epsilon_3 \quad (\text{elastic}) \quad (9.3)$$

but it will be negligible in metals because the elastic strains are never large. Taking an example of a very strong material, piano wire (high-carbon steel, cold-drawn) with $\sigma_y \simeq 3$ GPa, $E \simeq 210$ GPa, the elastic strains are $\epsilon_3 \simeq \sigma_y/E \simeq 1.5\%$, and with $\nu = 0.33$, the area shrinks only by 1%. Just considering the elastic response, the difference between the true stress and the engineering stress s ,

$$s \equiv \frac{P}{A_0} \quad (9.4)$$

is negligible. While constitutive relations between stress and strain $\sigma = \sigma(\epsilon)$ always relate the true stress and true strain, we are much more interested in the engineering stress for applications. We would like steel beams to support their loads P in service. We know the area A_0 the beams had when we put them into service and do not much care about (and cannot easily know) their area under loading $A(\sigma)$.

9.1.2 Engineering strain e

The *engineering strain*

$$e \equiv \frac{\Delta L}{L_0} \quad \Delta L = L_f - L_0 \quad (9.5)$$

tells us about the elongation of the beam to a final length L_f , normalized to its initial length L_0 . The difference with the true strain,

$$\delta\epsilon \equiv \frac{\delta L}{L} = d \ln L \quad (9.6)$$

becomes important only for large strains. Going from an initial length L_0 to a final length L_f , the true strain integrates to

L_0	L_1	L_2	L_3 (m)
1.0	1.1	1.21	1.321

Table 9.1: Sequence of 10% strains from L_0 to $L_f = L_3$.

$$\epsilon_{0,f} = \ln \frac{L_f}{L_0} \quad (9.7)$$

For the engineering strain,

$$e_{0,f} = \frac{L_f - L_0}{L_0} \quad (9.8)$$

$$\frac{L_f}{L_0} = 1 + e_{0,f} \quad (9.9)$$

so true strain is related to engineering strain through

$$\epsilon = \ln(1 + e) \quad (9.10)$$

In the limit of $e \ll 1$, there is no difference: $\ln(1 + x) \simeq x$ for small x .

Engineering strains do not sum The true strains have the convenient property that if we sum a series of smaller strains, going from e.g. L_0 to L_f in three steps L_1, L_2, L_3 , as shown, their sum is the same as the total strain. Consider a sequence of three elongations, each by 10%, as presented in Table 9.2. Each engineering strain $e_{i,i+1} = (L_{i+1} - L_i)/L_i$ is 10%, so that the sum of the engineering strains is 0.3. However, if we take the engineering strain from start to finish, $e_{03} = 0.321$, and

$$e_{03} \neq e_{01} + e_{12} + e_{13} \quad (9.11)$$

True strains, on the other hand, can be summed

$$\epsilon_{01} + \epsilon_{12} + \epsilon_{23} = 3 \ln 1.1 = \ln 1.1^3 = \epsilon_{03} \quad (9.12)$$

9.2 Volume conservation in plasticity

Empirically, when a metal begins to flow under an applied stress, its total volume is approximately conserved, to a precision of $\sim 10^{-3}$. This means that we can write

$$AL \simeq A_0 L_0 \quad (9.13)$$

Thus for any plastic elongation ΔL , there will be a reduction in area. We can define a fractional reduction in area q as

$$q \equiv \frac{A_0 - A_f}{A_0} \quad (9.14)$$

so volume conservation implies

$$(1 - q) A_0 (1 + e) L_0 \simeq A_0 L_0 \quad (9.15)$$

$$(1 - q) (1 + e) \simeq 1 \quad (9.16)$$

$$-q + e - qe = 0 \quad (9.17)$$

$$q = \frac{e}{1 + e} \quad (9.18)$$

The effect of this reduction in area is that plastic flow can be very unstable. Plastic flow starts locally, where some imperfection (typically at the surfaces) concentrates stress. This section elongates ($\Delta L > 0$) and becomes narrower ($\Delta A < 0$) transverse to the stress. For fixed load P , the stress $\sigma = P/A$ increases due to the reduction in area. This increased stress causes more plastic flow, further decreasing the area, in a positive feedback loop. In the absence of any countervailing tendency of the metal to become stronger under deformation, the plastic deformation would immediately become unstable and the sample would fail catastrophically.

Estimating the stress at failure is most convenient through the area, since the area reduction q can be measured post-mortem, locally, where the sample fractured. From $A_f = (1 - q)A_0$

$$\sigma = \frac{s}{1 - q} \quad (9.19)$$

Equivalently, if the elongation can be measured accurately in the vicinity of the plastic deformation, we can relate true stress and true strain as

$$\sigma = s(1 + e) \quad (\text{uniform}) \quad (9.20)$$

This equation together with Eq 9.10 allows us to convert from the engineering stress and strain to true stress and strain in an experiment. Using Eq 9.10, Eq 9.20 can be expressed as

Metal	Condition	n	K (MPa)
Cu	annealed	0.54	33
Cu ₇₀ Zn ₃₀ (brass)	annealed	0.49	92
0.6% C steel	quenched and tempered at 704° C	0.19	125
0.6% C steel	quenched and tempered at 534° C	0.10	160

Table 9.2: Tabulated strength coefficients K and strain hardening exponent n for different metals, processed different ways. From Dieter.

$$\sigma_u = s_u e^{\epsilon_u} \quad (9.21)$$

where the u subscript denotes properties at the *ultimate engineering stress*, found at the maximum load P_u sustained by the sample in tension.

9.3 The flow curve

Experimentally, it is often found that the true stress - true strain relationship for a metal in the plastic regime is followed by

$$\sigma = K \epsilon_p^n \quad (9.22)$$

where ϵ_p is the plastic strain, K is the *strength coefficient*, in Pa, and n is the dimensionless *strain hardening exponent*. Two limits can be considered for n . If $n = 0$, the material is perfectly plastic: increasing strain requires no increase in stress. In this limit, the material does not harden at all during deformation. If $n = 1$, the material is perfectly elastic, σ_0 is zero, and $K \sim E$. Otherwise, this relationship neglects elasticity. At the yield point,

$$\sigma_y = K \epsilon_{p,y}^n \quad (9.23)$$

where is a conventionally defined amount of plastic strain. In the USA, the convention for σ_y is $\epsilon_{p,y} = 0.002$.

The strain hardening coefficient n determines how much the metal strengthens as a result of plastic deformation. The metal becomes increasingly stronger with increasing plastic deformation ϵ because of the peculiar behavior of the line defects (dislocations) which dominate plasticity. We will pay greater attention to the microscopic behavior of dislocations in following chapters.

Taking a derivative of Eq 9.22 with respect to strain,

$$\frac{\partial \sigma}{\partial \epsilon} = nK \epsilon^{n-1} \quad (9.24)$$

$$\left(\frac{\partial \sigma}{\partial \epsilon} \right) = n \frac{\sigma}{\epsilon} \quad (9.25)$$

9.3.1 Instability in tension: Considère's criterion

As described in Section 9.2, the stress σ can increase at fixed load, and fixed engineering stress s , because the area in the region of plastic flow begins to drop. This phenomenon is called "necking" because of the appearance of the reduced area / increased elongation region. Strain hardening turns out to be essential to keep the metal from failing immediately, as soon as plastic deformation begins. However, there will be still be a *maximum load* P_u that the sample can bear. For this load, the weakening tendency of reducing the cross-sectional area balances with the strengthening tendency of the work hardening. At the instability¹

$$\left(\frac{\partial P}{\partial e} \right)_{e=e_u} = 0 \quad (9.26)$$

where the derivative is positive (strain hardening) for strains below the maximum and negative (weakening) for strains above the strain at maximum load e_u . We can express

$$dP = d(\sigma A) = 0 \quad (9.27)$$

$$0 = \sigma dA + Ad\sigma \quad (9.28)$$

$$\frac{dA}{A} = -\frac{d\sigma}{\sigma} \quad (9.29)$$

However, from conservation of volume,

$$d(AL) = 0 \quad (9.30)$$

$$\frac{dA}{A} = -\frac{dL}{L} \quad (9.31)$$

$$\frac{dA}{A} = -d\epsilon \quad (9.32)$$

Thus

¹This material is covered in Dieter, Ch. 8.3[dieterCh8p3]

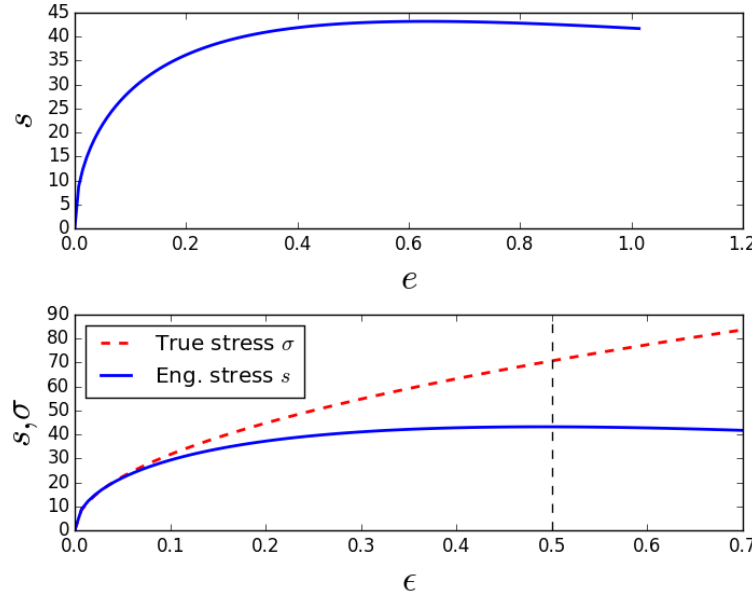


Figure 9.1: Illustration of tension test in plastic regime; stress in MPa, assuming $K = 100$ MPa, $n = 0.5$. The instability point from Eq 9.39 is illustrated.

$$\left(\frac{\partial \sigma}{\partial \epsilon} \right)_{\epsilon=\epsilon_u} = \sigma_u \quad (9.33)$$

This is Considère's criterion. Expressed graphically, it means that if we draw a tangent to the $\sigma(\epsilon)$ curve and extrapolate it to $\sigma = 0$, the distance in strain from the point at which we take the tangent to the ϵ axis intercept is equal to 1 for $\epsilon = \epsilon_u$. To see this, we can take the first Taylor series approximation to $\sigma(\epsilon)$ about a point ϵ_0

$$\sigma(\epsilon) \simeq \sigma(\epsilon_0) + \left(\frac{\partial \sigma}{\partial \epsilon} \right)_{\epsilon=\epsilon_0} (\epsilon - \epsilon_0) \quad (9.34)$$

Clearly this is a good approximation only for small deviations $\epsilon - \epsilon_0$, but that is not important here. This relation extrapolates to $\sigma = 0$ at a strain ϵ_1 :

$$-\sigma(\epsilon_0) = \left(\frac{\partial \sigma}{\partial \epsilon} \right)_{\epsilon=\epsilon_0} (\epsilon_1 - \epsilon_0) \quad (9.35)$$

Compare with Considère's criterion,

$$\left(\frac{\partial \sigma}{\partial \epsilon} \right)_{\epsilon=\epsilon_u} = \sigma_u \quad (9.36)$$

If we have taken the tangent from the instability point, $\epsilon_0 = \epsilon_u$, then we can substitute in

$$\sigma(\epsilon_u) = \sigma_u (\epsilon_u - \epsilon_1) \quad (9.37)$$

Thus we can identify the instability point, ϵ_u , as the point from which the distance in strain to the intercept is 1, $\epsilon_u - \epsilon_1 = 1$.

This gives us a graphical means to determine the strain-hardening exponent n . We can equate the derivative on the left hand side with the stress-strain relationship from strain hardening in Eq 9.25:

$$n \frac{\sigma_u}{\epsilon_u} = \sigma_u \quad (9.38)$$

which means that the strain hardening exponent can be identified from the strain at maximum load,

$$n = \epsilon_u \quad (9.39)$$

or from the engineering strain at maximum load e_u ,

$$n = \ln(1 + e_u) \quad (9.40)$$

Exercises

1. For a cylinder of power-law strain hardening metal, loaded along its axis by P and characterized by strength coefficient K and strain-hardening exponent n , with initial diameter D_0 , derive an expression for the maximum load P_u in terms of K, n and D_0 .

Chapter 10

Forces on a dislocation

Contents

10.1 Strain and dislocation density	170
10.1.1 Strain as a function of dislocation density	170
10.1.2 Strain rate as a function of dislocation velocity . .	170
10.1.3 Dislocation accumulation	170
10.2 Peach-Koehler forces	171
10.2.1 Edge dislocation under simple shear	171
10.2.2 Mixed dislocation under arbitrary σ	173
10.2.3 Glide force on a dislocation loop	175
10.3 Strain fields and self-energy of dislocations	177
10.3.1 Screw dislocation	177
10.3.2 Edge dislocation	180
10.3.3 Force between two dislocations	183
10.4 Line tension of a dislocation	184
10.5 Dislocation - point-defect interactions	188
10.5.1 Chemical force in dislocation climb	189
10.5.2 Glide pinned by point defects	193
10.6 Dislocation dynamics	196
10.6.1 Power-law creep	197
10.6.2 Strain rate	197
10.6.3 Tensile test: yield drop	199

10.1 Strain and dislocation density

Some of these relationships will be needed in the subsequent discussions.

10.1.1 Strain as a function of dislocation density

The macroscopic shear is proportional to the propagation of dislocations. This is relatively simple to understand. We can consider plastic deformation in a prism of dimensions L_x, L_y, L_z . In shear σ_{xy} of an edge dislocation with $\mathbf{b} = b\hat{x}$, the transit Δx of a dislocation by the full sample dimensions, L_x displaces the top face with respect to the bottom by the amount of the Burgers vector b . This gives us an engineering strain γ_{xy} of b/L_y

$$\gamma_{xy} = \frac{\Delta x}{L_x} \frac{b}{L_y} \quad (\text{single}) \quad (10.1)$$

for a single dislocation. The strain will be multiplied by the number of dislocations N_d in this area, which travel a similar distance Δx . In terms of the dislocation density $n_d = N_d/(L_x L_y)$,

$$\gamma_{xy} = b n_d \Delta x \quad (10.2)$$

10.1.2 Strain rate as a function of dislocation velocity

The strain rate is obtained by taking a time derivative. In terms of the dislocation velocity,

$$\dot{\gamma}_{xy} = b n_d v_d \quad (10.3)$$

Alternatively, in terms of the tensor shear strain,

$$\dot{\varepsilon}_{xy} = \frac{b}{2} n_d v_d \quad (10.4)$$

10.1.3 Dislocation accumulation

During plastic deformation, are generated in the crystal and can become stuck at pinning sites. Again considering that one dislocation is lost from the crystal for a motion of the top surface area $L_x L_z$ by a Burgers vector b ,

$$\frac{\partial N_d}{\partial \gamma} = \frac{1}{\frac{b}{L_y}} = \frac{L_y}{b} \quad (10.5)$$

the areal density in $L_x L_y$ changes by

$$\frac{\partial n_d}{\partial \gamma} = \frac{L_y}{b} \frac{1}{L_x L_y} \quad (10.6)$$

$$\frac{\partial n_d}{\partial \gamma} = \frac{1}{b L_x} \quad (10.7)$$

If instead, generated dislocations become stuck at mean free paths of Λ , rather than propagating to the edge of the crystal and disappearing, there is a net gain of dislocations found by taking $L_x \rightarrow \Lambda$:

$$\frac{\partial n_d}{\partial \gamma} = \frac{1}{b \Lambda} \quad (10.8)$$

10.2 Peach-Koehler forces

The Peach-Koehler formula determines the force per unit length which acts on a dislocation due to the application of a stress tensor σ_{ij} . We will start with the simplest force, acting on an edge dislocation under pure shear, in Section 10.2.1. The *Peach-Koehler formula* will be generalized to an arbitrary dislocation under arbitrary stress in Section 10.2.2. Finally, in Section 10.2.3, we will apply this formula to a circular dislocation loop, and show that it expands (or contracts) uniformly under the application of shear resolved to its slip plane.

10.2.1 Edge dislocation under simple shear

The simplest example of a force on a dislocation is that due to pure shear, causing an edge dislocation to glide. We will consider a crystal with top surface area $A\hat{\mathbf{y}} = L_x L_z \hat{\mathbf{y}}$, for a prism with lengths L_x, L_y, L_z . The dislocation line $\hat{\mathbf{l}}$ is taken to be $+\hat{\mathbf{z}}$. For a dislocation with additional half plane originating in the center of the crystal and extending to $-\hat{\mathbf{y}}$, the Burgers vector is $\mathbf{b} = +b\hat{\mathbf{x}}$, according to the *RH, fs* sign convention. (Similarly, one with half plane extending to $+\hat{\mathbf{y}}$ has $\mathbf{b} = -b\hat{\mathbf{x}}$.) The dislocation is pictured in Figure 10.1.

We know already that the force on the dislocation must be in $-\hat{\mathbf{x}}$, because plastic shear, as pictured, requires atoms to flow from the center to the bottom left (and top right) of the crystal. For the dislocation pictured, the extra half plane needs to move to the bottom left; this is dislocation motion in $-\hat{\mathbf{x}}$. After passage of one edge dislocation, as pictured, the top surface will have moved with respect to the bottom surface by an amount $\mathbf{b} = +b\hat{\mathbf{x}}$.

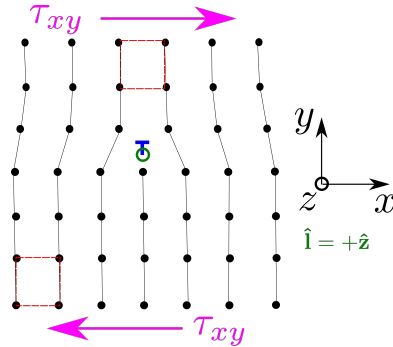


Figure 10.1: Profile of an edge dislocation, with Burgers vector $\mathbf{b} = b\hat{x}$, in a crystal subjected to a shear σ_{xy} . For the RH-fs sign convention of the edge dislocation, the Burgers circuit creating \mathbf{b} is a right-hand circuit about the line-vector $\hat{l} = +\hat{z}$, out of the page. The shear causes the dislocation to glide to the left ($-\hat{x}$) in the figure. Red boxes show that the lattice is nearly undistorted far away from the dislocation.

If a single dislocation inside the crystal moves by some distance less than that required to reach the sample edge, there will be no macroscopic plastic shear. The external dimensions of the sample do not change. However, if the dislocation glides all the way to the edge of the crystal, the additional half plane will hang off the edge, and there will be a net shear displacement of the top of the crystal with respect to the bottom by an amount b .

The force acting on a dislocation, \mathbf{f}_D , can be estimated through an energy balance, equating work done on the crystal and "work done" on the dislocation. In this discussion we should bear in mind that the dislocation is a sort of accounting trick, and that the real, irreversible work is done by externally applied forces which ultimately move atoms.

The work δW done *on the crystal* in plastic shear is

$$\delta W = \mathbf{f}_{\text{top}} \cdot \delta \mathbf{x} \quad (10.9)$$

where \mathbf{f}_{top} is the total force acting on the top surface of the crystal and $\delta \mathbf{x}$ is the distance through which the top surface moves. This work is irreversible and the energy added to the system goes directly into heat. Plastic strain is not recoverable, in contrast to elastic strain, so removal of the stimulus (σ) does not allow the response (ϵ_p) to return to zero.

Since the required shear is τ_{xy} , the force is $f_{\text{top}}\hat{x} = \tau_{xy}L_zL_x\hat{x}$, and the displacement is $\delta \mathbf{x} = b\hat{x}$, so the work done to move one dislocation across the whole crystal is

$$\delta W = \tau_{xy} L_z L_x b \quad (10.10)$$

However, we can equate the work done on the crystal for plastic shear with the work done "on the dislocation", by a force acting on the dislocation \mathbf{f}_d :

$$\delta W = \mathbf{f}_d \cdot (d\mathbf{s}) \quad (10.11)$$

where $\mathbf{s} = +s\hat{x}$ is the glide vector of the edge dislocation, the vector through which the dislocation glides. An infinite line can move only transverse to its length, so

$$\mathbf{s} \cdot \hat{\mathbf{l}} = 0 \quad (10.12)$$

i.e. the glide vector is transverse to the dislocation line. If the dislocation moves across the whole crystal, and we know its motion to be in $-\hat{x}$: $\mathbf{s} = -L_x\hat{x}$. Work can be done on the dislocation only if the force acting on the dislocation, \mathbf{f}_d , is also in $-\hat{x}$.

$$\delta W = -f_D L_x \quad (10.13)$$

Equating the two expressions for work, the force acting on the dislocation per unit length is

$$-f_D L_x = \tau_{xy} L_x L_z b \quad (10.14)$$

$$\frac{\mathbf{f}_d}{L_z} = -\tau_{xy} b \hat{x}$$

(10.15)

scaling proportionally with the shear stress, which is intuitive, and with the Burgers vector, which is on the order of atomic spacings. The force which acts on the dislocation ($\tau_{xy} L_z b$) is many orders of magnitude smaller than that exerted on the outer boundary of the crystal ($\tau_{xy} L_z L_x$), scaled down by an approximate number of atoms across the crystal $L_x/b \simeq L_x/a$.

10.2.2 Mixed dislocation under arbitrary σ

This derivation can be extended to an arbitrary (mixed) dislocation line under an arbitrary stress $[\sigma]$. This was done by Peach and Koehler in 1950[1]. Here we consider a differential element of the dislocation line $d\mathbf{l} = \delta l \hat{\mathbf{l}}$, slipping by a differential distance $d\mathbf{s} = \delta s \hat{\mathbf{s}}$. Again the unit vectors $\hat{\mathbf{l}}$ and $\hat{\mathbf{s}}$ are

orthogonal, since dislocation lines can move only normal to their direction \hat{l} (Eq 10.12.)

In evaluating the equivalent of Eq 10.9, the work on external surfaces, for arbitrary stress $[\sigma]$, we use the force acting on a differential area element,

$$\mathbf{F} = [\sigma] \delta \mathbf{A} \quad (10.16)$$

from Eq 3.9, the definition of the stress tensor as a proportionality. The differential area element uncovered by the slip of δl through δs is

$$\delta \mathbf{A} = \delta s \delta l \hat{l} \times \hat{s} \quad (10.17)$$

where the cross-product gives the area element. To keep track of the sign of this area element, the surface normal $\mathbf{A} = A \hat{n}$ will be in a right hand sense from $\delta \hat{l}$ and $\delta \hat{s}$. (For the example given in the last section, $\mathbf{l} = L_z \hat{z}$, $\mathbf{s} = L_x \hat{x}$, so this is $+L_z L_x \hat{y}$, corresponding to a force positive in \hat{x} positive for a positive shear σ_{xy} , as pictured in the figure.) This force does work on the crystal when it displaces atoms:

$$\delta W = \mathbf{F}_{\text{ext}} \cdot \mathbf{b} \quad \rightarrow \quad \delta W = ([\sigma] \cdot (ds \times dl)) \cdot \mathbf{b} \quad (10.18)$$

Atoms are displaced in "slip" direction \hat{b} (Burgers vector) Note that atoms are *not* displaced along the dislocation displacement vector (glide vector) δs ! This is coincidentally true for an edge dislocation, since $\hat{s} = \hat{b}$, but it is not true for a screw dislocation ($\hat{s} \cdot \hat{b} = 0$).

Next, we equate the work δW done on the outer boundaries of the crystal to work done *on the dislocation*, due to the *Peach-Koehler force* \mathbf{f}_D

$$\mathbf{f}_D \cdot ds = ([\sigma] \cdot (ds \times dl)) \cdot \mathbf{b} \quad (10.19)$$

Here we need a mathematical tool: if matrix $[A]$ is symmetric, multiplication with \mathbf{u} , projected on \mathbf{v} will be:

$$([A] \mathbf{u}) \cdot \mathbf{v} = ([A] \mathbf{v}) \cdot \mathbf{u} \quad (10.20)$$

which can be shown easily by expanding the matrices, matrix multiplication, and dot products for the 2D case. Rearranging,

$$\mathbf{f}_D \cdot ds = ([\sigma] \cdot \mathbf{b}) \cdot (ds \times dl) \quad (10.21)$$

We need another mathematical tool, for the scalar triple product:

$$\mathbf{u} \cdot (\mathbf{v} \times \mathbf{w}) = \mathbf{v} \cdot (\mathbf{w} \times \mathbf{u}) = -(\mathbf{u} \times \mathbf{w}) \cdot \mathbf{v} \quad (10.22)$$

Using this tool,

$$\mathbf{f}_D \cdot d\mathbf{s} = -(([\sigma] \cdot \mathbf{b}) \times \mathbf{l}) \cdot d\mathbf{s} \quad \rightarrow \quad \boxed{\frac{\mathbf{f}_D}{\delta l} = -([\sigma] \cdot \mathbf{b}) \times \hat{\mathbf{l}}} \quad (10.23)$$

Force on an edge dislocation Using the same coordinate system for the edge dislocation as shown before, $\mathbf{b} = b\hat{\mathbf{x}}$, $[\sigma] = \sigma_{xy} = \sigma_{yx} = \tau$, and $\hat{\mathbf{l}} = +\hat{\mathbf{z}}$, we can evaluate the Peach-Koehler formula:

$$[\sigma] = \begin{bmatrix} \cdot & \tau & \cdot \\ \tau & \cdot & \cdot \\ \cdot & \cdot & \cdot \end{bmatrix} \quad \rightarrow \quad \frac{\mathbf{f}_D}{\delta l} = - \left(\begin{bmatrix} \cdot & \tau & \cdot \\ \tau & \cdot & \cdot \\ \cdot & \cdot & \cdot \end{bmatrix} \begin{bmatrix} b \\ 0 \\ 0 \end{bmatrix} \right) \times \hat{\mathbf{l}} \quad (10.24)$$

$$\frac{\mathbf{f}_D}{\delta l} = -(\tau b \hat{\mathbf{y}}) \times \hat{\mathbf{l}} \quad (10.25)$$

This relationship is general for this Burgers vector \mathbf{b} and shear state τ and can be applied for other cases as well. For the edge dislocation, $\hat{\mathbf{l}} = \hat{\mathbf{z}}$,

$$\frac{\mathbf{f}_D}{\delta l} = -\tau b \hat{\mathbf{x}} \quad (10.26)$$

as shown in Eq 10.15 previously.

10.2.3 Glide force on a dislocation loop

What about a dislocation loop under the same shear? In a dislocation loop, the Burger's vector \mathbf{b} always has the same value, but the dislocation line vector \mathbf{l} creates a closed circuit. If the loop is a circle centered at the origin of the zx plane, radius R , the line vector will be in a counter clockwise, right-hand sense when viewed along $-\hat{\mathbf{y}}$. There are two pure-edge and two pure-screw-type sections:

- Edge: $\hat{\mathbf{l}} = +\hat{\mathbf{z}}, x = -R, \hat{\mathbf{l}} = -\hat{\mathbf{z}}, x = +R$
- Screw: $\hat{\mathbf{l}} = +\hat{\mathbf{x}}, z = R, \hat{\mathbf{l}} = -\hat{\mathbf{x}}, z = -R$

Substituting in,

$$(x = -R) \quad (\text{edge}) \quad \frac{\mathbf{f}_D}{\delta l} = -(\tau b \hat{\mathbf{y}}) \times \hat{\mathbf{z}} = -\tau b \hat{\mathbf{x}} \quad (10.27)$$

$$(x = +R) \quad (\text{edge}) \quad \frac{\mathbf{f}_d}{\delta l} = -(\tau b \hat{\mathbf{y}}) \times \hat{\mathbf{z}} = +\tau b \hat{\mathbf{x}} \quad (10.28)$$

$$(z = -R) \quad (\text{screw}) \quad \frac{\mathbf{f}_d}{\delta l} = -(\tau b \hat{\mathbf{y}}) \times (-\hat{\mathbf{x}}) = -\tau b \hat{\mathbf{z}} \quad (10.29)$$

$$(z = +R) \quad (\text{screw}) \quad \frac{\mathbf{f}_d}{\delta l} = -(\tau b \hat{\mathbf{y}}) \times \hat{\mathbf{x}} = +\tau b \hat{\mathbf{z}} \quad (10.30)$$

In this way, a circular dislocation loop under simple shear experiences a uniform radial force which tends to expand it uniformly, for positive shear, or contract it uniformly, for the opposite sense of shear. The expansion is an important step in the generation of net plastic flow (dislocation creation) from a Frank-Read source.

Dislocation climb Next, we can consider the simple edge dislocation under uniaxial compression along the Burgers vector direction, $[\sigma] = \sigma_{xx} = -\sigma$. The Peach-Koehler formula is now

$$[\sigma] = \begin{bmatrix} -\sigma & \cdot & \cdot \\ \cdot & \cdot & \cdot \\ \cdot & \cdot & \cdot \end{bmatrix} \quad \rightarrow \quad \frac{\mathbf{f}_d}{\delta l} = -\left(\begin{bmatrix} -\sigma & \cdot & \cdot \\ \cdot & \cdot & \cdot \\ \cdot & \cdot & \cdot \end{bmatrix} \begin{bmatrix} b \\ \cdot \\ \cdot \end{bmatrix} \right) \times \hat{\mathbf{z}} \quad (10.31)$$

$$\frac{\mathbf{f}_d}{\delta l} = -\sigma b \hat{\mathbf{y}} \quad (10.32)$$

Here, because the additional half-plane extends towards $-\hat{\mathbf{y}}$, the effect of the compression will be to push this half-plane out of the crystal. This means that the dislocation will move in $-\hat{\mathbf{y}}$, as illustrated by the Peach-Koehler force.

Note here that the force alone cannot tell anything about the acceleration and ultimate speed of the dislocation. The force can relate to the acceleration, and in the relevant viscous case to a terminal velocity, only through some dislocation "mass." This "mass" is much larger for dislocation climb than for glide because climb does not conserve volume in the crystal and it is a slower process to accomodate the atomic flow to the boundaries.

10.3 Strain fields and self-energy of dislocations

The atoms surrounding the core of a dislocation, and extending some distance away, are displaced from their equilibrium positions. Elastic strain is then built up around a dislocation, as a function of distance r away from a straight, infinitely long dislocation line. We will find the strain fields $\epsilon(r)$ for straight dislocations of screw and edge type. Since the elastic strain energy is quadratic in strain at any point, a finite elastic energy (self-energy) is associated with the dislocation.

10.3.1 Screw dislocation

For a screw dislocation, the strain can be found relatively straightforwardly. The material surrounding the core is under pure shear. We can take a cylinder of material with axis along the direction of the dislocation line \hat{l} and Burger's vector \mathbf{b} , collinear for a screw dislocation. The atomic displacements will be zero in the x and y directions.

In cylindrical coordinates (r, θ, z) , the atomic displacement increases proportionally to θ , the winding angle around the screw dislocation:

$$u_z = b \left(\frac{\theta}{2\pi} \right) \quad (10.33)$$

so, as the sub-atomic bug walks around the dislocation line, continuously increasing θ as $\theta = \omega t$, he continuously ascends. Each revolution sends him further by an amount of the Burger's vector, b . (At this rate, it will take him a while.) His progress is the same for each circuit around the core.

We can treat the problem in cylindrical coordinates, (r, θ, z) . Taking the gradient of scalar f in cylindrical coordinates,

$$\nabla f = \left(\frac{\partial f}{\partial r} \right) \hat{r} + \left(\frac{\partial f}{\partial \theta} \right) \hat{\theta} + \left(\frac{\partial f}{\partial z} \right) \hat{z} \quad (10.34)$$

where denominators of the derivatives are unit distances in the orthonormal set of directions $(\hat{r}, \hat{\theta}, \hat{z})$

$$\nabla f = \left(\frac{\partial f}{\partial r} \right) \hat{r} + \frac{1}{r} \left(\frac{\partial f}{\partial \theta} \right) \hat{\theta} + \left(\frac{\partial f}{\partial z} \right) \hat{z} \quad (10.35)$$

Now allowing f to be the displacement in the z direction, u_z ,

$$\frac{\partial u_z}{\partial x_\theta} = \frac{1}{r} \left(\frac{\partial u_z}{\partial \theta} \right) \quad (10.36)$$

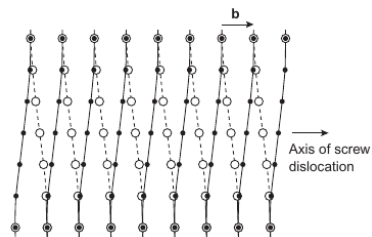


Figure 10.2: Atomic arrangements near a screw dislocation. From Hull.

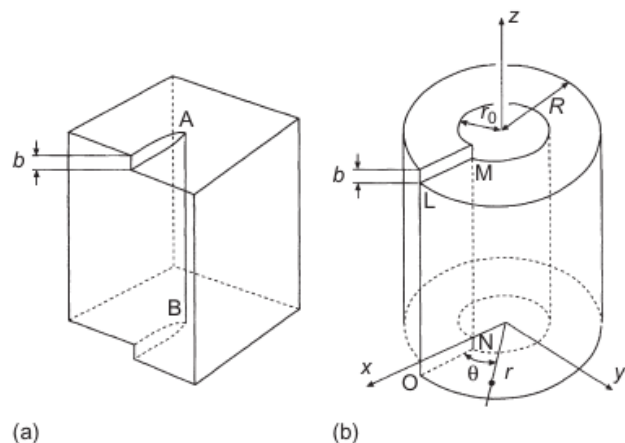


Figure 10.3: Elastic energy of a screw dislocation. From Hull.

and applying the formula for tensor shear,

$$\varepsilon_{z\theta} = \frac{b}{4\pi} \left(\frac{1}{r} \right) \quad (10.37)$$

The most important feature is that the strain falls off as $1/r$, the inverse distance away from the dislocation core.

Shear stress and strain energy

Shear stresses relate to shear strains only through the on-axis stiffnesses, $\sigma_4 = c_{44}\epsilon_4$, $\sigma_5 = c_{55}\epsilon_5$, $\sigma_6 = c_{66}\epsilon_{66}$, for cubic or isotropic materials. For simplicity we will consider only isotropic materials here, so

$$\sigma_{z\theta}(r) = 2G\varepsilon_{z\theta}(r) \quad (10.38)$$

$$\sigma_{z\theta}(r) = \frac{Gb}{2\pi} \left(\frac{1}{r} \right) \quad (10.39)$$

It then becomes possible to calculate the elastic strain energy associated with the screw dislocation, integrating over the volume:

$$U_s = \int_0^{2\pi} d\theta \int_0^\infty dr r \frac{1}{2} (\sigma_{z\theta}(r)\varepsilon_{z\theta}(r) + \sigma_{\theta z}(r)\varepsilon_{\theta z}(r)) \quad (10.40)$$

Because the σ_{ij} and ε_{ij} tensors are symmetric, the two terms are equal, so

$$U_s = \int_0^{2\pi} d\theta \int_0^\infty dr r \sigma_{z\theta}(r) \varepsilon_{z\theta}(r) \quad (10.41)$$

$$U_s = 2\pi \int_0^\infty dr r \frac{Gb}{2\pi} \left(\frac{1}{r} \right) \frac{b}{4\pi} \left(\frac{1}{r} \right) \quad (10.42)$$

$$U_s = \frac{Gb^2}{4\pi} \int_0^\infty \frac{dr}{r} \quad (10.43)$$

The limits for the integral are subtle. The integral diverges for $r \rightarrow 0$, so we take a cutoff radius R_c . Physically this can be justified by the fact that the displacements of the atoms right around the core are not absolutely constant. The cutoff is on the order of five atomic spacings ($R_c \simeq 1 \text{ nm}$). On the high side, the radius will be bounded by the physical dimensions of the sample. If the sample has a volume V , the average $\langle R_{max} \rangle$ would be $R \sim 0.5V^{1/3}$.

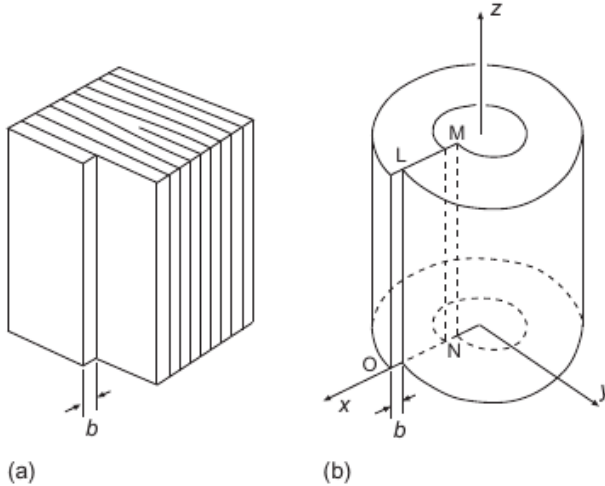


Figure 10.4: Elastic energy of an edge dislocation. From Hull.

$$U_s = \frac{Gb^2}{4\pi} \ln \frac{R_{max}}{R_c} \quad (10.44)$$

The term in the logarithm is relatively slowly varying with size. The most important part to see is the prefactor. The elastic energy of a dislocation is greater in stiffer material, proportional to G , and proportional to the square of the Burgers vector b . Therefore it will be energetically favorable for a dislocations to *dissociate* into smaller dislocations $\mathbf{b}_1, \mathbf{b}_2$ which achieve the same displacement, with $\mathbf{b} = \mathbf{b}_1 + \mathbf{b}_2$. If $b_1 = b_2 = b/2$, the elastic self-energy is cut roughly in half.

10.3.2 Edge dislocation

For an edge dislocation, we can again take the dislocation line along $\mathbf{l} = \hat{\mathbf{z}}$. Now the Burgers vector has to be orthogonal to \mathbf{l} , and we take $\mathbf{b} = +b\hat{\mathbf{x}}$. For a clockwise circuit around \mathbf{l} (right-handed sense), Burgers vector drawn from finish to start, this corresponds to the additional half-plane extending to $-\hat{\mathbf{y}}$.

Now the atomic displacements, in the direction of \mathbf{b} , will be in the $\hat{\mathbf{x}}$ direction, and there will be no variation of the displacements in the $\hat{\mathbf{z}}$ direction. The solution for the displacements is not as simple as for the screw dislocation case because a function like $u_x = b\theta/2\pi$ cannot not satisfy the

elastic equilibrium equations Eq 7.58, so additional terms are added in. (A full derivation for u_i near the edge dislocation is given in Weertman's text[2], pp. 37-8.)

Shear stress and strain energy We will skip over the relatively complicated expressions for the displacements and just write the result for stresses. The result for the stresses σ associated with the dislocation is relatively simple, however, very closely related to those in Eq 10.39. For the shear component,

$$\sigma_{r\theta} = -\frac{Gb}{2\pi(1-\nu)} \frac{\cos\theta}{r} \quad (10.45)$$

where the result is nearly identical except for the factor of $1 - \nu$. Additionally, there is a dependence on θ such that the shear is maximum in the xz plane, and minimum in the additional half-plane of the dislocation at $\theta = \pm\pi/2$. Unlike the case for the screw dislocation, there are also axial stresses:

$$\sigma_{rr} = \sigma_{\theta\theta} = \frac{Gb}{2\pi(1-\nu)} \frac{\sin\theta}{r} \quad (10.46)$$

Here there is a tensile stress for $+b$, with the additional half-plane extending to $-\hat{y}$, above the xz plane ($\theta = \pi/2$) and a compressive stress below the xz plane ($\theta = -\pi/2$). Additionally, there is even an axial stress along the dislocation line, due to the poisson expansion / contraction:

$$\sigma_{zz} = \frac{G\nu b}{\pi(1-\nu)} \frac{\sin\theta}{r} \quad (10.47)$$

Elastic self-energy Summing the elastic energies for the different terms leads to a result for the self-energy of the edge dislocation which is very similar to that of the screw dislocation,

$$U_e = \frac{Gb^2}{4\pi(1-\nu)} \ln \frac{R_{max}}{R_c} \quad (10.48)$$

where the only difference is the Poisson ratio term, which will tend to increase the energy of the edge dislocation by about 30% compared with that of the screw dislocation; see e.g. Hull[3], chapter 3.

Stress in Cartesian coordinates Next, we can convert these shears to the xy coordinate system through

$$a_{xr} = \cos \theta \quad a_{yr} = \sin \theta \quad a_{x\theta} = -\sin \theta \quad a_{y\theta} = \cos \theta \quad (10.49)$$

so

$$\sigma_{xx} = a_{xr}^2 \sigma_{rr} + a_{x\theta}^2 \sigma_{\theta\theta} + 2a_{xr} a_{x\theta} \sigma_{r\theta} \quad (10.50)$$

where the factor of two is from the symmetric $\sigma_{\theta r}$ component. The other stresses in Cartesian coordinates are

$$\sigma_{yy} = a_{yr}^2 \sigma_{rr} + a_{y\theta}^2 \sigma_{\theta\theta} + 2a_{yr} a_{y\theta} \sigma_{r\theta} \quad (10.51)$$

$$\sigma_{xy} = a_{xr} a_{yr} \sigma_{rr} + a_{x\theta} a_{y\theta} \sigma_{\theta\theta} + (a_{xr} a_{y\theta} + a_{x\theta} a_{yr}) \sigma_{r\theta} \quad (10.52)$$

substituting,

$$\sigma_{xx} = \frac{Gb}{2\pi(1-\nu)r} (a_{xr}^2 \sin \theta + a_{x\theta}^2 \sin \theta - 2a_{xr} a_{x\theta} \cos \theta) \quad (10.53)$$

$$\sigma_{xx} = \frac{Gb}{2\pi(1-\nu)} \frac{\sin \theta}{r} (1 + 2 \cos^2 \theta) \quad (10.54)$$

similarly

$$\sigma_{yy} = \frac{Gb}{2\pi(1-\nu)} \frac{\sin \theta}{r} (1 - 2 \cos^2 \theta) \quad (10.55)$$

$$\sigma_{xy} = -\frac{Gb}{2\pi(1-\nu)} \frac{\cos \theta}{r} (\cos^2 \theta - \sin^2 \theta) \quad (10.56)$$

In tensor form,

$$[\sigma] = \frac{Gb}{2\pi(1-\nu)r} \frac{1}{r} \begin{bmatrix} \sin \theta (1 + 2 \cos^2 \theta) & \cos \theta (\sin^2 \theta - \cos^2 \theta) \\ \cos \theta (\sin^2 \theta - \cos^2 \theta) & \sin \theta (1 - 2 \cos^2 \theta) \end{bmatrix} \quad (10.57)$$

10.3.3 Force between two dislocations

We can now see what the force between two dislocations will be. We can think of the mutual attraction or repulsion between two dislocations as analogous to the force between two charged particles: if we place one charge at the origin and consider it fixed, we can calculate the force on another charge some distance r away. Here, we place one dislocation at the origin; the elastic stress fields it produces at $x = r \cos \theta$, $y = r \sin \theta$ will be as given in Eq. 10.57. The orientation of the burgers vector and dislocation line 1, \mathbf{b}_1 and \mathbf{l}_1 , compared with those of the dislocation upon which we would like to calculate the force, \mathbf{b}_2 and \mathbf{l}_2 , is important; we will take the case where the dislocation lines are parallel and on $\mathbf{l} = \hat{\mathbf{z}}$, and the Burgers vectors are equal, $\mathbf{b}_1 = \mathbf{b}_2 = b\hat{\mathbf{x}}$.

Sign convention for Peach-Koehler formula : Here we follow the sign convention for \mathbf{l}, \mathbf{b} : positve \mathbf{b} is the direction of the $f \rightarrow s$ vector (linking finishing point to starting point) found taking a right-handed Burgers circuit (clockwise looking down the vector) about positive \mathbf{l} . Therefore, for $\mathbf{l} = \hat{\mathbf{z}}$, $\mathbf{b} = b\hat{\mathbf{x}}$, $b > 0$ means that the additional half-plane of atoms *extends to* $-\hat{\mathbf{y}}$. In the example taken for a simple shear previously, the force pushed the additional half-plane in the direction of the shear force on its nearest face. Therefore this force needs to be negative for this sign convention and we write

$$\frac{\mathbf{f}_d}{\delta l} = -([\sigma] \mathbf{b}) \times \hat{\mathbf{l}} \quad (10.58)$$

with an inverted sign. Evaluating Eq 10.58,

$$\frac{\mathbf{f}_d}{\delta l} = -\frac{Gb}{2\pi(1-\nu)r} \frac{1}{r} \begin{bmatrix} \sin \theta (1 + 2 \cos^2 \theta) & \cos \theta (\sin^2 \theta - \cos^2 \theta) \\ \cos \theta (\sin^2 \theta - \cos^2 \theta) & \sin \theta (1 - 2 \cos^2 \theta) \end{bmatrix} \begin{bmatrix} b \\ . \end{bmatrix} \times \hat{\mathbf{z}} \quad (10.59)$$

$$= -\frac{Gb^2}{2\pi(1-\nu)r} \frac{1}{r} [\sin \theta (1 + 2 \cos^2 \theta) \hat{\mathbf{x}} + \cos \theta (\sin^2 \theta - \cos^2 \theta) \hat{\mathbf{y}}] \times \hat{\mathbf{z}} \quad (10.60)$$

$$\frac{\mathbf{f}_d}{\delta l} = \frac{Gb^2}{2\pi(1-\nu)r} \frac{1}{r} [\cos \theta (\cos^2 \theta - \sin^2 \theta) \hat{\mathbf{x}} + \sin \theta (1 + 2 \cos^2 \theta) \hat{\mathbf{y}}] \quad (10.61)$$

A vector plot of the forces is shown in Figure 10.5. Here X is the dislocation-dislocation distance in the slip plane and Y is the dislocation-dislocation distance out of the slip plane. There are several points to notice in the plot:

- The force in \hat{y} is positive for $Y > 0$ (above the slip plane) and negative for $Y < 0$ (below the slip plane), so same-sign dislocations always *repel* each other normal to the slip plane.
- The glide force is zero in the slip plane for dislocations above or below each other, as shown with the vertical black solid line ($F_y = 0$ line).
- The glide force is *also* zero in the slip plane for dislocations at 45° angles to each other, even though a normal force remains, as shown with the orthogonal black solid lines.

Even though the glide force is zero for same-sign dislocations at $\theta = \pm\pi/4, \pm 3\pi/4$, same-sign dislocations cannot reach this state through the glide force.

- Dislocations separate in \hat{x} (in slip plane) if they separated more in the slip plane than they are out of the slip plane, but approach each other \hat{x} if they are separated by more out of the slip plane than they are in the slip plane.

This approach can be extended for other geometries of dislocations (screw-edge, edge-edge with different Burgers vectors, etc.)

10.4 Line tension of a dislocation

Whenever there is a bend in a dislocation line, elastic energy will tend to straighten it out. The (positive) elastic energy per length of dislocation line, expressed in U_e or U_s , implies that the dislocation will seek to minimize its length to decrease its energy. Increases in length will be opposed by a *line tension* $T = U$, in units of force (N),

$$T \simeq \frac{Gb^2}{4\pi} \ln \frac{R}{R_{min}} \quad (10.62)$$

where we have neglected any effect of the Poisson ratio ν or distinction between edge and screw dislocations.

The line tension is the one-dimensional analog of surface tension, as expressed in e.g. a soap bubble, which reduces its surface area by forming a

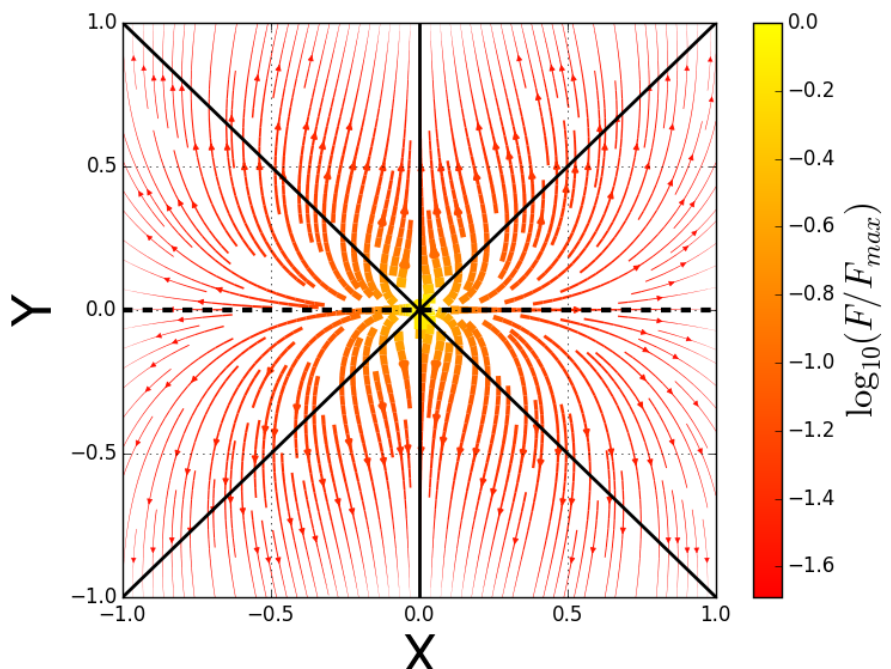


Figure 10.5: Vector plot of forces on a long, straight edge dislocation, $\mathbf{b} = b\hat{\mathbf{x}}$, located at (X, Y) , from a long, straight parallel edge dislocation at $(0, 0)$. Both dislocations have $\mathbf{l} = \hat{\mathbf{z}}$. The dotted black line shows where the Y -force is zero (normal to slip plane); the solid black lines show where the X -force is zero (in slip plane.)

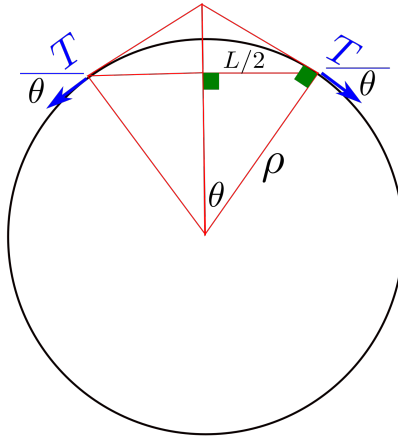


Figure 10.6: Line tension T creating a transverse force on a curved segment, length L , radius of curvature ρ .

sphere. The dislocation will attempt to remain straight unless it encounters some force transverse to \mathbf{l} .

We can consider a curved segment of dislocation line as pictured in Figure 10.6. For a given length L , with radius of curvature ρ , there will be a force acting transverse to the length at the two boundaries, due to the curvature. Here the downward force at the two sides is

$$F_y = -2T \sin \theta \quad (10.63)$$

$$F_y \simeq -2T \frac{L/2}{\rho} \quad (10.64)$$

$$\frac{F_y}{\delta l} \simeq -\frac{T}{\rho} \quad (10.65)$$

In order for the dislocation to remain stationary, there must be an equal and opposite force acting on the dislocation length in the positive $\hat{\mathbf{y}}$ direction.

Example: Frank-Read source We can now consider an edge dislocation, length L on $\hat{\mathbf{z}}$, Burgers vector $\mathbf{b} = b\hat{\mathbf{x}}$, pinned at both ends. If a shear stress σ_{xy} is exerted on the crystal, there is a glide force on the dislocation which opposes the line tension,

$$\sigma_{xy}b = \frac{T}{\rho} \quad (10.66)$$

$$\boxed{\sigma_{xy} = \alpha \frac{Gb}{\rho}} \quad \alpha \equiv \frac{\ln R/R_{min}}{4\pi} \quad (10.67)$$

The α parameter can be taken to be $\alpha \sim 1$. The expression says that the curvature of the dislocation line will be proportional to the applied shear, at least for small shears.

Elastic energy of a bent line A bend in the dislocation line also produces a small reduction in the line tension. In the limiting case of a dislocation loop, outside the loop, the elastic stress from the dislocation will drop off rapidly with increasing distance. The stress at any point will be the sum of opposite-sign components from opposite sides of the loop, because the sense of \hat{l} reverses with respect to fixed \mathbf{b} . So, integrated over all distance, the elastic energy will be lower, creating an upper limit R_{max} which is lower than the sample dimensions.

This rapid decrease with distance can be seen most easily for the stress from two parallel screw dislocations with equal Burgers vector $\mathbf{b}_1 = \mathbf{b}_2 = b\hat{z}$ and opposite line vector $\hat{l}_1 = -\hat{l}_2 = \hat{z}$. We can assume that they are separated in \hat{x} by d , so that dislocation 1 is at $x = -d/2$ and dislocation 2 is at $x = d/2$, and consider the sum

$$\sigma(x) = \sigma_1(x) + \sigma_2(x) \quad (10.68)$$

$$\sigma(x) = \frac{Gb}{2\pi} \left(\frac{1}{x - d/2} - \frac{1}{x + d/2} \right) \quad (10.69)$$

$$\sigma(x) = \frac{Gb}{2\pi} \frac{1}{x} \left[\left(1 - \frac{d}{2x} \right)^{-1} - \left(1 + \frac{d}{2x} \right)^{-1} \right] \quad (10.70)$$

For distances x far away from the dislocation pair, $x \gg d$, Taylor-expanding,

$$\sigma(x) \simeq \frac{Gb}{2\pi} \frac{1}{x} \left(1 + \frac{d}{2x} - 1 + \frac{d}{2x} \right) \quad (10.71)$$

$$\sigma(x) \simeq \frac{Gbd}{2\pi x^2} \quad (10.72)$$

We can see that the stress from this "dislocation dipole" drops off in distance r from the dipole as r^{-2} , whereas it drops off inverse in distance from a single infinitely straight dislocation as r^{-1} . Calculation of the full stress field from the loop, or from a curved segment, would be more complicated,

but it is clear that the stress field from a loop (localized to a radius ρ rather than infinitely long) would drop off even more rapidly with distance.

The greater containment of the elastic fields from a curved segment can be approximated by taking the radius of curvature as the upper limit of integration

$$R_{max} \rightarrow \rho \quad (10.73)$$

and if we take the dislocation core radius as

$$R_0 = 5b \quad (10.74)$$

the elastic energy U_s and tension T will be

$$T \sim \frac{Gb^2}{4\pi} \ln \frac{\rho}{5b} \quad (10.75)$$

This expression ignores any difference in the edge and screw dislocation energies from the Poisson ratio.

10.5 Dislocation - point-defect interactions

The lattice is strained near the dislocation. For a distance r away from an edge dislocation, $\hat{l} = \hat{z}$, $\mathbf{b} = b \hat{x}$, there is compression and tension in the glide plane, transverse to the line, as

$$\sigma_{xx} = \frac{Gb}{2\pi(1-\nu)} \frac{\sin \theta}{r} \quad (10.76)$$

where the additional half-plane for this sign of \mathbf{b} comes in from the bottom, extending to $y = -\infty$. Above the glide plane, $0 \leq \theta \leq \pi$, the lattice is in tension; below the glide plane, $\pi \leq \theta < 2\pi$, it is in compression.

Point defects will tend to have preferred sites near the dislocation line, depending upon whether they expand or contract the lattice:

- **Vacancies** can relieve compression by diffusing towards the additional half-plane ($-y$) below the dislocation line, as close as possible from the $1/r$ dependence.
- **Interstitial impurity atoms**, such as C or N in Fe, can relieve tension by filling the empty space above the additional half-plane ($+y$).

- **Substitutional impurity atoms**, such as Ni impurities in a Au host (or Au impurities in a Ni host) will find preferred sites depending upon their size relative to the host ($r_i > r$ diffuses above, $r_i < r$ diffuses below.)

Point defects find their equilibrium positions near the dislocation line through diffusion. Typically, at room temperature, atomic diffusion is slow compared with dislocation glide velocities, so the "solute environment" remains fixed in space, and the dislocation tries to move out of it under the influence of stresses. There will be reversible forces on the dislocation line restoring it to its equilibrium with respect to the solutes.

Because point defects impede the initial motion of dislocations, they strengthen the solid, raising the flow stress τ / yield stress σ_y . We will look at two types of interaction: first, where the point defects are *created* in the crystal through dislocation motion, second, where they are not. The first case is relevant for vacancies interacting with dislocation climb; the second case is relevant for solid-solution strengthening, impeding dislocation glide.

10.5.1 Chemical force in dislocation climb

Equilibrium concentration of vacancies

A finite concentration of point defects is always energetically favored at standard atmospheric conditions of constant pressure and temperature (P, T). Under these conditions, a crystal will spontaneously minimize its Gibbs free energy

$$\Delta G = \Delta H - T\Delta S \quad \Delta G \leq 0 \quad (10.77)$$

which includes a contribution from entropy, $-T\Delta S$, favoring increased disorder through a finite point defect concentration. To take the specific case of a number of vacancies N_v on a fixed number of atomic sites N , higher N_v allows a greater number of atomic configurations, raised from only one possible atomic configuration for a perfect crystal. The configurational entropy for N lattice sites, N_v defects, $N - N_v$ sites without defects, is

$$S_{config} = k_B \ln \frac{N!}{N_v! (N - N_v)!} \quad (10.78)$$

characteristic for a binary system. Using the lowest-order Stirling approximation

$$\ln x! \simeq x \ln x - x \quad (10.79)$$

for very dilute numbers of impurities $N_v \ll N$, this becomes

$$S_{config} = k_B N_v \ln \frac{N}{N_v} \quad (10.80)$$

and the additional configurational entropy associated with the addition of a vacancy, increasing N_v by one, is

$$S_{V,c} = k_B \ln \frac{N}{N_v} \quad (10.81)$$

We can divide the entropy associated with the introduction of a vacancy into two components, configurational and 'other', $S_V = S_{V,c} + S_{V,0}$. The change in Gibbs free energy from the addition of the vacancy will then be, at equilibrium,

$$\Delta G = 0 = Q_V - k_B T \ln \frac{N}{N_{v,0}} - k_B T S_{V,0} \quad (10.82)$$

where $Q_V = \Delta H_V = U + P\Delta V$ is the enthalpy for the vacancy at constant P and V_V is its volume. For a vacancy, volume e.g. $V_v \sim \pi a^3 / (12\sqrt{2})$ in a FCC metal where a is the lattice parameter, the PV_v product is roughly $5 \mu \text{ eV}$, negligible compared with $k_B T$, and we can take $Q_v \simeq E_v$, the formation energy. Finally

$$N_{V,0} = N \exp \frac{S_{V,0}}{k_B} \exp - \frac{E_V}{k_B T} \quad (10.83)$$

Equivalently, the fraction of sites occupied by a vacancy $x_V \equiv N_{V,0}/N$ is

$$x_V = \exp \frac{S_{V,0}}{k_B} \exp - \frac{E_V}{k_B T} \quad (10.84)$$

This expression assumes that the defect can take only one configuration in the crystal, which is the case for the vacancy. Equation 10.84 predicts that there will be an equilibrium concentration of vacancies which increases strongly with increasing temperature.

Measurement of the equilibrium vacancy concentration, and validation of Eq 10.84, did not come until the early 1960s. Simmons and Balluffi[4] took careful measurements on a heated Al single crystal, comparing the external dimensions of the crystal (L , measured using a microscope) with the lattice

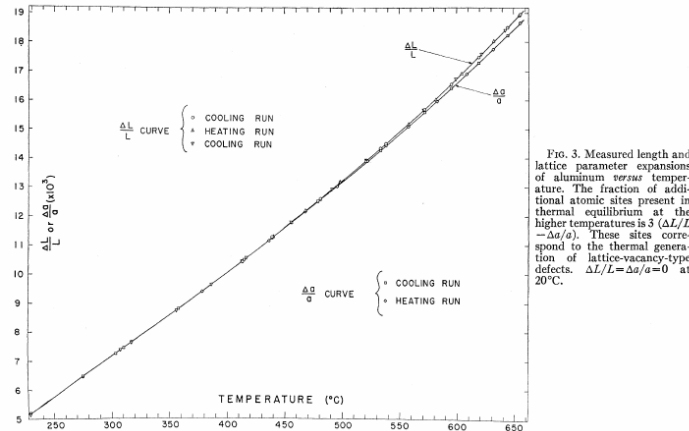


Figure 10.7: Simmons-Balluffi experiment, comparing thermal expansion of the lattice parameter a with thermal expansion of the external sample dimension L . The difference is attributed to vacancy formation at high T . From [4]

parameter a measured by x-ray diffraction, both in a heating vessel. In the absence of vacancies, $a(T)$ is described by the thermal expansion, and the external dimensions of the sample should increase by the same multiple as $a(T)$. Instead, they found that a and L varied similarly with temperature for low temperatures, but that the external dimensions started to increase much more quickly than the lattice parameter (which increases due to thermal expansion) for temperatures approaching the melting point.

The difference in dilation was attributed to vacancy formation with constant volume per vacancy:

$$x_v = 3 \left(\frac{\Delta L}{L} - \frac{\Delta a}{a} \right) \quad (10.85)$$

Based on the data in Figure 10.7, the authors extracted a vacancy energy in Al of $E_V = 0.74$ eV.

The "chemical force"

An edge dislocation with the configuration described previously ($\hat{l} = \hat{z}$, $\mathbf{b} = b \hat{x}$) will experience a climb force in $+\hat{y}$ for tension, $+\sigma_{xx}$, and a negative climb force in $-\hat{y}$ for compression, $-\sigma_{xx}$.

The applied compressive or tensile stress either "squeezes out" or "sucks

in" the additional half-plane of atoms. Dislocation climb then does *not* conserve the number of atoms. A line of atoms needs to be added along **1** for negative climb; a line of atoms needs to be removed for positive climb. Equivalently, negative climb requires the removal of a line of lattice vacancies, positive climb requires the addition of a line of lattice vacancies.

Vacancies break atomic bonds in the crystal, raise the energy of the bonding environment, and carry an internal energy penalty for the crystal U_v . If the boundaries of the sample are coated (in a thought experiment) so that no vacancies can diffuse in or out, dislocation climb then involves an energy penalty (energy reduction) for positive (negative) climb. To move the dislocation line in positive climb then requires additional work done on the crystal and additional stress σ_{xx} .

We can now consider the thermodynamics of vacancy formation through dislocation motion. We add to the equilibrium expression for Gibbs free energy for vacancy formation in Eq xx a term for the work done on the dislocation, when it moves through a lattice parameter distance $\Delta y = a$ in climb,

$$\Delta W = \Delta U = f_y a \quad (10.86)$$

In this motion, for a dislocation line length δl , there will be $\delta l/a$ vacancies created. The amount of mechanical work required to add a vacancy will then be

$$U'_v \sim \frac{f_y a}{\delta l/a} = a^2 \frac{f_d^y}{\delta l} \quad (10.87)$$

Comparing the equilibrium expression without the added term, creating an equilibrium number of vacancies $N_{v,0}$ in Eq 10.82, with the additional term creating a nonequilibrium number of vacancies N_v ,

$$0 = Q_V - PV_V - k_B T \ln \frac{N}{N_{v,0}} - k_B T S_{V,0} \quad (10.88)$$

$$0 = U'_v + Q_V - PV_V - k_B T \ln \frac{N}{N_v} - k_B T S_{V,0} \quad (10.89)$$

and subtracting,

$$0 = U'_v + k_B T \ln \frac{N_v}{N_{v,0}} \quad (10.90)$$

$$\frac{f_d^y}{\delta l} = \frac{k_B T}{a^2} \ln \frac{N_v}{N_{v,0}} \quad (10.91)$$

This is the "chemical force" on the dislocation. When there is a greater-than-equilibrium concentration of vacancies, the force pulls the dislocation upwards (positive climb) to annihilate them. When there is a lower-than-equilibrium concentration of vacancies, the force pushes the dislocation downwards (negative climb) to create them.

Expressed as a stress,

$$\sigma'_{xx} \sim (k_B T / a^2 b) \ln N_v / N_{v,0} \quad (10.92)$$

Putting representative numbers to Eq 10.92 (room temperature $k_B T \approx 25.86$ meV, $a \sim b \sim 0.36$ nm), the effect of the chemical force is nonnegligible: a supersaturation of vacancies by a factor of two produces a climb force equivalent to a compressive stress of 60 MPa.

10.5.2 Glide pinned by point defects

Point-defect "atmospheres," concentrated near dislocation lines, have a strong influence on the stress required for dislocation glide. We will assume that a point defect has diffused to the dislocation line, near its lowest energy state defined by its mismatch with the lattice, and evaluate the force required for the dislocation to move away from it. Here we will consider carbon (C) interstitials in Fe first, because their effects were identified in early studies on "mild" (low-carbon) steel[5].

Point-defect pinning of an edge dislocation

We can evaluate the interaction energy of a line of point-defects, parallel to an edge dislocation line, by considering its effect on elastic strain. We assume that there is a volume V_i associated with the defect. Introduction of the defect perturbs the volume of the lattice by a small amount $dV = V_i$. The elastic energy of the crystal can be expressed as

$$U_{el} = -PdV \quad (10.93)$$

where compression ($dV < 0$) increases the energy of the crystal. The dilation can be expressed in terms of the bulk compressibility β (inverse of bulk modulus, $\beta = 1/K$) and hydrostatic pressure P as

$$\Delta = \beta P \quad \rightarrow \quad P = K\Delta \quad (10.94)$$

thus the elastic energy change from the defect can be expressed in terms of the bulk modulus, dilation, and impurity volume

$$U_{el} = -K\Delta V_i \quad (10.95)$$

To evaluate the dilation near the edge dislocation, recall

$$\Delta = \frac{1-2\nu}{E} \sigma_{ii} \quad (10.96)$$

in dummy suffix notation for the normal stresses. We have already written expressions for the stresses around an edge dislocation, $\sigma_{rr} = \sigma_{\theta\theta}$, σ_{zz} ,

$$\sigma_{rr} = \sigma_{\theta\theta} = \frac{Gb}{2\pi(1-\nu)} \frac{\sin \theta}{r} \quad \sigma_{zz} = \frac{Gb\nu}{\pi(1-\nu)} \frac{\sin \theta}{r} \quad (10.97)$$

so the dilation is

$$\Delta = \frac{1-2\nu}{E} (\nu+1) \frac{Gb}{\pi(1-\nu)} \frac{\sin \theta}{r} \quad (10.98)$$

Substituting in for G in terms of E ,

$$\Delta = \frac{1-2\nu}{E} (\nu+1) \frac{E}{2(1+\nu)} \frac{b}{\pi(1-\nu)} \frac{\sin \theta}{r} \quad (10.99)$$

now the dilation is

$$\Delta = \frac{1}{2\pi} \left(\frac{1-2\nu}{1-\nu} \right) \frac{b \sin \theta}{r} \quad (10.100)$$

The compressibility can be expressed in terms of the shear modulus as

$$K = \frac{2G}{3} \left(\frac{1+\nu}{1-2\nu} \right) \quad (10.101)$$

So the elastic energy can be expressed as

$$U_{el} = -A \frac{\sin \theta}{r} \quad A \equiv V_i \frac{Gb}{3\pi} \left(\frac{1+\nu}{1-\nu} \right) \quad (10.102)$$

where A has units of $(J \cdot m)$ and the (extensive) elastic energy U_{el} is in units of energy, J . If the point defect increases the volume, $V_i > 0$, the elastic energy of the crystal will be reduced (favored position) if it goes in at $y > 0$, opposite the additional half-plane.

Force required for glide The point-defect will be at some distance y_0 normal to the glide plane. When a shear stress is applied to the crystal, the dislocation starts to move in the glide plane, in the \hat{x} direction, so the y coordinate does not change. The interaction energy of the dislocation and point-defect will be

$$U_{el}(x) = -A \frac{y_0}{r^2} \quad (10.103)$$

where $r^2 = x^2 + y_0^2$, $\partial r / \partial x = x/r$, and the force required to move the dislocation with respect to the stationary defect is

$$F = -\frac{\partial U_{el}(x)}{\partial x} = -A \frac{2x y_0}{r^4} \quad (10.104)$$

The maximum force during glide can be evaluated:

$$\frac{\partial F}{\partial x_m} = -2A\rho(r^{-4} - 4x_m^2 r^{-6}) = 0 \quad (10.105)$$

$$r^2 - 4x_m^2 = 0 \quad (10.106)$$

$$x_m = \pm \frac{1}{\sqrt{3}} y_0 \quad (10.107)$$

$$F_m = \frac{3\sqrt{3}}{8} \frac{A}{y_0^2} \quad (10.108)$$

and substituting the interaction parameter A ,

$$F_m = \frac{\sqrt{3}G b}{8\pi y_0^2} \left(\frac{1+\nu}{1-\nu} \right) V_i \quad (10.109)$$

Yield stress In a tensile test, overcoming this force requires a large enough uniaxial σ , with maximum resolved shear stress in a randomly oriented polycrystal of $\sigma/2$. The force per unit length on the dislocation line is

$$\frac{F_d}{\delta l} = \frac{\sigma_y b}{2} \quad (10.110)$$

Cottrell assumed that the length of dislocation line with which the point-defect interacts is on the order of the Burgers vector b , and that the C atoms are spaced by this amount along a line parallel to the dislocation line. A relatively small amount of C is sufficient to pin all dislocations in this way. A relatively high density of dislocations is $n_d \sim 10^{12} \text{ cm}^{-2}$. The planar atomic

density in Fe is a^{-2} , or $n_a \sim 1.2 \times 10^{15} \text{ cm}^{-2}$. This means that to have one C atom pinning each atomic plane in the dislocation requires $x_C \sim n_a/n_d$, or $x_C < 0.001$. gives an estimate for the yield strength of

$$\sigma_y = \frac{3\sqrt{3}A}{4y_0^2 b^2} \quad (10.111)$$

$$\sigma_y = \frac{\sqrt{3}}{4\pi} \left(\frac{1+\nu}{1-\nu} \right) \frac{V_i}{y_0^2 b} G \quad (10.112)$$

active at $T = 0$. We can now make an estimate of this effect in Fe with interstitial C. Taking the Burgers vector as $b = 0.25 \text{ nm}$, the off-glide-plane distance for the C interstitial of $y_0 = 0.7 \text{ nm}$, its volume as $V_i = 7.8 \text{ \AA}^3$, one estimates

$$\sigma_{y,0} \simeq 1.2 \text{ GPa} \quad (10.113)$$

At finite temperatures, the yield stress is reduced because small sections of the dislocation can be thermally activated past the maximum force point at x_m . σ_y drops by roughly a factor of 8 at 295 K (to $\sim 140 \text{ MPa}$.)

10.6 Dislocation dynamics

Plasticity is, fundamentally, a kinetically limited phenomenon. An applied tensile stress will create a glide force on a dislocation, for properly oriented Burgers vectors and glide planes. For the dislocation to glide, it will need enough energy to mount some energy barrier holding it in place: either a low barrier (Peierls force) for a perfect metal, or a higher barrier if the dislocation is pinned by a solute, as discussed in the previous section.

At temperatures of interest for structural metals, the lattice vibrates with a kinetic energy of $\sim k_B T$ per atom, as discussed in Section 1.3: the lattice heat capacity ranges between $\sim 1 - 3k_B$ per formula unit, and so the lattice has $\sim k_B T$ available to access higher-energy configurations.

this is 60 K for Ag, as shown in Figure 1.5.) The probability of the system being in states of higher energy will be

$$\frac{P(E)}{P(E_0)} \sim \exp - (E/k_B T) \quad (10.114)$$

and so there will always be, at finite temperature, be *some* probability that the dislocation will be excited over the energy barrier which holds it in

place against the P-K force. For high energies and low temperatures, this probability will be low, and the rate of dislocation advance will be very slow.

Yield or flow stresses are defined at given temperatures for experimental times, on the order of 10s to 100s of seconds for a typical tensile test. We will see that if the time scales of interest are much shorter, the yield stresses are larger; if the time scales of interest are much longer, the yield stresses are lower. As time goes to infinity, the yield stress always goes to zero.

10.6.1 Power-law creep

Experiments find that the dislocation velocity is a strongly nonlinear function of applied stress. The velocity can be expressed as

$$v = v_0 \left(\frac{\tau}{\tau_0} \right)^m \quad (10.115)$$

where τ is the shear and m is much larger than 1. τ_0 is the shear stress required to reach the characteristic velocity v_0 , conventionally taken as 1 m/s. The exponent can be extracted from a log-log plot of velocity as a function of applied shear. An example is shown for LiF in Figure 10.8, with $m \sim 25$. The power-law relationship in Equation 10.115 is an approximation for velocities far below the shear-wave velocity, which is the speed limit for dislocation motion.

The fact that dislocations reach a constant velocity under constant stress suggests that some drag force opposes their motion. This is not very surprising because atomic slip is an irreversible relative motion of atoms, which involves larger-amplitude motions than those in Snoek damping, for example, and is likely to lose elastic energy to heat. The damping apparently increases as the velocity approaches the shear wave velocity.

10.6.2 Strain rate

The strain rate can be expressed in terms of the dislocation velocity as

$$\dot{\epsilon}_p = b n_d(\epsilon_p) v(\tau) \quad (10.116)$$

where b is the Burgers vector (scalar), $n_d(\epsilon)$ is the dislocation density in m^{-2} , and $v(\tau)$ is the shear-dependent dislocation velocity. The dislocation density increases proportionally with increasing plastic strain as

$$n_d = \alpha_d \epsilon_p \quad (10.117)$$

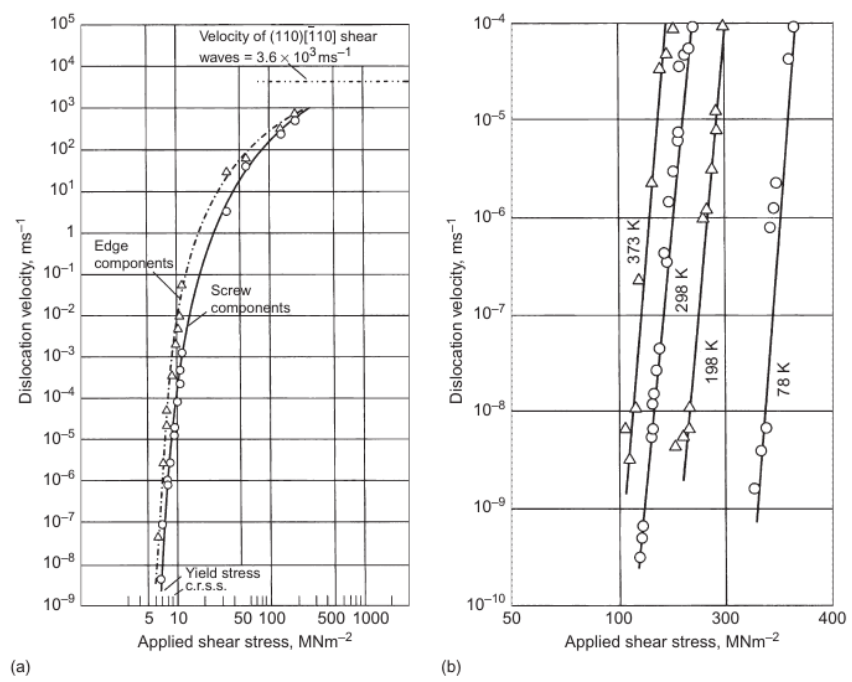


Figure 10.8: Dislocation velocities in LiF crystals. *Left:* saturation at high velocity. *Right:* extraction of exponent m . Johnston et al, refs [6, 7]

where $\alpha_d \sim 10^9 \text{ cm}^{-2}$ in LiF. From Eq 10.115, the strain rate will be strongly dependent on the applied stress:

$$\dot{\epsilon}_p = b \alpha_d \epsilon_p v_0 \left(\frac{\tau}{\tau_0} \right)^m \quad (10.118)$$

10.6.3 Tensile test: yield drop

We can consider a tensile test of a specimen exhibiting this sort of shear-dependent strain rate. The force exerted on the material over cross-sectional area A will be

$$\tau = \frac{F}{2A} \quad (10.119)$$

and the plastic strain $\epsilon_p = y_p/L_0$ can be related to the cross-head displacement y , assuming that there is a plastic component in series with an elastic stress $F = ky_{el}$, which may include elasticity of the apparatus,

$$y = y_p + y_{el} \quad (10.120)$$

$$y = L_0 \epsilon_p + \frac{F}{k} \quad (10.121)$$

where $y = S_c t$ is imposed by a constant cross-head displacement velocity S_c . The plastic strain ϵ_p can be expressed

$$\epsilon_p = \frac{1}{L_0} \left(y - \frac{2A\tau}{k} \right) \quad (10.122)$$

and the plastic strain rate

$$\dot{\epsilon}_p = \frac{1}{L_0} \left(\dot{y} - \frac{2A\dot{\tau}}{k} \right) \quad (10.123)$$

$$\dot{\epsilon}_p = \frac{1}{L_0} \left(S_c - \frac{2AS_c}{k} \left(\frac{\partial \tau}{\partial y} \right) \right) \quad (10.124)$$

$$\dot{\epsilon}_p = \frac{S_c}{L_0} \left(1 - \frac{2A}{k} \left(\frac{\partial \tau}{\partial y} \right) \right) \quad (10.125)$$

Substituting $\dot{\epsilon}_p$ in Eq 10.118,

$$\frac{S_c}{L_0} \left[1 - \frac{2A}{k} \left(\frac{\partial \tau}{\partial y} \right) \right] = b \alpha \epsilon_p v_0 \left(\frac{\tau}{\tau_0} \right)^m \quad (10.126)$$

and ϵ_p

$$\frac{S_c}{L_0} \left[1 - \frac{2A}{k} \left(\frac{\partial \tau}{\partial y} \right) \right] = b \alpha \frac{1}{L_0} \left(y - \frac{2A}{k} \tau \right) v_0 \left(\frac{\tau}{\tau_0} \right)^m \quad (10.127)$$

$$\left(\frac{\partial \tau}{\partial y} \right) = \frac{b\alpha}{S_c} v_0 \left(\frac{\tau}{\tau_0} \right)^m \left(\tau - \frac{k}{2A} y \right) + \frac{k}{2A} \quad (10.128)$$

Define, as a series elastic modulus of the tensile apparatus,

$$C \equiv \frac{k}{2A} \quad (10.129)$$

$$\left(\frac{\partial \tau}{\partial y} \right) = \frac{b\alpha}{S_c} v_0 \left(\frac{\tau}{\tau_0} \right)^m (\tau - Cy) + C \quad (10.130)$$

defining

$$B \equiv \frac{b\alpha}{S_c} \quad (10.131)$$

,

in units of m· s,

$$\left(\frac{\partial \tau}{\partial y} \right) = B v_0 \left(\frac{\tau}{\tau_0} \right)^m (\tau - Cy) + C \quad (10.132)$$

This is a differential equation for $\tau(y)$, or equivalently, stress σ vs. engineering strain e . Given an initial condition for $y = y_0$, which can be expressed in terms of the *initial* number of dislocations n_d

$$y_0 = L_0 \alpha_d n_d \quad (10.133)$$

added before the material is loaded into the tensile tester, Eq 10.132 can be integrated numerically and solved for $\tau(y)$.

Solutions for different initial dislocation densities, or *prestrain*, are shown in Figure 10.9, with parameters chosen to match the experiment. For the lowest amounts of prestrain and lowest initial number of dislocations, the *yield drop* is quite pronounced. As the sample is first loaded, the displacement in y is proportional. This is the effect of the elastic term (constant C). However, as the loading τ increases, the dislocation velocity starts to increase very abruptly near the characteristic stress, here taken as $\tau_0 = 5.3$ MPa, the stress at which the dislocation velocity reaches $v_0 = 1$ cm/s. This is due to the very large exponent $m = 16.5$. Plastic strain ϵ_p then increases rapidly

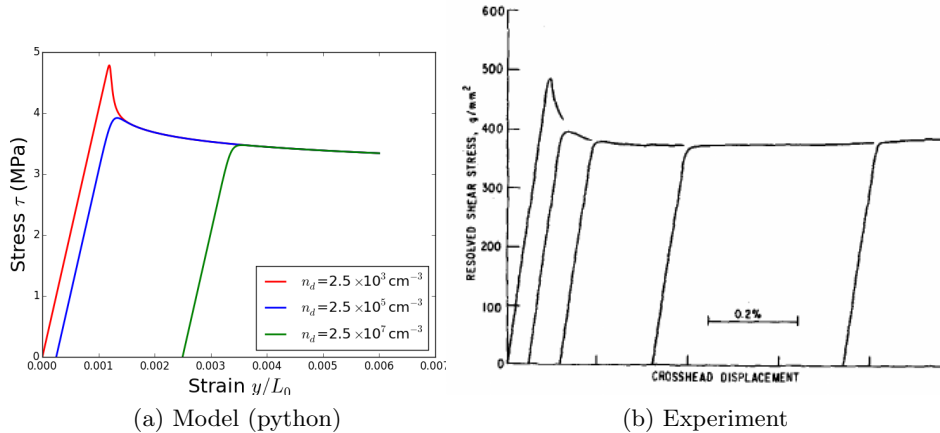


Figure 10.9: Numerical solutions of Eq 10.132 and experimental stress-strain data on LiF from Ref [7], variable prestrain controlling dislocation density.)

for stresses slightly in excess of τ_0 , and the elastic component of the stress drops. For increasing prestrain, the yield drop becomes less pronounced.

In the experiment, for larger strains, there is always a positive slope for $\tau(y)$. This is the effect of work hardening. We could take work hardening into account in Eq 10.132 by adding a constant term $\theta = \partial\tau/\partial y$, as will be described in Section 11.2.1.

Bibliography

- [1] M. Peach and J. S. Koehler. “The Forces Exerted on Dislocations and the Stress Fields Produced by Them”. In: *Phys. Rev.* 80 (3 Nov. 1950), pp. 436–439. DOI: [10.1103/PhysRev.80.436](https://doi.org/10.1103/PhysRev.80.436).
- [2] J. Weertman and J.R. Weertman. *Elementary dislocation theory*. Oxford, 1992.
- [3] D. Hull and D.J. Bacon. *Introduction to dislocations*. Pergamon, 2011.
- [4] R. O. Simmons and R. W. Balluffi. “Measurements of Equilibrium Vacancy Concentrations in Aluminum”. In: *Phys. Rev.* 117 (1 Jan. 1960), pp. 52–61. DOI: [10.1103/PhysRev.117.52](https://doi.org/10.1103/PhysRev.117.52).
- [5] A H Cottrell and B A Bilby. “Dislocation Theory of Yielding and Strain Ageing of Iron”. In: *Proceedings of the Physical Society. Section A* 62.1 (Jan. 1949), pp. 49–62. DOI: [10.1088/0370-1298/62/1/308](https://doi.org/10.1088/0370-1298/62/1/308).
- [6] W. G. Johnston and J. J. Gilman. “Dislocation Velocities, Dislocation Densities, and Plastic Flow in Lithium Fluoride Crystals”. In: *Journal of Applied Physics* 30.2 (1959), p. 129. DOI: [10.1063/1.1735121](https://doi.org/10.1063/1.1735121).
- [7] W. G. Johnston. “Yield Points and Delay Times in Single Crystals”. In: *Journal of Applied Physics* 33.9 (1962), p. 2716. DOI: [10.1063/1.1702538](https://doi.org/10.1063/1.1702538).

Exercises

1. Draw edge dislocations and Burgers circuits in FCC, BCC, and HCP material. (Show atomic arrangements near the core.) Use the sign convention that you are sighting along \mathbf{l} (directed into the page), the Burgers circuit has a right-hand, clockwise sense, and the vector \mathbf{b} connects the finish to the start of the circuit ($f \rightarrow s.$)
2. For two edge dislocations with parallel Burgers vectors $\mathbf{b} = b\hat{x}$, dislocation line $\hat{\ell} = \hat{z}$, with initial coordinates $(0,0)$ and $(0.25,0.5)$, sketch their motion for all time assuming that they move only under the influence of their mutual stresses.
3. Prove that the stress σ_{yy} never exerts a force on a dislocation with Burgers vector $\mathbf{b} = b\hat{x}$ regardless of the orientation of the dislocation line.
4. Consider two parallel screw dislocations, each with Burgers vector \mathbf{b} , separated by a distance R . Calculate the total strain energy of these dislocations. Show that the force between the dislocations found by differentiating this expression is the same as that determined by the Peach-Koheler formula.

Chapter 11

Strength of metals

11.1 Yield stress of perfect single crystals

11.1.1 Microscopic crystals

If metals were defect-free, without any dislocations, their yield stresses would be quite high. The strength can be estimated by the amount of elastic stress and strain required to make one full atomic plane slip with respect to the plane below it. A cartoon of such a strained situation, at the instability point, is shown below. Further shear will allow the third atomic layer to settle into atomic sites displaced by a close-packed atomic distance, with a total shear of $\gamma \simeq 30^\circ$. The shear γ_u at the instability point is roughly half this value, $\gamma_u \simeq 15^\circ = 0.26$ rad

The amount of shear stress required to reach γ_u is just $\tau_u = G\gamma_u$. We can estimate $\tau_y \sim G/4$ in this way. However, as the middle planes of atoms are moved with respect to each other, they require a smaller and smaller

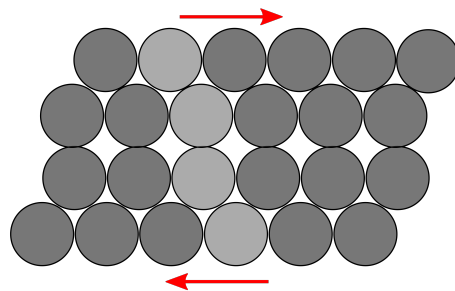


Figure 11.1: Illustration of elastic instability in shear for perfect crystal.

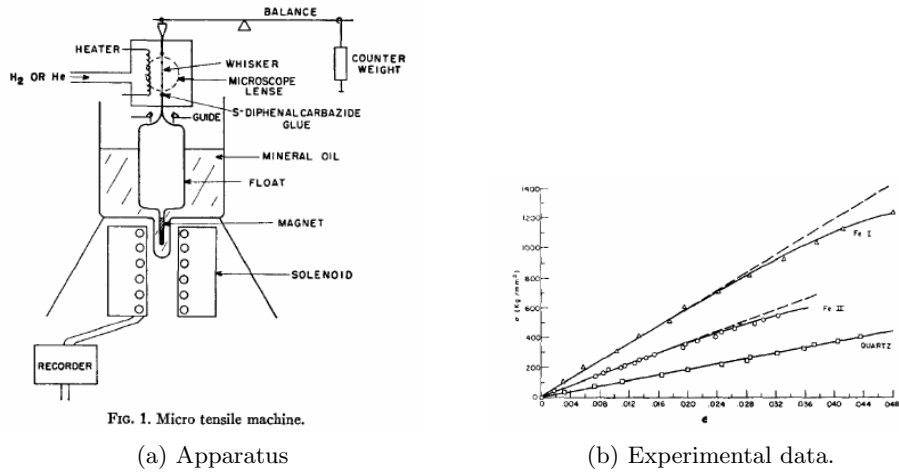


Figure 11.2: Microtensile experiments on $1\text{-}10 \mu\text{m}$ diameter, 1 mm length single-crystal whiskers, from [2]. The maximum yield stress reached for the Fe whisker is $\sigma_y = 12 \text{ GPa}$ (1200 kg/mm^2 .)

shear force to move, since in a hard-sphere model their resolved interatomic forces are less and less in-plane, until at the point pictured, that force is zero. $\tau_y \sim G/4$ is an overestimate then, even in the crudest picture. Estimates from bubble-raft experiments[1] found a lower bound of $\tau_y \sim G/30$, so the range of prediction is $0.03G \leq \tau_y \leq 0.25G$.

This value is usually presented as a hypothetical in textbooks on plasticity, but remarkably enough, the relevant experiment has been carried out on single crystals. It became possible in the 1950s to make single-crystal "whiskers" (now known as "nanowires") by reduction of their halides, e.g., FeCl_3 . The whiskers happen to grow without dislocations, but they can be only very small in length and diameter. Bulk single crystals, on the other hand, always have some dislocations present.

The ingenious experiment by Brenner et al[2] measured yield stresses in these tiny crystals by wax-mounting them to a solenoid actuated float tube in a bath. Sample data for Fe and quartz are shown on the right. Several features of the response of single-crystal Fe are worth noting

- Recoverable strains as large as $\epsilon = 0.05$ could be sustained in the Fe whisker.
- The elastic response is visibly anharmonic in Fe: the Young's modulus E is not constant with elongation

- The maximum yield stress seen in the Fe whisker is 12 GPa, compared with 5 MPa in a bulk crystal

Yield stresses for the whiskers were very high: $\tau_{max} = 0.060 \text{ G}$ for Fe, $\tau_{max} = 0.022 \text{ G}$ for Cu, $\tau_{max} = 0.031 \text{ G}$ for Ag. These values were in satisfactory agreement with the more realistic theoretical predictions.

11.1.2 Macroscopic crystals

The authors observed that the yield stress dropped rapidly as the whisker diameter increased, but with a great deal of random variation from one diameter to the next. This was attributed to the gradual, random introduction of dislocations. In the case of macroscopic, high-purity, annealed perfect single-crystal Cu, the yield stress is down all the way to $< 30 \text{ MPa}$ [3], difficult to measure precisely, because the elastic component is not clearly visible.

11.2 Strengthening mechanisms

We will take a look at several mechanisms which are used to strengthen metals. Work hardening, or cold work, will be described in Section 11.2.1. This is an important mechanism in wire drawing and stamping metal components, for example. Finite-size strengthening, or grain-boundary strengthening, has been understood through the Hall-Petch relationship, described in Section 11.2.4. Polycrystalline metals can be strengthened by making their grains smaller, for grain sizes below $\sim 5\mu\text{m}$; this mechanism is also important in pearlitic steels, the highest strength engineering metals known. Solid solution strengthening, described in Section 11.2.2, is relevant in a variety of metal alloys, particularly those used in jewelry, and is quite similar in mechanism to the C interstitial in Fe pinning described in Section 10.5.2. Finally, in Section 11.2.3, we will look at precipitation hardening, or second-phase strengthening, which has been critical for the development of Al alloys in aerospace and sports equipment.

11.2.1 Work hardening

Crystals can be strengthened through plastic deformation alone. We have referred to *strain hardening*, or *work hardening*, in our earlier discussion of $\sigma(\epsilon)$ relationships in plasticity. Without the tendency of the yield stress $\sigma_y(\epsilon)$ to increase with strain ϵ , metals would become immediately unstable

in tension. We saw that there was a relationship $\sigma(\epsilon) = K\epsilon^n$, where K is the strength coefficient and n is the strain-hardening exponent.

Understanding of work hardening was reviewed recently in ref [4]. This review, like earlier reviews, starts with despairing statements about how the problem is difficult and a general theory is remote.¹ We will look at simple models of work-hardening of single crystals, at low temperature and low dislocation density, since this behavior seems to be best understood.

Taylor relation

The microscopic origin of work hardening, at least in relatively pure crystals, is in the increase in dislocation density with increasing plastic strain. The larger number of dislocations interfere with each other and move less easily. Taylor[5] found a relationship between the flow stress and dislocation density of

$$\tau = \alpha G b \sqrt{n_d} \quad (11.1)$$

where G is the shear modulus, b the Burgers vector, and n_d the areal density of dislocations. α is a constant. This relation holds where the flow stress is controlled by dislocation-dislocation interactions alone. Experimental results on work hardening of Cu single-crystals through 1981 have been collected in [6]. The Taylor relationship is obeyed quite well over several decades of work hardening, with a maximum flow stress achieved of $\tau \sim 0.0025 G \simeq 200$ MPa.

Strain hardening rate

Differentiating Eq 11.1 with respect to shear strain γ ,

$$\frac{\partial \tau}{\partial \gamma} = \frac{\alpha G b}{2\sqrt{n_d}} \left(\frac{\partial n_d}{\partial \gamma} \right) \quad (11.2)$$

Next, defining the *work hardening rate* as the differential increase in flow stress with shear strain,

$$\theta \equiv \left(\frac{\partial \tau}{\partial \gamma} \right) \quad (11.3)$$

and substituting both the dislocation generation mean free path from Eq 10.8 and Eq 11.1 again,

¹This from Cotrell: "It is sometimes said that the turbulent flow of fluids is the most difficult remaining problem in classical physics. Not so. Work hardening is worse."

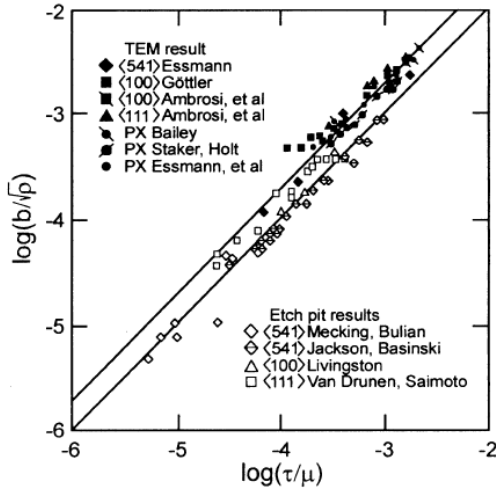


Figure 11.3: Work hardening in single-crystal Cu: validation of Eq 11.1. $\mu = G$ and $\rho = 1/n_d$ in our notation. From [4].

$$\tau \theta = \frac{(\alpha G b)^2}{2} \left(\frac{1}{b \Lambda} \right) \quad (11.4)$$

or substituting the Taylor relationship for τ ,

$$\alpha G b \sqrt{n_d} \theta = \frac{(\alpha G b)^2}{2} \left(\frac{1}{b \Lambda} \right) \quad (11.5)$$

Now the mean free path for dislocation storage is taken to be approximately equal to the dislocation spacing,

$$\Lambda \sim \frac{1}{\sqrt{n_d}} \quad (11.6)$$

and

$$\frac{\theta}{G} = \frac{\alpha}{2} \quad (11.7)$$

where α is a constant. Empirically, the work-hardening rate is indeed found to be constant for small amounts of work hardening and/or at low temperatures, for FCC single crystals,

$$\theta \simeq \frac{G}{200} \quad (11.8)$$

valid to within a factor of two[6].

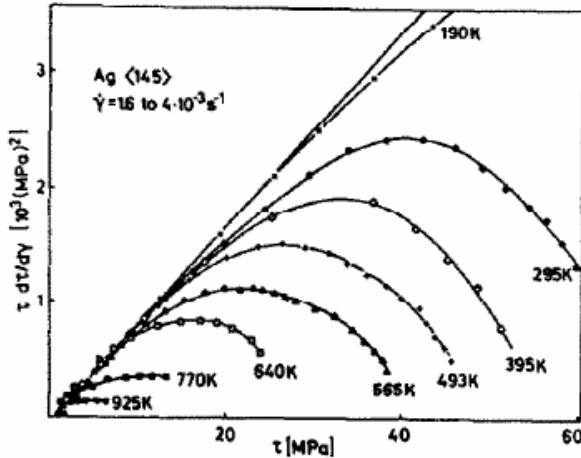


Figure 11.4: Work hardening in single-crystal Ag. The low-temperature data are consistent with Eq 11.8. From [6]

Thermal effects As temperatures increase from zero, the work-hardening rate θ becomes no longer constant as a function of work hardening. The experimental plot in Figure 11.4 shows the quantity $\theta \tau$, proportional to τ if θ is constant, as a function of flow stress τ . The deviation from the linear relationship increases with increasing temperature. Clearly work hardening becomes less effective as temperature increases. This behavior is attributed to *dynamic recovery*: as more thermal energy is available, the dislocations become better able to rearrange themselves so that they can glide past each other.

11.2.2 Solid-solution strengthening

We can estimate the shear stress required to move a dislocation line pinned by solutes with a mean spacing L in the glide plane. The estimate is credited to Fleischer[3] as presented in [7]. Under an applied stress, the line segments between the solutes will "bow out" and develop a radius of curvature ρ . The force per unit length on the line will be

$$\frac{f}{dl} = \frac{T}{\rho} \quad (11.9)$$

and substituting the Peach-Koehler force τb , the radius of curvature is given as

$$\rho = \frac{T}{\tau b} \quad (11.10)$$

where T is the line tension. Each time the dislocation line moves past an obstacle, it will sweep out the area subtended by the line bowing out from pinning points separated by L . For small-angle bowing, $\theta \ll 1$, the area A swept will be

$$A \simeq (\theta L) L \quad (11.11)$$

Substituting $\theta = L/(2\rho)$, as shown in Figure 10.6,

$$A \simeq \frac{L^3}{2\rho} \quad (11.12)$$

so

$$A \simeq \frac{L^3 \tau b}{2 T} \quad (11.13)$$

The dislocation is pinned essentially only by the solutes in its glide plane. As we saw in Eq 10.108, the solute-edge dislocation force falls off as y_0^{-2} , where y_0 is the distance from the solute to the glide plane. To estimate the glide-plane area per pinning site A_p , we take a thin-layer volume $A_p b$, with thickness of the Burgers vector, containing one solute atom (distributed with a volume concentration c):

$$b A_p c = 1 \quad (11.14)$$

$$A_p = \frac{a^3}{b x} \quad (11.15)$$

,

where x is the fractional atomic content of the solute. For the dislocation to move over large distances, past many obstacles, the criterion is that it must not be recaptured immediately by another solute. This implies that the area swept will be larger than the area per pinning site,

$$A \geq A_p \quad (11.16)$$

$$\frac{L^3 \tau b}{2 T} \geq \frac{a^3}{b x} \quad (11.17)$$

In equilibrium, the Peach-Koehler force on the dislocation, over line segment L between solutes, will be equal to the force f_0 exerted by each solute on the dislocation,

$$\tau b = \frac{f_0}{L} \quad (11.18)$$

which gives us an estimate of the length L in terms of the shear stress and f_0 ,

$$L^3 = \frac{f_0^3}{(\tau b)^3} \quad (11.19)$$

This is substituted back in. Taking $a \sim b$,

$$\frac{f_0^3}{(\tau b)^3} \frac{\tau b}{2T} \geq \frac{b^2}{x} \quad (11.20)$$

At the critical resolved shear stress τ_c , the areas are equal; solving for τ_c ,

$$\tau_c = \frac{f_0^{3/2}}{\sqrt{2T} b^2} x^{1/2} \quad (11.21)$$

Substituting in for the line tension, $T \sim G b^2$,

$$\tau_c = \frac{f_0^{3/2}}{\sqrt{2G} b^3} x^{1/2} \quad (11.22)$$

This gives the surprising result that the strengthening is proportional to the square root of the solute concentration x , rather than the simply proportional to x .

We have already estimated f_0 for an impurity atom in Eq 11.23:

$$f_0 = \frac{\sqrt{3}G b}{8\pi y_0^2} \left(\frac{1+\nu}{1-\nu} \right) V_i \quad (11.23)$$

$$\tau_c = \frac{\sqrt{x}}{\sqrt{2G} b^3} \left(\frac{\sqrt{3}G b}{8\pi y_0^2} \left(\frac{1+\nu}{1-\nu} \right) V_i \right)^{3/2} \quad (11.24)$$

As before, we estimate $y_0 \simeq 3b$, $\nu \sim 1/3$,

$$\tau_c = \frac{G}{Z} \epsilon^{3/2} \sqrt{x}$$

(11.25)

where ϵ is the volume difference between the impurity atom and the host,

$$\epsilon \equiv \left| \frac{V_i}{b^3} \right| \quad Z \equiv \sqrt{2} \left(\frac{36\pi}{\sqrt{3}} \right)^{3/2} \sim 750 \quad (11.26)$$

Example: 5% Au in Cu The lattice parameters differ as $a_{Au} = 0.4078$ nm, $a_{Cu} = 0.361$ nm, so $\epsilon = (0.4078^3 - 0.361^3) / 0.361^3 = 0.44$. The increase in yield stress will be

$$\Delta\tau \simeq \frac{G}{750} 0.44^{3/2} \sqrt{0.05} \simeq 8.7 \times 10^{-5} G \quad (11.27)$$

taking the shear modulus of copper as 48 GPa, we estimate a small strengthening of $\Delta\tau \simeq 4$ MPa. The experimental value[8] is $\Delta\tau = 53$ MPa/ $\sqrt{x_{Au}}$, or for $\sqrt{0.05} = 0.22$, $\Delta\tau = 12$ MPa. This is reasonable agreement given the many approximations made.

Improved estimate Fleischer took a few additional effects into account in his estimate. The substitutional impurity may have very different elastic properties from the host; a parameter η ,

$$\eta = \frac{\partial \ln G}{\partial x} = \frac{1}{G} \left(\frac{\partial G}{\partial x} \right) \quad (11.28)$$

was defined to quantify this effect. The change in lattice parameter was defined as

$$\delta = \frac{\partial \ln b}{\partial x} = \frac{1}{b} \left(\frac{\partial b}{\partial x} \right) \quad (11.29)$$

The full expression uses

$$\eta' \equiv \frac{\eta}{1 + |\eta|/2} \quad (11.30)$$

and ϵ becomes

$$\epsilon = |\eta' - \alpha \delta| \quad (11.31)$$

where $\alpha = 3$ for screw dislocations and $\alpha = 16$ for edge dislocations.

Fleischer's equation is as it was with the revised definition of ϵ and with $Z = 760$. The agreement between the revised Eq 11.25, with the revised definitions, and experimental solid-solution strengthening of Cu single crystals is remarkably good, as shown in Figure 11.5.

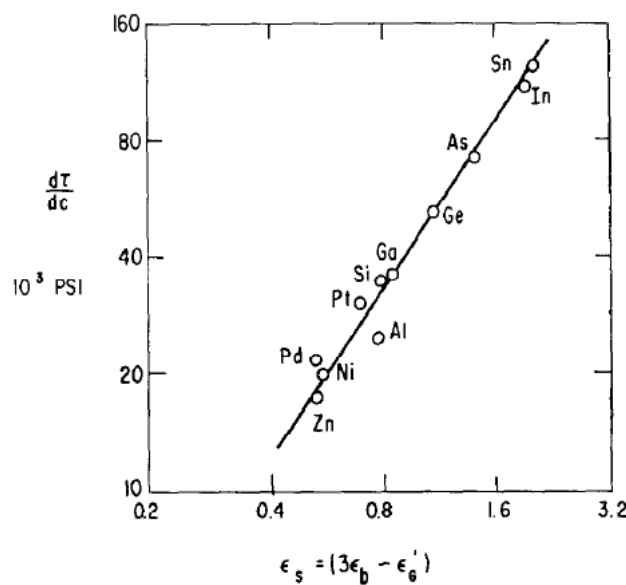


Figure 11.5: Solid solution strengthening in Cu alloys. The line is a fit to Eq 11.25. Note the double-logarithmic scale, showing $\tau \sim \epsilon^{3/2}$; 1 ksi = 6.9 MPa. From [3]

At higher concentrations, Labush showed

$$\tau_c = \frac{G}{Z_2} \epsilon^{4/3} x^{2/3} \quad (11.32)$$

where $Z_2 = 550$. Some experimental evidence for this form was presented by Jax et al[8].

11.2.3 Precipitation hardening

Small precipitates of a second phase can strengthen alloys to a greater extent than impurity atoms in a random solid solution can. *Precipitation hardening* is an important strengthening mechanism for Al-base alloys. For dilute precipitates, the mechanism can be understood similarly to solid-solution strengthening. When the precipitates occupy a larger volume fraction, the energy of the dislocation as it cuts through the precipitate or bends around the precipitate needs to be considered. Several mechanisms have been proposed for the strengthening. In FCC metals, like Al, in which dislocations separate into Shockley partials, one of the more successful approaches has been to consider the difference in stacking-fault energy as the dislocation cuts into the precipitate, or *stacking-fault strengthening*. The strengthening effect is given by

$$\Delta\tau_y = (\gamma_{sfm} - \gamma_{sfp})^{3/2} \sqrt{\frac{3\pi^2 f < r >}{32T b^2}} \quad (11.33)$$

where γ_{sfm} is the stacking fault energy of the dislocation in the matrix, γ_{sfp} is the stacking fault energy in the particle, f is the volume fraction of particles, $< r >$ is the radius of the precipitate, T is the line tension of the dislocation, and b is the Burgers vector. Data obeying this relationship for Al with $\sim 2\%$ Ag are shown in Figure 11.6.

11.2.4 Finite-size strengthening (Hall-Petch)

Consider N dislocations gliding together on the slip plane, all under the influence of an applied shear τ , in $+x$. Dislocation $N-1$, the most advanced in x , or "spearhead," is pinned at $x = 0$. The trailing dislocations form a pileup, technically here a stressed single pileup. The pinning exerts an opposing force

$$-\frac{f_0}{\delta z} \hat{x} \quad (11.34)$$

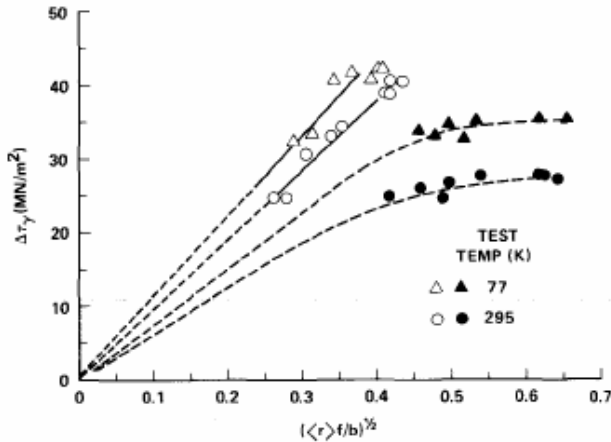


Fig. 13—The experimental data of Gerold and Hartmann⁵⁴ on age hardened monocrystalline Al-1.8 pct Ag. The open and filled symbols represent data on samples aged at 140 and 225 °C, respectively. The dashed curves schematically illustrate expected behavior.

Figure 11.6: Precipitation hardening in Al-Ag, from Ardell.[9]

on dislocation 0, which keeps it in equilibrium from the elastic forces from dislocations 0 to $N - 2$ and the external shear. If we take the whole ensemble of dislocations as one free-body, the total forces acting on them are zero, at equilibrium. The force acting on dislocation 0 then must balance all the individual Peach-Koehler forces,

$$\frac{f_0}{\delta z} = N \tau b \quad (11.35)$$

If no shear is applied, the dislocations spread out to infinite width in $-x$. In order for the N dislocations to fit on the domain $-l \leq x \leq 0$, there must be a large enough shear force pushing them to $+\hat{x}$, and so compressing the ensemble to a length l . We can then expect that the net dislocation density,

$$n = \frac{N}{l} \quad (11.36)$$

is proportional to the applied shear τb .

Equilibrium To express equilibrium for the dislocations, we have

$$f_{ij} = \frac{q}{x_i - x_j} \quad q = \frac{Gb^2}{2\pi(1-\nu)} \quad (11.37)$$



Figure 11.7: Calculated pileup profile behind pin at $x = 0$, for $\tau b = q$, $N = 15$ dislocations. The rightmost dislocations are too close together to be resolved.

where f_{ij} is the repulsive force (per unit length) acting between two same-sign dislocations i, j on the same slip plane. Writing the equilibrium equation for each dislocation i ,

$$0 = \sum_{j \neq i} \frac{q}{x_i - x_j} + (1 - N\delta_{i0}) \tau b \quad (11.38)$$

Dimensionless variables are convenient for numerical calculations; we can cast the expression in reduced units $X \equiv x/\lambda$, where

$$\lambda = \frac{q}{\tau b} \quad (11.39)$$

is a characteristic length. Then we have instead

$$0 = \sum_{j \neq i}^N \frac{1}{X_i - X_j} + (1 - N\delta_{i,N-1}) \quad (11.40)$$

Here the δ term represents the pinning force acting on the rightmost dislocation. It is possible to find the equilibrium positions for the N dislocations by solving for the roots of the N equations in Eq 11.40. A calculated single-sided stressed pileup for $N = 15$ dislocations, applied shear characterized by $\lambda = 1$, is shown in Figure 11.7.

Dislocation density We would like a relationship between the total length of the ensemble and the applied shear. The derivation in Eshelby's first paper[10] and in the textbook by Hirth and Lothe requires some advanced mathematics, but the result is simple:

$$l = 2N \frac{q}{\tau b} \quad (11.41)$$

showing that the dislocation density is indeed proportional to the applied stress. In reduced units,

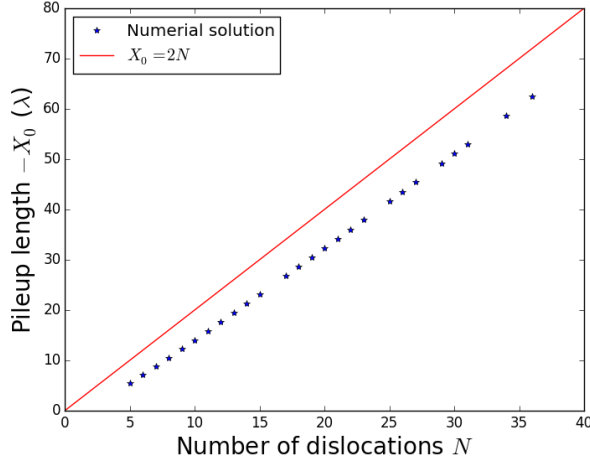


Figure 11.8: Total length $l = \lambda X_0$ of dislocation ensemble, as a function of number of dislocations N . Numerically calculated values are compared with the continuum limit in Eq 11.42.

$$X_0 = \frac{l}{\lambda} = 2N \quad (11.42)$$

Numerical validation of this expression is shown in Figure 11.8, looking at the calculated equilibrium length $X = l/\lambda$ of pileups of N dislocations. At higher values of N , appropriate for the continuum approach, the lengths appear converge to the theoretical result, however, the numerical solution becomes sensitive to initial guesses at high numbers of N .

Strengthening effect We assume that for slip to propagate from one domain – grain, or planar region – to another, the force per unit length on the spearhead dislocation must be greater than some value F_0 :

$$F_0 < N \tau_y b \quad (11.43)$$

We are interested in the effect of size on the strength of the metal. The dislocations are contained initially in a region of length l . This could be the size of the grain, $l = d_g$, or the width of lamellae, $l = w$. The N dislocations have to fit in the length l . We have $n = N/l = \tau b/2q$

$$F_0 < \frac{N}{l} l \tau_y b \quad (11.44)$$

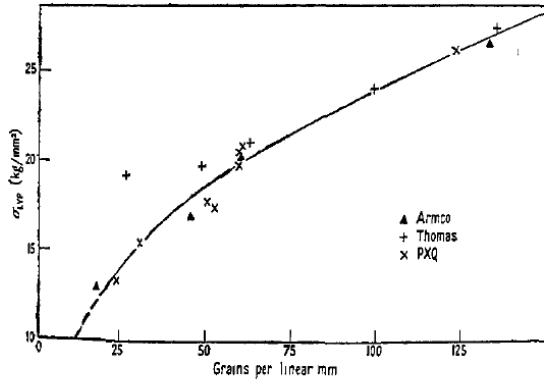


Figure 1.

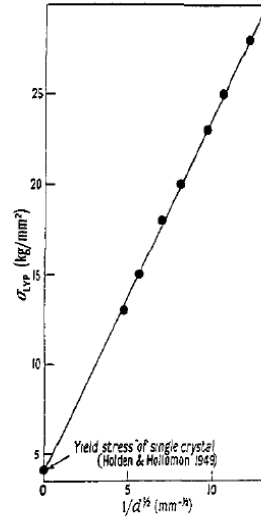


Figure 2.

Figure 11.9: First observation of grain-size strengthening, by Hall, motivating Eq 11.46. From Ref [11]

$$2q F_0 < l (\tau_y b)^2 \quad (11.45)$$

The product of the square of the yield stress and the grain size are constant, giving a relationship

$$\sigma_y = \sigma_y^0 + \frac{K}{\sqrt{d_g}} \quad (11.46)$$

This is the Hall-Petch relationship. Hall first observed this effect of grain size in mild (low-carbon) steels[11], as shown in Figure 11.9. The strengthening is substantial, roughly 210 MPa for $d_g = 10\mu\text{m}$. The mechanism is thought to be valid down to $d_g \sim 1\mu\text{m}$.

Exercises

1. If I apply a fairly rapid shear of 10/s, and the initial dislocation density is $10^{12}/\text{cm}^2$, how fast do the dislocations move, assuming $b=0.2 \text{ nm}$?
2. For a cold-worked metal, derive a relationship between shear strain and dislocation density, assuming no pinning sites from other strengthening mechanisms.
3. According to the Taylor relation, for a heavily drawn Cu wire
 - (a) What should be the dislocation density?
 - (b) What yield stress do you expect, if the sensitivity is constant?
4. Recall the strain-hardening factor and exponent. How would you relate to the sensitivity? Is there a relationship?
5. Estimate the pinning force of a dislocation line to a solute atom of Au in Cu. Convert your result to meV per atomic diameter and compare your result with $k_B T$.
6. Ni-Cu are perfectly soluble in each other in a FCC lattice. For 50:50% Ni-Cu, what strength do you expect due to solid solution strengthening? Use the simple (uncorrected) form equation, and compare with values from the plot.
7. Examine the precipitation hardening data for Al-1.8%Ag from the Ardell paper. a. Why do you think the filled symbols are to the right of the open ones? (read the legend) b. What is the radius of the smallest precipitates shown on the graph? (assume $b=0.2 \text{ nm}$) Approximately what is the difference in stacking fault energy?
8. Explain why annealing piano wire is likely to weaken it.
9. Explain why annealing nanocrystalline Ti is likely to weaken it.

Bibliography

- [1] Lawrence Bragg and W. M. Lomer. “A Dynamical Model of a Crystal Structure. II”. In: *Proceedings of the Royal Society of London A: Mathematical, Physical and Engineering Sciences* 196.1045 (1949), pp. 171–181. DOI: [10.1098/rspa.1949.0022](https://doi.org/10.1098/rspa.1949.0022).
- [2] S. S. Brenner. “Tensile Strength of Whiskers”. In: *Journal of Applied Physics* 27.12 (1956), pp. 1484–1491.
- [3] R.L. Fleischer. “Substitutional solution hardening”. In: *Acta Metallurgica* 11 (1963), p. 203.
- [4] U.F. Kocks and H. Mecking. “Physics and phenomenology of strain hardening: the {FCC} case”. In: *Progress in Materials Science* 48.3 (2003), pp. 171–273. DOI: [http://dx.doi.org/10.1016/S0079-6425\(02\)00003-8](http://dx.doi.org/10.1016/S0079-6425(02)00003-8).
- [5] G.I. Taylor. “The mechanism of plastic deformation of crystals, part I—theoretical”. In: *Proceedings of the Royal Physical Society of London* 145 (1934), p. 362.
- [6] H. Mecking and U.F. Kocks. “Kinetics of flow and strain-hardening”. In: *Acta Metallurgica* 29 (1981), pp. 1865–1875.
- [7] R. Labusch. “A statistical theory of solid solution hardening”. In: *Physica Status Solidi* 41 (1970), p. 659.
- [8] P. Jax, P. Kratochvil, and P. Haasen. “Solid solution hardening of gold and other FCC single crystals”. In: *Acta Metallurgica* 18 (1970), p. 237.
- [9] A.J. Ardell. “Precipitation hardening”. In: *Metallurgical Transactions A* 16A (1985), p. 2131.
- [10] J.D. Eshelby, F.C. Frank, and F. R. N Nabarro. “The equilibrium of linear arrays of dislocations”. In: *Philosophical Magazine* 42 (1951), p. 351.

- [11] E O Hall. "The Deformation and Ageing of Mild Steel: III Discussion of Results". In: *Proceedings of the Physical Society. Section B* 64.9 (1951), p. 747.

Chapter 12

Fracture

12.1 Griffith critical crack length

A brittle material under tension can fail catastrophically due to the propagation of a crack. The crack tip is a point where the externally applied tension σ becomes concentrated, reaching much higher local stresses than are seen in the bulk of the material. As the crack becomes longer, the intensity of the stress becomes larger, and more elastic energy would be released when the material breaks. This tendency is inhibited by the creation of two new surfaces in the crack, which have an associated surface energy. Since the stress concentration goes up rapidly with crack length l , and the surface area uncovered is simply proportional to l , there will be *critical crack length* at which the incremental reduction in elastic energy outweighs the incremental increase in surface energy with increasing length dl . At this point, the crack length becomes unstable, the crack grows rapidly, and the material fractures.

12.1.1 Square beam

The simplest system in which to see the critical crack length appear is a beam, under an applied tensile load per unit thickness at the edge, P/t , which tends to split the beam. Each side edge of the crack is displaced by an amount δ at the tip. A crack of length l grows in from the outside surface, as pictured in the Figure.

It can be shown relatively easily from elastic beam theory that the load-displacement ($P - \delta$) relationship for the beam is

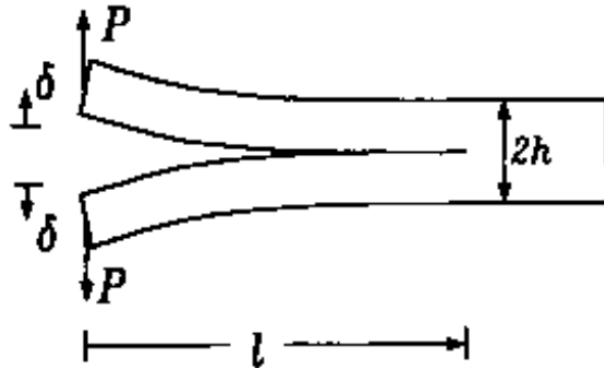


Figure 12.1: Split beam under tension. From ref. [1]

$$\frac{P}{t} = \frac{Eh^3}{4l^3}\delta \quad (12.1)$$

where h is the height of each leg and E is the Young's modulus. The elastic energy per thickness for the two beams ($(P/t)\delta/2$ in each) will be

$$\frac{U_{el}}{t} = \frac{P}{t}\delta \quad (12.2)$$

We will consider an experiment where the load P^* is constant and will not change with length, so

$$\frac{U_{el}}{t} = \frac{4l^3}{Eh^3} \left(\frac{P^*}{t} \right)^2 \quad (12.3)$$

This is a positive strain energy for the beam. When the crack propagates, the strain energy is released and the contribution to U_{el} is negative, $\delta U_{el} < 0$, for increasing crack length $\delta l > 0$. On the other hand, the surface energy change is positive for increasing crack length,

$$\frac{U_s}{t} = 2\gamma l \quad (12.4)$$

where γ_S is the surface energy of the solid (J/m².) Summing the two contributions,

$$\frac{\partial}{\partial l} \left(-\frac{U_{el}}{t} + \frac{U_s}{t} \right) \quad (12.5)$$

will be the net change in energy for a differential increase in crack length. If the crack is short, little elastic energy (as l^3) is released, the increase in surface energy impedes its motion, and the crack would have a tendency to shrink – but it cannot shrink because the surfaces do not fuse back together except under high pressure and temperature. If the crack is long, however, a lot of elastic energy is released, making the surface term insignificant, and the crack will grow with increasing velocity until the sample breaks.

Setting the derivative equal to zero for the crossover between the stable and unstable crack lengths, the critical crack length l_c is

$$\frac{6l_c^2}{Eh^3} \left(\frac{P^*}{t} \right)^2 = \gamma \quad (12.6)$$

finally,

$$l_c = \sqrt{\frac{E\gamma h^3}{p^2}} \quad (12.7)$$

where E is the Young's modulus, h is the height of the beam (m), and p is the constant loading force per unit thickness of the beam (N/m).

12.1.2 Elliptical crack

Griffith instead considered an elliptical crack with length $l = 2c$.[2], where the minor axis width of the ellipse goes to zero. The mathematics are much more complicated here but the basic elements (elastic energy and surface energy) are the same. Here the critical value of c is

$$c = \frac{E\gamma_S}{\sigma_c^2} \frac{2}{\nu\pi} \quad (12.8)$$

where ν is the Poisson ratio and σ_c is the critical stress, leading to fracture, for a crack with length $2c$. The expression has some similarities with the beam analysis: it contains the ratio of the Young's modulus - surface energy product to the square of the applied load. Nevertheless, Griffith's equation depends on these terms with a different power law. Griffith's expression can be recast as

$$\sigma_c \sqrt{c} = \sqrt{\frac{2E\gamma_S}{\nu\pi}} \quad (12.9)$$

where the right-hand side contains only material constants. This expression means that the yield stress will vary as $c^{-1/2}$, the inverse of the square root of the crack length.

Example Griffith evaluated the fracture of glass tubes onto which he scribed cracks of various lengths. The bursting stress (under pressure) was measured as a function of the crack length. What should be the bursting stress for a 3.8 mm length crack ($c = 1.9$ mm.) For glass, take $E = 62$ GPa, $\nu = 0.251$, and $\gamma = 0.54$ J m⁻², as reported by Griffiths. The rupture stress σ_c evaluates to 6.7 MPa, in reasonable agreement with his observed 5.96 MPa.

12.2 Weibull distribution

For a glass specimen which contains many tiny cracks, with a statistical distribution of crack lengths, what will be the fracture strength? The key insight is that the fracture strength is determined by the weakest link. If for an applied stress σ , any crack i , with length $2c_i$, is long enough that

$$\sigma > \sigma_{c,i} = \sqrt{2E\gamma/\pi\nu c_i} \quad (12.10)$$

the whole sample fails. Since we cannot know for sure what crack lengths are inside the solid, we can only assign a statistical probability of crack lengths, and therefore of failure, and then make sure that that probability is effectively zero for critical components.

Weibull[3] treated the statistical problem in general terms¹. If there is some quantity x_i (here σ_i) attributed to individuals i (cracks), $F(x)$ is the probability of an individual i having x_i less than x . This probability distribution function is not defined in the conventional way, which is where $P(x)$ is the probability of any value x_i falling between x and $x + \delta x$.

Gaussian example for $F(x)$ For a Gaussian distribution, now

$$P(x) = \frac{\sqrt{\pi}}{2} \exp -\frac{(x - x_0)^2}{\sigma^2} \quad (12.11)$$

the distribution will be peaked at x_0 (the mean value) with the probability of a member having $x_i = x_0 \pm \sigma$ (off by a standard deviation) falling off to ~ 0.27 of the peak probability. As $F(x)$ is defined,

¹"A statistical distribution function of wide applicability," W. Weibull, *Journal of Applied Mechanics* **293** (1951)

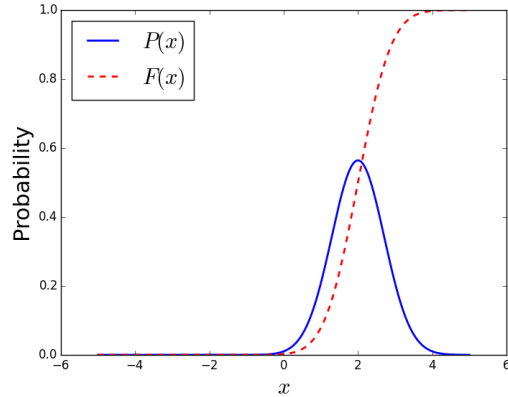


Figure 12.2: Comparison of $F(x)$ and $P(x)$. Standard deviation $\sigma = 1$, peak location $x_0 = 2$.

$$F(x) = \int_{-\infty}^x dx P(x) \quad (12.12)$$

Far above the peak value x_0 , $F \rightarrow 1$; far below x_0 $F \rightarrow 0$. In Figure 12.2, $F(x)$ is integrated numerically. The jump in $F(x)$ from 0.1 to 0.9 (10% of members i having $x_i < x$ to 90% of members i having $x_i < x$) is over the 2σ near the peak in the distribution. Columbia students are familiar with the definition of $F(x)$ in percentile scores on standardized tests, where your score x_i is surely such that $F(x_i) \rightarrow 1 - \delta$. In the same way, we would choose cracks such that $F(\sigma) \rightarrow 1 - \delta$ for the strongest material.

We now define a function $\phi(x)$ as a different way to express $F(x)$:

$$\exp(-\phi(x)) = 1 - F(x) \quad (12.13)$$

which is the probability of $x_i (\theta_i)$ being *higher* than x (applied σ). This is the *probability of nonfailure* of any link: elements (students) with high percentile scores are not likely to fail.

The probability of *nonfailure* for n links is the product of all individual probabilities: if each link fails 10% of the time, all of four links will not fail only $0.9^4 = 65\%$ of the time. If the chain fails with probability P_n , the probability of nonfailure is $1 - P_n$, given by the product

$$1 - P_n = (1 - F(x))^n \quad (12.14)$$

$$P_n = 1 - \exp(-n\phi(x)) \quad (12.15)$$

The only remaining step is to know what the expression for $\phi(x)$ is. We can first remark that a reasonable guess would be

$$\phi(x) = \frac{x}{x_c} \quad (12.16)$$

where x_c is a constant, characteristic value of x . If $x \gg x_c$, we expect $F(x) \rightarrow 1$. The exponential argument is large and negative and the exponential tends to zero. In our expression for P_n ,

$$P_n = 1 - \exp\left(-n \frac{x}{x_c}\right) \quad (12.17)$$

for large numbers of links n , P_n goes very rapidly to zero for $x > x_c$, and very rapidly to one for $x < x_c$. Weibull chose a more general distribution function

$$\phi(x) = \left(\frac{x - x_u}{x_0^{1/m}}\right)^m \quad (12.18)$$

This distribution function improves on the initial guess x/x_c by adding a parameter. The new parameter x_u is a nonzero value of x for which $P_n = 0$: no individual has X lower than x_u . The parameter x_0 controls the width of the distribution. The parameter m is more difficult to motivate. This assumption for $\phi(x)$ has similar features to the first: 1) it is positive for all $x > x_u$, 2) it increases with x , but it is otherwise still completely *ad-hoc*. Weibull remarks,

it is utterly hopeless to expect a theoretical basis for distribution functions of random variables such as strength properties of materials or of machine parts or particle sizes, the "particles" being fly ash, Cyrtidea, or even adult males born in the British isles

This gives the probability of any one of n individuals having a value x_i less than x as

$$P_n(x) = 1 - \exp\left[-n \left(\frac{x - x_u}{x_c}\right)^m\right] \quad (12.19)$$

or, in the case of fracture, the probability of any one of n links having σ_i less the applied stress σ as

$$P_n(\sigma) = 1 - \exp\left[-n \left(\frac{\sigma - \sigma_u}{\sigma_0}\right)^m\right] \quad (12.20)$$

Defining a volume density of cracks $\rho_c = n/V$, where V is the volume of the sample, and taking $\sigma_u = 0$ (so that there is a continuous probability distribution of crack lengths to large sizes), the failure probability is

$$P^f(\sigma) = 1 - \exp \left[-\frac{V}{V_0} \left(\frac{\sigma}{\sigma_0} \right)^m \right] \quad \sigma_u = 0 \quad (12.21)$$

where $V_0 = 1/\rho$ is the characteristic volume occupied by a crack and V_{eff} is the volume of the sample.² The *characteristic strength* σ_0 is that for which the failure probability is $1 - 1/e \sim= 0.63$. This is the two-parameter Weibull distribution.

The failure probability can then be estimated in a loglog - log plot as

$$\log \left[\log \left(\frac{1}{1 - P^f(\sigma)} \right) \right] = m \log \left(\frac{\sigma}{\sigma_0} \right) + \log \frac{V_{eff}}{V_0} \quad (12.22)$$

Plotting the experimental quantities of failure rate P^f vs applied load σ in this form helps to identify the *Weibull modulus* m . m is observed to be on the order of 10-15[4].

The scaling of yield strengths σ with size V_{eff} can be understood by taking a constant argument in the exponential. At the characteristic strength σ with 63% failure probability, if we consider two samples with different volumes V_1 , V_2 , their strengths σ_1 , σ_2 will be related through the Weibull modulus,

$$\sigma_2 = \left(\frac{V_1}{V_2} \right)^{1/m} \sigma_1 \quad (12.23)$$

The size dependence can be seen in the right hand graph of Figure 12.3. While there is a size dependence of failure stress σ , the $1/m$ exponent means that it is not very dramatic: a 10-fold increase in the sample volume reduces the strength by a factor $0.1^{1/m}$, or $\sim 15\%$ for $m = 15$ as observed for SiC. Increasing the volume by four orders of magnitude cuts the characteristic stress σ_0 in half.

²There is an additional constant factor in V_{eff}/V , taken to be = 1 here.

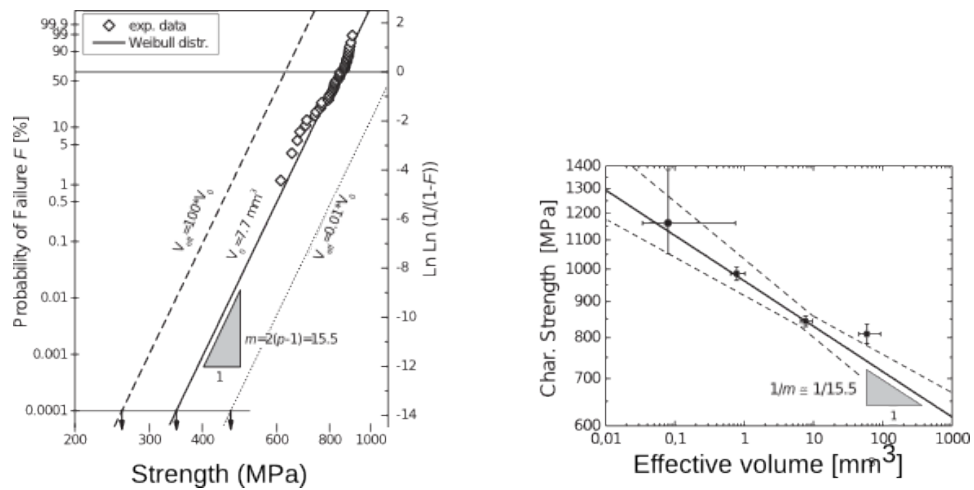


Figure 12.3: *Left:* Estimate of the Weibull modulus from loglog-log plot of failure probability vs bending stress, SiC fibers. Estimate of $\sigma_0 = 844$ MPa is shown with the solid horizontal line. Estimate of modulus m is shown with slope. *Right:* Scaling with volume: characteristic stress σ_0 vs volume V . From [4].

Bibliography

- [1] L.B. Freund. *Dynamic fracture mechanics*. Cambridge University Press, 1990.
- [2] A.A. Griffith. “The phenomenon of rupture and flow in solids”. In: *Proceedings of the Royal Society A* 587 (1920), p. 163.
- [3] Waloddi Weibull. “A statistical distribution function of wide applicability”. In: *Journal of Applied Mechanics* (1951), p. 293.
- [4] R. Danzer et al. “Fracture of Ceramics”. In: *Adv. Eng. Mater.* 10 (2008), p. 275. DOI: [10.1002/adem.200700347](https://doi.org/10.1002/adem.200700347).

Appendix A

Moments of inertia

There are two incompatible types of "moments of inertia:" area moments, and moments of mass. Unfortunately, both types have the same name and share the same set of symbols in many textbooks¹. To avoid "any confusion" (e.g. the instructor's) we will distinguish between them with different symbols in this note packet: I_x, I_y, I_z (or I_1, I_2, I_3) for area moments, and $\zeta_1, \zeta_2, \zeta_3$ for moments with mass attached; bear in mind that this nomenclature is not common.

A.1 Area moments of inertia

Take an arbitrary area S in the yz plane. Conventionally, the x direction is the direction along a beam, which motivates this choice. The moments *about axes in the yz plane* are defined through the integrals

$$I_y \equiv \int_S dA z^2 \quad (\text{A.1})$$

$$I_z \equiv \int_S dA y^2 \quad (\text{A.2})$$

where dA is an area element, $dA = dydz$. We see that the units are $I[=]\text{m}^4$. The integral I_z is important in the statics of beams, described in Section 2.5. The area moments of inertia can be taken for a cross-sectional area with normal along the long axis of the beam. One can also take the area moment of inertia about the normal (x -)axis,

¹see for example Beer and Johnston *Vector Mechanics for Engineers and Mechanics of Materials*.

$$I_x = \int_S dA \sqrt{y^2 + z^2} \quad (\text{A.3})$$

Example Let's calculate the ratio I_z/S of a rectangle, h in y , W in z . Here we have

$$\frac{I_z}{S} = \frac{1}{Wh} \int_0^W dz \int_{-h/2}^{h/2} dy y^2 \quad (\text{A.4})$$

$$\frac{I_z}{S} = \frac{h^2}{12} \quad (\text{A.5})$$

A.2 Mass moments of inertia

The moments of inertia of a mass relate the angular acceleration to a torque. For torques about x ,

$$\tau_x = \zeta_x \ddot{\theta}_x \quad (\text{A.6})$$

where θ_x is the rotational angle of the body about the x axis and $\ddot{\theta}_x$ is the angular acceleration. Clearly, because $\tau [=] \text{J}$ and $\ddot{\theta} [=] \text{s}^{-2}$, ζ has units of $\text{kg} \cdot \text{m}^2$, different from I . Taking our axis of rotation as x ,

$$\zeta_x = \int_V d^3\mathbf{x} \rho(\mathbf{x}) r_x^2(\mathbf{x}) \quad (\text{A.7})$$

where $\rho(\mathbf{x})$ is the mass density at any point and $r_x(\mathbf{x})$ is the distance from the x axis (of rotation) at any point.

Example: moment of inertia of a plate Take a plate with the same dimensions as shown before, $h \times W$ in yz , but Δx thick in x . Assume a uniform mass density ρ . The mass moment of inertia will be

$$\zeta_x = \Delta x \rho \int_{-W/2}^{W/2} dz \int_{-h/2}^{h/2} dy (y^2 + z^2) \quad (\text{A.8})$$

$$\zeta_x = \Delta x \rho \frac{hW}{12} (W^2 + h^2) \quad (\text{A.9})$$

which if we set $h = W = a$ becomes

$$\zeta_x = \rho \delta x \frac{a^4}{6} \quad (\text{A.10})$$

If a uniform torque per unit length is applied, $\tau_x/\Delta x$, the angular acceleration will vary as a^{-4} . For a cube with uniform density, we can take $\delta x = a$, and the mass $m = \rho a^3$. This gives $\zeta_x = ma^2/6$.